Strathclyde Institute for Pharmaceutical and Biomedical Sciences
Faculty of Science

The treatment of bacterial disease of plants by bacteriophage coated nanoparticles

Sara Filgueira Martinez

Thesis presented in fulfilment of the requirements for the degree of Doctor of Philosophy

2018

Declaration

This thesis is the result of the author's original research. It has been composed by the author and has not been previously submitted for examination which has led to the award of a degree.

Signed:

Date: 22/11/2018

Acknowledgements

I am taking this opportunity to thank everyone who supported me throughout the course of this project. Firstly, I would like to express my sincere gratitude to my supervisor Dr Paul Herron for his continuous support of my PhD, his patience and encouragement are very valued. Thanks also Dr Paul Hoskisson and Dr Nick Tucker, for your helpful advice and guidance in some experiments. I am also grateful to Dr Michael Mattey and Dr Gordon Smith for the industry and technological input, it was very practical to have your opinion on board. I am also grateful for the invaluable help provided by Dr Michaela Conley and Dr David Bhella from the University of Glasgow for some of the work.

I would like to thank my ex colleagues in the Microbiology Department in SIPBS, without whom this experience would have not been the same, for their support in times of need and for making me realise how important being part of a team can be. Thank you Jana, Talal, Sarah, Stu, Emilio, Cesar, Mireia, Alison, Kirsty, Leena, James, Danny, Vartul, Lauren, Flo, Sara, Maeidh and even Charles. I wish I could work along with most of you in the future.

To my family, for their lifelong support and. Thank you Paul for being there for me, for your invaluable help and encouragement, for joining me in Glasgow and for understanding how important this project has been for me, I could not have chosen a better companion. And last but not least, thank you Uxia for just being yourself, for making a better person of me and for giving me the strength that I needed (your hugs are the best!), this thesis is dedicated to you both.

Abstract

Bacterial phytopathogens are a recurring issue for agricultural plants. Traditional control measures include copper treatment and use of pesticides and antibiotics. The use of bacteriophages that selectively kill the causative pathogen as an alternative treatment has been delayed by technical difficulties associated with phage stability and deployment methods. In this project, we developed phage-coated nanoparticles for the control of tomato plant soft rot, caused by *Pectobacterium carotovorum,* as a model system. Scottish crops were used as a source to isolate new bacteriophages, followed by triple isolation of single plaques formed after infection. Using the enrichment technique, that uses bacteria to isolate the virus from a soil sample, twelve potentially different bacteriophages were recovered and fully characterised.

All of the phages isolated resemble T7 based on morphology by transmission electron microscopy; consistent with the genomic characterisation, electron microscopy revealed that the phages displayed a morphology characteristic of the *Podoviridae*. Subsequently, we covalently bound a collection of phages to the surface of different nanoparticles and the capacity of these phage coated nanoparticles to control bacterial plant disease was assessed.

This new technology fully retains the antimicrobial capacity of the bacteriophages and enhances its stability, particularly against dehydration, making this technology a potentially good candidate for use of biocontrol agents for crop pathogen treatment.

Table of contents

List of abbreviations

aa	amino acid
ABC transporter	ATP-binding cassette transporter
Abi	Abortive Infection System
AC	Alternating Current
AHL	N-acylhomoserine lactone
AI-2	AutoInducer-2
AMG	Auxiliary Metabolic Genes
ANI	Average Nucleotide Analysis
ANOVA	ANalysis Of VAriance
ASEN	Acquisition of SENsitivity
ATCC	American Type Culture Collection
BCA	Biocontrol Agent
BLAST	Basic Local Alignment Search Tool
bp	base pairs
BREX	BacteRiophage Exclusion System
BSA	Bovine Serum Albumin
°C	Celsius degrees
Car	1-carbapen-2-em-3-carboxylic acid
Cas	CRISPR-associated proteins
CBD	Cell-wall Degrading Domain
CCT	CGView comparison Tool
CDS	CoDing Sequence
cfa	coronafacic acid
cfu	colony forming units
CG	Cytosine Guanine
CLUSTAL	CLUSTer analysis of the pairwise ALignments
cm	centimeter
CRISPR	Clustered Interspaced Short Palindromic Repeats
crRNA	CRISPR RNA
crRNP	CRISPR ribonucleoprotein
cv	cultivar
DC	Direct Current
dCMP	deoxyCytidine MonoPhosphate
DGRs	Diversity-Generating Retroelements
DISARM	Defence Island System Associated with Restriction-Modification
DNA	DeoxyriboNucleic Acid
DNase	DeoxyriboNuclease
DPD	4,5-Dihydroxy-2,3-PentaneDione
dsDNA	double-stranded DNA
DSMZ	Deutsche Sammlung von Mikroorganismen und

DTR	Zellkulturem Direct Terminal Repeats
E. coli	*Escherichia coli*
EcRNAP	*E. coli* RNA Polymerase
EDTA	EthyleneDiamineTetraacetic Acid
EOP	Efficiency Of Plating
EPS	ExoPolySaccharides
eV	electronvolt
FAO	Food and Agriculture Organization of the United
FastME	Nations
FFT-NS-i	Fast Minimal Evolution
	Fast Fourier Transform-Normalised Similarity matrix-
FGenesV	iterative method
FP	Finding Genes in Viral genomes
g	Fixed-Phage
G	grams
GBDP	refers to “gravitational force” in centrifuges
GEPARD	Genome-BLAST Distance Phylogeny
GFF	Genome PAir Rapid Dotter
GLIMMER	General Feature Formet
gp	Gene Locator and Interpolated Markov ModelER gene product
HF	High Frequency
HGT	Horizontal Gene Transfer
HMM	Hidden Markov Models
HR	Hypersensitive Reaction
ICTV	International Committee on the Taxonomy of Viruses
ISPs	Ion Sphere Particles
k	thousand
kV	kilovolt
MAFFT	Multiple Alignment using Fast Fourier Transform
mg	milligram
ml	millilitre
MOI	Multiplicity Of Infection
mRNA	messenger RNA
MTase	Methyl Transferase
MUMmer	Maximal Unique Matches
mV	millivolt
NDM	New Delhi metallobeta-lactamase
NEB	New England Biolabs
ng	nanogram
nm	nanometre

nt	nucleotide
OD	Optical Density
O/N	OverNight
OPTSIL	OPTimising SILhouette Widths
ORF	Open Reading Frame
PA	Phage Adsorption
PAM	Photo-spacer adjacent motif
Pba	*Pectobacterium atrosepticum*
Pbb	*Pectobacterium betavasculorum*
Pbc	*Pectobacterium carotovorum*
PBS	Phosphate Buffer Saline
Pbw	*Pectobacterium wasabiae*
PCN	Phage-Coated Nanoparticle
PCR	Polymerase Chain Reaction
PCWDE	Plant Cell Wall Degrading Enzymes
PEG	PolyEthylene Glycol
Pfam	Protein families
pfu	plaque forming units
PGM	Personal Genome Machine
PHACTS	PHage Classification Tool Set
ppm	parts per million
PROKKA	PROKAryotic Annotation
psi	per square inch
qPCR	quantitative PCR
QS	Quorum Sensing
RAST	Rapid Annotation using Subsystem Technology
REN	Restriction Endonucleases
R-M	Restriction-Modification
RNA	RiboNucleic Acid
RNase	RiboNuclease
RNA-Seq	RNA Sequencing
rpm	revolutions per minute
SAM	S-AdenosylMethionine
SBS	Step-by-step
SCRI	Scottish Crop Research Institute
SDS	Sodium Dodecyl Sulfate
SM buffer	
SNP	Single Nucleotide Polymorphism
SPADES	Saint Petersburg genome Assembler
spp	species
SPR	Subtree Prunning and Regrafting
TA	Toxin-Antitoxin

TAE buffer	Tris, Acetic acid and EDTA buffer
TE buffer	Tris and EDTA buffer
TEM	Transmission Electron Microscope
TM buffer	Tris and Magnesium sulphate buffer
tRNA	transfer RNA
tRNAscan-SE	transfer RNA scan in genomic Sequence
tmRNA	transfer-messenger RNA
µg	microgram
µl	microliter
µm	micrometre
US	United States
UV	Ultra-violet
V	volts
VCE	VanComycin resistant Enterococci
V. harveyii	*Vibrio harveyii*
VICTOR	VIrus Classification and Tree building Online Resource
v/v	volume/volume
w/v	weight/volume
1SGC	one-Step Growth Curve
2D	biDimensional

1.0 Introduction

1.1 Importance of controlling crop pathogens

The demand for crop products has been increasing for the last few decades all over the world. This is the result of many factors, including population growth that is estimated to reach 9.6 billion by 2050, (United Nations, Department of Economic and Social Affairs, 2015), the increased levels of consumption in developing countries, such as China, and persistent poverty that has prevented millions of people from meeting their food needs (FAO, 2009). It has been predicted that crop supply should increase between 80 and 110% to meet these demands (Ray *et al.*, 2013); this need to increase crop production could come from expansion of crop land, harvest intensity and/or improvements in yield (FAO, 2009). Increasing the crop yield aims at maximising production, and this can be achieved by optimising water availability, use of fertilisers or pathogen control and it is likely to be the largest source of increased crop production in the future.

It is estimated between 10 and 25% of food produce is lost worldwide as a result of infectious plant diseases that include decay of infected crops by microbes (Strange and Scott, 2005), this damage causes economic losses for growers but also results in increased prices for consumers. It is estimated that the potato sector losses amounts to 65 billion kilograms and 16 billion dollars annually worldwide, and between 30 to 50% of these losses are caused by pectolytic bacteria (Oerke, 2006; Czajkowski *et al.*, 2011). Infection of plants in general can happen at any stage in the development: from the selection of seeds, to the field, harvest, transportation or even storage. The pathogens responsible include parasitic plants, oomycetes, nematodes, viruses, fungi and bacteria. Among the latter, there are over 200 plant pathogenic bacteria (Considina and Considine, 1995), and *Pectobacterium* spp. are within the eight most important (Mansfield *et al.*, 2012).

Potato (*Solanum tuberosum*) is the world's fourth most important food crop after rice, wheat and maize and the third in consumption (FAO, 2009). With Europe and Asia producing more than 80% every year (Figure 1-1), the UK is decreasing steadily its production and area harvested for the past twenty years (Figure 1-2). It is estimated that 22% of total production is lost as a result of pests and diseases; this corresponds to an average of over 65 million tonnes annually (Ross, 1986). Blackleg in potato seeds and tubers, caused mainly by *Pectobacterium* and *Dickeya* spp. (Charkowski, 2015), has been consistently the main cause for rejections and downgrading of potato seeds in most European countries (Czajkowski *et al.*, 2011); for example in the

Netherlands seed certification downgrades account for losses of up to 30 million euros annually (Toth *et al.*, 2011). In Scotland, downgrading of seed potatoes is mainly caused by *Pectobacterium atrosepticum* via contaminated seed tubers (Pérombelon, 2002) and its incidence has increased to levels not seen in 20 years (Davey *et al.*, 2016).

1.2 Crop losses caused by *Pectobacterium* spp.

It is estimated that losses vary between 15 and 30% of harvested crops (Agrios, 2005) and the severity of *Pectobacterium* infection is particularly high under warm and damp weather conditions. The bacteria can gradually grow on parent plants during storage, and be passed onto seed shoots every year, causing economic losses of between 50 to 100 million dollars worldwide every year (Pérombelon and Kelman, 1980). These bacteria are the main reason for production losses of stored potatoes (Harris, 1979; Pérombelon, 2002; Toth *et al.*, 2011) and they could be responsible for up to 85% of total losses (Fajola, 1979). Disease development depends on different factors including crop variety, environmental conditions during growing season or poor seed health (Davey et al., 2016). Unlike other plant pests like fungi, oomycetes and insects, there are no chemical treatments for these bacteria and preventative control measures rely on disease-free planting material (Table 1-1) (Czajkowski *et al.*, 2011), limiting the number of seed generations and good agronomical practices (Davey *et al.*, 2016), these include maintenance of crop rotation, selection of resistant varieties, correct entering of mineral fertilisers, enough distance between nursery plants and industrial ones, and careful destruction of the vegetation residues to name a few. Blackleg symptoms are detected visually on crop inspections, but these depend on the disease to be fully developed as a black, wet, rotting lesion developing from the base of the stem, though some yellowing and stunting may occur under dry conditions (Skelsey *et al.*, 2016), from the site of infection many bacteria are released into the soil and move to a distance of up to 10 metres (Graham and Harper, 1967) and survive for up to 10 months (Czajkowski *et al.*, 2011). Moreover, low inoculum levels of the bacteria on potatoes can still lead to high disease incidence under the right conditions (van der Wolf *et al.*, 2017), that include temperature and moisture levels can also facilitate disease development, for example the optimal temperature for pathogenicity is estimated to be between 15-20°C for *P. atrosepticum* and around 25°C for *P. carotovorum* (Perombelon and Salmond, 1995).

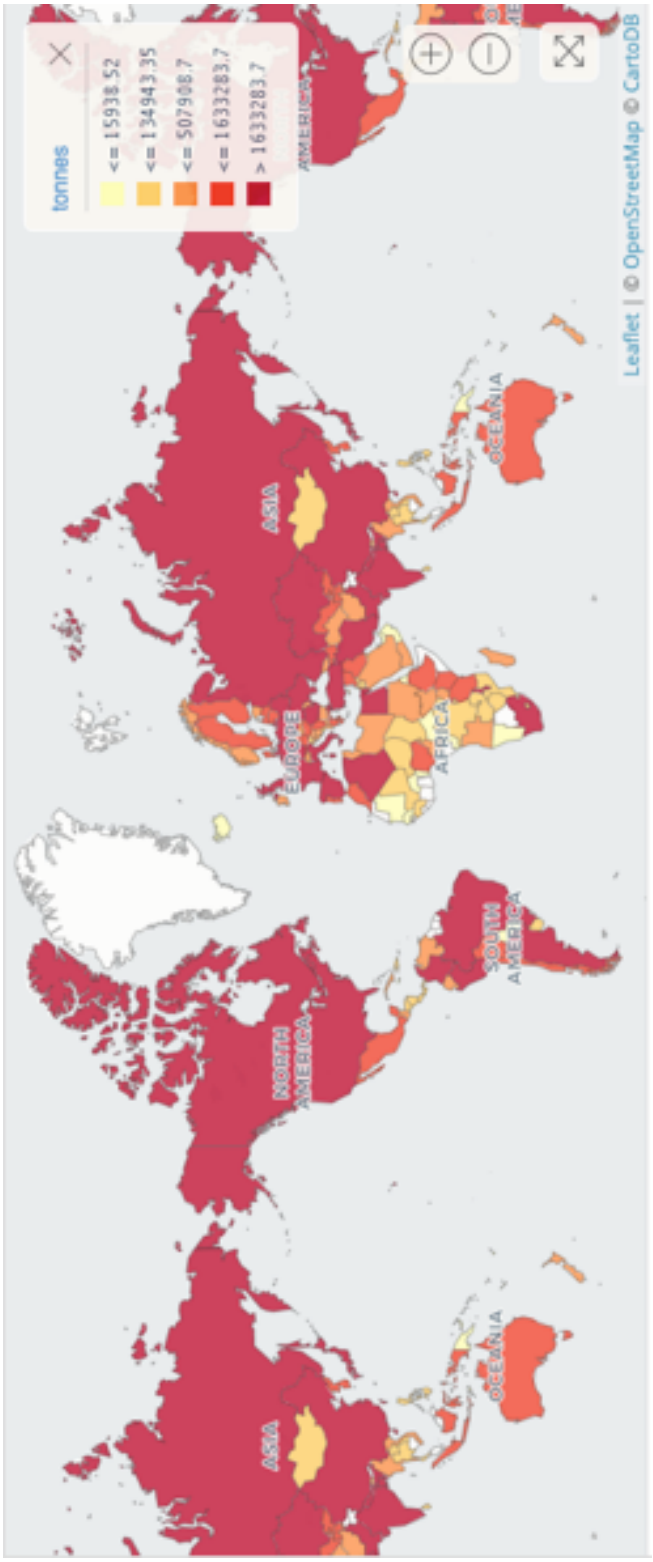

Figure 1-1: Average world production of potato between 1994 and 2016 (in tonnes). Crop production is higher in cold and temperate climates, mainly in developed countries (Anon, 2011).

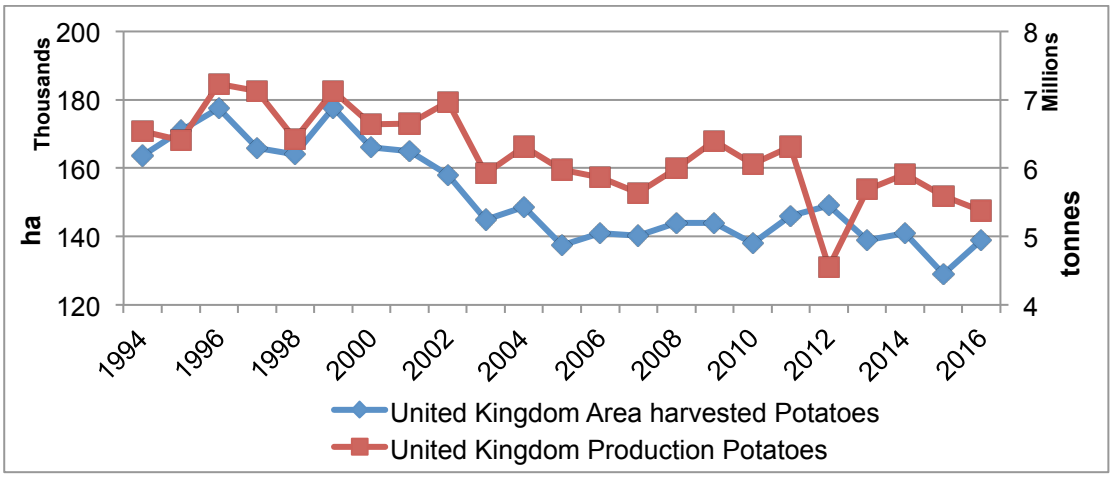

Figure 1-2: Production of potato in the United Kingdom between 1994 and 2016. Since 1992 the crop production has been decreasing moderately from approximately 8 to 6 million tonnes, the area dedicated for harvesting has been consistently decreasing from 180k to 140k hectares (Anon, 2014).

Control methods	Examples	Possible consequences of treatment
Seed selection	Seed Potato Classification Scheme (SPCS) in Scotland	High pathogen load after many generations, regular inspections
Pesticides treatments	Antibiotics, insecticides or fungicides	Pollution in the water and surrounding environment
Use of genetically-modified or cisgenic plants	Durable resistance against Phytophtora (DuRP) project	Possible insertional mutagenesis
Physical controls	Application of steam, hot water, UV or solar radiation	Damage crop product, accelerate plant degradation
Chemical controls	Antibiotics, inorganic and organic salts	Pollution in the water and surrounding environment, selection of resistant strains
Biological controls	Predatory bacteria and bacteriophages	Dysbiosis in the ecosystem, selection of resistant strains

Table 1-1: Different methods used for crop pathogen control. They should cover all the different stages of growth and commercialisation (Czajkowski *et al.*, 2011).

1.3 *Pectobacterium* spp.

Pectobacterium are pectinolytic, Gram-negative, facultatively anaerobic, nonsporing, motile bacteria, distributed in straight rods with petrichous flagellae and their colonies vary between one to two micrometres in diameter (Charkowski, 2006). The soft rot *Erwinia* group has been reclassified in recent years into two new bacterial genera (*Pectobacterium* and *Dickeya*), which are relatively different in terms of phage susceptibility (Czajkowski, 2016a), and seven *Pectobacterium* species are now described (Dees *et al.*, 2017):

Species	Abbreviation	Subspecies
Pectobacterium atrosepticum	Pba	
Pectobacterium betavasculorum	Pbb	
Pectobacterium carotovorum	Pbc	*carotovorum* (Pbc), *brasiliensis* and *odoriferum*
Pectobacterium wasabiae	Pbw	
Pectobacterium aroidearum		
Pectobacterium parmentieri		
Pectobacterium cacticida		

All these subspecies are widely distributed: *Pectobacterium carotovorum* has a worldwide distribution, being adapted to many climates, *Pectobacterium atrosepticum* is found in cold climates and *Pectobacterium betavasculorum* has been reported in Brazil, Israel, United States, New Zealand and South Africa (Ma *et al.*, 2007). These bacteria cause greater total crop losses of produce than any other bacterial disease, and they are responsible for a spectrum of disease symptoms, such as soft rot, blackleg and wilt, on eleven monocot and sixteen dicot families in a density-dependent manner (Ma *et al.*, 2007). *Pectobacterium* have also been found associated with many invertebrates, including fruit flies (Basset *et al.*, 2000; Muniz *et al.*, 2007; Nadarasah and Stavrinides, 2011), corn maggots (Gnanamanickam, 2006) and snails (Harrison *et al.*, 1977; Phillips and Kelman, 1982). *P. atrosepticum* causes infection on potato and closely related solanaceous crops, whereas *P. carotovorum*, *P. betavasculorum* and *P. wasabiae* are capable of infecting other plant species, therefore they are considered broad-host-range pathogens. Different *Pectobacterium* strains could share common virulence determinants associated with stem infection (Morschhäuser *et al.*, 2000), the detection of coronafacic acid (cfa) biosynthetic clusters in limited *Pectobacterum carotovorum* strains indicates that they were probably acquired from independent lateral gene transfer events (Panda *et al.*, 2016) and they contribute to more virulent blackleg symptoms (Morschhäuser *et al.*, 2000).

1.3.1 Virulence mediated by quorum sensing

Bacterial communication is based on the release in the surrounding microenvironment of small signalling molecules that can diffuse through the bacterial membrane. The accumulation of these membrane-diffusible molecules is coupled with gene expression, in a population-density-dependent mechanism known as quorum sensing (QS). There are at least two quorum sensing systems in *P. carotovorum* that use N-acylhomoserine lactones (AHL) and the autoinducer-2 (AI-2) as signalling molecules.

Virulence in *Pectobacterium* is triggered by quorum sensing, releasing plant cell-wall degrading enzymes (PCWDE) which break the host cell and initiate the rotting process (Toth and Birch, 2005). How the infection progresses depends on not only the bacterial strain but also the susceptibility of the host plant and the environmental conditions, such as temperature and humidity. Although it is widely accepted that quorum sensing is responsible for *Pectobacterium* virulence and infectivity (Barnard *et al.*, 2007), it is unclear why it happens. One theory behind the release of PCWDEs is the response to low nutrients in an environment with high cell densities, by breaking down the host cell walls, its incipient release of nutrients from the host plant would ensure further growth. Another theory explains antibiotic production in a quorum sensing system as a method of survival against other organisms; the fact that it is quorum sensing-directed would ensure that the levels of carbapenem antibiotic released are over the minimum inhibitory concentration for cell death (Barnard *et al.*, 2007). This highly specialised mechanism enables the synchronisation of entire bacterial communities resulting in increased effectiveness as a whole community rather than as individual bacteria. Many virulence factors depend on cell density in *Pectobacterium* (Whitehead *et al.*, 2002; Corbett *et al.*, 2005; Liu *et al.*, 2008), and they are induced at a density higher than 10^6 cells per millilitre (Toth *et al.*, 2003).

1.3.1.1 Protein secretion

In *P. atrosepticum,* PCWDEs are the main virulence determinants being responsible for tissue maceration at latter stages of infection (Py *et al.*, 1998). *P. atrosepticum* SCRI 1043 has 20 putative pectinase genes, such as cellulases and pectate lyases (Bell *et al.*, 2004). These proteins are secreted by the bacteria using the one-step type I secretion system in *P. carotovorum* (Delepelaire, 2004). Most of the main secreted virulence factors in *P. carotovorum* include multiple Pels, Peh, Cel and Svx and are secreted by a two-step type II secretion system known as Out (He *et al.*, 1991; Reeves *et al.*, 1993; Corbett *et al.*, 2005). Type III secretion systems, known as Hrp systems, are responsible for the defence response known as hypersensitive reaction (HR) in non-host or resistant plants (Barnard *et al.*, 2007). The genome of *P. carotovora* subsp. *atroseptica* contains a gene cluster within HAI7 very similar to both a plasmid conjugation system in *E. coli* and the pathogenicity-related type IV secretion system locus in *Agrobacterium tumefaciens* (Bell *et al.*, 2004).

PCWDE production is regulated by two quorum sensing systems: one comprising ExpI/AHL, modulating *rsmA* expression (Kõiv and Mäe, 2001; Chatterjee *et al.,* 2002) in the other system, Luxs/AI-2 PCWDE secretion

control is unclear. Full production of secreted virulence factors is dependent on functional *luxS* gene in some *Pectobacterium* (Põllumaa *et al.*, 2012), and there is a correlation between AI-2 levels and the production of pectinolytic enzymes (Laasik *et al.*, 2006), although accumulation of AHL signal is enough for PCWDE production, even in the absence of AI-2 signal (Brader *et al.*, 2005).

1.3.1.1.1 AHL-based quorum-sensing in Pectobacterium

AHL-producing bacteria can respond to concentrations of signalling molecules and high cell densities (approximately 10^{10} cell per ml) increasing the levels of AHLs in their environment. The LuxI type proteins are AHL synthases that use S-adenosylmethionine (SAM) to synthesize the homoserine lactone ring, and the acyl chains from lipid metabolism (Moré *et al.*, 1996; Parsek *et al.*, 1999). The LuxR type proteins are transcriptional factors that bind to the signal molecule, AHL, modulating the expression of its target genes (Zhu and Winans, 2001; Zhang *et al.*, 2002). The ExpR protein is a transcriptional regulator from the LuxR family that detects the AHL signal, transforms it into a cellular response and initiates the virulence response that leads to the release of PCWDEs. Despite this, some studies could not establish this role in some *Pectobacterium* strains (Cox *et al.*, 1998).

1.3.1.1.2 LuxS/Autoinducer-2-mediated quorum sensing in *Pectobacterium*

A different quorum-sensing system has also been described in Gram-negative bacteria: the AI-2 signalling system. First identified in the marine bacterium *V. harveyii* (Xavier and Bassler, 2005), where it is one of the three quorum-sensing systems that regulate bioluminescence and other phenotypes such as type III secretion systems (Bassler *et al.*, 1994; Henke and Bassler, 2004a; Henke and Bassler, 2004b). At high cell densities, AI-2 binds the receptor protein LuxP which, in turn, interacts with the hybrid sensor kinase LuxQ. This process initiates a dephosphorylation cascade that results in the dephosphorylation of the phosphotransfer protein, LuxU, and inactivation of the response regulator, LuxO. This allows the expression of Luxvh, which in turn activates the expression of the bioluminescence operon (Schauder *et al.*, 2001; Henke and Bassler, 2004; Miller *et al.*, 2004). Many Gram-negative and Gram-positive bacteria also have a *luxS* homologue and synthesise compounds that can activate the AI-2 sensor (Miller *et al.*, 2004).

The LuxS protein, which is highly conserved throughout bacteria, is responsible for the biosynthesis of AI-2. LuxS synthesizes 4,5-dihydroxy-2,3-pentanedione (DPD), that forms a series of DPD derivatives through

spontaneous rearrangements. In turn, these DPD derivatives interconvert into AI-2 (Miller *et al.*, 2004). Levels of AI-2 in *P. atrosepticum* increase during log phase and decline during stationary phase (Crépin *et al.*, 2012). Despite this, the expression of *luxS* is consistent throughout bacterial growth. A *luxS* mutation can affect bacterial motility, virulence and the initial stages of infection through the modulation of the expression of pectinolytic enzymes.

AI-2 might be a universal and/or interspecies signalling molecule since responses to AI-2 can be triggered by different AI-2 molecule types (Schauder *et al.*, 2001). Although production of AI-2 depends on the *luxS* gene, mutants in this gene have been reported to decrease type III secretion and motility in *E. coli* (Sperandio *et al.*, 1999; Sperandio *et al.*, 2001). As a result, it is still unclear how many of the phenotypes result in a signalling defect due to the absence of AI-2 (McGowan *et al.*, 1996) and how many are just the result of a metabolic defect due to the loss of methionine recycling (Vendeville *et al.*, 2005).

1.3.1.2 Antibiotic production

Parallel to the secretion of PCWDEs, a few strains of *Pectobacterium* produce low levels of the β-lactam antibiotic, carbapenem (1-carbapen-2-em-3-carboxylic acid or Car) (Brader *et al.*, 2005). The genes for biosynthesis and autorresistance functions are clustered in the *car*ABCDEFGH operon (Figure 1-3) (McGowan *et al.*, 1996; McGowan *et al.,* 1997). The proteins encoded by *carA, carB* and *carC* are responsible for carbapenem production (McGowan *et al.*, 1997). CarB produces carboxymethylproline, which is the first molecule in Car biosynthesis (Sleeman *et al.*, 2004). CarD and CarE may be involved in the supply of the precursors for this first step, but they are not essential for carbapenem production (McGowan *et al.*, 1997). CarA is the β-lactam synthetase, closing the β-lactam ring (Miller *et al.*, 2002; Miller *et al.,* 2003; Gerratana *et al.*, 2003). CarC forms the active carbapenem antibiotic by an epimerisation and desaturation reaction (Li *et al.*, 2000). *carF* and *carG* encode for antibiotic resistance (McGowan *et al.*, 1997), and this resistance mechanism occurs before biosynthesis of the antibiotic (Barnard *et al.*, 2007). CarI, a LuxI family member, produces three AHL signals, whereas CarR, a member of the LuxR transcriptional factors, is a DNA-binding transcriptional activator of the *carA-H* operon that functions in the presence of AHL. *CarR* is located 108bp upstream the operon *carA-H* (McGowan *et al.*, 2005), whereas the *carI* gene is located elsewhere in the genome. Some *Pectobacterium* strains that produce carbapenem have a single *CarI* gene to synthesize AHL, and two different LuxR homologues that control the expression of different genes but recognise the same AHL (Welch *et al.*, 2000).

Car production in *Pectobacterium* reaches a peak during the transition from late log to stationary phase of growth, decreasing its production afterwards (Barnard *et al.*, 2007).

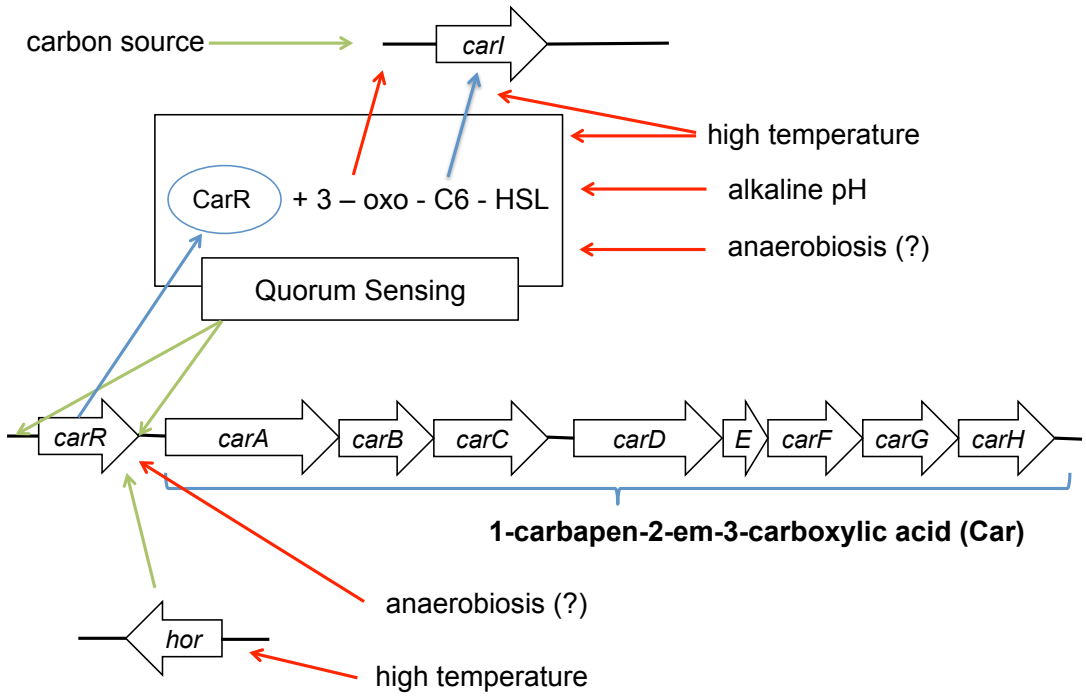

Figure 1-3: The regulation of carbapenem production in *Pectobacterium carotovorum* spp. *carotovorum*, adapted from (Barnard *et al.*, 2007)). Different environmental factors, such as temperature, pH, oxygen availability and carbon source also affect expression: green arrows indicate a positive effect, whereas red arrows indicate a negative effect. The (?) symbols indicate a possible effect.

1.3.1.2.1 Environmental factors influencing Car production

Apart from quorum-sensing regulation, Car production in *P. carotovorum* can be affected by environmental factors including temperature, anaerobiosis, pH and availability of a carbon source (Figure 1-3) (Byers *et al.*, 2002; McGowan *et al.*, 2005). These conditions can also affect the stability of the AHL signalling molecule, which becomes unstable over a narrow pH range (between 7 and 8) (Byers *et al.*, 2002; Yates *et al.*, 2002). When *Pectobacterium* strains are cultured in an unbuffered culture medium, Car production is switched off during stationary phase as the pH becomes alkaline. However, if the culture medium is buffered, Car production remains constant during the stationary phase (Byers *et al.*, 2002). This is an important

factor since one of the first recognisable responses *in planta* to infection is a pH increase of the apoplastic fluid surrounding the infection site (Nachin and Barras, 2000), that is an increase in the intercellular space from 6.2 to 8.3 (Baker *et al.*, 1990).

Another important environmental factor is temperature (McGowan *et al.*, 2005). Optimal temperatures for both *carA* transcription and Car production in *P. carotovorum* is 34°C, whilst higher temperatures are inhibitory, stopping completely at 37°C or over, being the transcription of *hor* also repressed at 37°C (McGowan *et al.*, 2005). The carbon source present in the media also affects Car production (McGowan *et al.*, 2005), using sucrose as the sole carbon source increases transcription of *carA* by 50% when compared to glucose as the only carbon source. This transcription is completely inhibited when using glycerol. Oxygen availability can also affect Car production, although Car production cannot be detected under oxygen-limiting conditions. AHL stability is favoured under anaerobic conditions because anaerobic metabolism produces weak acids; this may explain the persistence of AHL during stationary phase and explain why soft rot is favoured when oxygen is limiting (Pérombelon and Kelman, 1980).

1.3.1.3 Other transcriptional regulators in *Pectobacterium*

1.3.1.3.1 The Hor transcriptional regulator

The *hor* gene belongs to the SlyA family of transcriptional factors present in different bacteria. This family of proteins controls multidrug resistance, toxin production, virulence and secondary metabolite production. In *Pectobacterium* it activates Car and PCWDE production (Thomson *et al.*, 1997). The *hor* gene was identified as one of the two genes required for infection in *Drosophila* by a strain of *Pectobacterium* (Whitehead *et al.*, 2002).

1.3.1.3.2 The VirR regulator

The VirR regulator, from the LuxR family, negatively regulates virulence products in the absence of AHLs (Burr *et al.*, 2006). It binds directly to the promoter regions of the genes to prevent transcription, regulating virulence (Bell *et al.*, 2004). This protein has been described in *P. atrosepticum* but not in other *Pectobacterium*.

1.3.1.3.3 The Rsm regulatory network

RsmA is a homologue of CsrA in *E. coli*, which negatively regulates other metabolic pathways, such as glycogen formation and gluconeogenesis in post-exponential phases of growth. CsrA binds to selected mRNA transcripts,

blocking ribosome binding and promoting transcript degradation (Cui *et al.*, 1995). This protein also activates flagellum biosynthesis and motility in *E. coli* (Wei *et al.*, 2001). RsmB blocks the action of RsmA by binding on its mRNA targets (Liu *et al.*, 1998), promoting PCWDEs encoding genes. RsmC negatively controls the expression of *rsmB* and, indirectly, enhancing the expression of *rsmA* (Cui *et al.*, 1999).

1.3.1.3.4 KdgR

KdgR acts as a global repressor of genes involved in pectin degradation. It is a DNA-binding transcriptional repressor (Barras *et al.*, 1994; Liu *et al.*, 1999), targeting pectinases (Liu *et al.*, 1999), but also binds the promoter region of *rsmB* (Liu *et al.*, 1999).

Other regulators include: rexZ, a *kdgR* homologue that activates production of PCWDEs (Thomson *et al.*, 1999) and AepA, acts as a transcriptional activator, promoting the production of protease and cellulase (Liu *et al.*, 1993).

1.4 Biological control of plant pathogens

Plant pathogens cause great losses in the agricultural industry. In addition, the global antibiotic crisis has raised the issue of finding reliable alternatives (Debarbieux *et al.*, 2016) to current methods such as antibiotics and copper treatments that contaminate the soil (Balogh *et al.*, 2008). The pesticide market is worth 50 thousand million euros with the biopesticides being only between 1500 and 2500 million euros, however growth of the biopesticide sector is expected to outgrow other treatments in the future (Marrone, 2014). In 2016 98% of Scottish seed potato crops were treated, being 65% of these fungicides (other treatments included herbicides, insecticides and molluscicides), on stored potatoes the percentage of pesticide treatments lowered to 47% for seed potatoes and 11% on ware potatoes (Monie *et al.*, 2017). These were the main reasons that led to the re-evaluation of alternative biocontrol methods (Elphinstone *et al.*, 2018).

Soil microbiomes are extremely complex and diverse and display spatial geographic patterns (Green *et al.*, 2008; Andam *et al.*, 2016; Zhao *et al.*, 2016). The abundance of viruses in soils ranges between 10^7 and 10^9 virus-like particles per gram of soil (Williamson *et al.*, 2003; Williamson *et al.*, 2005; Swanson *et al.*, 2009; Srinivasiah *et al.*, 2015). Environmental factors, such as pH, temperature, rainfall and total nitrogen content play an essential role in shaping the bacterial and viral communities in soil (Narr *et al.*, 2017), application of fertilisers increase viral concentrations in soils (Chen *et al.*,

2014; Doan *et al.*, 2014) and virus included in agricultural soils are less diverse than those from forest soils (Williamson *et al.*, 2005).

In plants the root microbiota has diverse functions including plant growth promotion by providing nutrients, carbon sequestration and phytoremediation by destroying phytopathogens (Weyens *et al.*, 2009; Mendes *et al.*, 2011) or improving the plant resilience to heat, drought or salt (Firakova *et al.*, 2007; De Deyn *et al.*, 2008; Rodriguez *et al.*, 2008; van der Lelie *et al.*, 2009), thus enhancing crop productivity (Mei and Flinn, 2010). Moreover, roots influence soil pH, structure, oxygen availability, antimicrobial concentrations and quorum-sensing mimicry in their rhizosphere, as well as providing an energy source of dead root material and carbon-rich nutrients (Marschner *et al.*, 1986; Dennis *et al.*, 2010; Bulgarelli *et al.*, 2012). Some research suggests that microbial communities differ between plants (Hardoim *et al.*, 2008; Redford *et al.*, 2010).

Current seed prevention measures include physical treatments, such as hot water treatment (Mackay and Shipton, 1983; Afek and Orenstein, 2002), UV or fluorescent light (Rocha *et al.*, 2015) that proved to eliminate *Pectobacterium* from the tuber surfaces. These methods are expensive and can seriously damage the potato tubers (Robinson and Foster, 1987; Perombelon *et al.*, 1989). Chemical seed treatments included antibiotics such as streptomycin and oxytetracycline or streptomycin and mercury (Bonde and de Souza, 1954), kasugamycin or virginiamycin (Wyatt and Lund, 1981; J. Bartz, 1999) or other organic compounds like hydroxyquinoline (Harris, 1979), 5-nitro-8-hydroxyquinoline bromopol (2-bromo-2-nitropropane-1,3-diol) and 7-chloro-1-methyl-6-fluoro-1,4-dihydro-4-oxo-3-quinolinic carboxylic acid (Bartz and Kelman, 1986), organic and inorganic salts such as aluminium acetate, sodium metabisulphite, potassium sorbate, calcium propionate, sodium hypochloride or sodium bicarbonate to name a few (Mills *et al.*, 2006). All these treatments carry high phytotoxicity risks and they do not target specific bacteria. Biological control treatments include the use of *Pseudomonas* spp. (Cronin *et al.*, 1997; Kastelein *et al.*, 1999), lactic acid bacteria (Trias *et al.*, 2008), antibiotic-producing *Streptomyces* spp. (Baz *et al.*, 2012; J. W. Park *et al.*, 2012; Balaraju *et al.*, 2016) or bacteria that quench quorum sensing signal molecules, including *Agrobacterium, Bacillus, Mesorhizobium, Pseudomonas, Rhodococcus* or *Streptomyces* (Uroz *et al.*, 2003; Jafra *et al.*, 2006; Jafra *et al.*, 2006; Mahmoudi *et al.*, 2011; Crepin *et al.*, 2012; Crepin *et al.*, 2012; Chankhamhaengdecha *et al.*, 2013; Garge and Nerurkar, 2016). Recent focus has been the development of lytic bacteriophages for *Pectobacterium* and *Dickeya* spp. (Czajkowski, 2016a; des Essarts *et al.*, 2016).

Effective treatments have little or no effect on the surrounding environment and the host plant (and/or neighbouring organisms), and they also keep their stability at changing conditions: pH, temperature, UV radiation and moisture levels that are found in the environment.

One approach when using phage therapy is the application of mixed phages or “cocktails”, which would minimise the appearance of resistance in the host. Ideally, the coevolution between bacteria and phage should be fully understood to predict and limit resistance development (Samson *et al.*, 2013). Unlike chemicals, phage treatments can be adapted to overcome bacterial resistance that had developed over time (Buttimer *et al.*, 2017). However, EU regulations (1107/2009 EC) require that any changes in a phage formulation should be reregistered (Doffkay *et al.*, 2015). There are also different strategies when using phage treatment: phages are UV sensitive, thus phyllosphere application should be done either in the evening or at dawn (Balogh, 2002; Balogh *et al.*, 2003; Iriarte *et al.*, 2007). The use of protective formulations (Wang and Sabour, 2010), that is suspensions containing mainly milk, sugar and flour, have significantly increased the longevity of phages on tomato leaves under field and greenhouse conditions (Balogh, 2002). Instead of treating the phyllosphere, there are many studies supporting rhizosphere treatment, moreover translocation of phages from the root to the plant leaves through the plant vascular system has been tested (Iriarte *et al.*, 2012; Jones *et al.*, 2012). The soil provides a more stable environment, protected from UV radiation, where movement can happen through mechanical action or fluid flow (S.T. Abedon, 2011), in fact there is evidence that proved the persistence of phages in soil (Fujiwara *et al.*, 2011). Phages can play an important role modifying the soil environment, such as the mineralisation process and the release of secondary metabolites from bacteria (Karlovsky, 2008). In contrast, phages can be inactivated by electrostatic interaction to clay particles (Ye *et al.*, 2009), biolfilms that may trap the phage (Storey and Ashbolt, 2001) and low pH levels (Sykes *et al.*, 1981). The phage must encounter directly its host to be infective and its survival could be enhanced if they are inoculated together with a viable host (Buttimer *et al.*, 2017).

1.4.1 Bacteriophages

For decades, bacteriophages have been models for viral replication research and the model bacteriophages (lambda, T-even bacteriophages) have contributed to the early development of molecular biology such as identifying the basis of the genetic material, the code of nucleotide triplets to amino acids (Crick *et al.*, 1961), the restriction enzymes (Dussoix and Arber, 1962) and the first sequenced genome, of phage ϕX174 of *E. coli* (Sanger *et al.*, 1977).

There are 10^{31} viral particles in the biosphere, most of them are bacteriophages, or commonly known as phages. They need to infect bacteria to survive and they coexist with a ratio of 1:10 (Wommack and Colwell, 2000; Parikka *et al.*, 2017), killing between 4 and 50% of bacteria produced daily. Bacteria are constantly subjected to viral infection, with a rate of approximately 10^{24} viral infections per second. The entire population turns over every two days, and they provide the largest unexplored reservoir of new genetic diversity on Earth (Suttle, 2005). Their densities have been estimated to be up to 2.5×10^{8} particles per ml and 1.5×10^{7} particles per gram in aquatic and soil environments, respectively (Ashelford *et al.*, 2003).

1.4.2 Phage classification

A bacteriophage particle or virion consists of a single or double stranded DNA or RNA, encapsulated in a protein or lipoprotein coat. The International Committee on the Taxonomy of Viruses (ICTV) uses virion morphology and the nucleic acid composition to classify bacteriophages at the family and species levels (Simmonds and Aiewsakun, 2018). Over 95% of known phages belong to the order *Caudovirales* (tailed dsDNA phages with icosahedral heads) (Ackermann and Kropinski, 2007). Within this order, approximately 60% of the characterised phages are *Siphoviridae*, with long flexible tails, 25% belong to *Myoviridae*, with double-layered and rigid contractile tails, and 15% are *Podoviridae*, with short noncontractile tails (Figure 1-4).

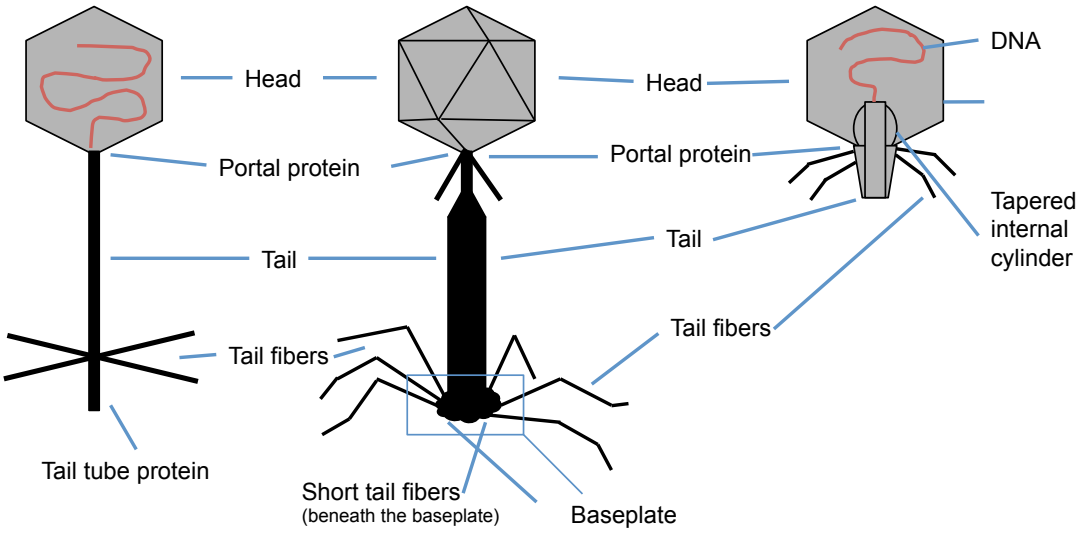

Figure 1-4: Basic morphology of the three families of the *Caudovirales*. From left to right, schematic drawings of a *Siphovirus* (with a long, non-contractile tail), *Myovirus* (with a long, contractile tail) and *Podovirus* (with a short tail) are shown. Adapted from (Leiman *et al.*, 2004) and (Serwer *et al.*, 2008).

The infectious cycle of virus replication comprises the moment when the virus contacts the cell until they divide and the progeny viruses are released. It is a complex process of adsorption (Chatterjee and Rothenberg, 2012), structural modification of both host and bacteriophage (Mahony and van Sinderen, 2012), transport of nucleic acid into the bacterial cell, and avoidance of degradation once inside the host (Richter *et al.*, 2012). Productive infections or lytic cycle, occur when the viral DNA is a separate molecule that replicates separately from the host, the release of the virions happens from the destruction of the infected cell and its membrane. By contrast, reductive infections or lysogenic cycle, are the ones that the phage survives but the infection does not produce viral particles immediately, in fact the phage nucleic acid is integrated into the host genome, which is then called “prophage”, its replication occurs during reproduction of the host and the viral particles are transmitted to daughter cells, these are called temperate phages. The outcome of a lytic or lysogenic cycle on λ phage depends on the interactions of five regulatory proteins called CI, CII, Cro, N and Q with a number of promoters in a regulatory region of the phage DNA. Destructive infections occur when phages do not survive (Abedon, 2011). The term “pseudolysogeny” is used when a lytic phage remains inside the bacterial host, without integrating with the host genome, until better conditions arise to complete the lytic cycle (Abedon, 2009). Transduction is a

process mediated by phages (depending on the type of terminases they carry) and it can be divided into generalised, when a fragment of DNA from the bacterial host is transferred to the phage but does not integrate in the bacterial chromosome, and specialised when specific set of genes from the host DNA are packaged inside the viral head, transferred and integrated into another bacterial genome, a different type of specialised transduction is the lateral transduction where several hundred kilobases of host genome can be packaged into the phage capsid (Chen *et al.*, 2018).

Temporal and spatial studies have demonstrated an inverse correlation between lytic and lysogenic cycles (Weinbauer *et al.*, 2003; Colombet *et al.*, 2006; Pradeep Ram and Sime-Ngando, 2010). The lytic cycle is dependant on environmental conditions and host physiology, and is commonly found in nutrient-rich environments with high host abundance and activity (Maurice *et al.*, 2013). On the other hand, the lysogenic cycle depends on the variability of prokaryote physiology, it improves the survival of both host and prophage under unfavourable conditions (Wommack and Colwell, 2000; Chibani-Chennoufi *et al.*, 2004), the host gets immunity against superinfection by closely-related bacteriophages but there would be a metabolic cost related to replication of the viral genome (Paul, 2008). Some bacteriophages can switch from lytic to lysogenic cycles depending on the abundance of a six-amino acid peptide called arbitrium released in the media (Erez *et al.*, 2017), its concentration allows the viral progeny to estimate the amount of phages that successfully completed a infectious cycle as the demand for viable hosts increases after every phage release (Ofir and Sorek, 2018), this could explain why at higher multiplicities of infection lysogenic cycles are more likely to happen (Weitz *et al.*, 2008). Nevertheless, some phages can also kill their bacterial hosts without carrying out a lytic cycle in a process known as ‘lysis from without’, that could reduce bacterial numbers when the lytic cycle is unlikely to happen (Ferguson *et al.*, 2013).

Generally, the molecules involved as phage receptors have essential roles in bacterial metabolism (Bertozzi Silva *et al.*, 2016). The few bacteriophages with receptor-binding to bacterial exopolysaccharides belong mostly to the *Podoviridae* order (Bertozzi Silva *et al.*, 2016). Upon receptor-binding, the phage tail triggers a series of conformational changes that will effectively inject the phage DNA and the core proteins inside the bacterial cytoplasm (Casjens and Molineux, 2012). After ejection, the phage tail and capsid collapse or disassemble, this step helps the resealing of the infected cell membrane (Hu *et al.*, 2013). Many phages need close interactions with other bacterial components such as chaperones and transcription factors to complete heir life cycles (Young and Gill, 2015). The host killing occurs prior to the lysis step when the phage converts its host into a factory for making

new phages (Kutter et al. 1994), they even increase the expression of host-encoded genes during infection in *Prochlorococcus* (Clokie *et al.*, 2011). In Gram-negative hosts, bacterial cell lysis is a coordinated process mediated by phage endolysins, that fusion the inner membrane with the outer membrane, spanins that disrupt the peptidoglycan layer in the periplasmic space (Rajaure *et al.*, 2015) and holins, that produce holes in the host membrane. It is worth mentioning that bacteriophages have broader host ranges immediately after release than a few hours afterwards (Whitehead *et al.*, 1953).

1.4.3 Bacteria-Phage coevolution

There is increased evidence that shows the role phages play regulating microbial populations (Fuhrman, 1999); the continuous interaction between phages and their hosts shapes and determines the evolution of both organisms, as they are subjected to related ecological selection pressures (Salathé and Soyer, 2008). Even some phages have been responsible for the development of bacterial virulence, as prophages or as vectors in horizontal gene transfer through transduction (Verheust *et al.*, 2010; Penadés *et al.*, 2015). Coevolution is ubiquitous and is thought to be primarily responsible for the world's biodiversity (Thompson, 2005), and it reflects an arms race dynamic where phages retain the ability to infect previously encountered bacteria and bacteria retain resistance to previously encountered phages (Buckling and Brockhurst, 2012) following the Red Queen hypothesis that describes predator/prey dynamics (Rodriguez-Brito *et al.*, 2010; Jover *et al.*, 2013; Lim *et al.*, 2015). This sort of coevolution between a parasite and a host, is called antagonistic coevolution, and its fate depends on different factors, such as the efficiency of attachment of phages to host cell surface receptors, lysis time or burst size, but also depends on the source of their diversity (either mutation, horizontal gene transfer or recombination), the environmental conditions and the effects associated with resistance and infectivity. Many lytic phage genomes are clearly shaped by vertical evolution (Ceyssens *et al.*, 2011). Bacterial species that are not infected by phages within the same environment will proliferate until nutrient availability becomes scarce or an infective phage is introduced (Koskella and Meaden, 2013).

Phage adsorption is essential for phage replication as phages must bind to a specific cell-surface receptor. From the perspective of the bacteria, survival relies upon the selection of cells that are resistant to infection, thus preventing viral proliferation and continuing the cell lineage (Avrani and Lindell, 2015). Any modification in the bacterial cell receptor could result in a

loss of this specificity (Rodriguez-Valera *et al.*, 2009) (Figure 1-5), thus avoiding infection, and it is usually associated to a fitness cost like reduction in growth rate (Chao *et al.*, 1977; Bohannan and Lenski, 2000; Middelboe, 2000; Lennon *et al.*, 2007) or increased susceptibility to other phages (Avrani *et al.*, 2011; Marston *et al.*, 2012; Castillo *et al.*, 2014). The effect and extent of cross resistance given by a resistance mutations depends mainly on genetic correlations between bacterial resistance traits and the different phage species (Wright *et al.*, 2018).

Some phages develop diversity-generating retroelements (DGRs) that contain two repeats (variable repeat and template repeat) and a reverse transcription gene, this system generates high diversity of potential tail fibres via reverse transcription of the template repeat in an error prone manner, with up to 10^{14} variants to overcome bacterial receptor mutations (Doulatov *et al.*, 2004). To prevent this, phages must target receptors that have an important function in the bacteria (Icho and Iino, 1978), then loss of phage receptors can be too costly for the bacteria. A strategy that some bacteria have developed to impede phage attachment is the production of an extracellular matrix (Labrie *et al.*, 2010), although there are phages that produce enzymes that break down alginate (Glonti *et al.*, 2010) and LPS-dependent phages have the broadest spectrum of activity (Evans *et al.*, 2010). Post-entry resistance mechanisms have also evolved in bacteria through different resistance mechanisms such as CRISPR, Restriction-Modification and Abortive Infection (Abi) Systems (Figure 1-5), but there is also strong evidence of phages overcoming these mechanisms (Chopin *et al.*, 2005; van der Oost *et al.*, 2009; Stern and Sorek, 2012). In addition, there are other defence mechanisms that have been discovered recently like bacterial Argonautes (Swarts *et al.*, 2014), the bacteriophage exclusion system (BREX) (Goldfarb *et al.*, 2015), the defence island system associated with restriction-modification (DISARM) (Ofir *et al.*, 2018) and others with yet unknown mechanisms of action (Doron *et al.*, 2018).

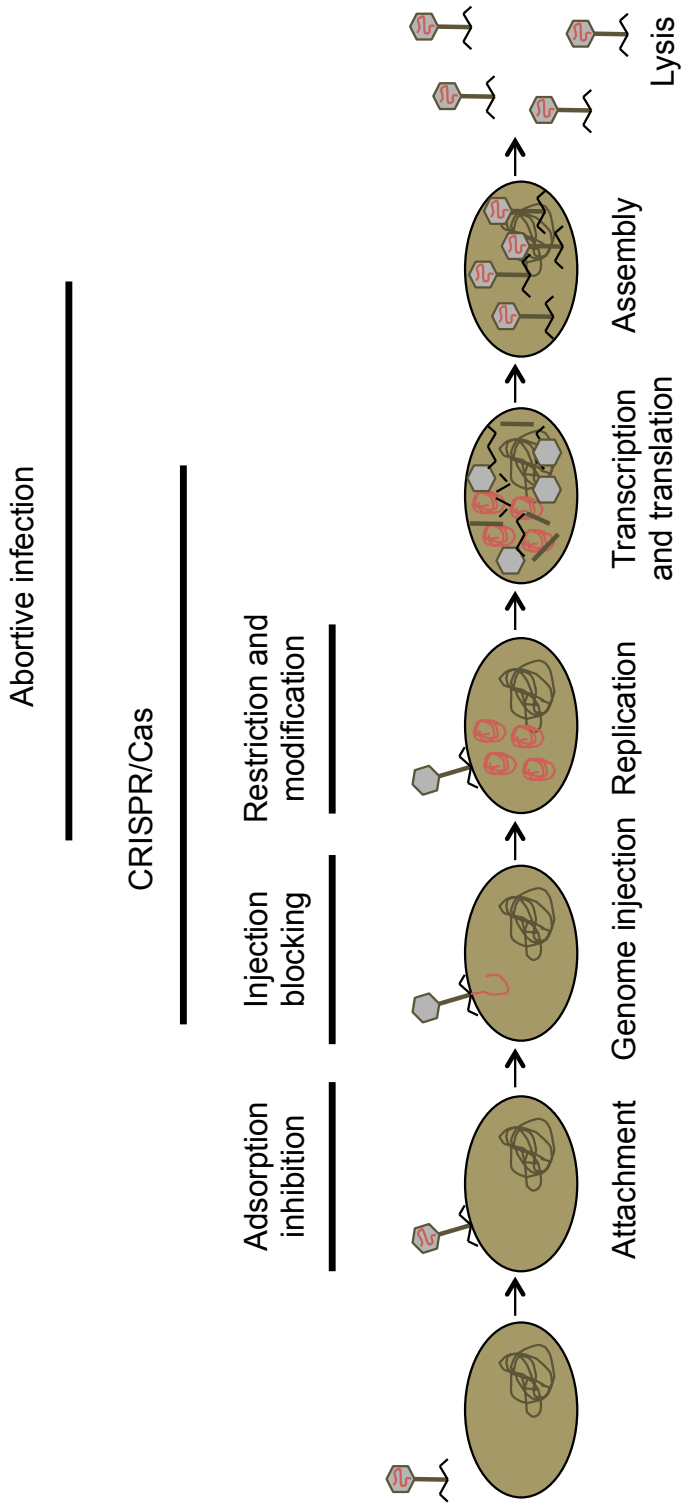

Figure 1-5: Different stages of bacteriophage infection and resistance mechanisms (adapted from (Frampton *et al.*, 2012)).

1.4.3.1 CRISPR

Clustered Interspaced Short Palindromic Repeats (CRISPR) confer host cell immunity to phages by targeting and degrading foreign nucleic acids (Barrangou *et al.*, 2007; Sorek *et al.*, 2013; Amitai and Sorek, 2016), it is equivalent to Lamarckian evolution where the phage infection causes heritable genetic mutations that confer an advantage against phage infection (Ofir and Sorek, 2018). Present in about 40% of sequenced bacteria (Al-Attar *et al.*, 2011), they are acquired by horizontal gene transfer (Haft *et al.*, 2005; Godde and Bickerton, 2006).

Despite their wide distribution, the mechanism of this bacterial immune system follows three basic steps: adaptation, expression and interference (García-Martínez *et al.*, 2018). Adaptation, or spacer acquisition, implies the integration of nucleic acids from foreign DNA (Amitai and Sorek, 2016), fragments of this foreign DNA (called protospacers) (Deveau *et al.*, 2008) are next to short conserved sequences or the photo-spacer adjacent motif (PAM) and they correspond to the specific nucleic sequences they target (Labrie *et al.*, 2010). The transcription of a CRISPR array generates a multispacer RNA (pre-crRNA) that requires the participation of Cas proteins (Brouns *et al.*, 2008), every resulting mature crRNA remains assembled to the Cas protein in a CRISPR ribonucleoprotein (crRNP) complex. During CRISPR interference, the crRNP complex recognises and cleaves the spacer-complementary sequences and results in the elimination of these molecules (Garneau *et al.*, 2010). Based on the composition of the interference complexes, the CRISPR-Cas systems can be divided into two classes: Class I systems are multi-subunit whereas Class II contain only one protein (Savitskaya *et al.*, 2016). Class I is subdivided into Types I, III and IV and Class II is subdivided into Types II, V and VI depending on the associated Cas protein.

CRISPR-Cas provides a heritable memory of past infections that is sequence-specific, but the bacterium must survive the viral infection (Abedon, 2012). Phages can overcome this resistance mechanism with a point mutation in the appropriate region of its own genome (Barrangou *et al.*, 2007) or with the presence of anti-CRISPRs that inhibit the activity of CRISPR-Cas systems that are very specific (Borges *et al.*, 2017). Bacteria can develop resistance to multiple phages as a result of coevolution. This system in phytopathogens is limited to *P. atrosepticum* (Przybilski *et al.*, 2011), *Erwinia amylovora* (Rezzonico *et al.*, 2011) and *Xanthomonas oryzae* (Semenova *et al.*, 2009). *P. atrosepticum* carries Type I-F CRISPR-Cas that recruits the *trans*-acting nuclease-helicase Cas2-Cas3 protein (Makarova *et al.*, 2015) that forms a complex with the protein Cas1 to acquire new spacers (Fagerlund *et al.*, 2017) and degrade the target molecule. Currently, the CRISPR-Cas system has many utilities in molecular biology, including

transcription repression (Luo *et al.*, 2015; Rath *et al.*, 2015), manipulation of bacterial communities (Bikard *et al.*, 2014) and loss of cell resistance to antibiotics (Bikard *et al.*, 2014).

1.4.3.2 Restriction-Modification

Restriction-modification systems are one of the most prevalent bacteriophage resistance mechanisms, present in approximately 90% of available bacterial sequences (Mohapatra *et al.*, 2014). Bacteria produce restriction endonucleases (REN) that cut unmethylated DNA at specific sites, thus protecting their own DNA by methylation (Tock and Dryden, 2005), like the toxin-antitoxin system restriction-modification systems mediate plasmid maintenance (Kulakauskas *et al.*, 1995). Simultaneously, phages have evolve diverse mechanisms to protect themselves, these include the loss of restriction enzymes, evolve their own methylase genes and the use of unusual bases (i. e. hydroxymethyl cytosine instead of cytosine in bacteriophage T4) (Labrie *et al.*, 2010). This mechanism is not essential for short-term coevolution but it serves as a metabolically inexpensive killing mechanism for targeting foreign DNA (Abedon, 2012).

1.4.3.3 Abortive Infection Systems (Abi)

This is an extreme response to phage infection that results in bacterial cell death, providing protection to the bacterial population but also has other important roles in bacterial physiology such as stress response (Wang and Wood, 2011), developmental processes (Kim *et al.*, 2009) and persister cell development (Gerdes and Maisonneuve, 2012). In the vast majority of cases they are encoded by chromosomal DNA (Sberro *et al.*, 2013). Abortive infection needs a toxic or bacteriostatic molecule along with another molecule that protects the host cell. Thus, there is a strong connection between Abi and toxin-antitoxin systems (Short *et al.*, 2018).

1.4.3.3.1 Toxin-Antitoxin (TA) Systems

This Abi system is homologous to the multiple “toxin-antitoxin” (TA) loci on the chromosomes of bacteria and archaea (Buts *et al.*, 2005). And they rely on the dual activity of a toxin and its antagonistic antitoxin (Gerdes *et al.*, 2005), which are unstable molecules that require to be constantly synthetised in order to inactivate the toxin (Gerdes *et al.*, 2005; Short *et al.*, 2018). TA loci fall into six categories depending on the nature and mode of action of the antitoxin: type I and III antitoxins are RNAs and type II, IV, V and VI are proteins (Goeders and Melderen, 2014). Acting as a protein-RNA TA pair, specifically it is a type III TA system where the RNA antitoxin interacts directly with the toxin protein (Dy *et al.*, 2014), these type III systems are

acquired by horizontal gene transfer (Blower et al. 2012) and result in slower phage maturation and reduced burst size (Fineran *et al.,* 2009).

In *P. atrosepticum*, ToxIN protects against phage infection using abortive infection. ToxN is a sequence-specific endoribonuclease that is needed for cell toxicity and phage defence (Blower *et al.*, 2011; Short *et al.*, 2013) and ToxI is both a substrate and inhibitor of ToxN. The *toxIN* locus is present in the pECA1039 plasmid (Fineran *et al.*, 2009; Samson *et al.*, 2013; Dy *et al.*, 2014), like most of these systems, its phylogenetic distribution is a result from horizontal gene transfer (Blower et al. 2012). ϕA2 and ϕM1 are clear examples of phages that are involved in this toxin system: single-base mutations in a single open reading frame evade the Abi system in ϕM1 (Blower *et al.*, 2017). ϕTE contains a locus that is similar to the sequence of ToxI (which gets amplified), this phage escapes the abortive system by mimicking the shape of ToxI antitoxin, ensuring viral replication within the host (Blower et al. 2012).

1.4.3.4 Phage genomics

There is clear evidence that phage diversity is very high even between phages that infect the same host (Kwan *et al.*, 2006). Phages that are almost identical at the nucleotide level can show variability in their phenotypic characteristics (Ceyssens *et al.*, 2011): for example small point mutations help the avoidance of restriction-modification systems (Labrie *et al.*, 2010), as well as mutations responsible for host-range interactions that accumulate in noncore genes in genomic islands (Avrani and Lindell, 2015). The infection process could potentially generate new genomic arrangements through recombination in the host cell (Pedulla *et al.*, 2003), a process likely to have occurred throughout bacterial evolution (Hendrix, 1999).

Caudovirales genomes are linear dsDNA, containing between 27 to over 600 genes tightly packed, highly clustered and normally arranged in large operons. Their genomes normally contains all the information encoding for DNA packaging, head, tail, DNA replication, transcription regulation, lysis genes and even homologous genes to their hosts (Clokie *et al.*, 2011).

The gene expression of phages is a highly coordinated process where groups of genes are sequentially expressed: the host RNA polymerase will recognise strong promoters in the phage genome leading to transcription of “early genes”. Phage infection triggers host stress response signals, if the virus has evolved to use these gene products it gains a fitness advantage (Lindell *et al.*, 2007). Along with this, when the phage genome is injected in the host cell some virion proteins are also be introduced (Guttman *et al.*,

2005), and these proteins hijack the host cell metabolism.

In some lytic cycles, the phage genomes are circularised (Figure 1-6) through complementary overhangs in the termini and the standard bacterial "theta" mode is used for circular-DNA replication (Kutter and Sulakvelidze, 2004), some circular DNA adopt the rolling-circle replication mechanism to generate several head-to-tail concatemers that will serve as substrates for the DNA packaging (Rao and Feiss, 2008). There are reported at least eight types of genomic termini in dsDNA phages (Table 1-2): lambdoid phages with 5' overhang cohesive ends, phages with 3' overhang cohesive ends, phages with direct terminal repeats and no circular permutation (these include T7 and T3 phages), phages with both terminal redundancy and circular permutation, phages with terminal redundancy and circular permutation but no obvious *pac* site (this incudes phage T4), phages with direct terminal repeats and protein adhering to each end of the genomic DNA, phages with host DNA fragments at each end of their genome and phages with short and variable length direct terminal repeats with a unique sequence at the left genome termini and differing sequences at the right genome termini, present in N4-like phages (Ohmori *et al.*, 1988; Catalano *et al.*, 1995; Casjens, 2005; Born *et al.*, 2011).

Assembly of the phage capsid occurs as a highly regulated process and is encoded by late genes (Casjens, 2008). They share a common mechanism for DNA packaging where the protein procapsid gets assembled first and the DNA molecule is then pumped into the procapsid by an ATP cleavage-powered DNA translocase (Catalano, 2005), a terminase is responsible for cutting the DNA both at the start and at the end of the genome packaging process (Casjens and Gilcrease, 2009).

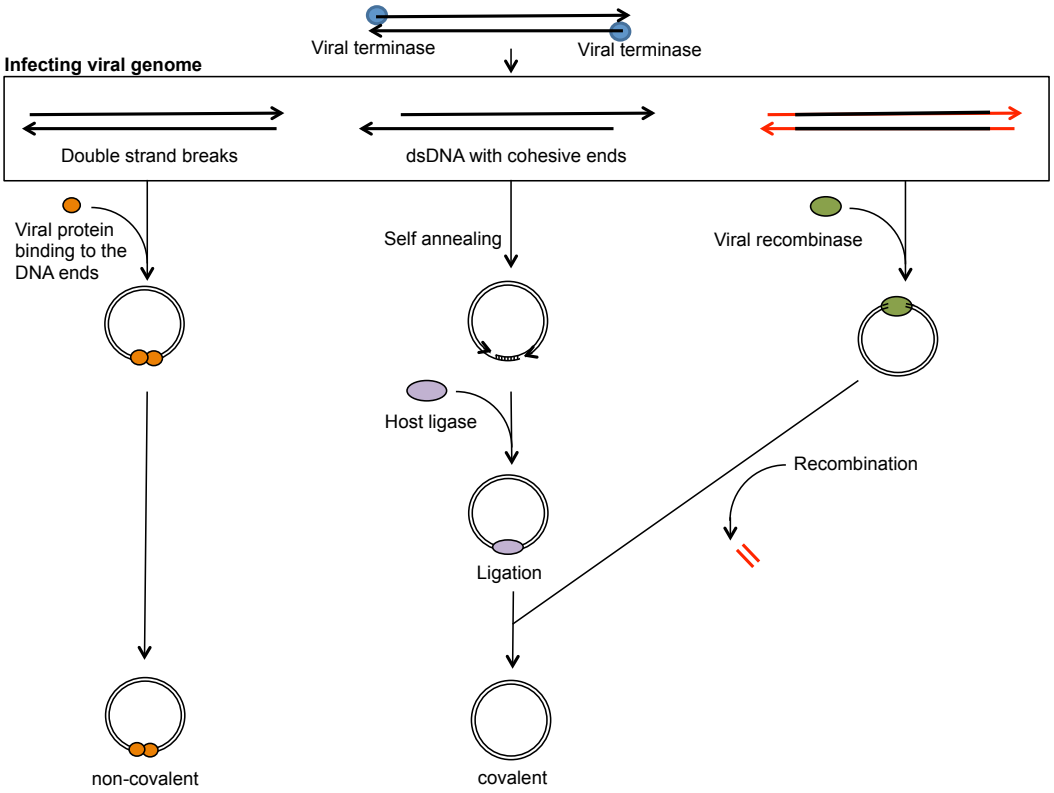

Figure 1-6: Viral genome circularisation in the host cytoplasm. Phage genomes circularise to avoid the host endonucleases, the different mechanisms depend on the nature of the genome terminal ends (adapted from (Swiss Institute of Bioinformatics, 2013)).

Phage	Incoming virion DNA	Replication strategy	End state replicated DNA
λ	Linear with 5' 12-base complementary ends (cohesive ends)	Closed circle switching to rolling circle	Linear concatemer
P22	Linear with 104% terminal redundancy	Recombination with extension via direct repeats	Linear concatemer
ϕ29	Linear with covalently attached gp3 at 5' ends	Gp3-primed extension, strand displacement	Unit length with gp3 covalently attached at 5' ends
T3 (T7)	Linear with 230 (160) base pairs direct repeats	Recombination with extension via direct repeats	Linear concatemer
T4	Linear with 102% terminal redundancy	Invasive strand initiated via terminal redundancy	Branched concatemer

Table 1-2: Viral DNA replication of different dsDNA bacteriophages. Phage DNA has different replication strategies based on the genomic termini (adapted from (Calendar and Abedon, 2005)).

1.4.3.4.1 Vertical evolution of T4-like genomes

T4-like phages are a clear example of vertical evolution in bacteriophages. About 90% of the known T4-like phages grow on *E. coli* or other enterobacteria. Their genomes consist of a conserved core that contains the essential genes for viral multiplication (Filée *et al.*, 2006). This genomic design provides a very successful multiplication strategy, but also the flexibility for adaptation to the environment. The most conserved genes encode for the structural components of the virion ("late genes") and genes encoding for replication (Comeau and Krisch, 2008). T4 recombines most efficiently early in infection (Krisch *et al.*, 1972) and it only requires 50bp of homology to recombine at a good frequency (Singer *et al.*, 1982). This process could replace one adhesion-recognising domain by another one, potentially changing the host range of the phage (Tétart *et al.*, 1998). This can be advantageous for the phage as it might give access to a new ecological niche.

1.4.3.4.2 Genetic mosaicism in temperate phages

Mosaicism is a common feature for some temperate phages, this characteristic arises from an exchange of gene modules between the host and the phage. This is a clear example of horizontal gene transfer (HGT), which is a major factor in phage evolution (Hendrix *et al.*, 2000; Hatfull, 2008), is a viral-mediated process called transduction. The recipient bacterium both survives and integrates the DNA into its genome through random nonhomologous recombination (Paolozzi and Ghelardini, 2006). Moreover, temperate phages also contain genes responsible for integration into the host genome, the integrases.

1.4.3.5 Endolysins

After the events of virion assembly and phage DNA packaging, all dsDNA phages degrade their host peptidoglycan layer using an essential genome-coding enzyme: the endolysins (Young *et al.*, 2000; Wang, 2006). There are at least six classes of endolysins described: N-acetyl-β-D-glucosaminidase, N-acetyl-β-D-muramidase, lytic transglycosilase, N-acetylmuramoyl-L-alanine amidase, L-alanoyl-D-glutamate endopeptidase and D-alanyl-glycyl endopeptidase (Young, 1992; Loessner, 2005; Fischetti, 2010; Schmelcher *et al.*, 2012; Schmelcher *et al.*, 2014), and they are composed of an active binding domain (CBD) and a cell wall-degrading domain that direct the enzyme to its target structure (Loessner, 2005). Each endolysin plays a different role within the lysing process that occurs within seconds of first contact with the bacterial cell wall, a tail-located lysin mediates the localised cell wall hydrolysis that allows the DNA translocation after host recognition (Letellier *et al.*, 2004; Sciara *et al.*, 2008). During infection, they accumulate

in the intracellular space until a small hydrophobic membrane spanning protein, a holin, produces pores in the inner membrane, revealing the peptidoglycan layer for the endolysin (Wang *et al.*, 2000; Young *et al.*, 2000; Young, 2002). The *N*-acetylmuramoyl-*L*-alanine amidases cleave the peptidoglycan bond between the *N*-acetylmuramic acid residues and L-alanine residues, the phage glycosidases belong to the lysozyme-like superfamily and they catalyse the glycolytic cleavage of the O-glucosidic bond of the bacterial peptidoglycan, and the endopeptidases cleave short peptides that link the sugar polymers of the peptidoglycan (Oliveira *et al.*, 2013), at some point the cell wall is no longer able to withstand the osmotic pressure within the cell and the virion particles are released with the consequent lysis. There is extensive research that uses these endolysins as biocontrol agents as they work in a species-specific manner (Loessner, 2005).

1.4.4 Use of bacteriophages as biocontrol agents (BCAs)

There are different steps required for using bacteriophages as BCAs, phage host-range, stability and the ability to lysogenise and transduce must be determined to ensure safety (Verheust *et al.*, 2010; Frampton *et al.*, 2012), as these could alter the pathogenic potential of their hosts (Young and Gill, 2015):

1.4.4.1 Collection of bacterial strains

It is essential to obtain a representative collection of the bacterial strains associated with the infection in the geographic location where the disease develops (Balogh *et al.*, 2010), preferably from reference collections (Casey *et al.*, 2018).

1.4.4.2 Isolation of phages

Phages can be obtained directly from infected plants, water or from the soil where they grow using the soft agar overlay technique and with a range of the host pathogens. Using the plaque assay, the phages that infect specific bacterial strains can be recovered and purified with three successive single-plaque isolations (Gill and Hyman, 2010).

It is essential to determine the host range of each phage to design an effective cocktail which will infect all known pathogenic strains, for example, by using polyvalent phage preparations, composed of phages that recognise different bacterial receptors (Blower *et al.*, 2010), as these bacteriophages do not compete with one another the host will not likely develop resistance

against the phages. Alternatively, the step-by-step (SBS) method of isolation that consists of the successive infection of phages with the strain of interest and a bacteriophage-insensitive mutant until a phage that is active against this strain is isolated, this process continues until the latest phage-resistant host is sensitive to the original phage (Casey *et al.*, 2018). Another option is using combination therapy: by using bacteriophage and antibiotic therapy combined to minimise resistance mechanisms (Casey *et al.*, 2018).

1.4.4.3 Phage characterisation

Phages need to be fully characterised to ensure that they are appropriate BCAs. Methods such as genome sequencing are used to detect any virulence factors, toxin-encoding genes (Koskella and Meaden, 2013), presence of integrases, site-specific recombinases and repressors of the lytic cycle (Weber-Dabrowska *et al.*, 2016), and it would allow the design of quantitative PCR strategies to track phages in future field trials (Lehman, 2007). Nevertheless, tailed phage families cannot be easily diagnosed using genomics alone and electron microscopy is also necessary (Ackermann and Kropinski, 2007). To determine the one-step growth curve at conditions likely to be found in the field such as temperature or pH, as well as host factors such as bacterial concentrations, metabolic state and/or presence of phage defence mechanisms (Barrangou, 2015; Barrangou and Van Der Oost, 2015; Bryan *et al.*, 2016). Optimal storage conditions for the phages is also an important factor to be considered (Balogh *et al.,* 2010).

1.4.4.4 Trials of phage as a BCA

Once phages have been characterised, it is necessary to scale-up phage preparations for the field trials, this requires knowledge about the characteristics of the phage (Ackermann *et al.*, 2004), and also determine possible interactions with their environment as some experiments suggested that some bacteriophages decreased plant growth or did not show any improvements when compared to common treatments (Gill and Abedon, 2003; Kocharunchitt *et al.*, 2009; Ye *et al.*, 2009). To measure the success or failure of phage treatment, traditional enumeration assays or qPCR can be used (Lehman, 2007). There are diverse factors that could determine the effectiveness of the treatment, that include the complexity of the natural environment, with complex interactions of the microbiome surrounding the infection site (Adriaenssens *et al.*, 2012), the presence of fertilisers or the type of water (Ravensdale *et al.*, 2007) and the stability of the phages under environmental conditions, including pH, temperature, UV and moisture levels (Iriarte *et al.*, 2007). Other factors like phage concentration, method of treatment (irrigation, use of solvents, etc.), application frequency and

application methodology, such as using a living bacterial cell delivery that ensures phage survival (Lehman, 2007; Svircev *et al.*, 2010), should also be taken into account.

Bacteriophages are ideal candidates as BCAs because they are often found within the infected plant, they are naturally-occurring, self-replicating, non-toxic to other eukaryotes, very specific, environmentally friendly and cheaper than antibiotics (Miedzybrodzki *et al.*, 2007).

The efficacy of several phage preparations to control bacterial pathogens has been successfully tested against fruit (Leverentz *et al.,* 2001), sausages (Whichard *et al.*, 2003; Guenther *et al.*, 2012), cheese (Modi *et al.*, 2001), seafood (Guenther *et al.*, 2012), eggs and milk (Guenther *et al.*, 2012; Marti *et al.*, 2013) and dried pet food (Heyse et al. 2015). Proof-of-concept experiments were used against *Pectobacterium carotovorum* subsp *carotovorum* (Eayre *et al.*, 1995), for prevention of potato tuber decay caused by *Pectobacterium atrosepticum* (Balogh *et al.*, 2010) and for control of *Pectobacterium carotovorum* subsp *carotovorum* infections in calla lily (Ravensdale *et al.*, 2007). Other experiments proved the efficiency of LIMEstone phage incubated with potato seed tubers in a field trial, and how these prevented maceration of tuber tissue (Adriaenssens *et al.*, 2012). The Scottish company APS Biocontrol has developed a bacteriophage-based wash solution that prevents soft rot development on potato tubers (Branston, 2012).

1.5 Nanoparticles

A new approach aimed at exploiting bacteriophages for use as vectors or as matrices for use in nanomedicine (Hemminga *et al.*, 2010; Rakonjac *et al.*, 2011; Fan *et al.*, 2012; Hyman, 2012), these are called bionanoparticles or bioorganic particles. Richard Feynman was the first to highlight the potential of nanomaterials for our society during his famous lecture “There is plenty of room at the bottom” at Caltech University (Feynman, 2012). By definition, nanoparticles would include all particles with a diameter size between 100 and 2500 nanometers. They are of great interest in science, because at nanoscale dimension, the properties of the material may change dramatically compared to their bulk counterparts. As the size of the material decreases, the proportion of surface atoms increases, augmenting their reactivity (Hanemann and Szabó, 2010). As a result, nanotechnology is envisaged to become the cornerstone for a diverse number of industrial sectors, including textile, micro-informatics, energy, paper, agronomy and many more (Linkov

et al., 2009), with an estimated annual turnover of 75.8 billion US dollars by 2020 (Research and markets, 2015).

1.5.1 Synthesis

Nanoparticles can be obtained from various materials using physical, chemical or biological methods. Evaporation-condensation and laser reduction ablation are among the physical methods (Iravani *et al.*, 2014). The synthesis of nanoparticles using chemical methods has been proved to be more effective, but they have been associated with environmental toxicity (Kango *et al.*, 2013), these include chemical reduction using sodium citrate, ascorbate, Tollens reagent and polymeric compounds as an example. The biological methods for nanoparticle synthesis has proven to be a good alternative, these include the use of microorganisms (Konishi *et al.*, 2007; Shivaji *et al.*, 2011), enzymes (Willner *et al.*, 2006), fungi (Vigneshwaran *et al.*, 2007; San Chan and Mat Don, 2013) and plants or plant extracts (Ahmad *et al.*, 2011; Akhtar *et al.*, 2013).

1.5.2 Attachment of organic molecules onto nanoparticles

The covalent conjugation to polymers and polymeric surfaces is a particularly important modification for the preparation of proteins and protein complexes (Jutz and Böker, 2011), and is linked to the progress in the elaboration of well-defined functional polymers via controlled polymerisation techniques. Techniques for immobilising enzymes can be generally divided into two categories: chemical and physical methods. Chemical methods are irreversible and they rely on the formation of a least one covalent bond between one or more of the molecules to be attached to the polymer matrix. Physical methods form reversible bonds and they include adsorption by electrostatic interaction and entrapment within microcompartments. This latter process involves entrapment of the molecules of interest within gel matrices or semi-permeable microcapsules for example. A corona discharge method or the modification of macromolecular biological drugs and drug-delivery complexes with polyethylene glycol (PEG), which is an established method to enhance blood circulation time and stability, avoiding non-specific binding and immunogenicity (Jain and Jain, 2008). More recent research applied to bacteriophages used a combination of both methods: the electrostatic interactions between the viruses and a surface were used for the correct orientation of the bacteriophages, followed by plasma polymerisation to bond covalently to the polymer used (Wang *et al.*, 2016; Zhou *et al.*, 2017).

1.5.3 Immobilisation technique: corona discharge

Different techniques have been developed to bind phages to different surfaces, including gold (Singh *et al.*, 2009; Arya *et al.*, 2011) or silica (Cademartiri *et al.*, 2010). A corona discharge is, by definition, a gas discharge where electrode geometries control and confine ionisation processes of gases in a high-field ionisation treatment (Goldman *et al.*, 1985). The corona geometry is called positive, negative, bipolar, alternating current (AC), direct current (DC) or high frequency (HF), depending on the polarity of the active electrode. All corona discharges present a large low field drift region located between the ionisation zone and the passive electrode (Denes and Manolache, 2004). Ion and electrons entering the drift space undergo neutralisation, excitation and recombination reactions (Figure 1-7).

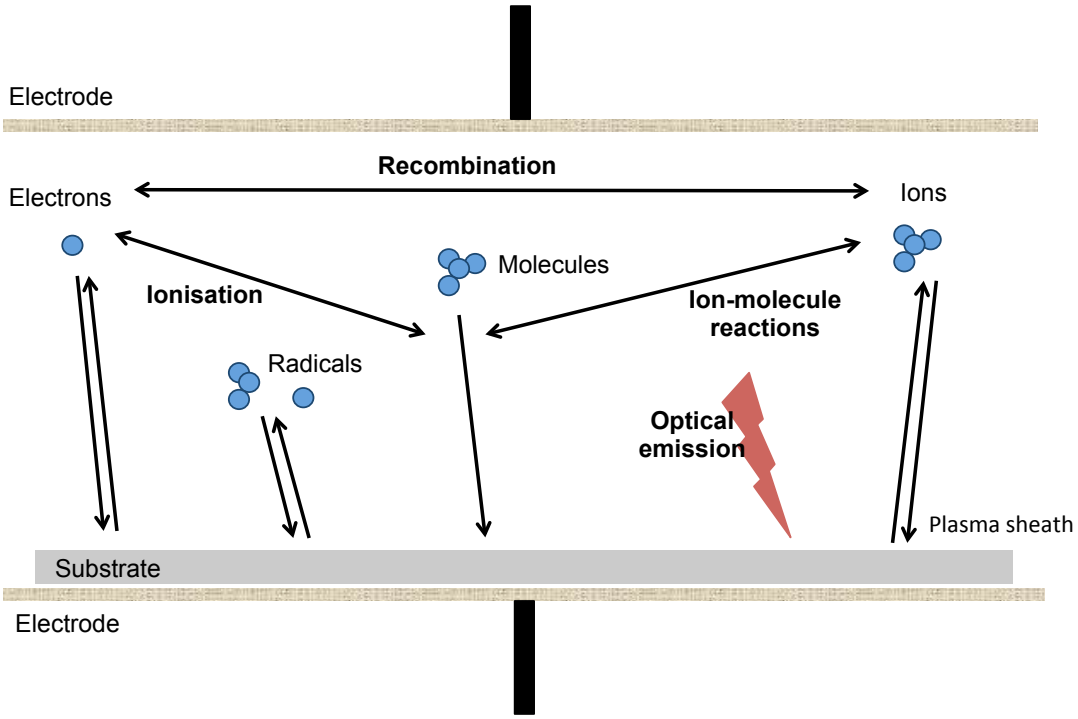

Figure 1-7: Interactions of plasma-generated species with the substrate. These include electrons, ions, molecules and free radicals formed in the drift region of the corona discharge (adapted from (Denes and Manolache, 2004)).

The drift region is characterised by its neutral chemistry formed by the ionisation energies and the species escaping the ionisation zone (with lower energy) (Figure 1-8). There are two very different types of DC and low frequency AC coronas:

Unipolar conduction coronas (positive-, negative-, glow coronas, negative Trichel pulsed coronas, and positive-glow coronas), the ionisation regions are located very closed to the stressed electrode, the drift region currents depend on the voltage and the nature of the "dielectric gap".

Bipolar conduction coronas (Streamers), with a point-to-plane electrode configuration and with higher current values at the positive point polarity, as a consequence, an ionising positive plasma channel (or streamer) originates from the point electrode towards the plane electrode. This plane cathode is subjected to a pulse glow discharge with ion energies as high as 100eV.

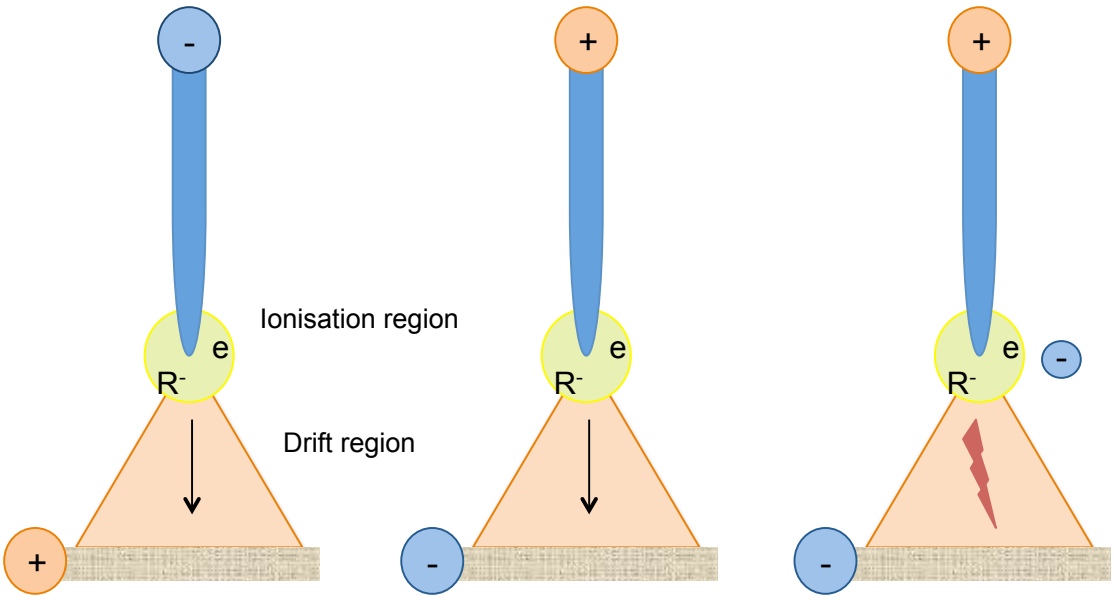

Figure 1-8: Drift region in different corona discharges. The ionisation regions from the corona discharge are immediate to the stressed electrode, the drift regions, between the ionisation region and the passive electrode, are characterised by its neutral chemistry (adapted from (Denes and Manolache, 2004)).

An “electric wind”, which is a charged particle flux, is formed from the transfer of energy from the charged particles to neutral gas molecules due to inelastic collisions. During this cold-plasma-mediated process, gas phase and surface reaction mechanisms occur, creating charged species, including atoms, molecules, free radicals, ions (+ or -), excited species, electrons and photons (Denes and Manolache, 2004). Ozone is one of the compounds created by this process, and it rapidly dissociates to molecular oxygen and oxygen radicals, that could result in crosslinking any polymers used. This covalent-bonding method has been used successfully with bacteriophages on polyhydroxyalkanoate surfaces (Wang *et al.*, 2016), retaining both good phage activity and high surface density. The hydroxyl groups, carboxyl groups and peroxide groups formed during the plasma treatment improved bacteriophage attachment (Wang *et al.*, 2016).

Over time, treated surfaces returned to their initial unattached state, due to the rearrangement of polar chemical groups from the surface of the material to the bulk (Schamberger *et al.*, 1994) and the diffusion of functional groups into the polymer matrix (Paynter, 2000).

1.6 Project aims

The main hypothesis for this project is to test the ability of phage-coated nanoparticles to control bacterial disease in plants.

The control of bacterial diseases of crops using bacteriophages that selectively kill the causative pathogen. Bacterial diseases of plants affect their growth and spoil their products post harvest. Disease control relies on preventing the spread of bacteria rather than plant treatment as, at present, no economical treatment exists. As an alternative to chemical control, it may be possible to use phages for the prevention of plant diseases. It is the aim of this project to address the use of phage-coated nanoparticles (PCNs) for the control of plant bacterial diseases and increase the efficiency and sustainability of crop production in the food chain. The targeted use of phages to control plant disease removes the negative environmental impacts of broad-spectrum antibacterial agents.

Fixed-Phage (FP) specialises in the immobilisation of phages onto surfaces and nanoparticles, which dramatically increase phage persistence. The evaluation of PCNs for the control of bacterial plant disease and to test the hypothesis that PCNs protect plants against bacterial pathogens.

The project involves the application of microbiology, molecular biology, microscopy and plant pathology techniques and it has the following objectives:

Isolation of a set of bacteriophages against different species of *P. carotovorum* and *P. atrosepticum.*
Characterisation of these phages using general microbiology, sequencing and microscopy, as well as evaluating the kinetic properties of the infective process.
Immobilisation onto nanoparticles by corona discharge and test their stability as compared to free phages.
Treatment of tomato plant seedlings and potato slices with the PCNs and test phage uptake and survival *in planta* using microscopy.

This multidisciplinary project develops a partnership between the academic and industrial partner increasing the understanding of phage-host relationships in the environment as well as to generate a novel system for the control of plant bacterial disease, respectively.

2.0 Materials and methods

2.1 Bacterial strains, culture and storage

Bacteria	Reference	DSMZ/ATCC number	Isolation sample	Growth conditions
Pectobacterium carotovorum subsp. *carotovorum*	(Jones, 1901)	DSM 30168	*Solanum tuberosum*	Nutrient agar at 26°C
Pectobacterium atrosepticum	(Van Hall, 1902)	DSM 18077	*Solanum tuberosum*	Nutrient agar at 30°C
Pectobacterium wasabiae	(Goto and Matsumoto, 1987)	DSM 18074	*Eutrema wasabi*	Nutrient agar at 28°C
Pectobacterium atrosepticum SCRI 1043	(Van Hall, 1902)	ATCC BAA-672	*Solanum tuberosum*	Nutrient agar at 26°C

Table 2-1: Bacterial strains used for this project. All bacterial strains used for this project were acquired from Deutsche Sammlung von Mikkroorganismen und Zellkulturen (DSMZ) and the American Type Culture Collection (ATCC), all belonged to the same risk group 1.

All bacteria were revived upon arrival and stored at -80°C (Table 2-1). Glycerol stocks were prepared by mixing 670µl of overnight grown liquid culture and 330µl of sterile 80% (w/v) glycerol, and stored at -80°C. Stock cultures were prepared on solid media monthly from these glycerol stocks and incubated at 30°C for 48 hours, the plates were then stored at 4°C for up to a month. Liquid culture was inoculated from an individual colony and incubated overnight at 30°C with shaking at 180rpm.

2.2 Media

Plant and bacterial media were made following the recipes displayed in Table 2-2.

Media	Composition (per litre)
Nutrient broth (Oxoid)	1g "Lab-Lemco" powder 2g yeast extract 5g peptone 5g NaCl
Nutient agar (Oxoid)	13g nutrient broth 20g agar
Soft nutrient agar (Oxoid)	13g nutrient broth 7g agar
Plant media	4.3g Murashige and Skoog basal salt mixture (Sigma-Aldrich)* 15g sucrose 7g agar 1ml vitamin mix**

Table 2-2. Composition of different bacterial and plant growth media. All media were sterilised by autoclaving at 121°C for 20 minutes (15 psi).
* Commercial media used for plant tissue culture, composition (per litre): 1650mg $(NH_4)NO_3$, 6.2mg H_3BO_3, 332.2mg $CaCl_2$, 0.025mg $CoCl_2 \bullet 6H_2O$, 0.025mg $CuSO_4 \bullet 5H_2O$, 37.26mg Na_2-EDTA, 27.8mg $FeSO_4 \bullet 7H_2O$, 180.7mg $MgSO_4$, 16.9mg $MnSO_4 \bullet H_2O$, 0.25mg $Na_2MoO_4 \bullet 2H_2O$, 0.83mg KI, 1900mg KNO_3, 170mg KH_2PO_4,, 8.6mg $ZnSO_4$.
** Vitamin mix solution (per litre): 0.5mg thiamine HCl (vitamin B1), 2mg glycine, 5mg nicotinic acid, 0.5mg pyridoxine HCl (vitamin B6), 0.05mg folic acid***, 0.1mg biotin (vitamin B7) and 10mg myo-inositol. This solution was added to cooled-down media after sterilisation using 0.22µm filter.
*** Dissolved 50mg folic acid in 0.5ml 1N NaOH and diluted down to 10ml of ddH_2O.

2.3 Bacterial growth

Nutrient broth (100ml) in a 250ml conical flask was inoculated with bacterial strains and grown overnight to give a final OD of 0.001. This culture was incubated at different temperatures (10, 20 and 30°C) under shaking conditions (200rpm). Growth was measured using OD at 600nm, every 30 minutes approximately, until no further growth was detected (up to 10 hours). The natural logarithm of the OD values were then plotted against time and the growth rate "µ" was calculated (Hall *et al.*, 2014), for each type strain and temperature, as the slope formed during the exponential phase of growth

(straight line formed when using the logarithm to the base of 10 of the data) plot against time (Madigan *et al.*, 2014).

2.4 Bacteriophage isolation, titration and storage

2.4.1 Double-agar overlay technique

Double-gar overlay technique was performed as described by Cormier (Cormier and Janes, 2014). The bottom layer of 2% nutrient agar was first poured into Petri dishes. Subsequently, a top layer of 0.7% soft nutrient agar and 100µl of overnight-grown bacteria were added and allowed to solidify at room temperature under sterile conditions. A 100µl solution of the bacteriophage tested was either mixed with the top layer before it was poured or spot-inoculated onto this top layer. These plates were left at room temperature overnight and checked for plaque formation the following morning.

2.4.2 Bacteriophage isolation: enrichment method

Environmental samples (soil, potato peelings or infected potatoes) were mixed with nutrient broth and 100µl of an overnight grown bacterial culture in a test tube, and incubated overnight at room temperature. This solution was filter-sterilised (using a 0.22µm membrane filter) and tested for plaque formation.

In the case plaques were formed, a single plaque was removed from the top agar layer, submerged in PBS (Table 2-3) and incubated for at least 2 hours at room temperature. The lysate was then filtered through a 0.22µm membrane filter. This procedure was repeated 3 times for newly isolated bacteriophages.

2.4.3 Bacteriophage stock production

Stocks were recovered from 20 round (9cm diameter) or 6 square Petri dishes (120 x 120cm). Buffer (PBS or SM) was poured onto the plates to cover the agar and let to incubate at room temperature for a minimum of 2 hours, this buffer was then filter-sterilised and centrifuged at 35000 x g at 4°C for 20 hours using the high speed centrifuge Avanti J-301 and rotor JA30-10. The supernatant was discarded and the pellet was resuspended in 1-2ml of buffer. The stock was kept in the fridge for up to one year and its titre was determined.

2.4.4 Bacteriophage titration and storage

Stock solutions of bacteriophages were serial-diluted using either PBS or SM buffer, 10µl of each solution was spot-inoculated onto the top agar layer containing the bacteria of interest (in triplicate). Plates were let to dry and incubated at room temperature overnight. The number of plaques was counted and the concentration of the original viral stock was calculated by multiplying the dilution factor and the volume used, as per plaque-forming units per ml.

Phage stocks were kept in PBS or SM buffer (Table 2-3) at 4°C for medium to short-term storage, these stocks were renewed annually to keep a high titre. Long-term storage was used for initial stocks, in PBS or SM buffer, at -80°C.

Buffer	Composition (per litre)
PBS (Phosphate-buffer saline) (Oxoid)	8g NaCl 0.2g KCl 1.15g Na_2HPO_4 0.2g KH_2PO_4
SM buffer	5.8g NaCl 2g $MgSO_4 \bullet 7H_2O$ 50ml 1M Tris HCl (pH 7.4)
TE buffer	10ml 1M Tris-HCl (pH 7.5-8) 2ml 0.5M EDTA (pH 8.0)
50X TAE buffer (Tris Acetate-EDTA)*	242g Tris base 57.1ml Glacial acetic acid 100ml 0.5M EDTA (pH 8.0)**
10X DNA loading dye	3.9ml glycerol 500µl 10% (w/v) SDS 200µl 0.5M EDTA 0.025g bromophenol blue up to 10ml with distilled sterile water

Table 2-3. Different buffers used for storage and serial dilution of the bacteriophages as well as for DNA storage and manipulation.
* 50X TAE buffer should be diluted down to 1X before use.
** pH was adjusted to 7.2 and distilled sterile water was added to a final volume of 1000ml.

2.5 Plaque morphology

The properties of the plaques formed upon infection were part of the characterisation of each bacteriophage, these included not just the morphology but also the transparency, presence of a halo, homogeneity of the plaques formed and the size when comparing plaques formed using the same media and incubation conditions.

A minimum of 20 plaque images were taken and their contrasts were enhanced using Adobe® Photoshop® software. The images pixels were transformed into millimeters and the plaque areas were selected by hand using ImageJ 1.50i software, the plaques areas were exported to Microsoft® Excel® for Mac 2011 (version 14.7.2) and their median, Q1, Q3, minimum and maximum values calculated and plotted. Values had a normal distribution, and an ANOVA two-tailed t-test with $p \leq 0.001$ was performed using StatPlus for Mac LE (version 6.2.21).

2.6 Host range and efficiency of plating

The phage stocks with concentrations of approximately 10^8pfu/ml were spot-inoculated onto a lawn culture of each of the *Pectobacterium* strains (Table 2-1) using the double agar overlay technique (section 2.4.1). The presence of plaques on the lawn indicated that the phage was infective against that strain.

Once the host range was determined, the bacteriophage stock was serially diluted 10-fold and a 10µl aliquot of each dilution was spot-inoculated onto a bacterial lawn for each susceptible strain as mentioned above. The relative efficiency of plating (EOP), that is the titer of the phage on a given bacterial cell line compared to the maximum titer observed (Kutter, 2009), was calculated for each phage-host system as follows:

$$\text{Efficiency of plating} = \frac{\text{number of plaques formed (per ml)}}{\text{number of plaques formed in host lawn (per ml)}}$$

The ratios obtained were divided into 4 categories (Viazis *et al.*, 2011): high production for ratios equal or above 0.5, medium production for ratios between 0.1 and 0.5, low production for ratios between 0.1 and 0.001 and inefficient production with ratios below or equal to 0.001 (less than 0.1% than the original strain).

2.7 Transmission electron microscopy (TEM)

Stocks containing 10^{10}pfu/ml were used for electron microscopy. Formvar carbon-coated on 200 mesh thick copper grids were placed in a pump vacuum to induce hydrophilicity, 50µl of the high titre lysate was loaded onto the grid and left for 2 minutes, the excess sample was blotted using filter paper and the grid was placed on a drop of water (this wash step was repeated three times), the grid was placed on a drop of 2% (w/v) uranyl acetate (this step was repeated twice) and the uranyl acetate drop was left on the grid for about 5 minutes before blotting using filter paper. The grids were examined at 200kV with 20K and 40K magnification in a JEOL 2200 FS microscope and images were recorded on a TVIPS 4kX4k CCD camera. The images pixels were transformed into millimeters and the diameters of at least 10 bacteriophages within each stock (with and without tail) were selected by hand using ImageJ 1.50i software, the diameters were exported to Microsoft® Excel® for Mac 2011 (version 14.7.2) and their median, Q1, Q3, minimum and maximum values calculated and plotted. Values had a normal distribution, and an ANOVA two-tailed t-test with $p \leq 0.001$ was performed using StatPlus for Mac LE (version 6.2.21).

2.8 Kinetics of infection

2.8.1 One-step growth curve and phage adsorption

The protocol used was adapted from Clokie and Kropinski (2009). Bacteria were grown until 0.1 OD or 10^8 cfu/ml (exponential phase of growth) and 10ml were pipetted into two flasks containing 100ml of nutrient broth at room temperature (labelled G, for growth and C, for control), as seen in Figure 2-1. After 5 minutes the first 1ml uninfected sample was taken and transferred into an Eppendorf tube (labeled S0) and placed on ice. At the same time as the timer was started, a 0.1ml phage stock solution containing 10^7 pfu/ml (MOI=0.001) was added to flask "G". After mixing well flask "G", a 1ml aliquot was transferred to flask "G2" and after mixing well, another 1ml aliquot was transferred to flask "G3" (yielding a 10^{-4}-fold dilution, both flasks contained 100ml of nutrient broth). One minute after the initial infection, 1ml samples were taken into S1 and L1 Eppendorf tubes and placed on ice (S, for sample and L, for lysis). Every 20 minutes additional 1ml "S" and "L" samples were taken. This continued up to 240 minutes at 180 rpm at room temperature. All the "S" samples were immediately filtered through a 0.22µm filter membrane in order to recover all unattached phages, all the "L" samples contained 50µl of chloroform to lyse the bacterial cell membrane and allowed the recovery of the total amount of phages (both attached and unattached). OD measurements were taken in triplicate for both "G" and "S" samples during the experiment.

The initial sample "G0" was serially diluted in PBS and 10µl were spot-inoculated onto nutrient agar plates and incubated at 30°C for 48 hours. All the other samples (both "S" and "L") were serial-diluted and spot-inoculated onto a bacterial lawn (in triplicate). All the results obtained were transformed into pfu/ml and plotted against time.

The phage adsorption constant was determined during the one-step growth curve experiment: 1ml samples were taken every minute for the first 15 minutes from the "G" flask after the phage was added. Each sample was filter-sterilised, serial-diluted and spot-inoculated onto a bacterial lawn (in triplicate). The adsorption rates were estimated by using the following equation (Krueger, 1931):

$$k = \frac{2.3}{Bt} \log \frac{Po}{P}$$

where k is the adsorption rate constant in ml/min, B is the concentration of bacteria in cfu/ml, t is the time in minutes, P_o and P are the original the final phage titres in pfu/ml (Barry and Goebel, 1951).

All the data obtained was calculated using Microsoft® Excel® for Mac 2011 (version 14.7.2), average readings were plot as percentage of free phage

against time for the phage adsorption constant. On the other hand, average readings were plot as log base 10 plaque-forming units against time in minutes for the one-step growth curve. The relative error was calculated for each time point, as the results were obtained from the same experiment.

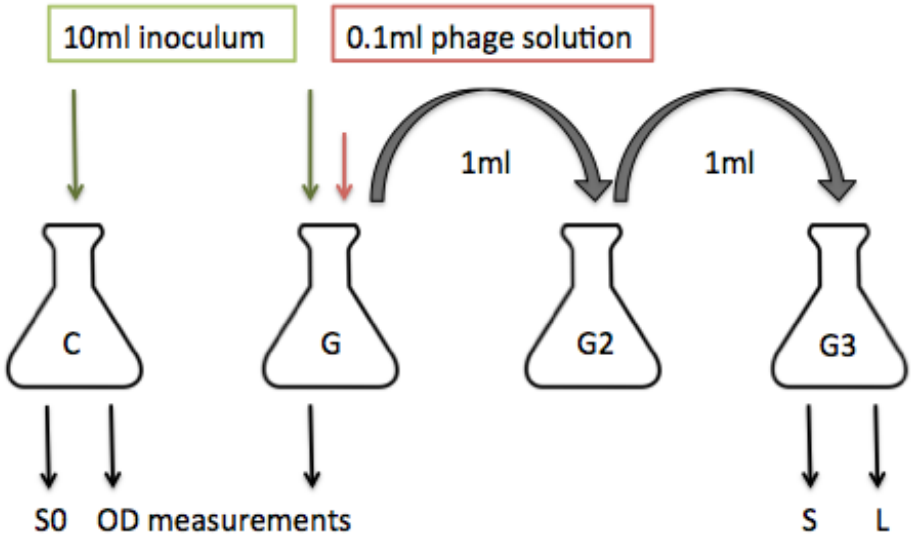

Figure 2-1: One-step growth curve experiment diagram. 10ml inoculum was added to flasks "C" and "G" but only flask "G" was infected with 0.1ml of phage stock. After mixing well, 1ml from flask "G" was added to flask "G2" and 1ml from flask "G2" was added to "G3". Only sample "S0" was taken from flask "C" to check the inoculum, OD measurements were taken from flasks "C" and "G", lysis samples ("L") and "S" samples (for unattached phages) were taken from flask "G3".

2.8.2 Bacterial cell growth during infection experiments

2.8.2.1 OxoPlate®

A 96-well OxoPlate® OP96U was set up to obtain real-time data of bacterial cell viability (measuring oxygen availability) during viral infection. These plates contain sulforhodamin covalently attached to polystyrene particles as the reference dye, and a platinum porphin as the indicator dye. The sensor has a thickness of 10µm and its fixed at the bottom of each of the 96 round-bottom wells in the plate (Greiner, Monroe, NC, USA).

An overnight culture of the test bacteria was inoculated in fresh media and grown until exponential phase, this bacterial suspension was diluted using nutrient broth to approximately 10^8 cfu/ml, 10µl were then used to inoculate each well for this experiment. The bacteriophage stocks were diluted down to

the appropriate pfu/ml (between 10^8 and 10^4 pfu/ml), 10µl of lysate was used to infect the bacteria at different MOIs (between 1 and 0.000001) and each well was filled up to 200µl using nutrient broth (the positive control only contained bacteria in nutrient broth and the negative control only contained nutrient broth), an example of the layout used is shown in Figure 2-2.

The OxoPlate® experiment was set up to test the infectivity of ϕSFM002 immobilised to cellulose nanoparticles: free bacteriophages were tested at different MOIs (between 1 and 0.000001), the bacteriophage-coated nanoparticles included two different 1:10 dilutions (of unknown MOI), the positive and negative controls were the same, as above and an additional negative control that included sterile nanoparticles was added.

The experiment measured time-resolved fluorescence as a function of oxygen concentration every 2 minutes for up to almost 9 hours at room temperature. Two sets of raw data were recovered from the run (both used the same excitation wavelength at 540nm, but the emission wavelength was 650nm for the indicator and 590nm for the reference filter pairs), and all data was normalised for each time point:

$$I_R = \frac{I_{indicator}}{I_{reference}}$$

The calibration constants (k_0 and k_{100}) were calculated by taking the average values for each normalised well containing the calibration solutions. Finally, the results were calculated as the oxygen partial pressure in percentage air saturation per well per time point:

$$pO_2 = 100 \times \frac{\left(\frac{k_0}{I_R} - 1\right)}{\frac{k_0}{k_{100}} - 1}$$

The results were plotted as pO_2 (in percentage) per time point, being each value the result from six different readings using Microsoft® Excel® for Mac 2011 (version 14.7.2). A decrease in pO_2 during the experiment during the experiment was used to determine the viral latent period.

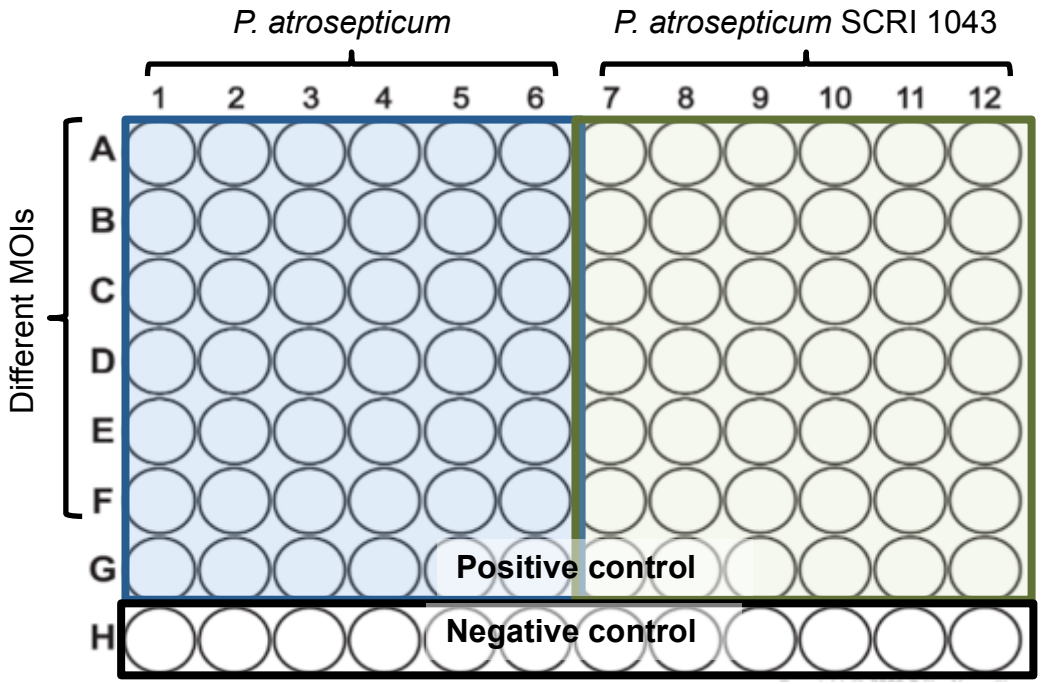

Figure 2-2: Layout used for the OxoPlate® experiment. The plate was divided into two halves (one per bacteria tested), 10µl of bacterial suspension were loaded into all wells (from row A to row G) and a 10µl of varying bacteriophage dilutions were loaded onto a different row (each phage was tested in 6 wells, a total of 6 different dilutions from row A to row F), all the wells were filled up to 200µl with nutrient broth. Row G contained bacteria and nutrient broth (positive control) and row H contained nutrient broth only (negative control).

2.8.2.2 Time-lapse microscopy

Bacterial infection was followed under the microscope for up to 30 hours, by taking an image every 5 minutes under 1000X magnification. An overnight grown bacterial solution was diluted down to 10^8 cfu/ml, 10µl were mixed with 10µl of 10^8 pfu/ml (MOI = 1), spot-inoculated onto 2% nutrient agar and left to dry under sterile conditions. A plug containing the dried solution was transferred to imaging chambers (IBIDI GmbH) and then placed onto the microscope.

Samples were monitored using a Nikon TE2000S inverted microscope and observed under the 100X objective using immersion oil and the 1.3 objective lens and captured using a Hamamatsu Orca - 285 Firewire Digital CCD Camera. The captured images were processed using ImageJ 1.50i software (http://rsb.info.nih.gov/ij/), by tracking bacteria in sequential frames and measuring their mean size and bacterial numbers. The results obtained were exported and plotted using Microsoft® Excel® for Mac 2011 (Version 14.7.2). The bacterial doubling time was measured from at least 10 different readings

in each experiment as the time between one bacterial division to the following. The latent period was estimated from at least 6 different measurements (apart from ϕSFM003, ϕSFM005, ϕSFM006 and ϕSFM007 where it was not possible), from the time a bacteria occupied a previously burst cell until it burst.

2.9 Viral DNA isolation

Two different methods were used for isolation of DNA.

2.9.1 Phenol-chloroform method (Clokie and Kropinski, 2009)

High density phage stocks (between 10^8 and 10^{10}pfu/ml) were mixed with 18µl of 1mg/ml DNase I (Sigma-Aldrich) and 8µl of 12.5mg/ml RNase A (Roche), and incubated for 30 minutes at 37°C. 46µl of 20% (w/v) SDS and 18µl of 10mg/ml of proteinase K (Sigma-Aldrich) were then added and incubated for another 30 minutes at 37°C. A 0.5ml aliquot was placed on a Phase-lock gel Eppendorf tube (VWR International), mixed with 0.5ml phenol:chloroform:isoamyl alcohol (25:24:1, Sigma-Fluka) and centrifuged at 1500 x g for 5 minutes. The supernatant was put into another Phase-lock gel tube and mixed with 0.5ml phenol:chloroform:isoamyl alcohol (25:24:1) and centrifuged at 1500 x g for 5 minutes. The supernatant was then placed on another Phase-lock gel tube and mixed with 0.5ml chloroform:isoamyl alcohol (24:1, Sigma-Fluka) and centrifuged at 6000 x g for 5 minutes. The supernatant was put into a 1.5ml Eppendorf tube with 45µl of 3M sodium acetate (pH 5.2) and 0.5ml of 100% isopropanol (or two volumes of ethanol) were added and incubated at room temperature for 20 minutes. The samples were centrifuged at 20000 x g for 20 minutes, the supernatant was discarded and the DNA pellet was washed twice with 70% ethanol (v/v) and let to dry. The DNA was resuspended in 50µl RNase-free water before sequencing or TE buffer (pH 8.0) for long-term storage at -20°C.

2.9.2 ISOLATE II Genomic DNA Kit (Bioline)

High titre 1ml stocks (between 10^8 and 10^{10}pfu/ml) were mixed with 25µl of proteinase K Buffer PR and 200µl of Lysis Buffer G3 (prepared by transferring Buffer G1 to Buffer G2), vortexed for 10-20 seconds vigorously and incubated at 70°C for 10-15 minutes. 210µl of ethanol (96-100%, v/v) were added to the sample, vortexed and loaded onto an ISOLATE II Genomic DNA Spin Column (inserted in a Collection Tube). The lysate was centrifuged for 1 minute at 11000 x g until all the sample was filtered through the matrix. The column was placed in a new Collection tube, added 500µl of Wash Buffer GW1 and centrifuged for 1 minute at 11000 x g. The flow-through was discarded and the Collection tube reused. 600µl of Wash Buffer GW2 were added to the column (16ml of 96-100% ethanol were added to the

Wash Buffer GW2 Concentrate) and centrifuged for 1 minute at 11000 x g. The flow-through was discarded and the Collection Tube was reused. The sample was centrifuged for 1 minute at 11000 x g and the ISOLATE II Genomic DNA Spin Column was placed in an Eppendorf tube. 50µl of RNase-free water preheated at 70°C were added directly onto the silica membrane and incubated at room temperature for 1-2 minutes, centrifuged for 1 minute at 11000 x g and the sample stored at -20°C for sequencing or long-term storage.

2.10 DNA Quantification

Viral DNA was quantified using two different methods: NanoDrop and Qubit.

2.10.1 NanoDrop 2000™ Spectrophotometer (Thermo Scientific)

All DNA samples used in this project were measured using the NanoDrop. 1.5µl of a sample was used to both quantify and assess the quality for further analysis ($A_{260/280}$ and $A_{260/230}$).

2.10.2 Qubit™ Fluorometer (Thermo Fisher)

Reagent	Amount per reaction (µl)
Qubit® dsDNA HS Reagent	1
Qubit® dsDNA HS Buffer	199
Qubit® dsDNA HS Standard #1	10
Qubit® dsDNA HS Standard #2	10
Sample	1

Table 2-4. Reagents used for dsDNA quantification using the Qubit™ Fluorometer.

All DNA samples used for sequencing were quantified using the Qubit™ Fluorometer. A fresh working solution was made by mixing the Reagent and the Buffer from the kit, the standards and samples were mixed separately with the working solution to a volume of up to 200µl as shown in Table 2-4, and the tubes were incubated at room temperature for 2 minutes following the kit protocol. The samples were quantified using the Qubit® Fluorometer.

2.11 Restriction enzyme analysis

Reagents	Amount
DNA sample	500ng
Restriction enzyme	1µl (10 units)
10X Buffer	2µl
BSA	2µl
Sterile distilled water	up to 25µl per reaction

Table 2-5. Reagents used for the restriction enzyme analysis. One unit of restriction enzyme could digest 1µg of λ DNA in one hour at 37°C in a total volume of 50µl. All the restriction enzymes and their buffers were from Promega and New England BioLabs (NEB).

The restriction digest was prepared according to Table 2-5. Once all reagents were mixed, the samples were incubated at 37°C (50°C for BssH II) for 3 hours with a further heat inactivation for 20 minutes at either 65°C or 80°C, if required. Loading dye (5µl) was added to each reaction tube for analysis using gel electrophoresis.

2.12 Agarose gel electrophoresis

Agarose (3g) was added to 200ml 1X TAE buffer to prepare a 1.5% agarose gel. This solution was heated in a microwave for about 5 minutes, swirling frequently to dissolve the agarose. When the mixture was well dissolved, it was left to cool down to 50-60°C before pouring into a gel tray with the well comb in place. Once solidified, the comb could be removed and the gel placed in an electrophoresis tank. The electrophoresis unit was filled with 1X TAE buffer, enough to cover the gel. A molecular weight ladder was loaded into the first lane of the gel (λ DNA-HindIII digest), followed by the DNA samples mixed with a loading dye. An electrical field was used to move the samples according to size and weight, in this case 60V were used for 5 hours. After the run, the gel was stained using GelRed™ or ethidium bromide (15µl of GelRed™ 10000X stock reagent, and 5ml 1M NaCl to 45ml water or 5µl of ethidium bromide per 100ml of water or TAE buffer) in a tray with approximately 200ml of distilled water and left with agitation for 30 minutes at room temperature. The stained gel was viewed and images taken using an Azure™ c200 transilluminator (302nm) for the GelRed™ or UV light using the ethidium bromide.

2.13 Sequencing of bacteriophage DNA

Varying amounts of phage DNA (between 0.4 and 0.6µg) were used for sequencing.

2.13.1 Library preparation (NEBNext® Fast DNA Fragmentation & Library Prep Set for Ion Torrent™)

All the reagents from Table 2-6 were mixed with the samples and incubated in the thermal cycler for 20 minutes at 25°C, for 10 minutes at 70°C and a final hold at 4°C, with this incubation the DNA samples were fragmented. More reagents from Table 2-7 were added to the samples (in this step the barcodes to sequence multiple samples were added), and incubated in the thermal cycler for 15 minutes at 25°C, for 5 minutes at 65°C and a final hold at 4°C, before 5µl of Stop Buffer were added.

Reagents	**Volume (µl)**
Sample DNA	1-15.5 depending upon sample concentration
NEBNext DNA Fragmentation Reaction Buffer	2
Sterile water	up to a final volume of 18.5
NEBNext DNA Fragmentation Master Mix	1.5

Table 2-6. Reagents used for the first step of the library preparation.

Reagents	Volume (µl)
T4 DNA Ligase Buffer for Ion Torrent™	4
Sterile water	1
Ion Xpress™ Barcode Adapters	10 (5 of each)
Bst 2.0 WarmStart DNA Polymerase	1
T4 DNA Ligase	4

Table 2-7: Preparation of adaptor ligated DNA.

The Adaptor ligated DNA was cleaned: 81µl of AMPure XP Beads were added and the sample left to incubate for 5 minutes at room temperature. The Eppendorf tube was placed in a magnetic rack for 2-3 minutes until the solution cleared. The supernatant was removed and 200µl of freshly prepared 80% ethanol were added. This last step was repeated once more and the tube was left with the cap open to dry for further 5 minutes at room temperature. The magnetic beads were resuspended in 25µl of 0.1X TE buffer and left incubating at room temperature for 2 minutes. The tube was placed again in the magnetic rack and approximately 20µl of supernatant were taken to a clean tube.

The selection of the fragment sizes was done using an E-Gel Precast Agarose Electrophoresis System (Thermo Fisher). The samples were loaded onto the gel and let to run between 14 and 18 minutes to get the required size, before being collected. After selecting the required sample fragments, the reagents from Table 2-8 were added to the samples and amplified using the PCR run from Table 2-9.

Reagents (for 10 to 100ng)	**Volume (µl)**
Adaptor Ligated DNA	1-40
Primers	4
Sterile water	up to 100
NEBNext Q5 Hot Start HiFi PCR Master Mix	50

Table 2-8: PCR amplification of Adaptor Ligated DNA.

Step	**Temperature (°C)**	**Time**	**Number of cycles**
Initial denaturation	98	30 seconds	1
Denaturation	98	10 seconds	12
Annealing	58	30 seconds	12
Extension	65	30 seconds	12
Final extension	65	5 minutes	1
Hold	4	Indefinitely	

Table 2-9. PCR Cycling conditions for the amplification of Adaptor Ligated DNA.

AMPure XP Beads (90µl) were added to the samples and left to incubate for 5 minutes at room temperature. The tubes were put in a magnetic rack for 2-3 minutes until the solution was clear, the supernatant was taken and 200µl of freshly prepared 80% ethanol were added. The samples were incubated for 30 seconds at room temperature before the supernatant was taken. This last wash step was repeated and the tubes were left to dry for further 5 minutes at room temperature with the caps opened. The magnetic beads were resuspended in 25µl of 0.1X TE buffer and left to incubate for 2 minutes at room temperature. The samples were put again in the rack until the solution was clear and 20µl were transferred to a new Eppendorf tube.

2.13.2 Quantity and quality controls of the library

Samples were quantified using the Qubit™ Fluorometer (see section 2.10.3) and their quality assessed using the Bioanalyzer (Agilent Technologies). The gel-dye mix was left at room temperature for 30 minutes to equilibrate (25µl of DNA dye concentrate mixed to a DNA gel matrix vial from the kit). The

DNA chip was put in the priming station and set up to load the samples (the gel-dye mix, the markers and the ladder were loaded following the protocol), 1µl of each sample was loaded into one well and the chip was vortexed for one minute at 2400rpm before the chip was ready to be run in the Agilent 2100 bioanalyzer. From these readings, the molarity of the samples was calculated and the samples were diluted down to 100pM.

2.13.3 Preparation of template-positive Ion Sphere™ Particles (ISPs) containing amplified DNA

Following the instrument display, the instrument lid was opened and 150µl of Ion OneTouch™ Breaking Solution was put into both recovery tubes and these were placed into the instrument, as well as a Recovery Router in between these recovery tubes and the lid was closed. The Amplification Plate was inserted into the heat block and installed following the instructions manual. Both the Ion OneTouch™ Oil and the Ion OneTouch™ Recovery Solution were installed. The 100pM library samples were pooled and diluted by mixing 2µl of the libraries with 23µl of nuclease-free water, and added to the amplification solution (shown in Table 2-10). The amplification solution was loaded into an Ion OneTouch™ Reaction Filter, then 1.7ml of Ion OneTouch™ Reaction Oil was also added to the Reaction Filter before this Reaction Filter was installed on the instrument and the run started.

Reagent	**Volume (µl)**
Ion PGM™ Hi-Q™ Reagent mix	800
Nuclease-free water	25
Ion PGM™ Hi-Q™ Enzyme Mix	50
Diluted library	25
Ion PGM™ Hi-Q™ ISPs	100

Table 2-10. Ion PGM™ Hi-Q™ ISPs amplification solution.

At the end of the run (approximately 6.5 hours), the sample was centrifuged and all the supernatant but 100µl was taken from both Recovery Tubes. 500µl of Ion OneTouch™ Wash Solution were added to each Recovery Tube before the contents from both Recovery Tubes were mixed and centrifuged for 2.5 minutes at 15500 x g. All the supernatant but 100µl was taken and discarded.

A quality assessment of the template-positive ISPs was done by mixing 2µl of the ISPs sample with 20µl of Ion Probe Master Mix (consisted of 19µl of annealing buffer and 1µl of ion probes) in a 0.2ml PCR tube. The sample was incubated in a thermal cycler for 2 minutes at 95°C and for another 2 minutes at 37°C. The unbound probes were washed from the sample 3 times: 200µl of Quality Control Wash Buffer were added to the sample, vortexed,

centrifuged at 15500 x g for 1.5 minutes and the supernatant removed (10µl were left in the tube). 190µl of Quality Control Wash Buffer were added and the sample was measured in the Qubit™ Fluorometer following manufacturer's instructions (the Alexa Fluor™ 488 and the Alexa Fluor™ 647 Calibration Standard reagents were used and the raw fluorescence data were input in the Qubit™ Easy Calculator spreadsheet to evaluate the template ISPs). Values between 10 and 30% were considered of good quality for sequencing according to the manufacturer's manual.

2.13.4 Enrichment of the template-positive Ion PGM™ Hi-Q™ ISPs

The 8-well strip was loaded as shown in Table 2-11 and put on the Ion OneTouch™, the instrument was set up and the run started according to the manufacturer's manual.

Well number	Reagent to dispense	Volume (µl)
1	Template-positive ISP sample	100
2	Dynabeads™ MyOne™ Streptavidin C1 Beads in MyOne™ Beads Wash Solution*	130
3	Ion OneTouch™ Wash Solution	300
4	Ion OneTouch™ Wash Solution	300
5	Ion OneTouch™ Wash Solution	300
6		Empty
7	Melt-Off Solution**	300
8		Empty

Table 2-11. Reagents used to enrich the template-positive Ion PGM™ Hi-Q™ ISPs.
* Dynabeads™ MyOne™ Streptavidin C1 Beads (13µl) were transferred to a new Eppendorf tube and placed on a magnet rack for 2 minutes. The clear supernatant was removed and 130µl MyOne™ Beads Wash Solution were added and mixed to the Dynabeads™ MyOne™ Streptavidin C1 Beads.
** Melt-Off Solution was freshly prepared by mixing 280µl of Tween™ Solution with 40µl of 1M NaOH. Its final composition was 125mM NaOH and 0.1% (w/v) Tween™ 20 detergent.

2.13.5 Cleaning and initialisation of the Ion PGM™ Sequencer

The Ion PGM™ Sequencer was cleaned according to manufacturer's instructions (a water cleaning and a chlorite cleaning), followed by an initialisation step. The chip to be used in the run was checked by the instrument before being loaded with the sample, and a new plan was created in the Torrent Browser for the sequencing run (including information such as

number of flows, type of kit used, assign the barcodes to the samples, type of sample and reference sequence, if possible).

2.13.6 Loading of the sequencing chip

To prepare the sample, 5µl of Control Ion Sphere™ Particles were added to the template-positive ISPs, mixed and centrifuged before the supernatant was removed (but 15µl). Sequencing Primer was added (12µl) and the samples were incubated in a thermal cycler run for 2 minutes at 95°C and for 2 minutes at 37°C. The Ion PGM™ Sequencing 200 v2 Polymerase (3µl) was added to the sample and incubated at room temperature for 5 minutes. The template-positive ISPs sample was loaded into the chip following manuals instructions (after emptying the chip from any liquid, the sample was loaded at a rate of approximately 1µl per second in a 45° angle). Once the chip was loaded, it was placed in the Ion PGM™ Sequencer and the sequencing run was started. The PGM™ sequencer detects the shift in pH caused by the release of protons (or hydrogen ions) every time a nucleotide triphosphate is added as part of the activity of the DNA polymerase during DNA synthesis.

2.13.7 Bioinformatic analysis

2.13.7.1 Trimming, *de novo* assembly and phage termini determination

Reads were individually trimmed using CLC Genomics Workbench v7.5.1 (CLC Bio-Qiagen, Hilden, Germany) to a minimum quality score of 0.01 (equivalent to Phred quality score of 20), a maximum length of 220bp, and were trimmed of any adaptor and repetitive telomere sequences. *De novo* assembly was performed using SPAdes v3.5.0 (Bankevich *et al.*, 2012) within Galaxy platform (Cuccuru *et al.*, 2014; Afgan *et al.*, 2016). Restriction enzyme analysis was performed to test for cohesive ends and the program PhageTerm v1.0.11 (Garneau *et al.*, 2017) was used to determine bacteriophage termini and packaging mode.

2.13.7.2 Genome annotation and protein similarity determination

The resulting viral genomes were annotated using PROKKA v1.12 (Seemann, 2014), RAST v2.0 (Aziz *et al.*, 2008; Overbeek *et al.*, 2014; Brettin *et al.*, 2015), FGenesV (Softberry Inc, Mount Kisco, NY) and Glimmer v3.02 (Salzberg *et al.*, 1998; Delcher *et al.*, 1999; Delcher *et al.*, 2007), all these programs use Hidden Markov Models (HMMs) to predict the functionality of the sequences. Protein similarity was evaluated with BLASTP, and structural predictions and motif searches were performed using Pfam v31.0 (Aziz *et al.*, 2008; Finn *et al.*, 2016) and InterProScan v56.0 (Jones *et al.*, 2014; Finn *et al.*, 2017).

2.13.7.3 Presence of tRNA and bacterial toxins

Presence of putative tRNAs was predicted using tRNA Scan-SE v2.0 (Lowe and Chan, 2016) and ARAGORN v1.0.0 (Laslett and Canback, 2004), and presence of bacterial toxins was predicted using BTXpred server (Saha and Raghava, 2007).

2.13.7.4 Phage lifestyle prediction and dot-plot analysis

Whole bacteriophage proteome was used to predict the lifestyle of each isolated bacteriophage as virulent or temperate, using the program PHACTS (McNair *et al.*, 2012). Nucleotide dot-plots were generated using GEPARD v1.40 (Krumsiek *et al.*, 2007).

2.13.7.5 Phylogenetic analyses

The bacteriophage DNA and RNA polymerases and the DNA sequence of the large subunit of the telomerase gene were used for phylogenetic analysis. The DNA sequences of these two genes from all bacteriophages were aligned using both Clustal Omega (Thompson *et al.*, 1994; Sievers *et al.*, 2011) and MAFFT v7 online (Katoh and Standley, 2013; Kuraku *et al.*, 2013; Katoh *et al.*, 2017) and visualised using Archaeopteryx.js (Zmasek and Eddy, 2001; Han and Zmasek, 2009). The RNA polymerases of all the isolated bacteriophages and those infecting *Pectobacterium* spp., together with the type strains for all six genera present in the subfamily *Autographivirinae* (Table 2-12) were used to form a phylogenetic tree in the phylogeny.fr platform (Dereeper *et al.*, 2008), using MUSCLE alignment v3.8.31 (Edgar, 2004), with default settings and the maximum likelihood method in PhyML program v3.1/3.0 (Castresana, 2000; Guindon and Gascuel, 2003) and the final representation of the phylogenetic tree was performed using TreeDyn v198.3 (Chevenet *et al.*, 2006; Anisimova and Gascuel, 2006).

Genome	Accession	Reference	Length (nt)	Genera
Pectobacterium phage Peat1	NC_029081	(Kalischuk *et al.*, 2015)	45633	Unassigned
Pectobacterium phage PP16	NC_031068		43902	Unassigned
Pectobacterium phage PP90	NC_031096		44570	Unassigned
Pectobacterium phage PPWS1	LC063634.2	(Hirata *et al.*, 2016a)	44539	*Phikmvvirus*
Acitenobacter phage Abp1	NC_021316	(Huang *et al.*, 2013)	42185	*Fri1virus*
Acitenobacter phage AB3	NC_021337	(Zhang *et al.*, 2015)	31185	*Fri1virus*
Acitenobacter phage Fri1	NC_028848		41805	*Fri1virus*
Pantoea phage LIMElight	NC_019454	(Adriaenssens *et al.*, 2011)	44546	*Kp34virus*
Klebsiella phage F19	NC_023567.2	(Lin *et al.*, 2014)	43766	*Kp34virus*
Klebsiella phage KP34	NC_013649	(Drulis-Kawa *et al.*, 2011)	43809	*Kp34virus*
Klebsiella phage NTUH-K2044-K1-1	NC_025418	(Lowe and Chan, 2016)	43871	*Kp34virus*
Pantoea phage LIMEzero	NC_015585	(Adriaenssens *et al.*, 2011)	43032	*Phikmvvirus*
Pseudomonas phage LUZ19	NC_010326	(Lammens *et al.*, 2009)	43548	*Phikmvvirus*
Pseudomonas phage phiKMV	NC_005045	(Lavigne *et al.*, 2006)	42519	*Phikmvvirus*
Xanthomonas phage f20	KU595432.1	(Retamales *et al.*, 2016)	43851	*Pradovirus*
Xanthomonas virus Xp10	NC_004902	(Yuzenkova *et al.*, 2003)	44373	*Pradovirus*
Xylella phage Prado	NC_022987	(Ahern *et al.*, 2014)	43940	*Pradovirus*
Salmonella virus SP6	NC_004831	(Dobbins *et al.*, 2004)	43769	*Sp6virus*
Escherichia virus K1-5	NC_008152	(Scholl *et al.*, 2004)	44385	*Sp6virus*
Escherichia virus K1E	NC_007637	(Stummeyer *et al.*, 2006)	45251	*Sp6virus*
Erwinia amylovora phage Era103	NC_009014	(Vandenbergh and Cole, 1986)	45445	*Sp6virus*

Kluyvera phage Kvp1	NC_011534	(Lingohr *et al.*, 2008)	39472	*T7virus*
Enterobacteria phage T3	NC_003298	(Pajunen *et al.*, 2002)	38208	*T7virus*
Enterobacteria phage T7	NC_001604	(Cheng *et al.*, 1994)	39937	*T7virus*
Escherichia phage K30	NC_015719		40940	*Kp32virus*
Klebsiella phage KP32	NC_013647		41119	*Kp32virus*
Klebsiella phage K11	NC_011043		41181	*Kp32virus*

Table 2-12. Phage genomes used for the phylogenetic tree using the RNA polymerases. The strains used included strains that infect *Pectobacterium* spp. as well as representative strains and type strains from each one of the seven genera belonging to the subfamily *Autographivirinae.*

2.13.7.6 Average nucleotide identity (ANI), core genome and whole genome analysis

Average nucleotide identity (ANI) was calculated using autoANI.pl with default settings (Davis Ii *et al.*, 2016). Comparative genome analysis was carried out using Roary v3.11.2, with "-i 50" input (Page *et al.*, 2015). A core-gene phylogeny was constructed using FastTree v2.1.4 (Price *et al.*, 2010). For whole-bacteriophage sequence phylogeny, the program VICTOR (Meier-Kolthoff *et al.*, 2013; Meier-Kolthoff and Göker, 2017) was used: all pairwise comparisons of the nucleotide sequences were performed using the Genome-BLAST Distance Phylogeny (GBDP) method with settings recommended for prokaryotic viruses (Meier-Kolthoff and Göker, 2017), the resulting intergenomic distances were used to infer a balanced minimum evolution tree with branch support via FASTME including SPR postprocessing (Lefort *et al.*, 2015), branch support was inferred from 100 pseudobootstrap replicates each. Trees were rooted at the midpoint (Farris, 1972). Taxon boundaries at the species, genus and family level were estimated with the OPTSIL program (Göker *et al.*, 2009), the recommended clustering thresholds (Meier-Kolthoff and Göker, 2017) and an F value of 0.5 (Meier-Kolthoff *et al.*, 2014). The global genomic similarity of the isolated bacteriophages was performed using VIPTree v1.3 (Nishimura *et al.*, 2017), including all the Podoviridae family and Gammaproteobacteria reference genomes.

2.13.7.7 Whole genome comparison

All the genomes were manually colinearised, placing the arbitrary starting point at the start of the open reading frame of the large terminase subunit gene (Abatángelo *et al.*, 2017). The genome organisation of the phages and comparative BLASTN for both nucleotides and coding sequences with figures were created using CGView Comparison Tool using the build_blast_atlas_all_vs_all.sh.script (Grant *et al.*, 2012), detail of regions of interest were formed using the create_zoomed_maps.sh script (using magnifications between 10 and 30) (Grant *et al.*, 2012). Whole genome alignments using tBLASTX were visualised with Easyfig v2.2.2 (Sullivan *et al.*, 2011) with a 21% identity cut-off and modified using Adobe® Photoshop® Software.

2.14 Corona discharge method for attachment

Nylon (20nm) and cellulose (50µm) nanoparticles were used for bacteriophage attachment using the corona discharge method. The amount of nanoparticles used was measured (as a function of area and phages,10^8pfu per cm^2, as explained in Table 2-13), before using the corona discharge the bacteriophages in PBS were added to the particles and mixed at room temperature. The bacteriophage-nanoparticle solution was poured onto the conductor surface of the instrument and a corona discharge was applied. Two passes at 7.5kV were used at a speed of 10 meters per minute. The samples were recovered, dried, washed between two and three times to discard unattached phages (mixed in PBS and centrifuged) and their ability to form plaques determined (as mentioned in section 2.4.3).

Material	Size (nm)	Surface area (nm^2)	Density (g/cm^3)	Volume (nm^3)	Ratio (surface area/volume)	Grams required
Nylon	20	1260	3.5	4190	0.3	$4.6\ 10^{-6}$
Cellulose	50×10^3	7850×10^6	0.6	65.5×10^{12}	0.12	2×10^{-3}

Table 2-13. Conversion units for area and volume of spheres depending on their sizes. It was decided to attach the nanoparticles as a function of number of bacteriophages per area so these parameters could be optimised ($4cm^2$ for the nylon and $4mm^2$ for the cellulose nanoparticles). From the required area ($2 \times 2cm^2$), the number of particles needed was calculated based on their surface area. The number of particles was then multiplied by their volume and converted into cm^3 ($1cm^3 = 1 \times 10^{21} nm^3$), this value was multiplied by the material density to get the weight in grams, for the requested area it was 4.6×10^{-6}g and 2×10^{-3}g for the nylon and the cellulose, respectively.

2.14.1 Stability test of immobilised bacteriophages

The stability of immobilised ϕSFM002 onto cellulose nanoparticles was tested at different temperatures and the results were compared to free ϕSFM002 stocks. Starting solutions of free ϕSFM002 were 10^9pfu/ml and for attached phages was 10^7pfu/ml (apart from the sample at 37°C that was 10^6pfu/ml) and they were incubated at 4°C, room temperature, 30°C and 37°C for up to six days for free ϕSFM002 and for up to four weeks for immobilised ϕSFM002. The ability to form plaques was tested every day for free bacteriophages and every week for attached ones in triplicate for each time point (as mentioned in section 2.4.3) and the results were plotted using Microsoft® Excel® for Mac 2011 (version 14.7.2).

2.14.2 Translocation of cellulose nanoparticles *in vivo* using confocal microscopy

Confocal microscopy was used to test cellulose nanoparticle uptake by the plant with autofluorescence. Tomato seeds (*Solanum lycopersicum* cv Moneymaker) were germinated in presence of sterile cellulose nanoparticles and allowed to grow for 28 days, a negative control without nanoparticles was used and a positive control consisting of unattached cellulose suspension in PBS. Samples were taken from roots, stems and leaves using a scalpel and transferred onto glass slides with no fixation. The samples were analysed using a Leica TCS SP/2 Laser Scanning Confocal Microscope (Leica Microsystems). Image processing was accomplished using LAS-AF Lite 2.6.3 software (Leica Microsystems).

2.15 Infectivity tests

2.15.1 Effect of different treatments on seed development

Tomato seeds (*Solanum lycopersicum* cv Moneymaker) were surface-sterilised: the seeds were submerged in 30% (v/v) commercial bleach for 15 minutes, followed by three more washes in distilled water. At least three seeds were dipped into different solutions for approximately 5 minutes: free bacteriophages (10^{10}pfu/ml), clean cellulose nanoparticles only, clean cellulose nanoparticles and bacteria, bacteriophages and bacteria, coated cellulose nanoparticles and bacteria, coated cellulose nanoparticles, a bacterial solution as the positive control (10^8cfu/ml) and distilled sterile water as the negative control, for ease of this experiment ϕSFM002 was the only bacteriophage used and *Pectobacterium atrosepticum* SCRI 1043 was the only bacteria. The seeds were transferred onto half-strength MS agar (see Table 2) and left in dark conditions at 25°C for about a week to allow germination, then they were transferred to an incubator at 25°C with a long

day photoperiod (16L/8D) (Schwarz *et al.*, 2014). Stem growth was measured every day for the first two weeks after seed sterilisation, data obtained included germination time, stem, cotyledon and leaf development. All this data was plotted against time using Microsoft® Excel® for Mac 2011 (version 14.7.2). Bonferroni's means comparison test, (one-way analysis of variance (ANOVA) with $p \leq 0.05$) was performed using StatPlus for Mac LE (version 6.2.21).

2.15.2 Potato tuber infection assay

Potato tubers (*Solanum tuberosum*) Marys Piper variety were used for the *in vivo* assays of the phage-coated nanoparticles on preventing soft rot development. The surface of the potatoes were sterilised using a 10% sodium hypochlorite solution for ten minutes followed by washing three times in distilled sterile water. After air-drying under sterile conditions for 30 minutes, tubers were cut into 1cm slices and placed in sterile Petri dishes.

An overnight culture of *Pectobacterium atrosepticum* and *Pectobacterium atrosepticum* SCRI 1043 in nutrient broth were diluted to an OD_{600nm} of 0.1 (Bell *et al.*, 2004), these samples were used separately as positive controls.

The different treatments included free ϕSFM002, free ϕSFM010, coated cellulose nanoparticles, coated nylon nanoparticles, two negative controls (one with distilled sterile water and the other with PBS) and the two positive controls above mentioned. Inoculation was performed by spot-inoculating three 10µl drops per potato slice (3×10^8 cfu/ml for the positive controls, and 3×10^{10} pfu/ml for each bacteriophage treatment). The samples were incubated for 3 days under different incubation temperatures (4°C, room temperature and 30°C) and the level of degradation was followed daily until the completion of the experiment. The area of degradation was manually selected on the pictures taken by using ImageJ 1.50i software and comparing it to the total tissue area available (Shabuer *et al.*, 2015a), the results were plotted using Microsoft® Excel® for Mac 2011 (version 14.7.2). This experiment was conducted only once independently with at least three replicates in each trial. Bonferroni's means comparison test (ANOVA two-tailed t-test with $p \leq 0.05$) was performed using StatPlus for Mac LE (version 6.2.21).

2.16 Statistical analysis

Plaque and bacteriophage morphology results using TEM had both a normal distribution, an ANOVA two-tailed test with $p \leq 0.001$was performed.

Bonferroni's means comparison test was used for the infectivity tests: one-way analysis of variance with $p \leq 0.05$ was used on the effect of treatments on seed development. ANOVA two-tailed t-test with $p \leq 0.05$ was performed on the potato tuber infection assay.

All calculations were performed using StatPlus for Mac LE (version 6.2.21).

3.0 Results

Isolation and description of isolated *Pectobacterium* spp. bacteriophages using plaque morphology, host range and TEM

3.1 Introduction

3.1.1 Characterisation of bacteriophage based on host range and morphology

Bacteriophages can be lethal to bacteria and this can be used to prevent the development of bacterial infections and, in the case of crops, spoil consumer products. The critical first step for the development of phage-based biocontrol agents involves the efficient isolation of bacteriophages. All these bacteriophages must be characterised before designing the bacteriophage cocktail to be used as a biocontrol agent.

Bacteriophages can be defined by their host range, that is described as the spread of organisms that a parasite can infect and kill (Hyman and Abedon, 2010). It is generally accepted that a broad host range refers to the ability to infect at least two or three bacterial species, whereas a narrow host range can only infect different strains within a bacterial species (Hyman and Abedon, 2010). The host range relies on a series of factors such as specificity of host-binding proteins, biochemical interactions during infection, presence of prophages and bacterial phage-resistance mechanisms (Adams, 1959; Hyman and Abedon, 2010; Diaz-Munoz and Koskella, 2014). In this work, host range is defined as the ability to form plaques, as there are a variety of processes when phages can be infective, but infection does not result in the production of phage particles, such as with lysogenic infections (Abedon and Yin, 2009). The development of plaques on different host strains is used to confirm a lytic infection of such strain. Additionally, the efficiency of plating refers to the plaque titre of a phage stock using a new bacterial host, that is relative to the estimate of the concentration of phage particles using the original host, which is usually higher (Adams, 1959).

The Genus *Pectobacterium* (formerly *Erwinia*) is divided into seven species: *P. atrosepticum, P. betavasculorum, P. carotovorum, P. cacticida, P. aroidearum, P. parmentieri* (Khayi *et al.*, 2016) and *P. wasabiae* (Hauben *et al.*, 1998). Recent studies have re-evaluated the taxonomy of the genera *Dickeya* and *Pectobacterium* (Zhang *et al.*, 2016), both included in the family *Pectobacteriaceae* (Adeolu *et al.*, 2016). Their complexity has been reflected in different studies (Dees *et al.*, 2017), where both *P. atrosepticum* and *P. atrosepticum* SCRI 1043 were shown to be closely related, followed by *P. wasabiae* (very similar to Dickeya species) and *P. carotovorum,* being the least similar of the type strains used for this project (see section 2.1 in Materials and methods).

The plaque assay is the gold standard for phage quantification. A phage plaque is formed by successive cycles of infection and virion release in a bacterial host lawn, comparable to the traveling wave of an epidemic (You and Yin, 1999). There are different factors to take into account when determining plaque morphology: plaque size, clarity, border definition and

distribution should be characterised as they provide information of the growth and virulence factors of the virus (Baer and Kehn-Hall, 2014). Plaque development occurs in four phases (Koch, 1964): the primary adsorption event, the first round of viral multiplication, the enlargement phase and the final phase in which viral multiplication ceases, although phage T7 continues to increase in size for up to fifty hours after inoculation (Yin, 1993). Plaque size depends on intrinsic viral infection characteristics, such as adsorption rate, lysis time and burst size, but also on the external conditions where the infection takes place; for example higher agar concentration impedes viral diffusion (Abedon and Yin, 2009). The initial adsorption also depends on three factors: bacterial density, agar concentration and phage adsorption constant (Abedon and Yin, 2009), delays in adsorption result in smaller plaques and/or varied plaque sizes. The latter is due to the time these phages mature and form plaques when the host has already reached stationary phase (Adams, 1959). On the other hand, highly-adsorbing phages also produce small plaques as the concentration of phages formed is small within plaques (Gallet *et al.*, 2011). Lysis time, or the time a phage takes from adsorption to the subsequent host lysis, is also a factor to take into account as optimal lysis time is independent of the adsorption rate for plaque size (Gallet *et al.*, 2011); shorter lysis times result in smaller burst sizes (Wang, 2006a) since they produce less progeny phages to diffuse, thus forming smaller plaques. However, long lysis times also develop smaller plaques for the same reasons as with longer adsorption rates (Gallet *et al.*, 2011). Therefore, maximum plaque sizes are reached when the lysis time is long enough to produce enough viral progeny but short enough to allow viral diffusion in the agar (Gallet *et al.*, 2011). Additionally, higher burst sizes can increase plaque dimensions but only when higher than 10 (Carlson and Miller, 1994) and smaller phages produce greater plaques as they diffuse easily in the agar (Elford and Andrews, 1932). Generally, viral multiplication stops when bacteria reach their stationary phase of growth.

3.1.2 The structure of phages

Electron microscopy is the only tool to visualise viral particles and it is the easiest, the fastest and the least expensive way for phage identification. Bacteriophages are classified in families and genera based on their external morphology (tail type, polyhedral, filamentous or pleomorphic capsid, presence of envelope) and their nucleic acid composition as stated in the Baltimore classification (dsDNA, ssDNA, dsRNA or ssRNA) (Ackermann, 2011; Adriaenssens and Brister, 2017). Other intrinsic phage characteristics that can be used for their classification include weight and buoyancy of the viral particle, number and composition of their proteins and lipids, inactivation by heat, UV or chloroform, restriction enzyme analysis and viral physiology characteristics such as adsorption rate, burst size, host range, latent period and DNA assembly to name a few. Of some consideration are tail lengths as they give information about viral endurance: short-tailed and non-tailed

bacteriophages are more resistant and do not lose infectivity as much as long-tailed ones (Aprea *et al.*, 2015).

3.1.3 Aims and objectives

A first aim within this project was to successfully isolate novel bacteriophages, active against *Pectobacterium* spp., and to characterise them in terms of plaque morphology, host range, efficiency of plating and determination of their morphotypes using transmission electron microscopy.

The success of phage isolation depends on the season, location, external conditions and presence of putative hosts (Gross *et al.*, 1991; Marsh and Wellington, 1994; Miller, 2001). Bacteriophages are frequently found at the site of infection, within close proximity to their host (Wommack *et al.*, 2009; Czajkowski *et al.*, 2014; Czajkowski *et al.*, 2015), and this is why potato and soil samples were chosen for the bacteriophage isolation.

Another objective of this chapter was to use the different characterisation techniques to ascertain the infective properties and discriminate between the different bacteriophages.

3.2 Bacteriophage characterisation

Pectobacterium bacteriophages were isolated from a variety of locations (Table 3-1) and their activity was tested against the bacterial type strains (Table 2-1) according to the methods described in Section 2.4 (in Materials and methods). Each plaque was subjected to three rounds of single plaque purification. Following this process, a set of 12 bacteriophages were selected for characterisation (Table 3-1).

Bacteriophages	Date of isolation	Sample	Shop and address
ϕSFM001 ϕSFM002	June 2013	Scottish new potatoes	Andersons Greengrocers 190 Byres Road Glasgow G12 8SN
ϕSFM003 ϕSFM004 ϕSFM005 ϕSFM006 ϕSFM007 ϕSFM008 ϕSFM009 ϕSFM010	December 2013	Maris Peer and Maris Piper from Scotland	Cessnock Food Store 374 Paisley Road West Glasgow G51 1BG
ϕSFM011 ϕSFM012	April 2014	Jersey Royals from Ayrshire	Morrisons Partick 1-2 Merkland Court Glasgow G11 6BB

Table 3-1: All the bacteriophages were isolated from potato samples. List of the 12 bacteriophages, including date and type of sample from where the isolation took place as well as the shop from where these samples were purchased.

3.2.1 Host range and efficiency of plating

In order to determine if there were any differences in host range, all twelve bacteriophages were tested against the four type strains of *Pectobacterium* (*P. atrosepticum* SCRI 1043, *P. atrosepticum, P. carotovorum* subsp *carotovorum* and *P. wasabiae*) (Figure 3-1). The titre from the infective phages was measured and compared to that from the titre obtained from the original strain to obtain the efficiency of plating (Table 3-2), the production ratio of each phage was divided into high, medium, low and inefficient when compared to the original host (see section 2.6).The bacteriophages isolated were only infective against two of the bacterial strains: ϕSFM010 could infect clearly *P. atrosepticum*, whereas all the other bacteriophages infected predominantly *P. atrosepticum* SCRI 1043, although they could produce plaques with the other host (Figure 3-1). No bacteriophages were found with a high production ratio when compared to the original host (higher or equal to 0.5), and only ϕSFM003 had a medium production ratio (between 0.1 and 0.5), low EOP was found in ϕSFM001, ϕSFM002, ϕSFM011 and ϕSFM012 (between 0.001 and 0.1), and all the other bacteriophages were found to have inefficient production (less that 0.1% compared to the original strain). All the bacteriophages had a narrow host range and ϕSFM010 was different as it was the only virus to infect *P. atrosepticum*. On the other hand, based on their efficiency of plating they were divided into 3 groups: ϕSFM003 (medium production ratio), ϕSFM001, ϕSFM002, ϕSFM011 and ϕSFM012 (low production ratio) and all the remaining (inefficient production ratio). Nevertheless, the efficiency of plating alone was not enough to conclude that these were different phages and more characterisation, such as morphology of the plaques and viral particles, were required.

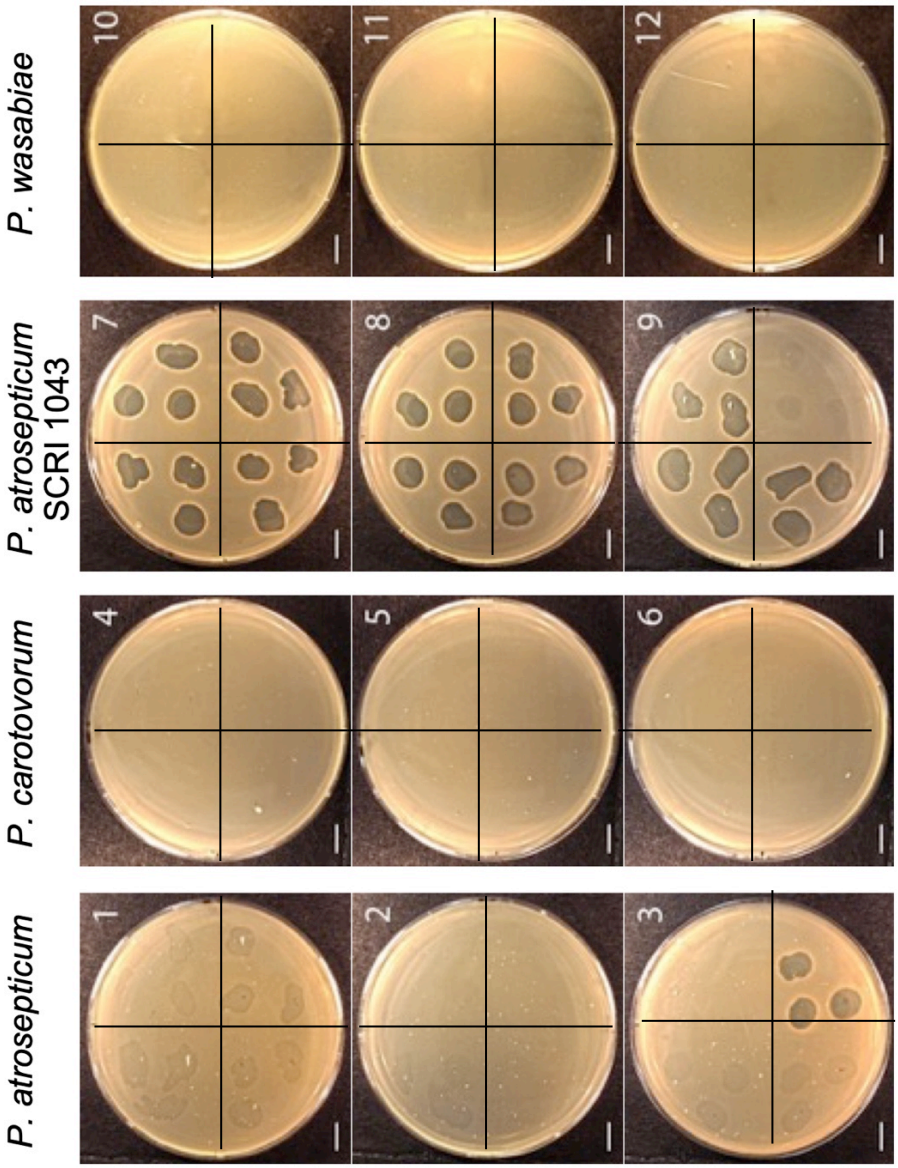

Figure 3-1: Host range analysis of the isolated bacteriophages using the double agar overlay technique. Host range analysis using *P. atrosepticum* (first column, 1-3), *P. carotovorum* (second column, 4-6), *P. atrosepticum* SCRI 1043 (third column, 7-9) and *P. wasabiae* (fourth column, 10-12). Phage dilution-stocks (MOI = 1) were spot-inoculated onto the bacterial lawn on triplicate (from top right, clockwise): ϕSFM001 (first quadrant), ϕSFM002, ϕSFM003 and ϕSFM004 are shown in the top row images (1,4,7 and 10), ϕSFM005 (top quadrant in the second row), ϕSFM006, ϕSFM007 and ϕSFM008 are shown in the middle row pictures (2, 5, 8 and 11), ϕSFM009 (top right quadrant), ϕSFM010, ϕSFM011 and ϕSFM012 are shown in the bottom row pictures (3, 6, 9 and 12), all 1cm scale bars are shown.

	P. atrosepticum SCRI 1043	*P. atrosepticum*	*P. carotovorum* subsp. *carotovorum*	*P. wasabiae*
ϕSFM001	1.0	0.049 ± 0.009	0	0
ϕSFM002	1.0	0.016 ± 0.008	0	0
ϕSFM003	1.0	0.166 ± 0.027	0	0
ϕSFM004	1.0	< 0.001	0	0
ϕSFM005	1.0	< 0.001	0	0
ϕSFM006	1.0	< 0.001	0	0
ϕSFM007	1.0	< 0.001	0	0
ϕSFM008	1.0	< 0.001	0	0
ϕSFM009	1.0	< 0.001	0	0
ϕSFM010	< 0.001	1.0	0	0
ϕSFM011	1.0	0.007 ± 0.009	0	0
ϕSFM012	1.0	0.066 ± 0.020	0	0

Table 3-2. All bacteriophages infected *Pectobacterium atrosepticum* and *Pectobacterium atrosepticum* SCRI 1043. Values calculated for the efficiency of plating (EOP) were obtained from the average of the phage titre with each host in triplicate with their standard deviations. Each EOP value is the mean of three measurements, followed by its standard deviation. The plating on the original strain of isolation (EOP = 1.0) is marked in bold.
[a] A value < 0.001 indicates that the PFU of the actual phage on the target bacterium is more than 1000 times less than on the primary host.
[b] A value of 0 means that bacteria did not show sensitivity in a spot test.

3.2.2 Comparative analysis of plaque morphology and viral particles

To further characterise the different bacteriophages, plaque comparison was done. A minimum of twenty plaques per isolate were formed together and under the same conditions (apart from using a different host for ϕSFM010), in order to compare them to each other (see section 2.3 in Materials and methods) (Figure 3-2). All areas were measured in square millimeters and plotted using their median, Q1, Q3, minimum and maximum values (Figure 3-3), since the area distribution of the plaques fell into a normal distribution, a one-way ANOVA was performed using a p-value of 0.05. All phages produced plaques that were very similar: they all formed clear round plaques with no halos and some had more variable plaque sizes than others (Figure 3-2). Statistical analysis of the results showed that two or more of the bacteriophages were significantly different but the one-way ANOVA test could not discriminate which bacteriophages were different.

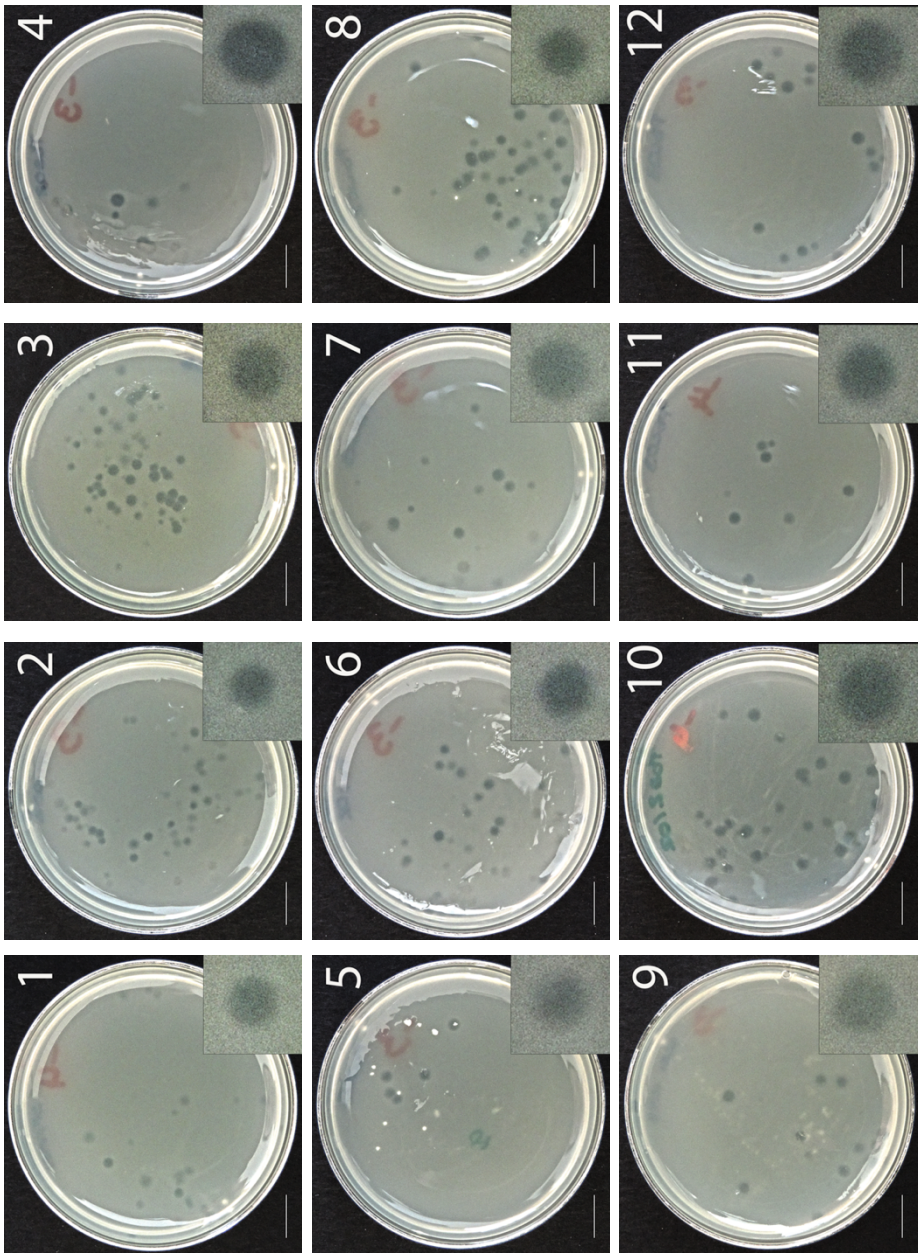

Figure 3-2: Plaque morphology of the twelve bacteriophages was very similar. Pictures labeled as 1 to 12, in ascending order: ϕSFM001, ϕSFM002, ϕSFM003, ϕSFM004, ϕSFM005, ϕSFM006, ϕSFM007, ϕSFM008, ϕSFM009, ϕSFM010, ϕSFM011 and ϕSFM012. Using 0.7% nutrient agar and a bacterial lawn with *P. atrosepticum* SCRI 1043, apart from image number 10 that had a bacterial lawn with *P. atrosepticum,* and MOIs of 0.1. Plaques had their contrasts enhanced and their areas measured, 1cm scale bars are shown.

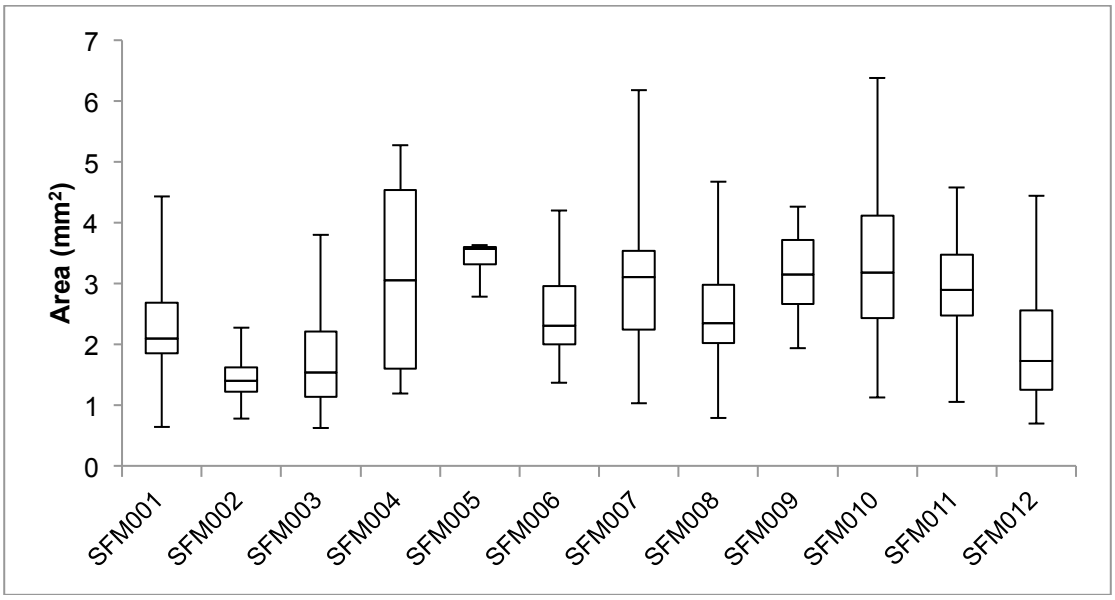

Figure 3-3: Comparison of plaque sizes of the twelve bacteriophages. Area measurements were calculated in square milimeters using ImageJ 1.50i software from the images shown in figure 3-2, and plotted using their median, Q1, Q3, minimum and maximum values using Excel.

3.2.3 Phage morphology using TEM

In order to continue with the characterisation, electron micrographs were used to determine the bacteriophage morphotypes (see section 2.7 in Materials and methods) (Figure 3-4). The capsid diameters were measured in nanometers and plotted without tails (Figure 3-5 a) and with tails (Figure 3-5 b) using their median, Q1, Q3, minimum and maximum values. A one-way ANOVA test with a p-value of 0.05 was used to determine differences between all the bacteriophages. Bonferroni's means comparison test, ANOVA two-tailed test with a p-value of 0.05 was also used to compare the plaque morphology values above mentioned together with the bacteriophage lengths (with and without tails). All bacteriophages displayed a morphology similar to that shown by bacteriophages of *Podoviridae* with an icosahedral head and a small non-contractile tail (Figure 3-4). The head diameters range between 56nm (ϕSFM004) and 138nm (ϕSFM008) (Figure 3-5 a), and the tail lengths vary between 15nm (ϕSFM005 and ϕSFM007) and 37nm (ϕSFM002) (Figure 3-5 b). The one-way ANOVA indicated that there were two or more significantly different bacteriophages, a p-value of 0 indicated that there were at least two significantly different bacteriophages but could not discriminate which ones and the Bonferroni test saw differences between ϕSFM008 with ϕSFM001, ϕSFM003, ϕSFM004, ϕSFM006, ϕSFM007 and ϕSFM011, In conclusion, it was clear that ϕSFM008 was significantly different than the others based on the results and on the *post hoc* analysis.

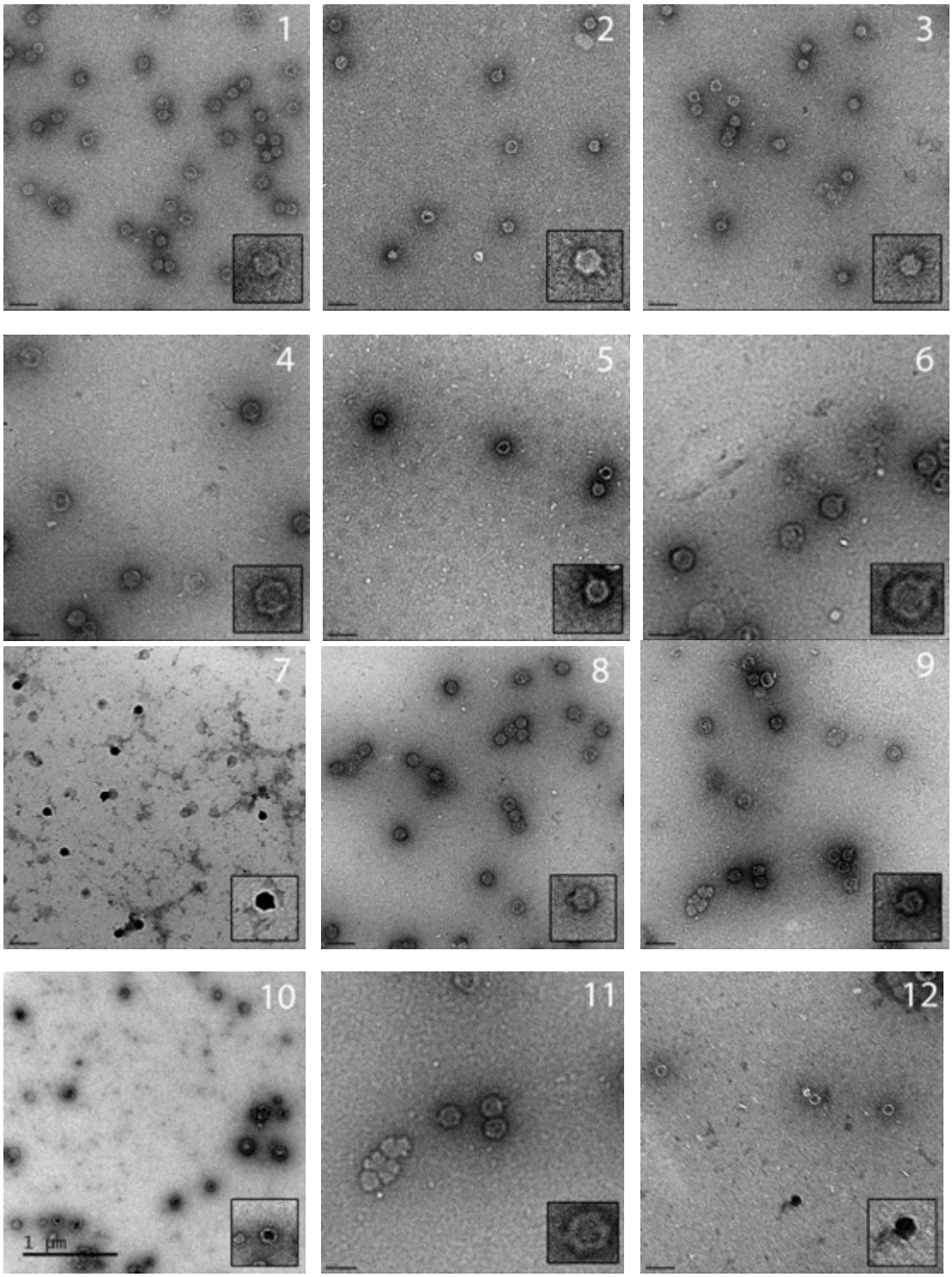

Figure 3-4: TEM images of the twelve bacteriophages. TEM images of ϕSFM001, ϕSFM002, ϕSFM003, ϕSFM004, ϕSFM005, ϕSFM006, ϕSFM007, ϕSFM008, ϕSFM009, ϕSFM010, ϕSFM011 and ϕSFM012 (in ascending order). The scale bars correspond to 200nm apart from ϕSFM010 which is 1µm. Double size close ups of each phage are shown at the right hand corners.

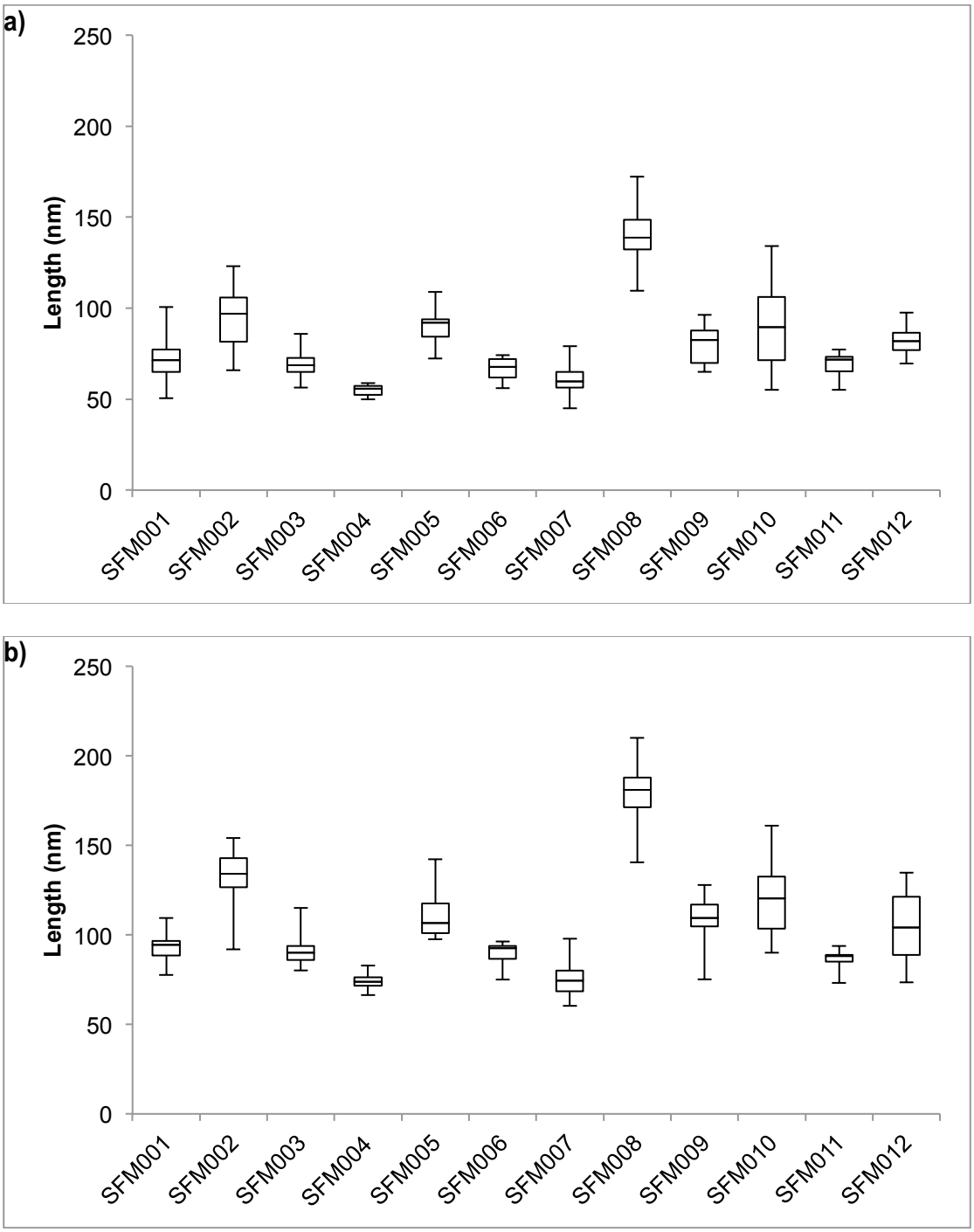

Figure 3-5 (a and b): Comparison of bacteriophage capsids based on TEM images. Using imageJ 1.50i software to calculate their diameters from the images shown in figure 3-4 and Excel for descriptive statistics, median, Q1, Q3, minimum and maximum values were calculated using at least 10 measurements per phage.

3.3 Discussion and conclusions

The use of bacteriophages as biocontrol agents requires a complete characterisation of the viruses to be carried out; the determination of their infectivity properties allows the most appropriate treatment to be developed. Host range is a key property for phage therapy (Ross *et al.*, 2016). It should be wide to the generic level as this is equivalent to a broad spectrum antibiotic (Ross *et al.*, 2016), but not so that would alter the bacterial community of the surrounding environment. It was suggested that some phage genes are involved in productive phage infection, like *ompC* that encodes an outer membrane receptor in *E. coli* (Yu and Mizushima, 1982; Cowley *et al.*, 2018); phages with these receptors have a broad host range for *E. coli*. The isolated bacteriophages in this project have a narrow host range as they infect primarily *P. atrosepticum* SCRI 1043 and no other closely related type strains. The permissiveness of this bacteria for the isolated bacteriophages suggest certain regionalism since all the samples isolated were from Scotland, just like the SCRI 1043 bacterial strain (samples from other regions such as Israel and Spain were not successful for phage isolation).

The plaques formed for all phages were clear and with no halos that is representative of lytic phages; the best candidates for a phage cocktail were ϕSFM001, ϕSFM002, ϕSFM003, ϕSFM010, ϕSFM011 and ϕSFM012 as they could infect one or more strains more efficiently than others. Plaque morphology is the first evidence of viral infection, its use as a characterisation method has many limitations except for determination of host range, as it relies on many different factors such as incubation conditions and/or other aspects such as host fitness, media composition or agar concentration. There are other factors that can affect plaque development, for instance the presence of “ghost” particles that do not contain DNA, but retain some lytic activity as they still retain cell-wall-degrading enzymes; this is known as lysis from without. Despite this they cannot replicate within the host (Barlow *et al.*, 2009; S. T. Abedon, 2011) and they can form a plaque though no viral replication takes place and result in an inefficient production ratio from the efficiency of plating results, this should be the case for ϕSFM004, ϕSFM005, ϕSFM006, ϕSFM007, ϕSFM008 and ϕSFM009 when using *P. atrosepticum* as the host (Table 3-2).

The bacteriophages isolated have icosahedral heads, with short tails and diameters that includes them in the C1 morphotype (Ackermann and Eisenstark, 1974) of the *Podoviridae* family. All the samples differed greatly in capsid sizes, from 56nm of ϕSFM004 to 138nm of ϕSFM008. When taking the tails sizes into consideration, most phages had a short tail between 15 and 25nm long, apart from ϕSFM002, ϕSFM010 and ϕSFM008, which were significantly different to all the other bacteriophages. Although ϕSFM008 was clearly bigger than any other phage, this did not reflect the plaque size; smaller presumably, due to lower diffusion of this phage in the agar (Elford and Andrews, 1932).

ϕT7 is the 'type' virus of the podoviruses (Kutter and Guttman, 2001), with a 56nm capsid and a 14nm tail (Ackermann and Nguyen, 1983; Dunn *et al.*, 1983; Sandaa, 2009) and it forms bulls eye plaques (plaques with halos). Only ϕSFM004 and ϕSFM007 have a similar size capsid to that of ϕT7 (56 and 60nm, respectively), and based on the tail length many of the bacteriophages were similar to ϕT7 including ϕSFM004 and ϕSFM007 (18 and 15nm, respectively), but none produced plaques with halo or plaques that would have grow larger if left incubated for 10 hours or over (data not shown).

It was suggested that soft rot enterobacteria-infecting podoviruses are difficult to isolate and that these phages are unusual in the environment (Ackermann, 2011), though they are more frequently isolated where the host bacteria is found (Czajkowski *et al.*, 2015). Out of the 2203 phage genomes published to date at the National Center for Biotechnology Information (NCBI), 31 are infective against different *Pectobacterium* spp. and 17 are podoviruses: ϕPP1 (Lee *et al.*, 2012), ϕPP2 (unassigned), ϕPPWS1 (Hirata *et al.*, 2016a), ϕPP16 (unassigned), ϕPP81 and ϕPPWS4 are all active against *P. carotovorum* subsp. *carotovorum*, ϕPeat1 (Kalischuk *et al.*, 2015), ϕPP90 (unassigned), vB_PatP_CB1 (unassigned) and vB_PatP_CB3 (unassigned) are active against *P.* atrosepticum, ϕA38 (Smolarska *et al.*, 2018) and ϕA41 (Smolarska *et al.*, 2018) are active against *P.* parmentieri, ϕPP74 (unassigned) is active against *P.* wasabiae. Other podoviruses that infect *Pectobacterium* spp. include ϕDU_PP_I (unassigned), DU_PP_III (unassigned), DU_PP_IV (unassigned) and DU_PP_V (unassigned). Not all these phages have been completely characterised, but from the available data, ϕPP2, ϕA38 and ϕA41 have similar dimensions to the bacteriophages isolated, and only these last two podoviruses resemble ϕT7 with a capsid diameter of 60nm and a tail of about 20nm, but they create very small plaques.

Overall, the first stages of characterisation have shown that from the host range there were at least two different groups of phages (ϕSFM010 and all the others) and from plaque morphology and TEM analysis combined there was another phage (ϕSFM008). Further characterisation is required at this stage as these results alone are not enough to discriminate between bacteriophages.

4.0 Results

Phage growth kinetics determination

4.1 Introduction

4.1.1 Phage infection kinetics

After first characterising the bacteriophage isolates using plaque and bacteriophage morphology, experiments that determine the *in vitro* functional characterisation of each phage-host interaction were required in order to justify the selection of a phage as a biocontrol agent (Abedon, 2017). The likelihood that an individual phage will find its host depends on the phage diffusion rate and the density of phage-susceptible bacteria, with more bacteria meaning faster phage adsorption (Kasman *et al.*, 2002). The generation time of a virus comprises this extracellular search for a host followed by a latent period (Abedon *et al.*, 2003), which is the time between phage adsorption and virion release (see Figure 4-1) and it can be measured through the release of mature phages or through the decrease of infected bacteria as the media turbidity decreases. Likewise, the eclipse period is the time when phage proteins and nucleic acids are synthesised but no phages have yet been assembled inside of the cell. This eclipse period is followed by a post-eclipse period when the phage progeny mature within the infected bacteria (Hyman and Abedon, 2009). It was observed that when the latent period decreased, the progeny production rate and burst size increased as the host growth rate also increased (You *et al.*, 2002). The release of phages ends the so-called constant period and starts the rise period that is always achieved with the burst of the bacterial host, using a phage-encoded lysis protein or a holin-endolysin system (Young, 1992a; Young *et al.*, 2000; Ing-Nang Wang *et al.*, 2000). This burst or yield can happen in one or two steps, with an eclipse period in between. The number of phages released per bacterial burst, as well as the time required for completion of the lytic cycle are all specific for each bacteria-host interaction, and this can be visualised in a one-step growth curve (Ellis and Delbruck, 1939; Hyman and Abedon, 2009). Lytic phages that have short latent periods and large burst sizes spread faster in bacterial populations, hence they are more successful evolutionarily (Abedon *et al.*, 2001; Chibani-Chennoufi *et al.*, 2004; Wang, 2006b). For example, phage T7 is a lytic bacteriophage that infects *E. coli* and produces approximately 100 progeny viruses per infected cell within 40 minutes at 30°C (Dunn *et al.*, 1983).

4.1.2 Lifecycle characteristics and stages

Bacteriophage life cycles are divided into lytic and lysogenic depending on their ability to integrate into the host genome. In terms of developing a bacteriophage treatment, the best candidates are those with lytic growth since these are more efficient in controlling bacterial populations without any exchange of genetic material between the bacteria and virus that may develop any defense mechanism against future phage infections. The infection cycle of virulent bacteriophages consists of an adsorption period,

virion attachment and nucleic acid uptake, latent period and virion release by disruption of the host membrane (Adams, 1959; Hyman and Abedon, 2009).

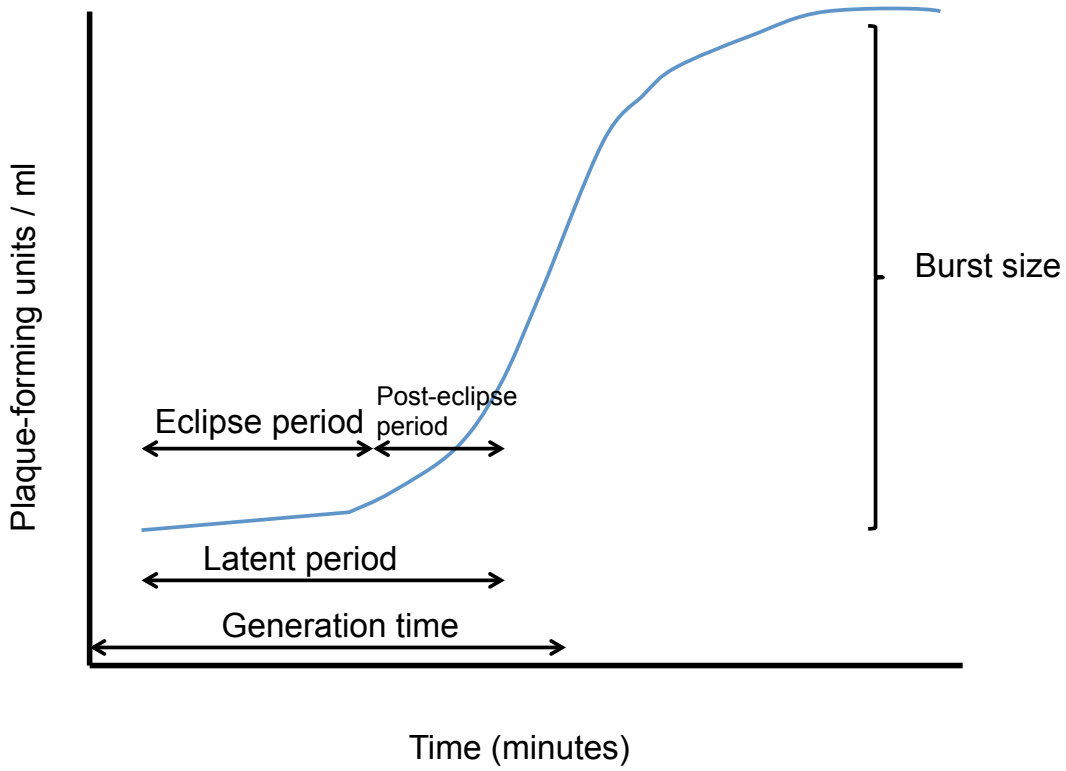

Figure 4-1: Diagram of a typical one-step growth curve. The generation time is the time that a bacteriophage takes to complete an infection cycle under optimal conditions, from its addition to the media to the first release of virions after infection. Within this generation time, the latent period comprises the moment a phage is attached to its host and/or its nucleic acid uptaken and lasts until the end of infection, upon viral release. The latent period can also be subdivided into the eclipse period or constant period when no viral particles are yet produced, but when phage proteins and nucleic acids are being synthesised, and it is followed by a post-eclipse period when the viral particles mature. The latent period and/or post-eclipse period are followed by a rise period, characterised by the release of virion progeny until the levels remain constant, the amount of virions released per phage infection is characteristic for the bacteriophage and bacteria tested and that is the burst size.

Adsorption is the point of contact between virus and host and starts the infection process, it shows host-range specificity and consists of three steps: initial contact, reversible binding and irreversible attachment (Duckworth, 1987). The first step requires random collisions caused by diffusion, flow dispersion or Brownian motion, during the second step the phage can still detach from the host, and the third step occurs between the bacterial receptor and the phage-binding domain, and it is irreversible (Kokjohn and Miller, 1992). The adsorption constant is the slope of the logarithm of free phages versus time (Hyman and Abedon, 2009) and measures the uptake of viral particles by their host, it follows a first-order kinetics (Krueger, 1931):

$$k = \frac{2.3}{Bt} \log \frac{Po}{P}$$

where k is the adsorption rate constant in ml/min, B is the concentration of bacteria in cfu/ml, t is the time in minutes, P_o and P are the original and the final phage titres in pfu/ml (Barry and Goebel, 1951).

Nonetheless, in some cases such as with lambda phage, ϕT4 and ϕT7, the decrease of free bacteriophages corresponds to a double-exponential function with a fast followed by a slower decay time; the fast decay depends strongly on bacterial concentration whereas the slower is a result of the interaction with their receptor; LamB for lambda phage (Schlesinger, 1932; Moldovan *et al.*, 2007; Kropinski, 2009). The requirements for optimal phage adsorption should be characterised as they depend on physical-chemical factors such as temperature, pH, osmolarity, electrolyte requirements (Ca^{+2} and Mg^{+2}), mixing conditions, glucose, ammonia, lipopolysaccharides on the bacterial membrane or if nutrient limitation is required for a protein to be expressed in the host membrane (such as OmpC for phage T4) (Nabergoj *et al.*, 2018).

After adsorption, the bacteriophage prepares to inject its DNA into the host cell and this process has been characterised in T4 and T7 phages. After binding to the host membrane lipopolysaccharides, the base plate of phage T4 modifies its structure forming a hole, then the outer sheath contracts and the internal tube creates a hole through the outer membrane, peptidoglycan and periplasm of the bacteria, the viral DNA is then injected in about 30 seconds (Trun and Trempy, 2003), within 1 to 3 minutes after infection the host DNA swiftly binds to the cell membrane and all host metabolism is inhibited (Kutter *et al.*, 2018). Close to the head-proximal end of the tail are six fibers, with a N-terminal domain that is attached to the tail and proximal and distal tail fibers, the latter being responsible for the interaction with the host (Steven *et al.*, 1988; Garcia-Doval and van Raaij, 2012). The core proteins are ejected through the portal-tail complex into the cell creating a trans-envelope channel used for DNA translocation (Molineux, 2001; Kemp *et al.*, 2005; Chang *et al.*, 2010) upon adsorption and it takes between 9 to 12 minutes (Zavriev and Shemyakin, 1982; Garcia *et al.*, 1995) to reach the bacterial cytoplasm as its tail cannot contract (Trun and Trempy, 2003).

Additionally it requires two phage proteins to be synthesized in a 4-minute process, after which these two proteins form a toroid structure that is responsible for the molecular mechanism that pulls the viral genome into the cytoplasm (Molineux, 2001; Kemp *et al.*, 2004; Chang *et al.*, 2010). *In vivo* tests have shown that all transcription during phage T7 infection is completed after 12 minutes (McAllister and Wu, 1978; Zhang and Studier, 1995).

It is established that phage early proteins interfere with bacterial proteins, hence affecting their host metabolism. Once this is achieved, the phage metabolic enzymes take over and catalyse the reactions that produce the metabolites needed for viral replication (Chevallereau *et al.*, 2016), such as nucleotide depolymerisation that are supplied for phage DNA synthesis. In addition, prevention of osmotic stress seems to be significant among phage clades (Matthews and Allen, 1983; Adriaenssens *et al.*, 2012; Chevallereau *et al.*, 2016). The enzyme deoxycytidine monophosphate (dCMP) hydroxymethylase was the first phage enzyme discovered that was involved in nucleotide production (Flaks and Cohen, 1957). It is made between 3 and 8 minutes after infection initiation and it is present in T-even phages that use nucleotides from their hosts (Matthews and Allen, 1983). This degradation of host DNA occurs between 6 and 20 minutes after infection in phage T4 and it is a two-step process where different exonucleases take part (Kutter, 1968), whereas in phage T7 this degradation occurs between 7.5 and 15 minutes after the start of infection (Sadowski and Kerr, 1970) when approximately 85% of the host DNA is degraded by the phage endonucleases and exonucleases (Sadowski and Kerr, 1970). Phages require not only protein and nucleic acid precursors, but also the translation machinery of the host to complete their life cycle as well as the DNA polymerase and its replisome to operate as an effective production-line complex (Matthews and Allen, 1983). The growth of phage T7 is highly dependent on ribosome numbers, thus the rate-limiting stage of this bacteriophage is the synthesis of phage proteins (You *et al.*, 2002), the next limiting factor is the host transcription rate that is directly linked to the concentration of EcRNAP (*E. coli* RNA polymerase), if both concentration levels are high the next limiting factor is the phage's own DNA synthesis (You *et al.*, 2002).

Late proteins are required for procapsid assembly, failure to produce these in required high levels will decrease the burst size (You *et al.*, 2002), this is also affected by cell volume, as larger cell volumes decrease concentrations of procapsid proteins and smaller cell volumes can decrease the rate of protein expression (You *et al.*, 2002).

4.1.3 Effect of external factors on phage infection development

Bacteriophages not only depend on the physicochemical conditions of their surroundings but also they depend on the physiological state of their hosts (Hadas *et al.*, 1997; You *et al.*, 2002; Golec *et al.*, 2014), that depend subsequently on the media used (Cohen, 1949; Heden, 1951; Hadas *et al.*,

1997), temperature (Ellis and Delbruck, 1939; Kutter *et al.*, 1994), oxygen tension (Kutter *et al.*, 1994) and any pretreatment (Cohen, 1949; Heden, 1951; Adams, 1959; Hadas *et al.*, 1997). An energised membrane is required for genome translocation but not for adsorption (Zimkus *et al.*, 1986; Kemp *et al.*, 2004; Hu *et al.*, 2013).

In the wild, bacteria are rarely in an exponential growth phase, although the bacterial growth rate is important as higher growth rates produce higher burst sizes in a linear relationship (You *et al.*, 2002). Despite this, the adsorption constant and the latent period decrease with higher bacterial growth rates (You *et al.*, 2002; Nabergoj *et al.*, 2018).

The effect of different MOIs under nutrient limitation conditions was also characterised in phage T4 (Bryan *et al.*, 2016): infection with low MOIs resulted in infection and killing of the host followed by a long senescence period when no phage production was observed, addition of glucose or casamino acids resulted in a fast production of progeny phage. On the other hand, the use of high MOIs allowed successful bacterial killing, characterised by a small burst size of about one phage per bacteria released between 120 and 180 minutes after infection and nutrient addition did no affect phage production. Despite this, the mechanisms that regulate this behavior are not yet understood though late-gene transcription in exponential phase is directly linked to DNA replication (Williams *et al.*, 1994; Geiduschek and Kassavetis, 2010).

4.1.2 Aims and objectives

The *in vitro* functional characterisation of bacteriophage infection is specific for each bacteriophage-host system, thus it is necessary their determination as part of their selection as biocontrol agents. Using the one-step growth curve (1SGC), phage adsorption and the OxoPlate® experiments to determine the kinetic properties of infection in optimal conditions, and the use of time-lapse microscopy to calculate the latent period in solid media for each phage-bacteria was carried out in order to aid in the differentiation between isolates. Ideally, bacteriophages with shorter latent periods and larger burst sizes would be selected as biocontrol agents, as these spread faster within a bacterial population (Abedon *et al.*, 2001; Chibani-Chennoufi *et al.*, 2004; Wang, 2006a).

4.2 Determination of phage infection kinetics

4.2.1 Determination of latent period and burst size using one-step growth curve

In order to determine the phage adsorption constant for each bacteriophage, a phage adsorption experiment was performed. After inoculation of bacteriophage to exponentially growing bacteria (*P. atrosepticum* SCRI 1043 was used for all the bacteriophages apart from ϕSFM010 when *P. atrosepticum* was used) to a MOI of 0.001, 1ml samples were taken every minute for the first 15 minutes and the amount of free phage remaining within the media was measured (see section 2.8.1 in Materials and methods). Phage levels remained constant throughout the sampling for all the isolates without a clear drop in numbers (data not shown), with these conditions it was not possible to determine the phage adsorption rate precisely.

To characterise the infection kinetics under optimal conditions, the one-step growth curve experiment was done. After inoculation of bacteriophage to exponentially growing bacteria (*P. atrosepticum* SCRI 1043 was used for all the bacteriophages apart from ϕSFM010 when *P. atrosepticum* was used) to a MOI of 0.001, two 1ml samples were taken every 20 minutes up until 4 hours: one of the samples was used to measure the free bacteriophages in the media and the other was mixed with 50µl of chloroform in order to measure the total number of phages. Similarly to what happened in the phage adsorption experiment, the results from the one-step growth curve have shown constant levels of phage throughout the duration of the experiment (4 hours in total) for most samples. Yet, results for phage ϕSFM002 gave a fast latent period of 15 minutes, followed by two bursts with a 45-minute eclipse period (a total rise period of 3 hours), and a burst size of 132 virions (Figure 4-2). Only 1SGC data could be retrieved for ϕSFM002.

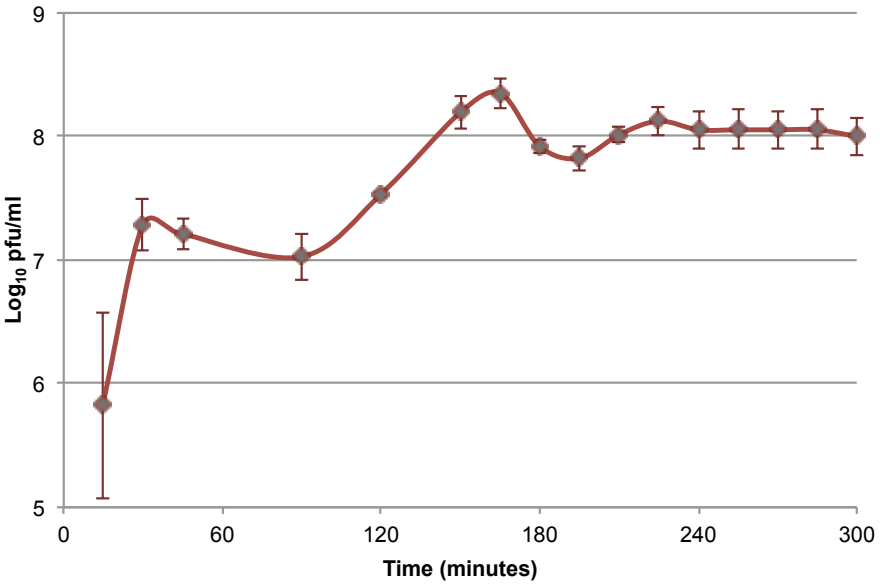

Figure 4-2: One-step growth curve obtained for ϕSFM002. 1ml samples were taken every twenty minutes after initial inoculation for up to five hours, each sample was then serial diluted 10-fold and spot-inoculated onto a bacterial lawn in triplicate.

4.2.2 Phage kinetics determination on solid media

To test the efficiency of bacteriophages in preventing bacterial growth on solid media, time-lapse microscopy was undertaken. An overnight grown bacterial suspension was mixed with a phage stock suspension (using a MOI of 1), spot-inoculated onto nutrient agar and placed onto the microscope. Images were taken every five minutes for up to 30 hours using 1000X magnification, processed using ImageJ software and plotted as bacterial number as a function of time (Section 2.8.2.2 in Materials and methods). When analysing each bacteriophage separately, ϕSFM001 cleared most bacteria 13 hours after the start and bacterial densities dropped for approximately 45 minutes (Appendix a, a and b), whereas ϕSFM002 only took 5 hours to lyse the bacteria and it lasted for 2 hours (Figure 4-3 a and b), ϕSFM003 had its main release approximately at 15 hours and cells continued bursting until the end of the experiment 15 hours afterwards (Appendix b, a and b), ϕSFM004 cleared most of their host approximately 10 hours after inoculation and this lasted until the end of the run over 20 hours later (Appendix c, a and b), ϕSFM005 displayed low bacterial lysis 20 hours after the start, until then bacterial were steadily growing on the agar (Appendix d, a and b). ϕSFM006 killed most bacteria from the start of the experiment, a few survivors grew for 22 hours until they were also burst (Appendix e, a and b), ϕSFM007 killed their hosts approximately 8 hours from the beginning of the experiment and it lasted for 2 hours (Appendix f, a and b), ϕSFM008 was released from the bacteria 8 hours from the start and bacteria kept bursting until the end of the run (over 22 hours) (Appendix g, a and b), during ϕSFM009 infection bacteria grew fast for the first 8 hours and they were constantly released until the end of the run 22 hours later (Appendix h, a and b), ϕSFM010 only slowed down bacterial growth slightly and these bacteria only started to burst 15 hours after the start of the experiment to remain more or less constant throughout (Figure 4-4 a and b), ϕSFM011 had its bacterial burst 13 hours after the beginning and this lasted until the end of the experiment (Appendix i, a and b), bacteria infected with ϕSFM012 grew for 17 hours until the phage was released from the infected hosts (Appendix j, a and b), bacterial populations recovered slowly with few isolated bursts until the end of the experiment, the calculated latent and rise periods using these methods are show together in Table 4-1.

Taken together the videos show that phages impaired bacterial growth and they showed common features of infection such as a similar pattern of initial and isolated bacterial bursts followed by a phase of bacterial growth and then another cycle of bacterial burst that killed most bacteria, followed by another cycle of bacterial growth. The bacteriophages isolated were effective in keeping bacterial densities low on solid media yet they never killed off their host completely.

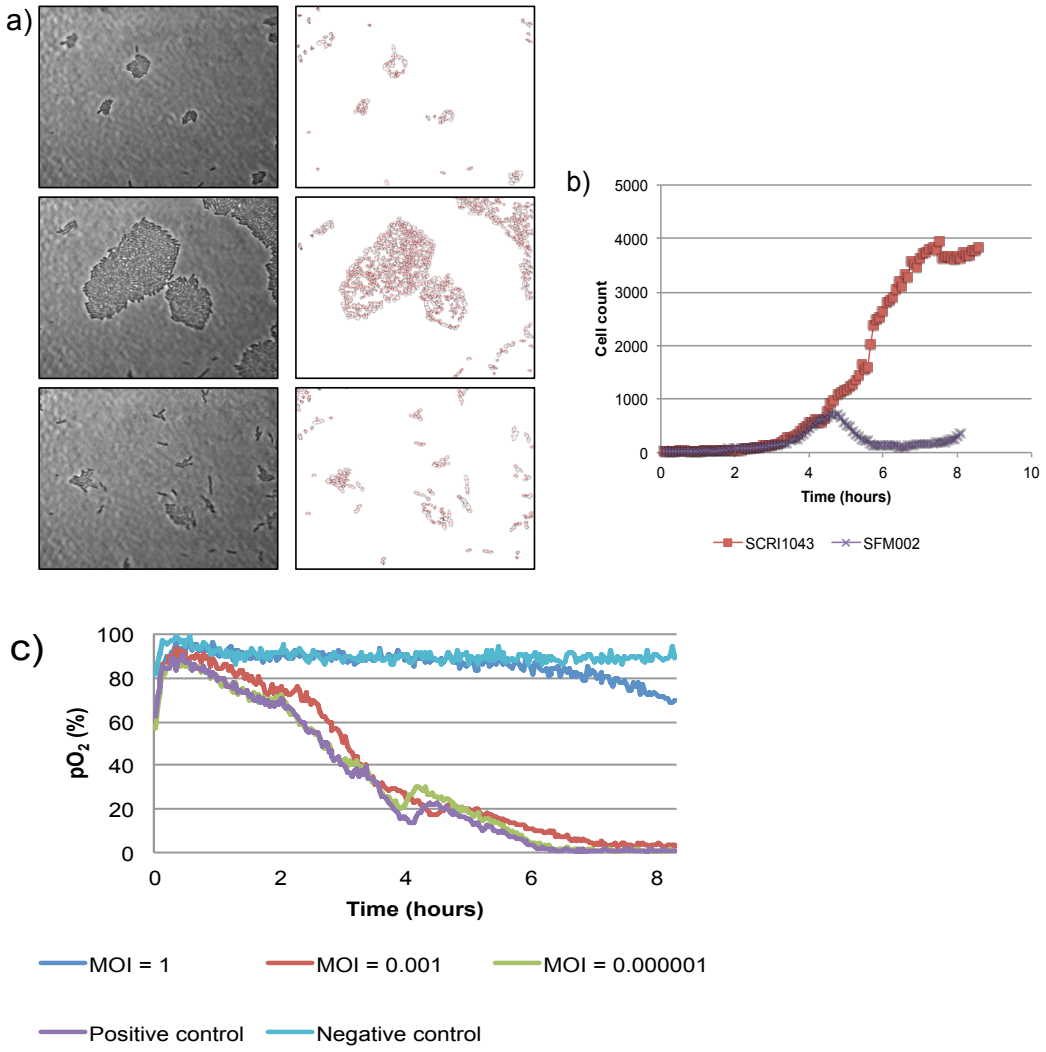

Figure 4-3: Infection kinetics on solid and liquid media experiments. (a) Images were taken every 5 minutes for up to 10 hours at 1000X magnification using a Nikon TE 2000S inverted microscope and a Hamamatsu Orca-285 Firewire Digital CCD Camera (left column images in a). These images were then processed and quantified using ImageJ 1.50i software (right column images in a) and the results were plotted and compared to a positive control using the growth of their host bacteria alone (red line, b). The OxoPlate® method (c) measured fluorescence intensity every 2 minutes for eight hours, the results were normalised and plotted as pO_2 (in percentage) per time point using *Pectobacterium atrosepticum* SCRI 1043 under the same conditions, being each value the result from six different readings. These were the results obtained from bacteriophage ϕSFM002.

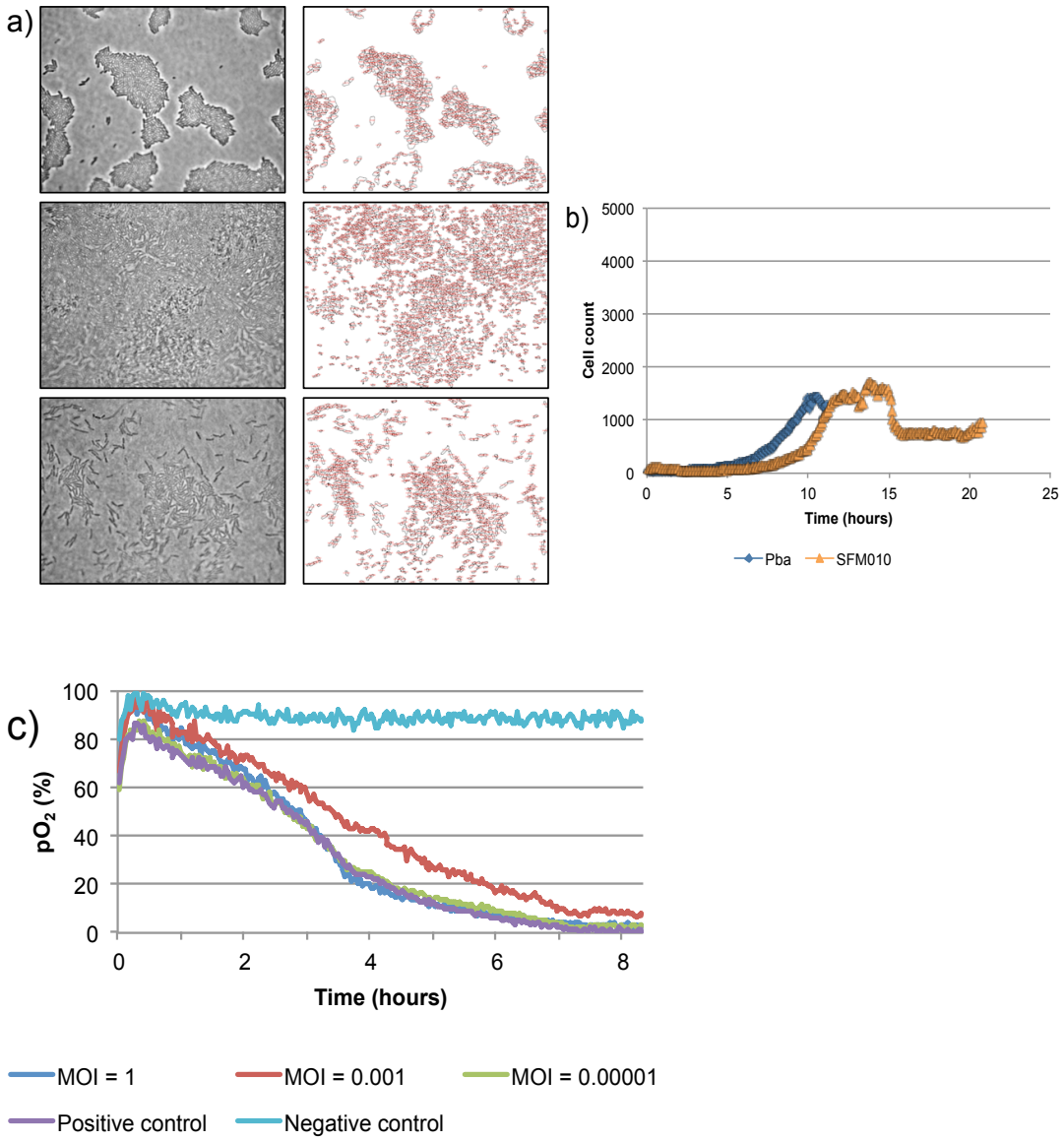

Figure 4-4: Infection kinetics on solid and liquid media experiments. (a) Images were taken every 5 minutes for up to 20 hours at 1000X magnification using a Nikon TE 2000S inverted microscope and a Hamamatsu Orca-285 Firewire Digital CCD Camera (left column images in a). These images were then processed and quantified using ImageJ 1.50i software (right column images in a) and the results were plotted and compared to a positive control using the growth of their host bacteria alone (blue line, b). The OxoPlate® method (c) measured fluorescence intensity every 2 minutes for eight hours, the results were normalised and plotted as pO_2 (in percentage) per time point using *Pectobacterium atrosepticum* SCRI 1043 under the same conditions, being each value the result from six different readings. These results were obtained from bacteriophage ϕSFM010.

4.2.3 Use of bacteriophages to prevent bacterial growth in liquid media

To ascertain the efficiency of each bacteriophage in controlling bacterial populations in liquid media and to test the best MOI the bacterial viability was measured. A bacterial inoculum in exponential phase was used (both *P. atrosepticum* SCRI 1043 and *P. atrosepticum* were used) and a phage stock using different MOIs (between 1 and 0.000001), the OxoPlate® experiment measured time-resolved fluorescence every 2 minutes for up to 9 hours at room temperature. Data from the experiment was normalised and the partial oxygen pressure (as a percentage) was calculated per time point for the average from 6 different replicates and plotted (Section 2.8.2.1 in Materials and methods). ϕSFM001 slowed bacterial growth slightly when using lower MOIs (0.01 and 0.0001) but no effect was seen when using MOI of 1 (Appendix a, c), the most effective MOI observed for ϕSFM002 was 1 (with no bacterial growth for the first 6 hours) and MOIs of 0.001 and 0.000001 only slowed bacterial growth: an initial burst happened 2 hours after inoculation that lasted for about 30 minutes when using MOI of 0.001 (Figure 4-3 c), all the MOIs used for ϕSFM003 impaired bacterial growth yet the best MOIs were 0.01 and 0.0001 (Appendix b, c), not a clear effect was seen when using ϕSFM004 for any MOI used (Appendix c, c) and a small decrease in growth compared to the positive control was seen for any MOI used with ϕSFM005 (Appendix d, c), medium and low MOIs were more effective against their host using ϕSFM006 though only small (Appendix e, c), ϕSFM007 also had a small effect on bacterial growth with any of the MOIs used although MOIs of 1 and 0.0001 were a bit more effective (Appendix f, c), only a small burst was observed 6 hours after the start of the experiment when using ϕSFM008 at MOI of 0.01 up until then there was no difference with the positive control (Appendix g, c) and a similar pattern happened when using ϕSFM009 but at the slowest MOI used (0.0001) (Appendix h, c), ϕSFM010 was tested on *P. atrosepticum* growth (Figure 4-4, c) and only the MOI of 0.001 had a clear effect on bacterial growth throughout as the other MOIs did not have an effect when compared to the positive control, whereas all MOIs used for ϕSFM011 were effective in a dose-response manner (Appendix l, c) being the highest MOI of 1 the most efficient, in the case of ϕSFM012, medium and lower MOIs were effective to a small degree though a clear effect was seen with MOI of 1 (Appendix j, c). The calculated latent and rise periods are shown for all bacteriophages in Table 4-1. In general, the effect of bacteriophages in liquid media was small and only affected bacterial growth briefly, on the other hand, bacteria grew slowly during this experiment and took 5 or more hours to start exponential phase with the exceptions of the ϕSFM002 and ϕSFM010 when growth started after 2 hours (as indicated by the decrease in pO_2), in both cases MOIs of 0.001 were the most effective as compared to MOIs of 0.00001, 0.000001 or 1.

	Solid media (microscopy)		Liquid media (OxoPlate®)	
	Latent period	Rise period	Latent period	Rise period
ϕSFM001	12	0.75	5.5	0.5
ϕSFM002	5	2	2	0.5
ϕSFM003	15	5	5	0.75
ϕSFM004	10	5	-	-
ϕSFM005	20	5	5	1
ϕSFM006	22	2	4.5	0.5
ϕSFM007	8	2	6.5	1
ϕSFM008	8	3	6	1
ϕSFM009	8	2	6	1
ϕSFM010	15	5	-	-
ϕSFM011	13	5	6	0.5
ϕSFM012	17	2	6	0.5

Table 4-1: Comparison between latent and rise periods using solid and liquid media. Comparison between liquid and solid media phage infection experiments: solid media results were from one replicate during time-lapse microscopy whereas liquid media results were from six replicates using the OxoPlate®, all results are shown in hours.

4.3 Discussion

The rate of phage adsorption is fundamental to phage ecology as it estimates the impact on cell populations (Kropinski, 2009). The results from the phage adsorption experiment have not shown a clear trend (data not shown), in most cases the titre reduction would not be pronounced and never below 10% of the initial inoculum as with ϕT7 (Barry and Goebel, 1951), instead there was a cyclical component of bacterial bursts followed by bacterial growth.

Generation of a one step-growth curve requires the synchronisation of phage infections, yet there seems to be some discordance regarding the MOIs to be used for this experiment, some research suggest that it is better to use MOIs lower than one to ensure that only one phage will infect the host and to avoid subsequent phage adsorption, thus a 100-fold dilution of the growth media is suggested (Hyman and Abedon, 2009), other groups have used higher MOIs of 1 (Wei *et al.*, 2017). It may be that different bacteria require different MOIs, as seen with the OxoPlate® experiments. The only one-step growth curve shown was obtained without the media being diluted 1:100. The MOIs used could have been far too low for these experiments creating a Poisson distribution after the serial-dilution that made the results oscillate greatly. The one-step growth curve also depends on the development of a productive infection, the time required for these to become visible along with the manual handling required carries over some error, in the case of ϕSFM010 no results were obtained as the bacterial lawn did not grow enough and the plaques were too small to be quantified. In addition, most of the one-step growth curves are shown in log base 10 against time (Hyman and Abedon, 2009; Brown *et al.*, 2016; Gao *et al.*, 2018) while others are shown as relative burst size against time (Jun *et al.*, 2016; Wei *et al.*, 2017), we have chosen the first option as is the most common in the literature.

The results from phage ϕSFM002, with a latent period of 15 minutes and a total burst size of around 132, differ greatly from those of phage T7, with a latent period between 30 and 50 minutes and a burst size of approximately 200 (You *et al.*, 2002; Xiaoxue Wang *et al.*, 2012). None of the other *Pectobacterium* phages have been yet characterised for their kinetic properties.

The use of OxoPlate® and time-lapse microscopy experiments helped to understand how the infection develops from the point of view of the host, both methods were easy to set-up and they can give results in real-time, the disadvantages include the impossibility of incubating the culture at lower temperatures (in this case at 20°C) and that no phage quantification could take place, therefore no eclipse and/or burst size determination was possible. Also, the impossibility to accurately measure the bacterial number during the time-lapse microscopy limits the usage of this instrument to certain bacterial densities as both contrast and cell size changed as the experiment

developed and the image analysis software could only measure at a set threshold, this underestimation of infected cells has already been reported elsewhere (Culley *et al.*, 2016). By use of the OxoPlate®, it is possible to test different MOIs and bacteria under the same conditions, but some of the experiments did not show that the bacteriophage used was clearly lytic as seen using other methods; this may be due to poor bacterial growth at the time or an example of phage-insensitivity (Sanders and Klaenhammer, 1984; Danis-Wlodarczyk *et al.*, 2015). The results obtained could not be compared to other methods as they used different settings, liquid and solid media or mixing and static conditions, but they provide a reference as how infection develops over time.

All the time-lapse microscopy experiments had common features: an early first burst of isolated bacteria, followed by the growth of other colonies that would eventually disappear in a second main burst that lasted beyond the end of the experiment in many cases. The first burst suggests that phages do infect the bacteria very early on, perhaps within the 10-20 minutes taken, to set up the experiment, thus the phage adsorption experiment should have shown a decrease in the number of viral particles within this time frame. The latent period after the first burst was extremely long, and this could be due to the experiment being undertaken in solid media, which should reflect field conditions more than when using liquid media, in fact the lack of results from liquid media could derive from the high shear forces of this environment that difficult their reversible first adsorption. In some of the videos it was clear that some bacteria stopped or slowed down growth (data not shown), rather unlikely from nutrient depletion as other neighboring bacteria did overgrow them without slowing down their growth. The “hibernation” mode refers to a persister but reversible dormant state, when the bacteria produce some phage enzymes, and slow phage development until some nutrients become available to resume phage production (Nabergoj *et al.*, 2018). These dormant bacteria could result from a phage infection and perhaps enact defense mechanisms to slow their metabolism or stop it altogether. On the other hand, the second burst happened like a coordinated event in many cases, suggesting that the release of phage-encoded molecules by infected bacteria could happen in a quorum-sensing manner (Erez *et al.*, 2017).

Efficacy of phage treatment increased when using higher phage titres in previous studies, and it was suggested that phage-resistance rates were higher when using higher MOIs; this is indicative of phage-bacteria interactions (Carvalho *et al.*, 2010). Recently, it was observed that high MOIs helped phages to complete the infection process when they encoded anti-CRISPRs and their respective hosts CRISPRs, but this was not necessary when the host lack CRISPR-Cas immunity, so low MOI ended in a successful viral replication (Borges *et al.*, 2018). This mechanism consisted of a first wave of infection when phage succumbed to the host CRISPR-Cas system but still got to deliver the anti-CRISPR proteins that immunosuppressed the bacteria, leaving it susceptible to a second wave of infection (Landsberger *et al.*, 2018). In other work, phage treatment was effective in controlling

bacterial populations, yet after 24 hours bacterial regrowth was observed due to the selection of resistant variants (Luria and Delbrück, 1943; Pires *et al.*, 2011; Oechslin *et al.*, 2017).

4.3.2 Future work

The completion of phage-adsorption and one-step growth curve experiments should be the main priority, as well as to obtain biological replicates for time-lapse microscopy. For the one-step growth curve, using quantitative real-time PCR (qPCR) for enumerating phage particles instead of using a traditional plaque assay would increase the sensitivity (Anderson *et al.*, 2011), though previous design of specific primers for each bacteriophage should be done and this can only be achieved when phage genomic sequencing is completed. As an alternative, there are other automated methods that measure virus replication using plate-reading fluorescence microscopy (Culley *et al.*, 2016).

There are a few points that could be addressed to help understand the interactions between phage and host. For example, bacteriophages must find a functional receptor to avoid unspecific binding, therefore it is advantageous to find the membrane receptor that our phages bind to, for example, phage T7 has been reported to bind to membrane lipopolysaccharides (Lindberg, 1973), but also to the proteins FhuA and TonB (Rakhuba *et al.*, 2010), this was achieved through molecular characterisation. Also, to understand the possible effect that temperature has on the receptor, if it produces conformational changes like being well dispersed throughout the bacterial membrane at high temperatures or by aggregating into a single patch at low temperatures (Moldovan *et al.*, 2007), this would help the development of predictive models of virulence under certain conditions.

In order to understand the phage-host interaction upon infection, the use of ^{14}C- or ^{35}S-labelled amino acids can elucidate what proteins are being produced in a given time period, this technique together with the two-dimensional (2D) polyacrylamide gel electrophoresis technique (O'Farrell, 1975) was effective in identifying many encoded proteins by phage T4 (Kutter *et al.*, 2018). For example, the use of ^{14}C-labelled mixed amino acids instead of ^{35}S-labelled methionine and cysteine helped to know the exact ratios of all the different proteins in early T4 infection (Kutter *et al.*, 2018) such is the case of the internal protein I, II and III that are highly synthesised early in infection and also during late expression, when the structural proteins are made (Kutter *et al.*, 2018). Recent whole-transcriptome studies using RNA-sequence (RNA-Seq) data have improved gene annotations, finding of regulatory elements and clarification of temporal transcriptome patterns, as well as the effect on host transcription regulation after viral infection (Ceyssens *et al.*, 2014; Chevallereau *et al.*, 2016; De Smet *et al.*, 2016).

It has been reported that resistant cells can be lysed by phages in the presence of sensitive cells, this acquisition of sensitivity (ASEN) provides a previously unidentified route for horizontal gene transfer. As bacteria in nature coexist in multispecies communities this may be a common occurrence (Tzipilevich *et al.*, 2017), from the release of phage-encoded holins that break down the host membrane and posterior release of mature virions (Calendar and Abedon, 2005). A similar experiment should be performed to determine the possibility of horizontal gene transfer in this manner, and measure the consequences that a phage-based treatment could have for the surrounding plants and microsystems treated, and subsequently to the environment. Studying phage infection under different conditions more similar to those encountered in nature, including anaerobic conditions, stationary phase of growth and/or use of different bacteria will help the development of mathematical models.

5.0 Results

De novo sequencing and comparative genomics of *Pectobacterium* spp. bacteriophages

5.1 Introduction

5.1.1 General characteristics of bacteriophage genomes

Morphological and infective characteristics of phages are not enough either for classification or for use as a biological control agents, thus genomic sequencing is required. Phage genomes present a modular organisation (Hendrix *et al.*, 2000; Hendrix *et al.*, 2003), and mosaicism is very common, with individual or groups of genes present in unrelated bacteriophages as a result from horizontal gene transfer during evolution.

The infective process is a choreographed event (Lee and Richardson, 2011) that involves a co-ordinated event of protein synthesis. Once the phage genome enters the cytoplasm, it down-regulates cellular functions and reprograms the bacterial cell for production of viral progeny. During phage T7 infection, the denominated early genes or class I are transcribed and translated by the host RNA polymerases and ribosomes, these include proteins that degrade the cytosine-containing host DNA (Trun and Trempy, 2003) and in general terms they serve to establish favourable conditions in the host for phage infection. Middle genes or class II are involved in DNA metabolism and T7 RNA polymerase recognises middle and late stage-specific promoters to initiate transcription (Savalia *et al.*, 2010). Late or class III proteins are involved in DNA packaging, virion assembly and lysis functions (You *et al.*, 2002). The major capsid protein (gp10A, Figure 5-1 a) is specially important as it is required in the largest quantities for each T7 virion (Steven and Trus, 1986). Procapsid assembly and packaging of phage DNA by terminases are the last stages before virion release.

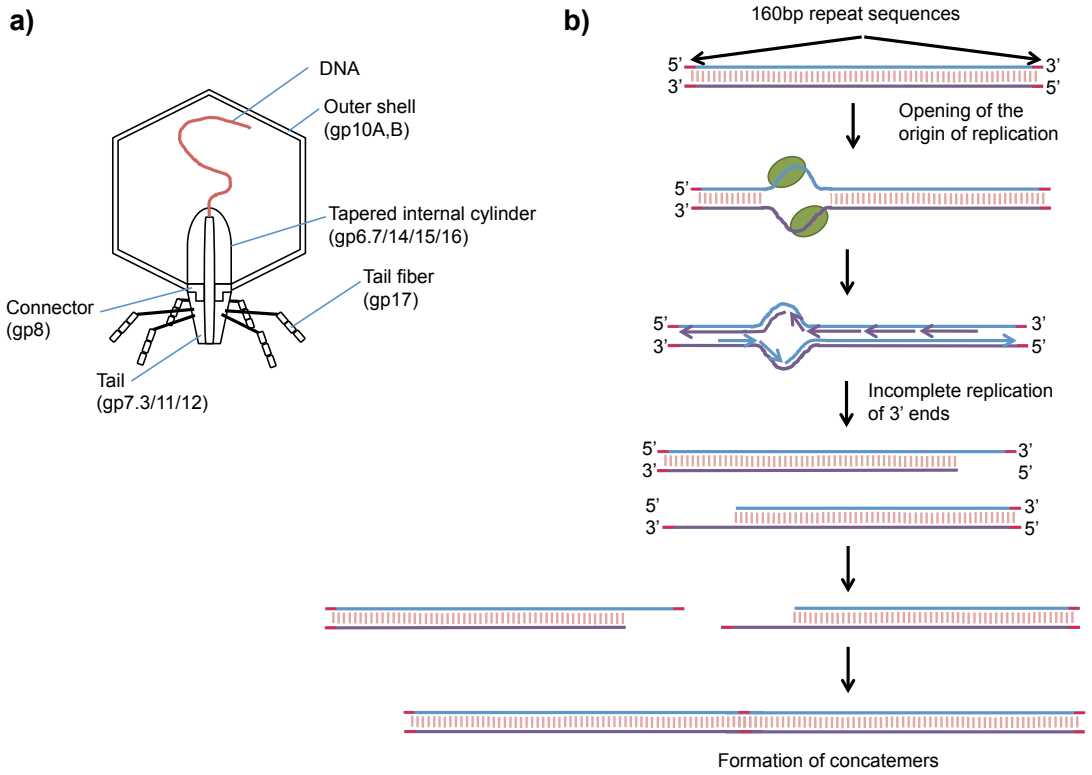

Figure 5-1: a) External structure of ϕT7. All components that conform the virion structure of phage T7 and their correspondent gene product (gp) numbers, within the genome each component appears in ascending order as part of the late genes. Once transcribed they will assemble to create an "empty shell" or procapsid that will be filled with a newly-transcribed phage DNA genome by the telomerase (adapted from Serwer *et al.,* 2008).

b) Linear replication mode typical of T7-like phages. Phage T7 has a linear dsDNA genome with 160bp short direct repeats on both genome ends, the viral replisome opens both strands at the origin of replication and starts the replication that is bidirectional, leaving incomplete replication at both 3' ends which is rapidly finished by the viral DNA polymerase and DNA ligase, the end result is a concatemer that contains between 5-10 complete genomes ready to be translocated to empty procapsids. Adapted from Chaconas and Chen (2005) and viralzone.expasy.org website from the SIB (Swiss Institute of Bioinformatics).

5.1.2 Methylation of phage DNA

The genomes of lytic phages are highly methylated to overcome the restriction-modification system in their hosts (Klumpp *et al.*, 2012). Approximately 90% of bacterial and archaeal genomes include genome-encoding restriction-modification (R-M) systems (Roberts *et al.*, 2015), their main function is to recognise and target any foreign DNA with restriction enzymes and to protect its own DNA by using methyltransferase (MTase) activity. There are four types of R-M systems (I, II, III and IV) that differ in the functional arrangement of the restriction endonuclease and the methyltranferase activities and the requirement for specific subunits and cofactors (Wilson and Murray, 1991). The type I R-M systems are formed by three subunits: the S or specificity subunit, the M or methyltransferase subunit and the R or restriction endonuclease subunit (Murray, 2000). The type II R-M systems are the most common and they normally work as two different proteins (Sistla and Rao, 2004). Type III R-M systems are formed by the product of at least two different genes, *res* and *mod* (Bickle and Kruger, 1993; Su *et al.*, 1999). The type IV R-M systems have both methyltransferase and endonuclease activities combined in a single enzyme (Janulaitis *et al.*, 1992; Lepikhov *et al.*, 2001). These R-M systems may be obtained by the phage through horizontal gene transfer (Jeltsch and Pingoud, 1996) and they can play a role in regulating host functions (Messer and Noyer-Weidner, 1988).

5.1.3 Bacteriophage DNA replication

Phage T7 is a model for DNA replication and it is bidirectional on a linear DNA molecule (Figure 5-1 b), three of the phage proteins along with a host protein serve as a functioning replisome (Figure 5-2) (Lee and Richardson, 2011). During replication, the helicase domain of the primase/helicase protein (gp4) unwinds dsDNA to supply the DNA polymerase (gp5) with a ssDNA template. The leading strand is synthesised continuously by the DNA polymerase in conjunction with host thioredoxin. At the same time, the primase domain synthesizes the oligonucleotides used as primers for the synthesis of Okazaki fragments (Lee and Richardson, 2011). T7 ssDNA-binding protein (gp2.5) has many functions, on one side it is essential in the coordination of the synthesis of leading and lagging strands (Lee *et al.*, 1998), but also binds to the complex DNA polymerase/host thioredoxin and allows them to catalyse strand-displacement DNA synthesis (Lee and Richardson, 2011). Both DNA polymerase and the ssDNA-binding protein contain a phenylalanine in the C-terminal tails, this increases their affinity as proved by suppressor mutation experiments (Ghosh *et al.*, 2009).

After replication of late genes, DNA packaging is accomplished in a directional process in all tailed phages characterised so far (Li *et al.*, 2014). Genome packaging is initiated by the packaging enzyme after recognition of a specific packaging site on the concatemeric DNA and cut at or near the site

(pac for ϕT4, ϕSPP1 and ϕP22 and *cos* for ϕT7, ϕT3 and ϕλ). In the *cos* mode of phage DNA packaging the cleavage sites are more specific and the packaging lengths are more accurate (Catalano *et al.*, 1995; Fujisawa and Morita, 2003), whereas the headful mode (*pac* mode) does not always have sequence specificity (Fujisawa and Morita, 2003; Casjens *et al.*, 2005). The terminase gene consists of a small subunit that cleaves the DNA and a larger subunit that contains a prohead-binding activity: with an ATPase activity that translocates the cleaved DNA into the prohead in only one direction from the cleavage point, and a nuclease activity which cuts the concatemeric DNA and generates the genome terminus (Sun *et al.*, 2012). Phages such as T7 and T3 contain termini with short direct repeats (SDR), these are a few hundred base pairs long and non-permuted (they are the same in every virion chromosome) (Casjens and Gilcrease, 2009).

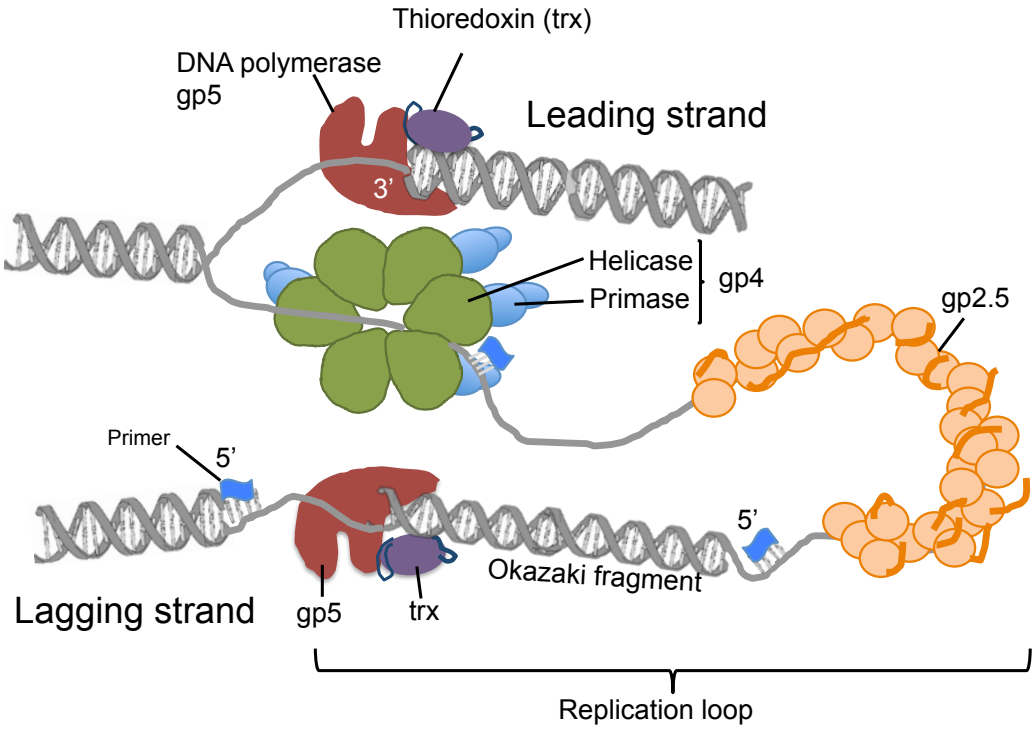

Figure 5-2: Model of the ϕT7 replisome. The phage T7 replisome consists of four proteins: DNA polymerase (gp5) and its processitivity factor, the host thioredoxin (trx), single-stranded DNA-binding protein (gp2.5) and the bifunctional DNA primase/helicase (gp4). The lagging strand forms a loop so that the replication proteins in both strands can touch. The active form of the helicase/primase protein is hexameric and binds to ssDNA, hydrolyses nucleotides, translocates on ssDNA and separates dsDNA (adapted from Lee and Richardson, 2011 and Kulczyk *et al.,* 2017).

5.1.2 Aims and objectives

To sequence the complete genomes of the isolated bacteriophages was the main objective before pursuing any plant treatment, as it would inform on the replicative properties and the real differences between each other and with other *Pectobacterium* phages.

General genomic features such as genome size, GC content, number of coding sequences or presence of tRNA will help determine the main differences between the phages. Analysis of the GC skew in adenoviruses ass found to switch polarity close to replication origins and it changes linearly across the linear genomes (Grigoriev, 1999). For example, in the papillomavirus genome, the GC skew is positive in one half and its close to zero in the other half (Grigoriev, 1999). The examination of the GC skews could point out the origins of replication and the terminus location of the phage genomes.

The use of different genomic comparison tools such as dot plot analysis allows the comparison of all genomes in one graphic. Genomic dot plot analysis consists of placing the nucleotide sequences across both the X- and Y-axis: a dot is placed where the sequences are identical, and results in a diagonal line down the centre of the plot when a sequence is compared to itself.

The analysis of coding regions can elucidate the lifestyle of the bacteriophages. For example, the detection of the ability to integrate in the host genome by the presence of integrases, the presence of bacterial toxin genes or virulence factors that can induce toxicity in the host or its environment upon infection, and the type of different endolysins that would explain the lysis mechanism.

Finding host defense mechanisms in the form of modified bases or the presence of DNA methyltransferases in the genome. Thus altering the host restriction-modification, but also inhibitor of toxin/antitoxin systems, the presence of auxiliary metabolic genes (AMG) or host- derived genes that may facilitate viral production (Rohwer and Thurber, 2009; Breitbart, 2012) or limit the host range (Verheust *et al.*, 2010) can explain how the infective cycle develops.

By establishing the DNA termini of the genomes, we might confirm the DNA replication mechanism and the DNA packaging method. The determination of genomic termini needs to be analysed together with restriction enzyme analysis, since short direct repeats will result in equimolar fragments that will not be altered by heating and cooling as with *cos* sites (Casjens and Gilcrease, 2009).

Another analysis involves the genomic comparison of our isolates: current guidelines for defining a phage species suggest that any two bacteriophages with an average nucleotide identity (ANI) > 95% should be considered the same species (Adriaenssens and Brister, 2017).

All soft rot enterobacterial phages sequenced to date contain dsDNA (Czajkowski, 2016a). TEM analysis of our phages included them as part of the *Podoviridae* family (section 3.2.3 in chapter 3). Moreover, phages of the subfamily *Autographivirinae* encode for an RNA polymerase (Lavigne *et al.*, 2008), and includes seven Genera: *Phikmivirus*, *Kp32virus*, *Kp34virus* (Eriksson *et al.*, 2015), *Sp6virus*, *Fri1virus*, *Pradovirus* and *T7virus*. The presence of a phage RNA polymerase will place our phages in this subfamily, and by producing a phylogenetic tree including the main representative viruses from each genera we can classify the phages up to this level.

Phylogenetic analysis will also position our phages with respect to other *Pectobacterium* phages and even other *Enterobacteria* phages. The introduction of the small subunit rRNA as a phylogenetic marker enabled a better understanding of diversity and role of bacterial communities (Fox *et al.*, 1980; Lane *et al.*, 1985; Hugenholtz *et al.*, 1998). There is no such conserved protein or gene that allows the classification or characterisation of phages, as an example, the polymerases only worked for several viral families (Culley *et al.*, 2003; Breitbart *et al.*, 2004), and there is not a single protein present in all phages (Rohwer and Edwards, 2002). The more characters that two or more organisms share, the more closely related that they are, this is why more approaches are based on the comparative analyses of one or more genes, like the terminase sequence (Serwer *et al.*, 2004; Casjens and Gilcrease, 2009; Lim *et al.*, 2014), polymerase genes (Buttimer *et al.*, 2018), structural genes (Chibani-Chennoufi *et al.*, 2004), or whole proteomes (Rohwer and Edwards, 2002; Lavigne *et al.*, 2009) have been proposed to classify phages. A phage proteomic tree summarises many morphological aspects used for ICTV classification (Rohwer and Edwards, 2002), and it would reflect any genetic recombination between phage groups within the same environment (Hendrix *et al.*, 1999) as well as it would reveal any common ancestors (Rohwer and Edwards, 2002), because nucleotide sequences diverge more quickly.

5.2 Characterisation of bacteriophage genomes

For the purpose of deciphering the lifecycle, presence of toxins and/or determining the closest model bacteriophage to our isolates, genomic sequencing was performed. All twelve bacteriophages were sequenced over a period of 2 years, during this time, the DNA isolation method was changed and the sequencing protocol improved. Bacteriophages ΦSFM002 and ΦSFM003 were sequenced first; the phenol-chloroform method (see section 2.9.1 in Materials and methods) was used to isolate their DNA and both were sequenced within the same sequencing chip, whereas the remaining bacteriophages had their DNA extracted using a commercial kit (see section 2.9.2 in Materials and methods) and were all sequenced using two sequencing chips.

5.2.1 General genomic features of the isolates

With the purpose of comparing all twelve samples, once the genomes were trimmed and assembled their general genomic features could be investigated. Through the use of restriction enzyme digestions and the use of different software programs, the general genomic features were determined (see section 2.13.7 in Materials and methods). Based on restriction enzyme analysis, all genomes had circular (Figure 5-3, a to d), dsDNA, with no cos ends and with short direct terminal repeats (DTR) of just over 200bp (Figure 5-4, a and b), with sizes ranging between 39865 (ΦSFM003) and 40538bp (ΦSFM010) and coverage ranging from 7 (ΦSFM008) to 285 (ΦSFM011) (Table 5-1). These results mean that these isolates very similar to each other and comparable to ϕT7 as it also contains short terminal repeats.

a)

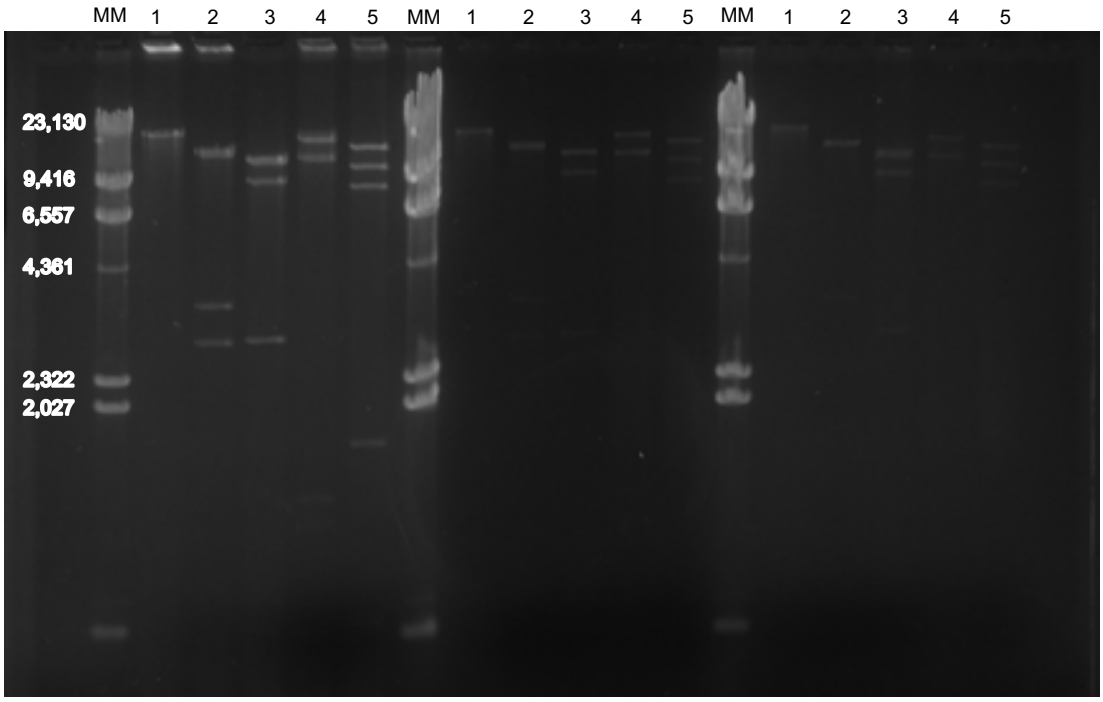

Figure 5-3 (a): RE digestion profiles of ϕSFM001 (first 5 sample columns), ϕSFM002 (second 5 sample columns) and ϕSFM003 (last 5 sample columns). MM: molecular marker is λ HindIII for all the gels, and all the restriction enzymes are in the same order: 1 is PacI, 2 is BsshII, 3 is BglII, 4 is AvaI and 5 is SpeI. 0.5µg of phage DNA sample were used per RE digestion, and it was left incubating for 2-3 hours at the required temperature, the 1% gel was run for 5-6 hours.

b)

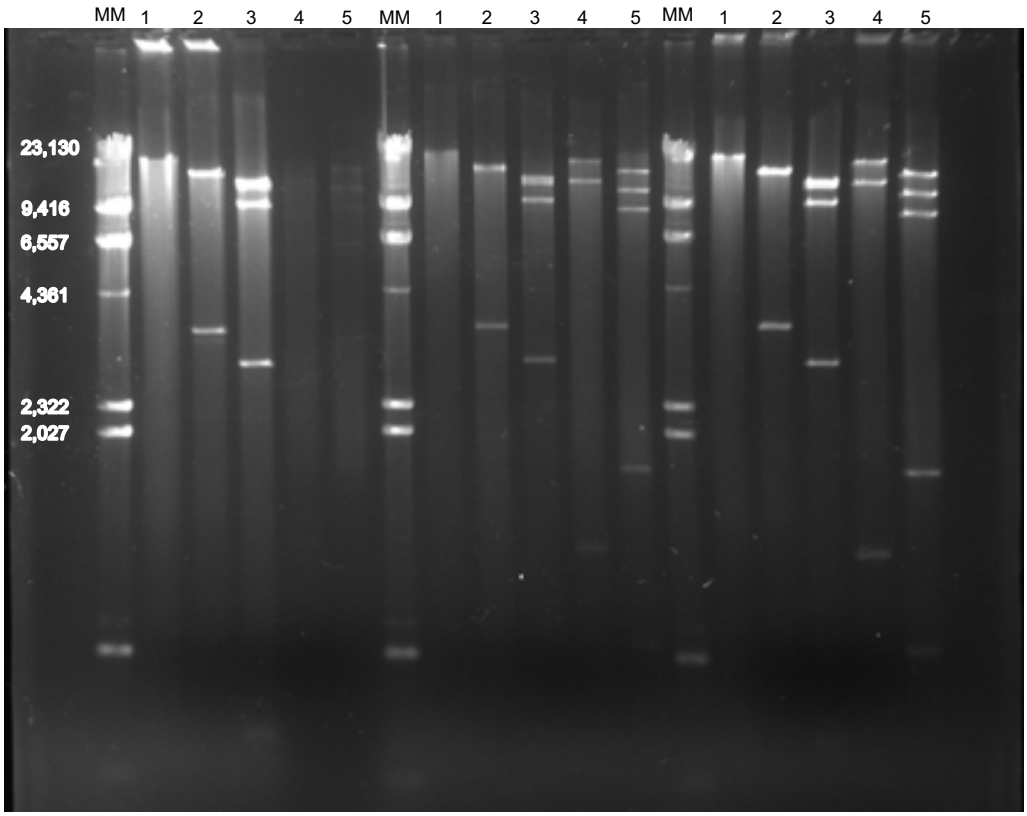

Figure 5-3 (b): RE digestion profiles ϕSFM004 (first 5 sample columns), ϕSFM005 (second 5 sample columns) and ϕSFM006 (last 5 sample columns). MM: molecular marker is λ HindIII for all the gels, and all the restriction enzymes are in the same order: 1 is PacI, 2 is BsshII, 3 is BglII, 4 is AvaI and 5 is SpeI. 0.5µg of phage DNA sample were used per RE digestion, and it was left incubating for 2-3 hours at the required temperature, the 1% gel was run for 5-6 hours.

c)

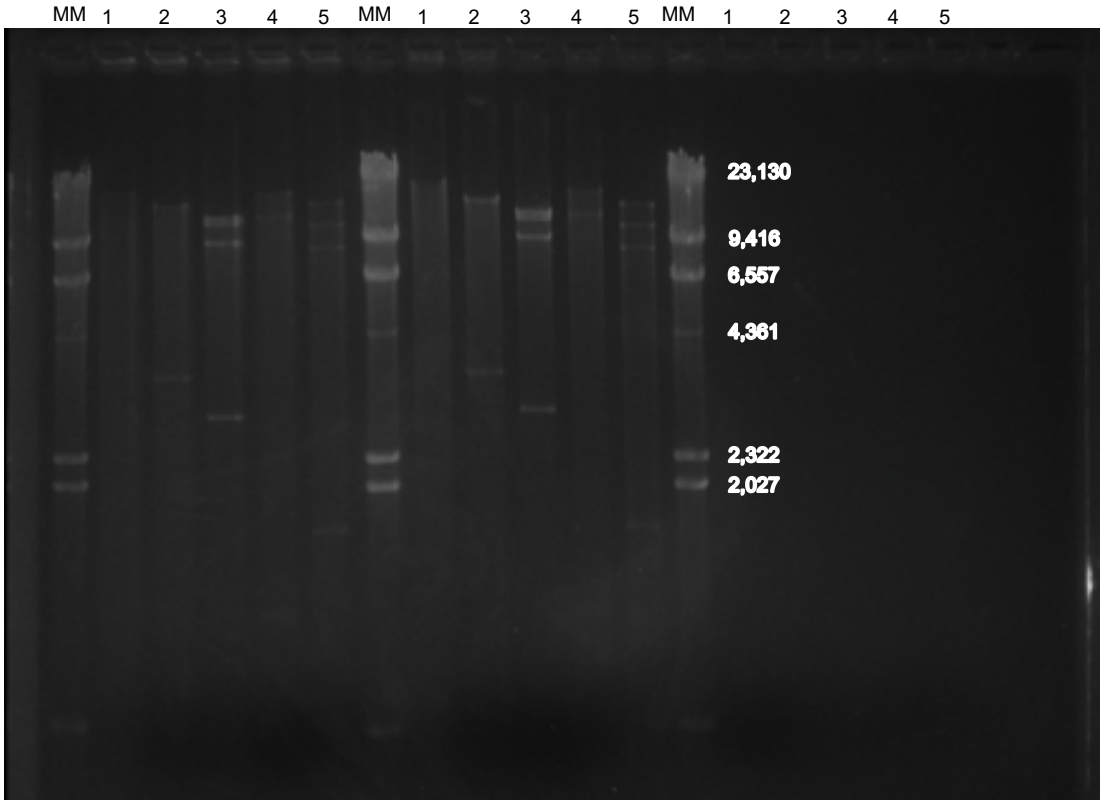

Figure 5-3 (c): RE digestion profiles of ϕSFM007 (first 5 sample columns), ϕSFM008 (second 5 sample columns) and ϕSFM009 (last 5 sample columns). MM: molecular marker is λ HindIII for all the gels, and all the restriction enzymes are in the same order: 1 is PacI, 2 is BsshII, 3 is BglII, 4 is AvaI and 5 is SpeI. 0.5µg of phage DNA sample were used per RE digestion, and it was left incubating for 2-3 hours at the required temperature, the 1% gel was run for 5-6 hours.

d)

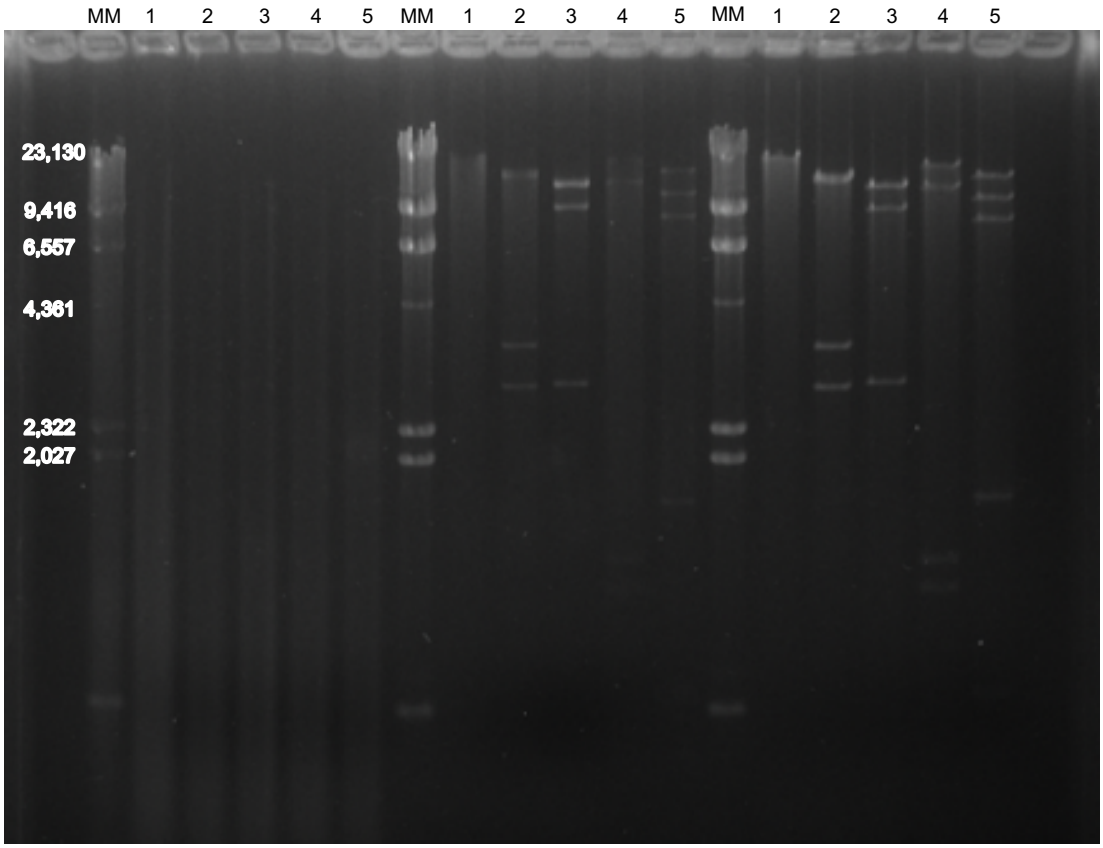

Figure 5-3 (d): RE digestion profiles of ϕSFM010 (first 5 sample columns), ϕSFM011 (second 5 sample columns) and ϕSFM012 (last 5 sample columns). MM: molecular marker is λ HindIII for all the gels, and all the restriction enzymes are in the same order: 1 is PacI, 2 is BsshII, 3 is BglII, 4 is AvaI and 5 is SpeI. 0.5µg of phage DNA sample were used per RE digestion, and it was left incubating for 2-3 hours at the required temperature, the 1% gel was run for 5-6 hours.

a)

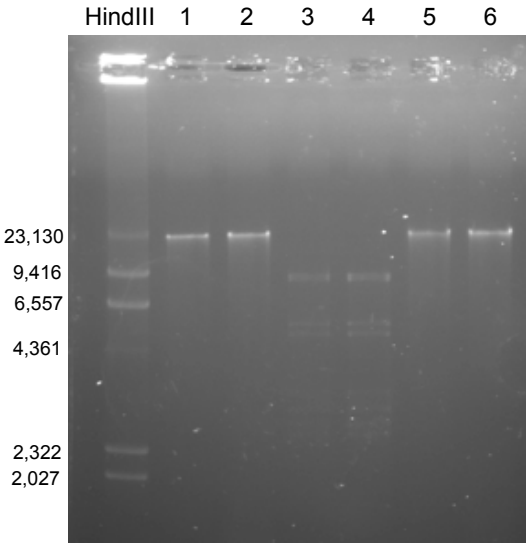

b)

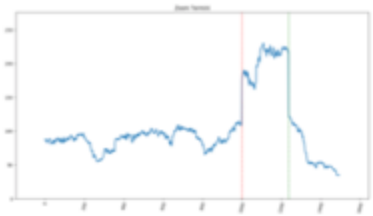

Statistical Method

Ends	Left (red)	Right (green)	Permuted	Orientation	Class	Type
Redundant	Preferred	Preferred	Yes	NA	DTR (short)	-

**Direct Terminal Repeats: 238 bp*

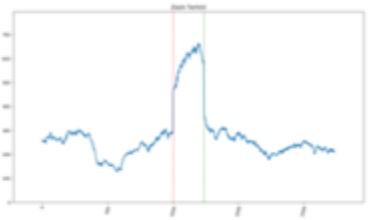

Statistical Method

Ends	Left (red)	Right (green)	Permuted	Orientation	Class	Type
Redundant	Preferred	Preferred	Yes	NA	DTR (short)	-

**Direct Terminal Repeats: 238 bp*

Figure 5-4 (a and b): Terminus analysis using HindIII and PhageTerm analysis. a) 1% gel using λ HindIII as a marker and restriction enzyme digestions using BamHI (lanes 1 and 2), EcoRI (lanes 3 and 4) and PstI (lanes 5 and 6) to digest the ϕSFM001 genome. The second digested sample (lanes 2, 4 and 6) was incubated at 70°C for further 10 minutes in order to determine *cos* end presence. b) PhageTerm analysis of phage ends disclosed the terminus characteristics and packaging mode of our isolates.

Phage name	Size (bp)	Coverage	GC content (%)	Predicted genes (PROKKA)
ΦSFM001	40329	133	50.2	47
ΦSFM002	40315	24	50.2	49
ΦSFM003	39865	103	50.2	53
ΦSFM004	39882	98	50.2	46
ΦSFM005	39882	80	50.2	46
ΦSFM006	39882	132	50.2	46
ΦSFM007	39882	45	50.2	46
ΦSFM008	40047	7	50.2	46
ΦSFM009	39898	184	50.2	47
ΦSFM010	40538	191	50.2	47
ΦSFM011	40329	285	50.1	47
ΦSFM012	40335	8	50.2	49

Table 5-1: The general genomic characteristics. After trimming of the samples, genome size and G + C content were determined, and several programs were used for annotation, including PROKKA, FGenesV, Glimmer and RAST.

The average GC content of these genomes was 50.2 (all apart from 50.1 in ΦSFM011), which was the same GC content associated with the host bacterium *P. atrosepticum* at 50-51% (Bell *et al.*, 2004), like ϕPP1 (Lee *et al.*, 2012), ϕPP2, ϕPPWS1 (Hirata *et al.*, 2016b) and ϕPeat1 (Kalischuk *et al.*, 2015) that also infect *Pectobacterium* spp.. Thus, the G+C content of all the genomes closely matched their host. Detection of any tRNAs in the genome was done using the programs ARAGORN and tRNA Scan-SE. No tRNAs were revealed, that indicated that all the bacteriophages used similar amino acids to their bacterial hosts (Delesalle *et al.*, 2016).

Presence of bacterial toxins in the phage genome is indicative of mobility of genetic elements within prophages (Abedon and Lejeune, 2007). It was analysed using the BTXpred server (see section 2.13.7 in Materials and methods). No bacterial toxins were found, thus all the bacteriophages were safe for use as a biocontrol agent as no known toxins or virulence factors could be released to the environment.

In order to determine the number and function of all the coding sequences in each phage genome, different software was used and every open reading

frame (ORF) was manually checked for protein function and/or structure using BLASTP, Pfam and InterProScan, and the coding sequences obtained from PROKKA were chosen over the others (RAST, Glimmer and FGenesV) as the most accurate. The number of ORFs varied depending on the software used: PROKKA and RAST predicted between 46 and 53 different ORFs, with an average of 47 per bacteriophage (Table 5-1), whereas Glimmer predicted between 52 and 75 ORFs with an average of 54, and finally FGenesV predicted between 39 and 50 ORFs with an average of 45 per genome. Whole genome analysis did not show homology to previously reported bacteriophages of both *Pectobacterium* and *Dickeya* spp., and from BLASTP analysis of individual ORFs, the most closely-related phages included ϕT7, ϕPP74 and ϕDU_PP_II (both infecting *P. atrosepticum*) and *Yersinia* phage AP10, that infects *Vibrio*, with similar genome sizes (40kbp) and number of coding sequences (approximately 50 in ϕT7 and ϕAP10). All predicted ORFs were located in the same strand, apart from one located in ϕSFM010 (Figure 5-8 d). All bacteriophages showed the same genomic organisation, and the general features were put together (Table 5-2), an example of detailed features and e values for ϕSFM002 was also completed (see Appendix k). Hypothetical proteins were found to total between 30 to 40% within each phage genome (data not shown). No integrase, excisionase, or repressor genes were detected, suggesting that all phages have a lytic lifecycle, this was also supported by the PHACTS program (Figure 5-5).

Consequently, whole genome sequencing analysis showed bacteriophages with a linear, dsDNA molecule with no cos ends and short terminal repeats, with GC content between 50 and 51%, no tRNAs or bacterial toxin genes and containing approximately 50 coding sequences. All bacteriophages showed high similarity with no unusual features from other *Pectobacterium* spp. phages, and further analysis, such as genomic mapping and comparison of core genomes were required to discriminate between them.

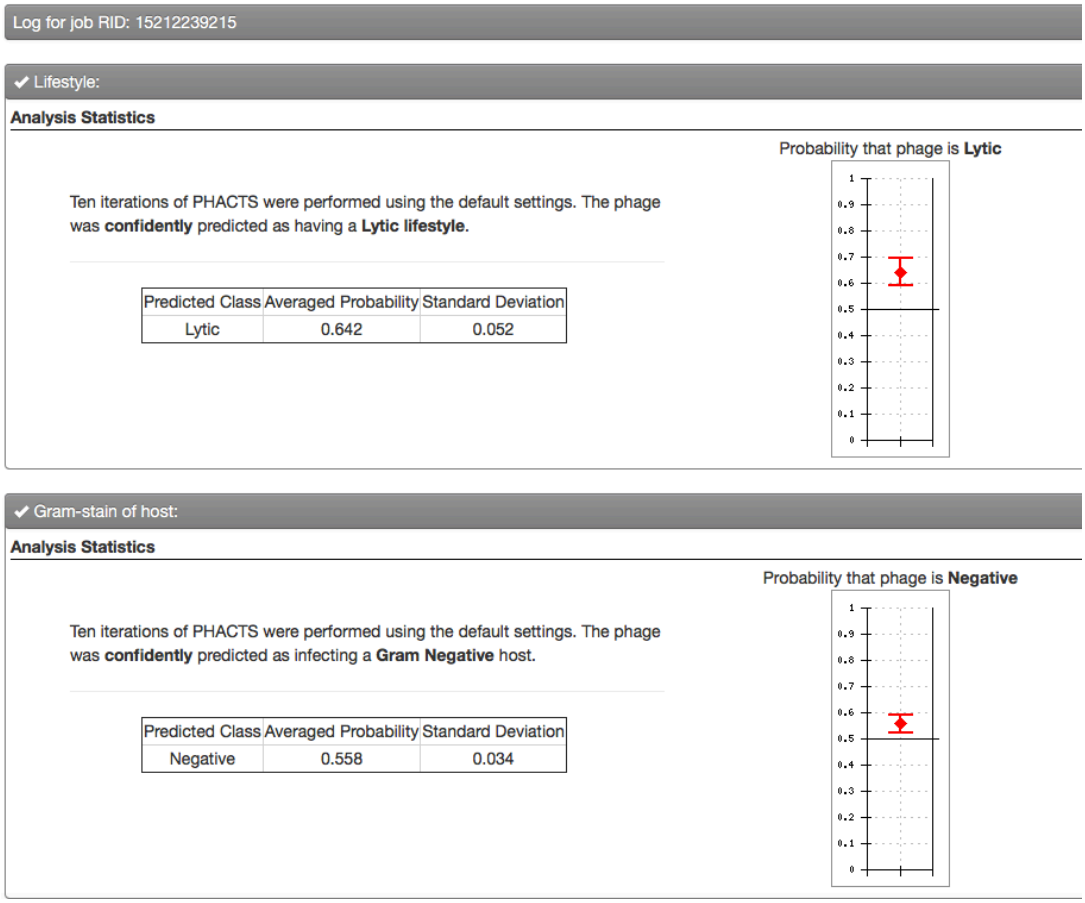

Figure 5-5: Prediction of the bacteriophages lifestyle against their Gram negative host according to the PHAge Classification Tool Set (PHACTS) analysis. All sequences were submitted individually to PHACTS (hosted by PhAnToMe.org) with default settings. PHACTS uses a similarity algorithm and a supervised Random Forest classifier to predict the lifestyle of a phage, using proteome data with a 99% precision rate.

Gene number	Function
gp 19	Terminase (DNA packaging protein)
gp 7	Protein kinase (for the host RNA polymerase)
-	RNA polymerase
-	DNA ligase
-	Bacterial RNA protein inhibitor
-	Endolysin
gp 4	DNA primase/helicase
gp 5	DNA poplymerase
gp 2.5	ssDNA binding protein
-	Portal protein
-	HNS-binding protein
-	Exonuclease
-	Tail assembly protein
gp 8	Head-to-tail joining protein
gp 9	Capsid assembly protein
gp 10A	Major capsid protein
gp 11 and gp 12	Tail tubular proteins
gp 14, gp 15 and gp 16	Internal virion proteins
gp 17	Tail fiber proteins

Table 5-2: General genome organisation and function of the isolated bacteriophages. All predicted CDS were individually checked for their function and a general table with the main coding sequences for the genomes was drawn.

5.2.2 Genomic organisation and nucleotide comparison of the bacteriophage genomes

On the basis of genomic analysis, it seemed that all of our bacteriophages were safe to use in plant treatment, thus we had to discriminate between them in order to design the most effective phage cocktail.

An easy way to compare genomes at the nucleotide level is by producing a dot plot alignment and a CCT map, all twelve nucleotide sequences were compared to one another and also to their closest phage genomes from the previous BLASTP search. Dot plot analysis revealed remarkable similarities between our sequences (Figure 5-6 a), and this similarity was even more remarkable when the closest genome sequences from other bacteriophages were added (Figure 5-6 b). Some features clearly stand out, like phage ϕSFM003 where there were clear indels when compared to the other samples (seen as overlapping edges), or that some phages looked like they were identical to each other, such as ϕSFM001, ϕSFM004, ϕSFM005, ϕSFM006 and ϕSFM007 or ϕSFM009 and ϕSFM012 (characterised as a unique diagonal line). The CCT map using nucleotide analysis gave a similarity of at least 98% or more, such was the case for ϕSFM001,

ϕSFM010 and ϕSFM011 that had 100% (Figure 5-7 a and c, and for individual analysis see Appendix I), seen as a black line on the outer ring. Another interesting feature from the CCT map was a large deletion in ϕSFM003, ϕSFM004, ϕSFM005, ϕSFM006, ϕSFM007, ϕSFM008 and ϕSFM009, approximately 200-300 nucleotides long located in the structural region (the absence of a gap within the ring indicated this deletion where the tail tubular protein or gp 11 is, seen in detail in Figure 5-7 b and d). The dot plot results suggested the presence of 3 distinct groups of phages based on completely similarity and presence of indels or extra gene copies, whereas from the CCT map results there were three different groups based on being 100% similar and the presence of a 200-300 nucleotide deletion. All the bacteriophages are highly similar to one another at the nucleotide level and more comparisons should be performed such as comparison of core genomes, average nucleotide identity (ANI) or different phylogenetic analysis.

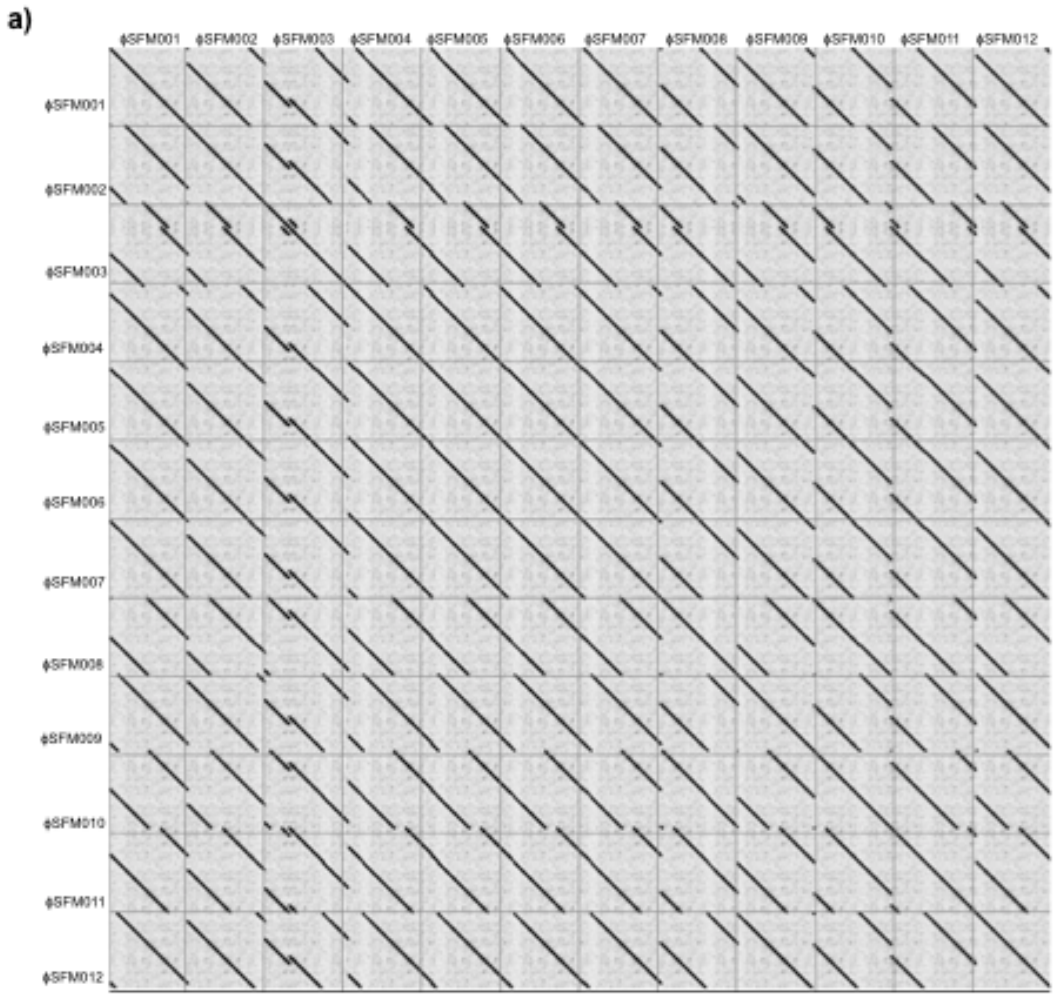

Figure 5-6 (a): Nucleotide comparison between all the bacteriophages isolates using dot plot analysis. Dot plot alignment of nucleotide sequences from twelve isolated bacteriophage genomes. Where necessary, genomes were reverse complemented and/or colinearised. Black diagonal lines parallel to the main diagonal indicate perfect sequence similarity while grey lines indicate weaker sequence correspondence. Parallel lines to the main diagonal indicate repeated regions in the same reading direction on different part of the sequences, indels are shown as overlapping edges.

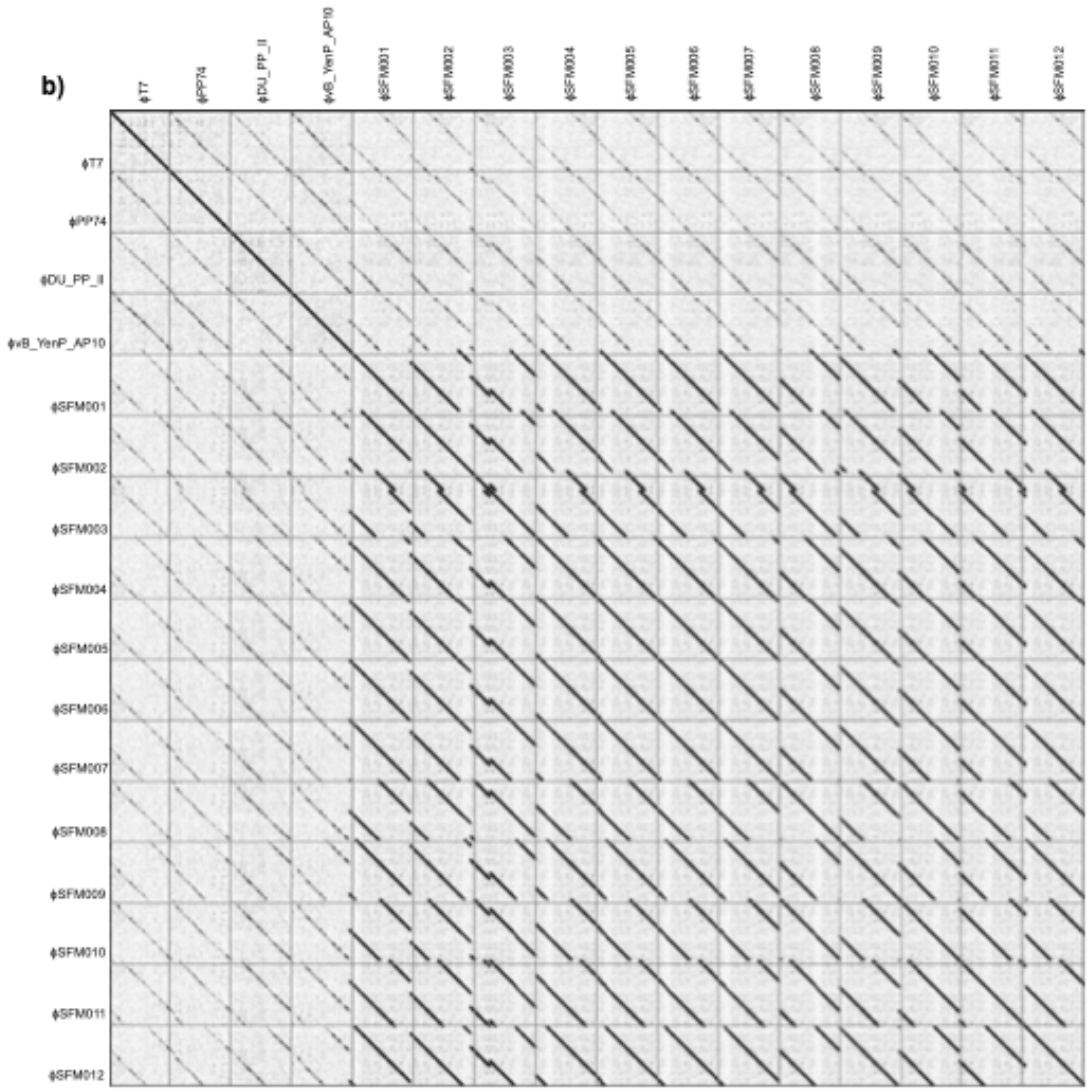

Figure 5-6 (b): Nucleotide comparison between all the bacteriophages using dot plot analysis. Dot plot alignment of nucleotide sequences from the twelve isolated bacteriophage genomes along with ϕT7, ϕPP74, ϕDU_PP_II and ϕvB_YenP_AP10 phages, these phages were added as they shown the most similarity when performing BLASTP analysis on their coding regions. Where necessary, genomes were reverse complemented and/or colinearised. Black diagonal lines parallel to the main diagonal indicate perfect sequence similarity while grey lines indicate weaker sequence correspondence. Indels are shown as overlapping edges and repeated regions are paralell lines in the same reading direction to the main diagonal.

In order to determine the origin of replication of the phage genomes, visual analysis of the GC skew in the CCT map (two inner rings, Figure 5-7 a and c) showed that it was positive in one half on the genome and the other half was close to zero as previously seen in other genomes (Grigoriev, 1999). This effect was replicated in all the phage genomes. From this analysis the origin of replication would be placed upstream of the terminase genes, at the top right corner of each figure (detailed in Figure 5-8, b and e).

To compare the genomes at the coding sequence level, another CCT map and a pairwise comparison map were produced In the pairwise comparison maps ORFs were divided into six groups according to their functions: transcriptional regulation, phage replication, transcription of structural elements, tail fibre, cell lysis and DNA packaging (Figures 5-8 and 5-9). When using CCT to compare between the coding regions (Figure 5-8), the similarities reached between our phages were even higher that when using nucleotide maps, and we included ϕSFM001, ϕSFM010, ϕSFM011 and ϕSFM012 together as they shown 100% BLAST similarity, another group that had almost 100% identity overall was formed by ϕSFM004, ϕSFM005, ϕSFM006, ϕSFM007 and ϕSFM008 (see Appendix m). Also, most of the variability could be traced to two main regions: the immediate region before the RNA polymerase (Figure 5-8, b and e) and within the structural proteins region (Figure 5-8, c and f). Pairwise comparison of the genome maps just corroborated the high homology between the bacteriophages and that the main differences between sequence lengths resided within the structural regions and an indel in the replication module in ϕSFM011 (Figure 5-9 a), this analysis seems to reinforce the hypothesis that there are more gene copies en some of the bacteriophages as opposed to deletions in the genome as these do not appear as such. The addition of their closest homologs in the comparison only served to highlight the more conserved regions, interspersed by stretches with lower homology (Figure 5-9 b). The use of genome maps served to point out the high similarity between these genomes and how different they are from previously sequenced bacteriophages (shown at the bottom of Figure 5-9 b).

To further compare these genomes, their core genomes were analysed. The core-genome and accessory genome phylogeny trees were obtained using Roary and FastTree programs (section 2.13.7 in Materials and methods). The core genome was identified as a set of 39 genes (Figure 5-10 a), accounting for approximately half of the genome (identified a total of 79 genes using this software, data not shown), since this tree could not differentiate between genomes, an additional tree was created using their accessory genes (Figure 5-10 b). From the core and accessory gene analysis, the main differences between our isolates included few hypothetical proteins downstream from the terminase genes (arbitrary starting point in Figures 5-7 and 5-8, it corresponds to the first and last coding sequences in Figure 5-9 a) or upstream from the inhibitor of the toxin/antitoxin system genes (“other function” gene in between two replication genes in Figure 5-9 a), the presence of two DNA ligases with the same size (1109bp, Table 5-3)

that are exclusively present in the genomes of all apart from ϕSFM003 and ϕSFM011 that contain both, and the presence of different copies of RNA polymerases (with differing sizes) in ϕSFM002 (3 copies), ϕSFM003 (2 copies) and ϕSFM012 (2 copies), being the RNA polymerase from the *Yersinia* ϕAP_10 the most common as it is present in all the genomes, the other polymerases are from the *E. coli* ϕCICC 80001 (present in ϕSFM003 and ϕSFM012) and ϕT7 and another *Enterobacteriaceae* polymerase (presence of both in ϕSFM002), other interesting features included the presence of an additional exonuclease and DNA polymerase in ϕSFM004 (Table 5-3), an additional bacterial RNA polymerase inhibitor in both ϕSFM003 and ϕSFM011 genomes and an additional tail tubular protein and peptidoglycan hydrolases (three in total) in ϕSFM003 genome (Table 5-3). These results highlight the main differences between our bacteriophages, whose core genomes are very similar apart from having alternative or extra copies of certain genes.

In order to investigate more thoroughly the main differences between these genomes, functional searches for each individual CDS using Pfam, InterProScan and BLAST identified some interesting features. All DNA polymerases were similar to the Klebsiella ϕK5 (with the only exception of ϕSFM004, where the similarity was with ϕT3), all primase/helicase proteins were identical to *Yersina* ϕphiYE F10 and *Serratia* ϕ2050H2, and most ssDNA-binding proteins were similar to *Pectobacterium* ϕPWS4 (ϕSFM004 to ϕSFM012) with the exception of ϕSFM002 and ϕSFM003 with similarity to *Serratia* ϕSM9-3Y and *Citrobacter* ϕSH1. Structural genes were more similar between the samples but they still contained some differences: all tail assembly proteins, tail tubular proteins, major capsid proteins and tail fibre proteins were similar to those from *Pectobacterium* phage DU_PP_II, all head-to-tail joining proteins were similar to the *Yersinia* ϕvB_YenP_AP10 and all capsid assembly proteins were like the *Yersinia* ϕvB_YenP_AP5 (with the exception of ϕSFM001 that did not have one, and ϕSFM002 that had an additional one similar to *Enterobacteria* ϕT3. The internal virion proteins (a, b, c and d) were all similar, in the following order: a was similar to *Pectobacterium* ϕPP74, whereas b, c and d were similar to Yersinia ϕvB_YenP_AP10 (but ϕSFM003 had an additional internal virion protein D similar to *Pectobacterium* ϕDU_PP_II). All terminase genes (both subunits) from all the phages were similar to *Yersinia* ϕvB_YenP_AP10. These results highlighted the main differences within the bacteriophages in terms of coding regions, and it explained the indels previously observed on the dot plot analysis of ϕSFM003.

a)

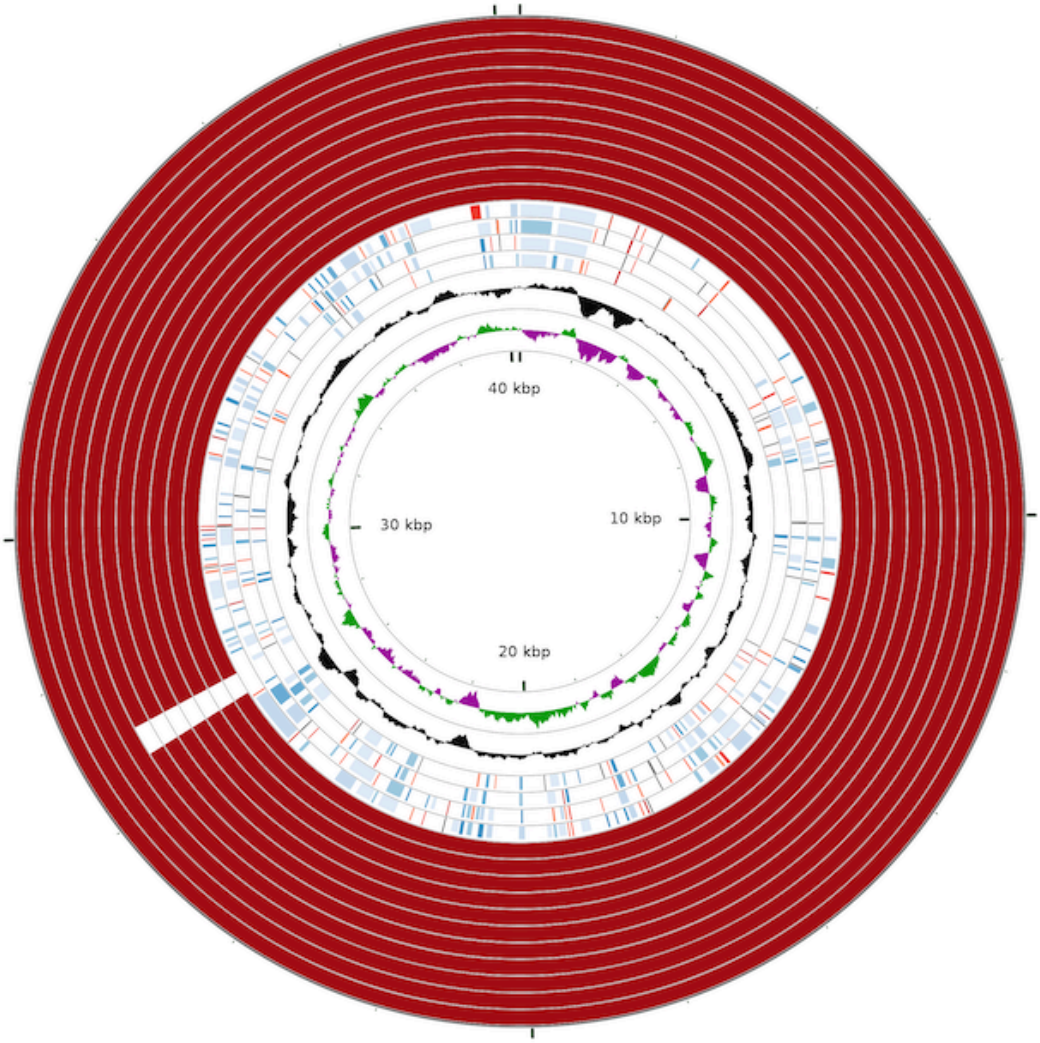

Figure 5-7 (a): Nucleotide comparison between all the bacteriophages with ϕSFM002 using CCT view. All phage genomes were manually colinearised placing the starting arbitrary point at the start of the open reading frame of the large terminase subunit gene (1), then each phage was compared individually to each other and the four closest phages from BLASTP results were added (ϕDU_PP_II, ϕPP74, ϕT7 and ϕvB_YenP_AP10 in the internal ring), dark red shows 90% similarity whereas black shows 100%. GC content and GC skews (+ and -) were shown as the innermost rings.

b)

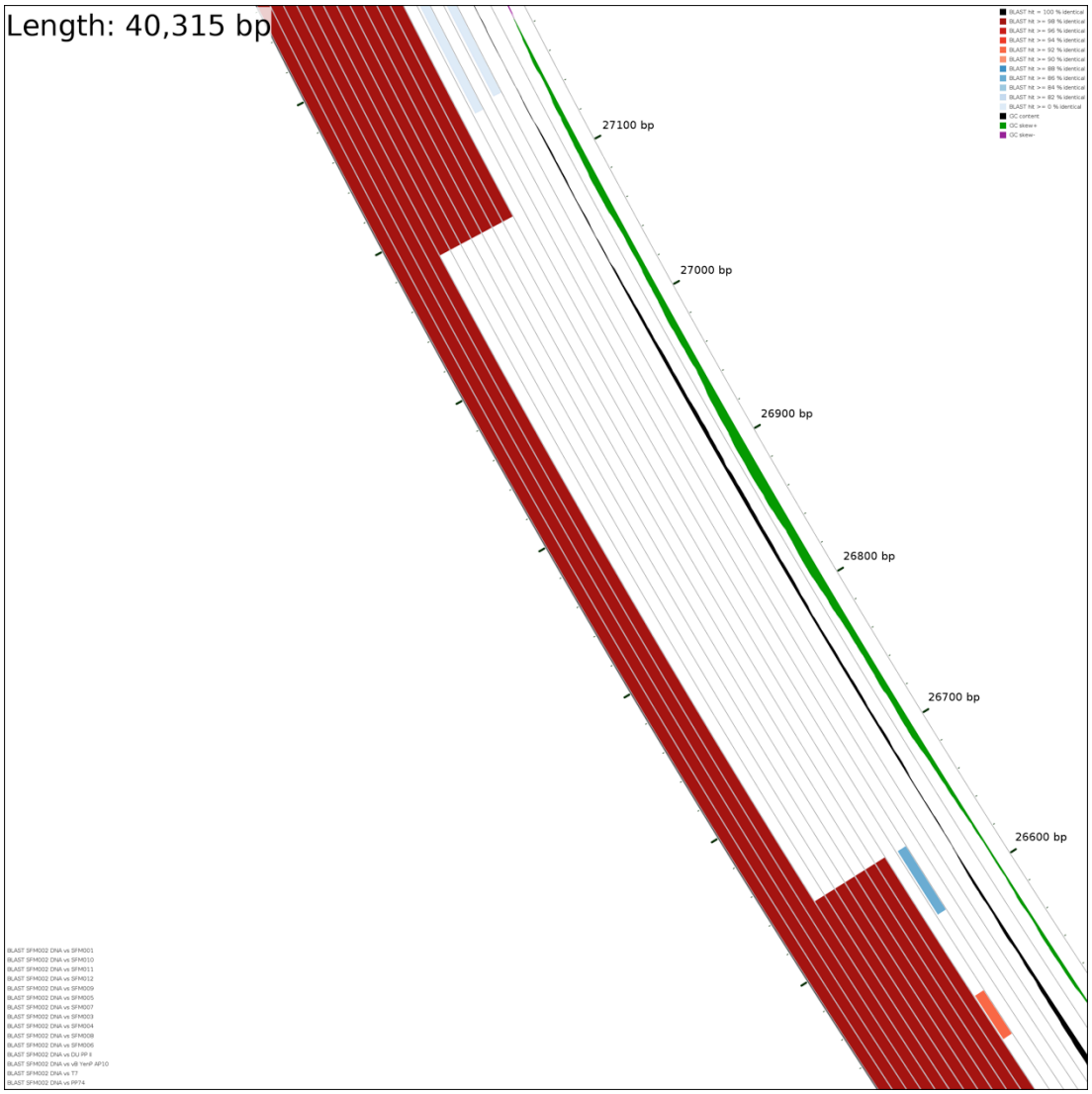

Figure 5-7 (b): Detail of nucleotide comparison between all the bacteriophages with ϕSFM002 using CCT view. Close-up image of the nucleotide sequence with highest variability surrounding the structural region (approximately 26900nt from the starting arbitrary point, the terminase gene), dark red shows 90% similarity whereas black shows 100%. GC content and GC skews (+ and -) were shown as the innermost rings.

c)

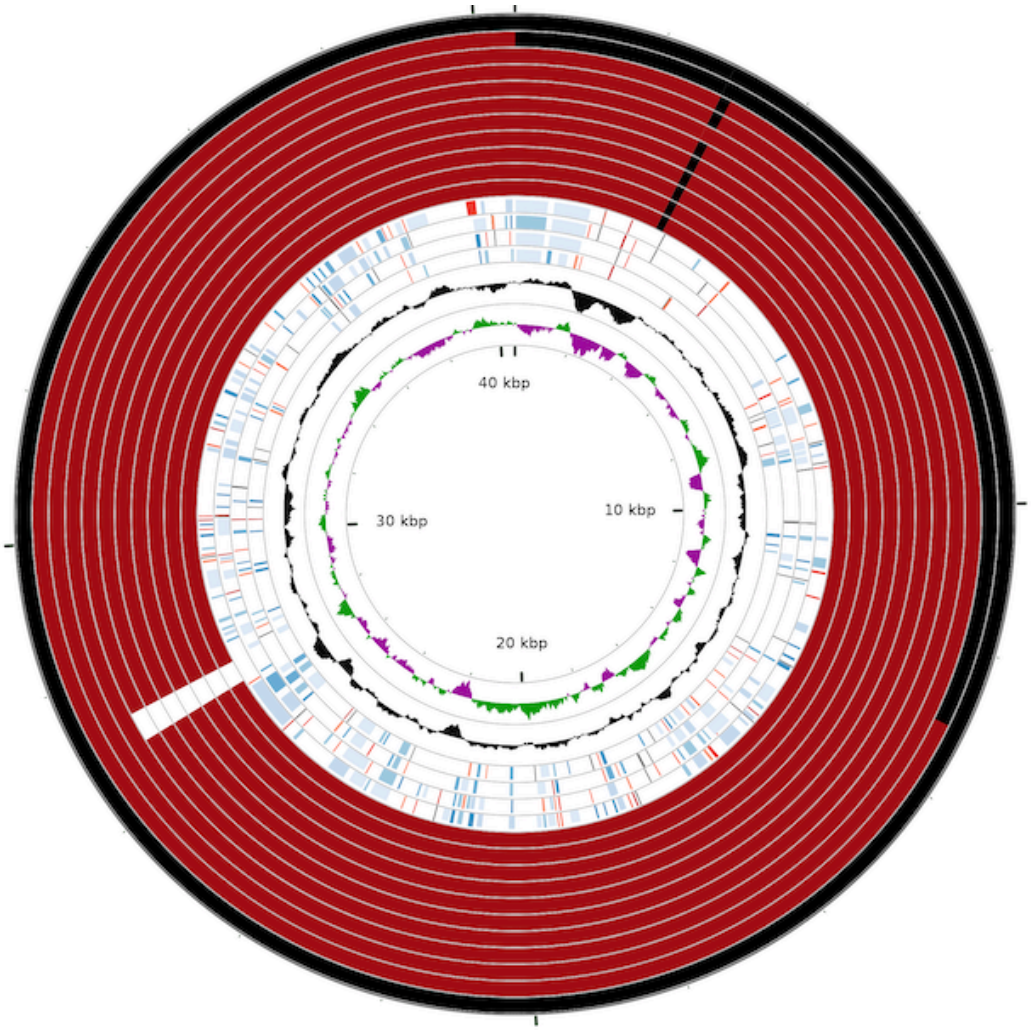

Figure 5-7 (c): Nucleotide comparison between all the bacteriophages with ϕSFM010 using CCT view. All phage genomes were manually colinearised placing the starting arbitrary point at the start of the open reading frame of the large terminase subunit gene (1), then each phage was compared individually to each other and the four closest phages from BLASTP results were added (ϕDU_PP_II, ϕPP74, ϕT7 and ϕvB_YenP_AP10 in the internal ring), dark red shows 90% similarity whereas black shows 100%. GC content and GC skews (+ and -) were shown as the innermost rings.

d)

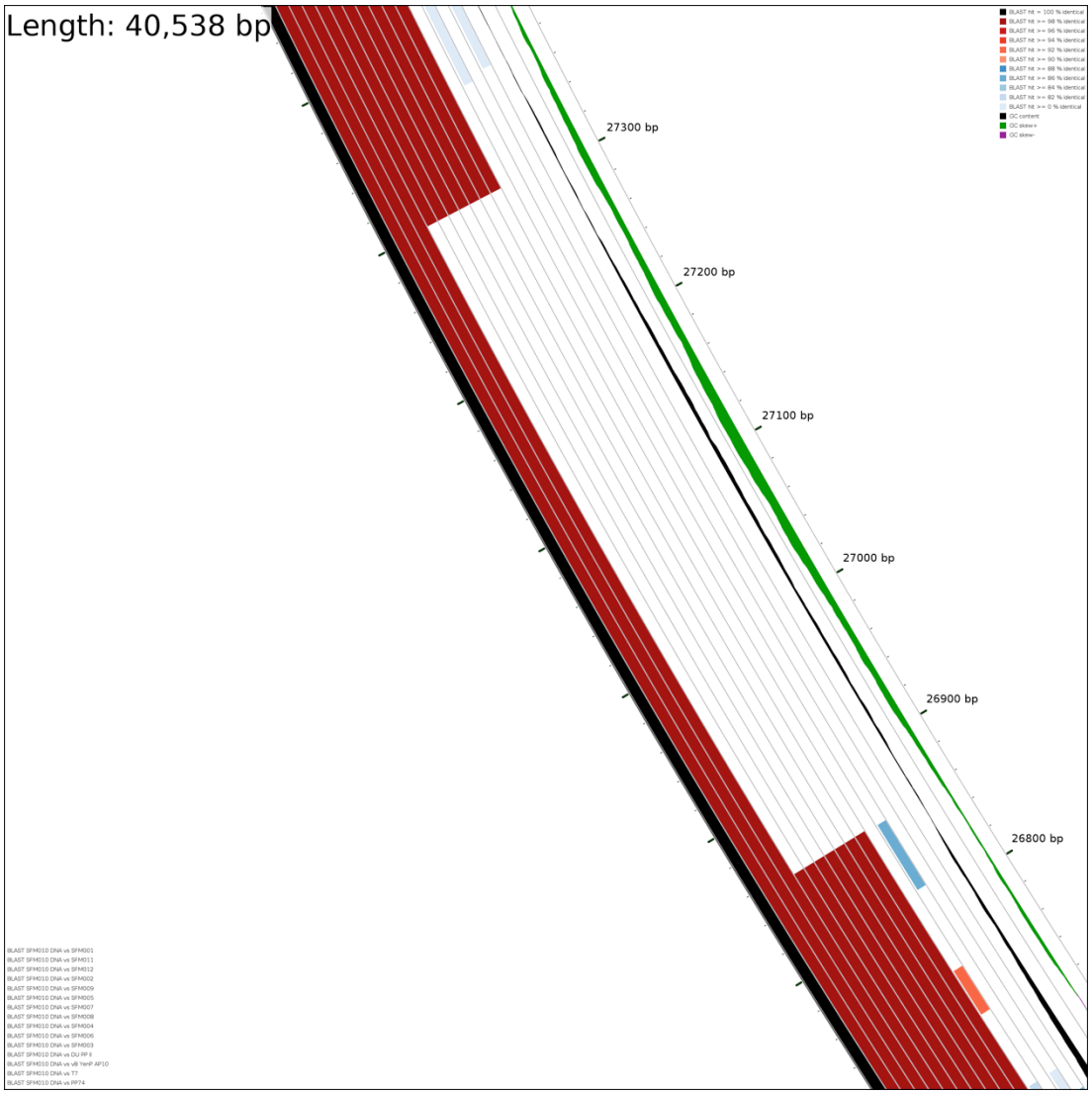

Figure 5-7 (d): Detail of nucleotide comparison between all the bacteriophages with ϕSFM010 using CCT view. Close-up image of the nucleotide sequence with highest variability surrounding the structural region (approximately 27100nt from the starting arbitrary point, the terminase gene), dark red shows 90% similarity whereas black shows 100%. GC content and GC skews (+ and -) were shown as the innermost rings.

a)

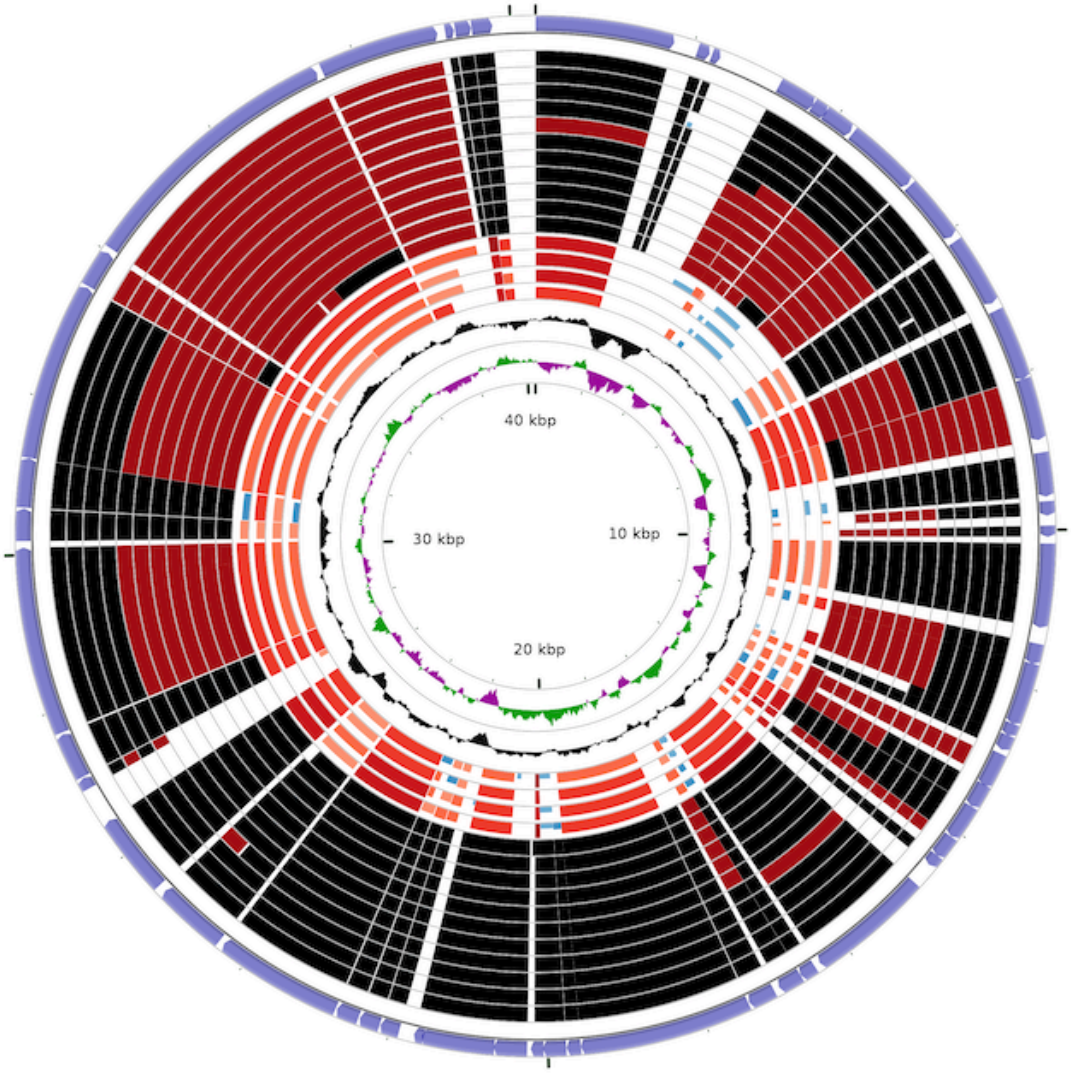

Figure 5-8 (a): Phage genome organisation comparison with ϕSFM002 using CCT view. All phage genomes were manually colinearised placing the starting arbitrary point at the start of the open reading frame of the large terminase subunit gene (1), then each phage was compared individually to each other and the four closest phages from BLASTP results were added (ϕDU_PP_II, ϕPP74, ϕT7 and ϕvB_YenP_AP10 in the internal ring), dark red shows 90% similarity whereas black shows 100%. GC content and GC skews (+ and -) were shown as the innermost rings.

b)

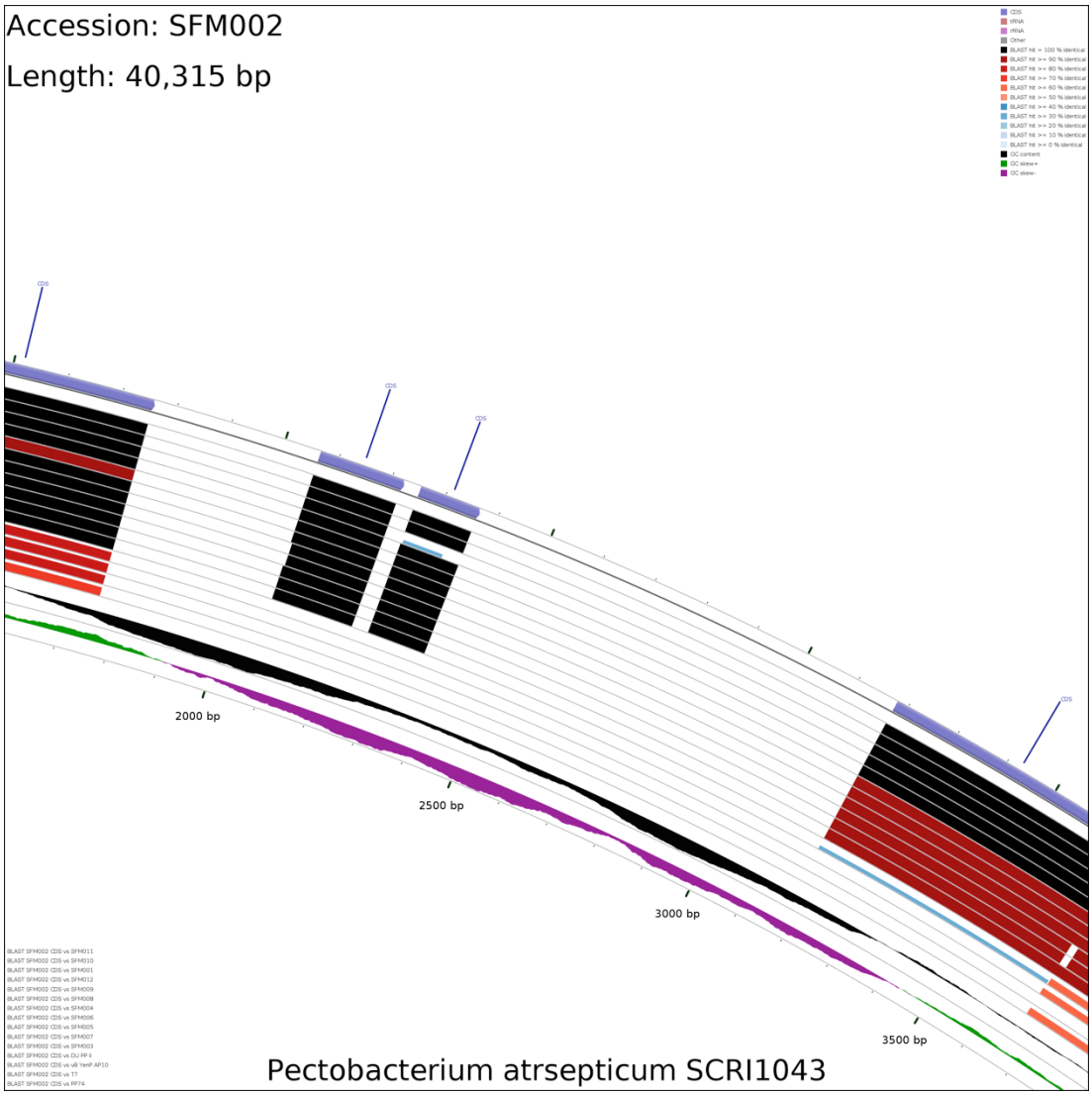

Figure 5-8 (b): Detail of nucleotide comparison between all the bacteriophages with ϕSFM002 using CCT view. Close-up image of the nucleotide sequence with indels or extra genes copies surrounding the early genes region (approximately 2500nt from the starting arbitrary point, the terminase gene), dark red shows 90% similarity whereas black shows 100%. GC content and GC skews (+ and -) were shown as the innermost rings.

c)

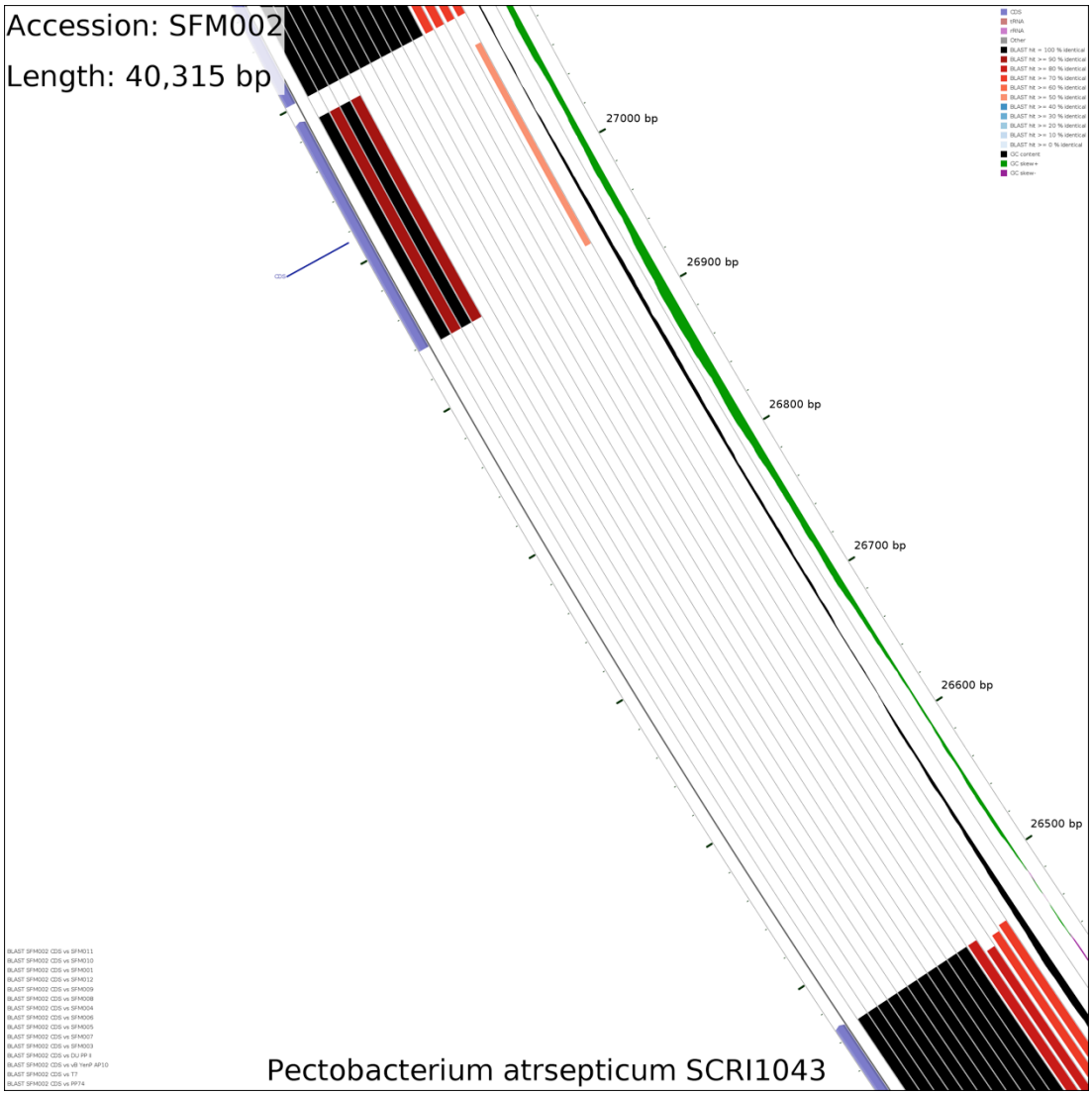

Figure 5-8 (c): Detail of nucleotide comparison between all the bacteriophages with ϕSFM002 using CCT view. Close-up image of the nucleotide sequence with highest variability surrounding the structural region (approximately 26800nt from the starting arbitrary point, the terminase gene), dark red shows 90% similarity whereas black shows 100%. GC content and GC skews (+ and -) were shown as the innermost rings.

d)

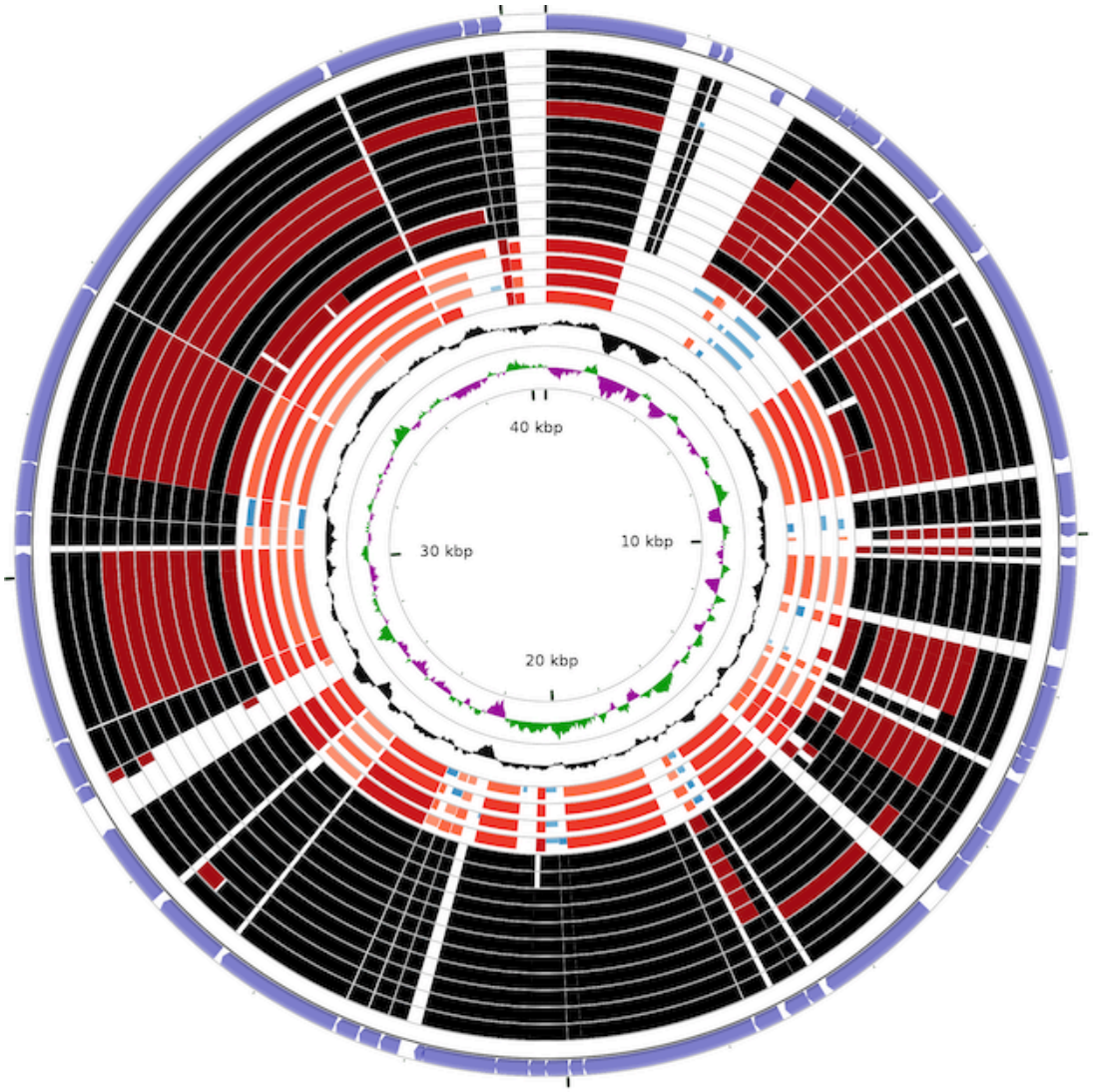

Figure 5-8 (d): Phage genome organisation comparison with ϕSFM010 using CCT view. All phage genomes were manually colinearised placing the starting arbitrary point at the start of the open reading frame of the large terminase subunit gene (1), then each phage was compared individually to each other and the four closest phages from BLASTP results were added (ϕDU_PP_II, ϕPP74, ϕT7 and ϕvB_YenP_AP10 in the internal ring), dark red shows 90% similarity whereas black shows 100%. GC content and GC skews (+ and -) were shown as the innermost rings.

e)

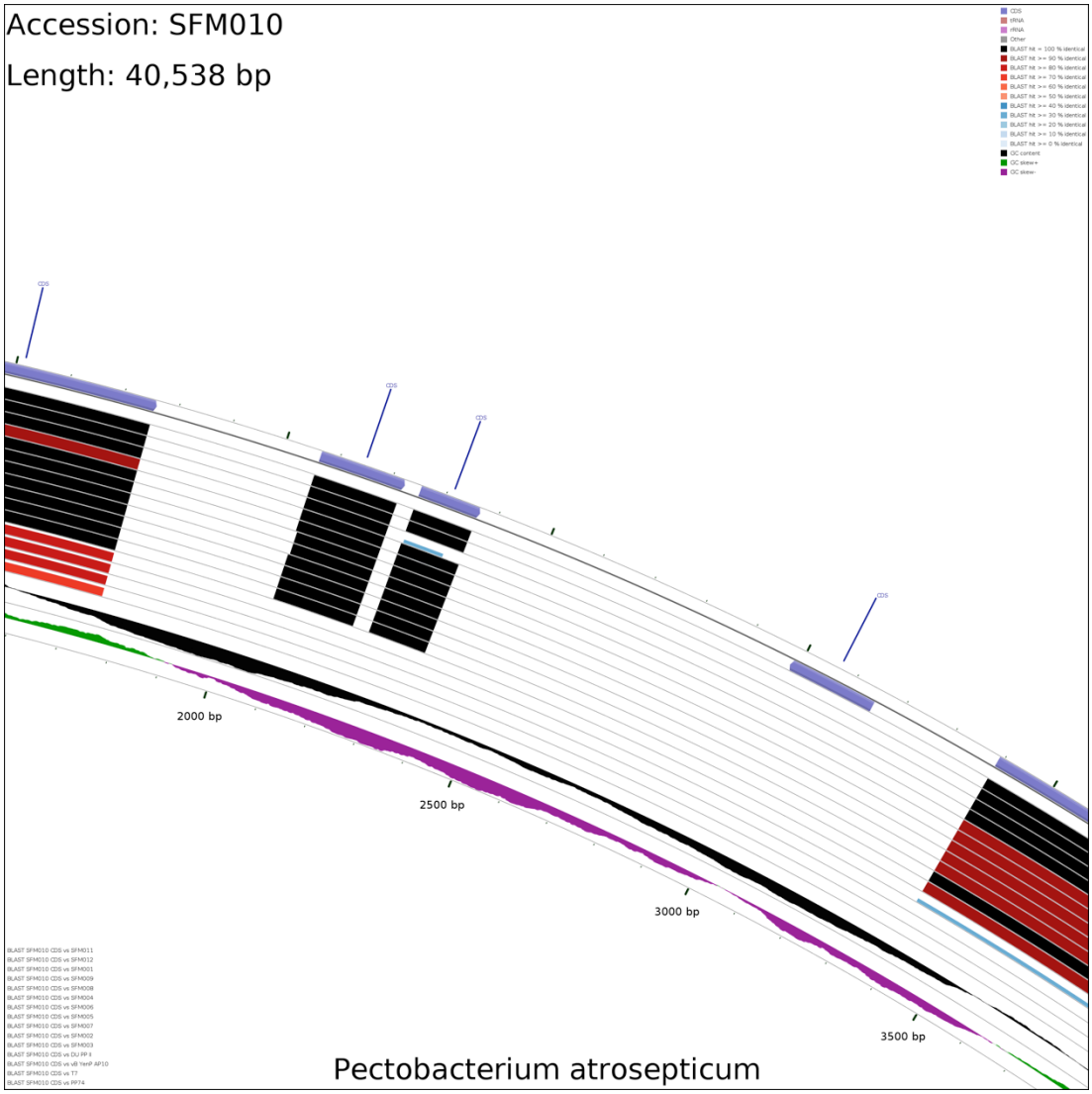

Figure 5-8 (e): Detail of nucleotide comparison between all the bacteriophages with ϕSFM010 using CCT view. Close-up image of the nucleotide sequence with indels or extra genes copies surrounding the early genes region (approximately 2500nt from the starting arbitrary point, the terminase gene), dark red shows 90% similarity whereas black shows 100%. GC content and GC skews (+ and -) were shown as the innermost rings.

f)

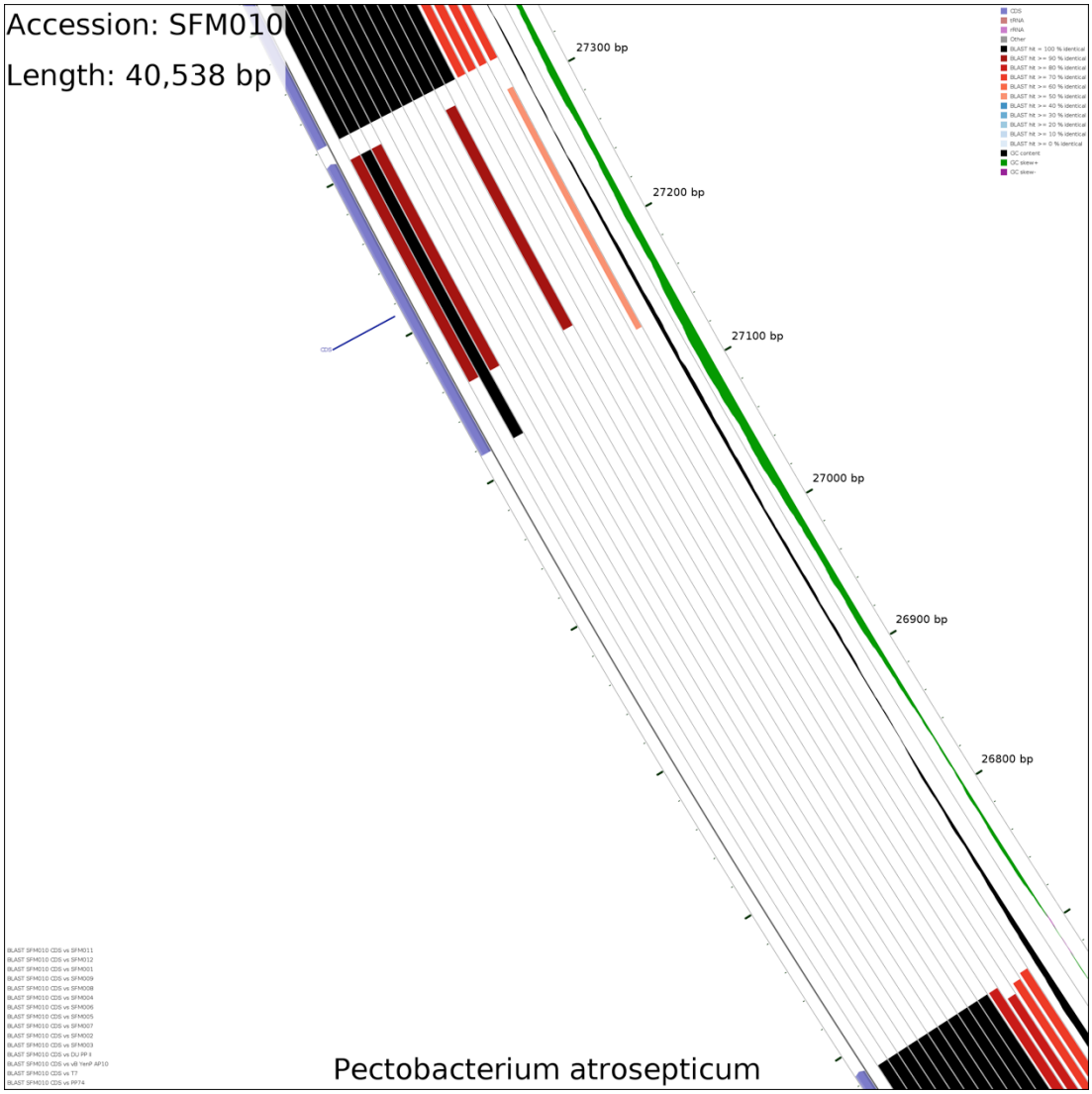

Figure 5-8 (f): Detail of nucleotide comparison between all the bacteriophages with ϕSFM010 using CCT view. Close-up image of the nucleotide sequence with highest variability surrounding the structural region (approximately 27050nt from the starting arbitrary point, the terminase gene), dark red shows 90% similarity whereas black shows 100%. GC content and GC skews (+ and -) were shown as the innermost rings.

a)

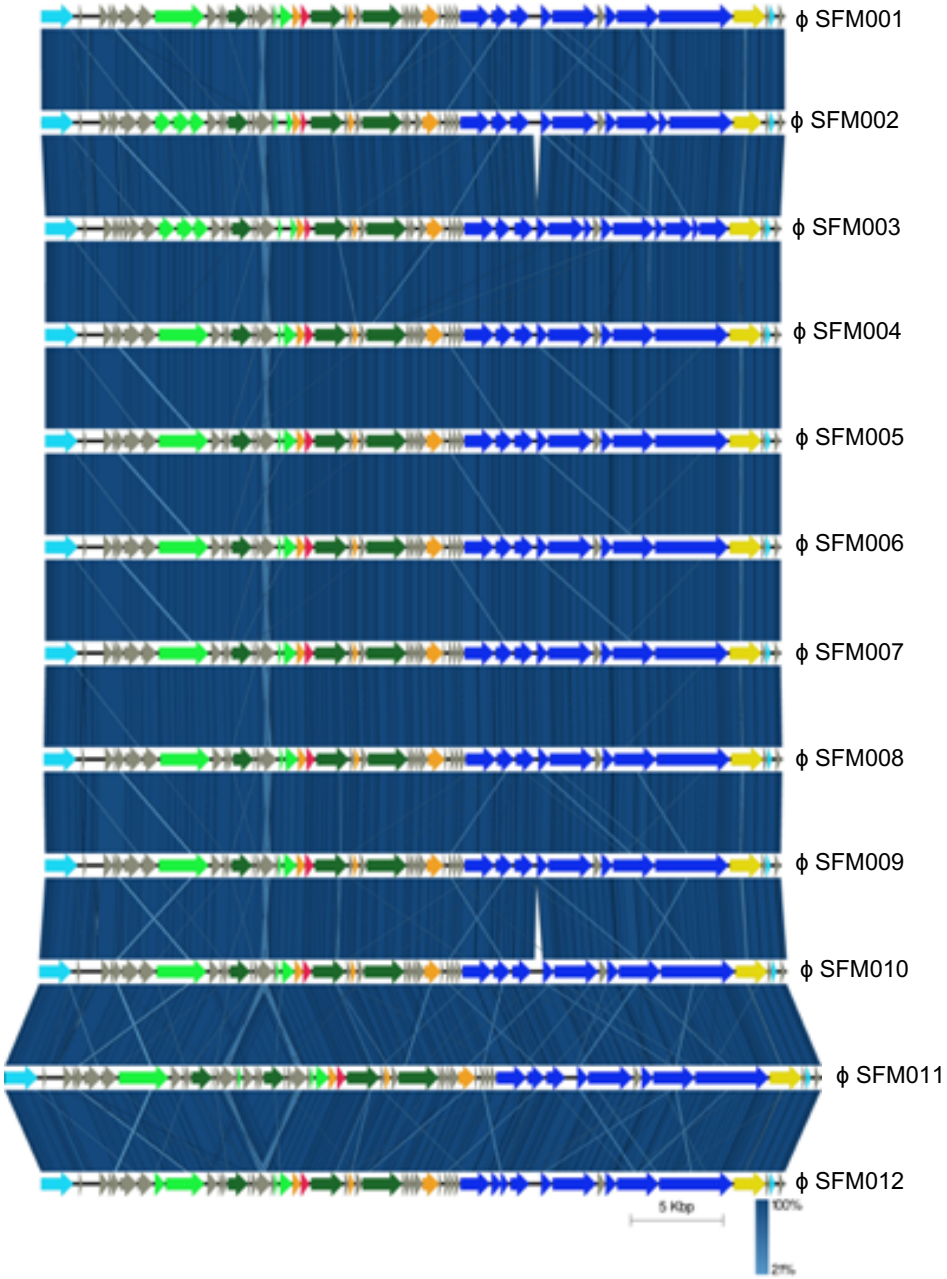

Figure 5-9 (a): Phage genome organisation comparison using tBLASTX. The top twelve genomes correspond to the phage samples. Arrowheads are genes, where the identity cut-off is set at 21%. They were classified in 5 categories: (1) DNA packaging included both terminase subunits, (2) transcriptional regulation included the DNA-directed RNA polymerase, the bacterial RNA polymerase inhibitor and the single-stranded DNA binding protein, (3) replication included the DNA ligase, the DNA primase/helicase and the DNA polymerase, (4) cell lysis included the amidase and (5) structural included the head-to-tail connector potein, the capsid assembly protein, the major capsid protein, the tail tubular protein, and the internal virion proteins, the "Other" function category included the endonuclease I, the inhibitor of the toxin/antitoxin system and the exonuclease I.

b)

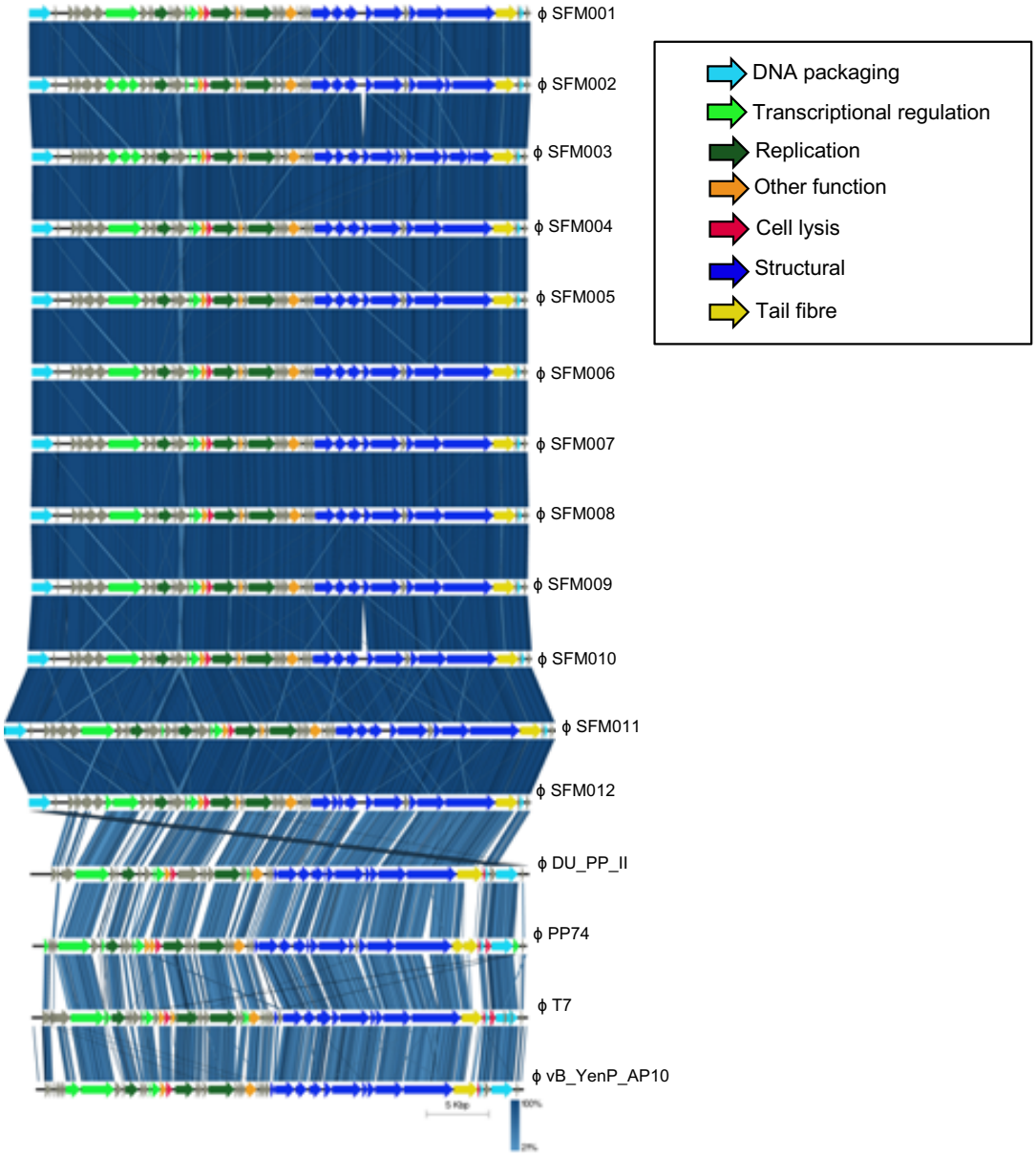

Figure 5-9 (b): Phage genome organisation comparison using tBLASTX. The top twelve genomes correspond to the phage samples and the bottom four corresponded to ϕDU_PP_II, ϕPP74, ϕT7 and ϕvB_YenP_AP10. Arrowheads are genes, where the identity cut-off is set at 21%. They were classified in 5 categories: (1) DNA packaging included both terminase subunits, (2) transcriptional regulation included the DNA-directed RNA polymerase, the bacterial RNA polymerase inhibitor and the single-stranded DNA binding protein, (3) replication included the DNA ligase, the DNA primase/helicase and the DNA polymerase, (4) cell lysis included the amidase and (5) structural included the head-to-tail connector protein, the capsid assembly protein, the major capsid protein, the tail tubular protein, and the internal virion proteins, the "Other" function category included the endonuclease I, the inhibitor of the toxin/antitoxin system and the exonuclease I.

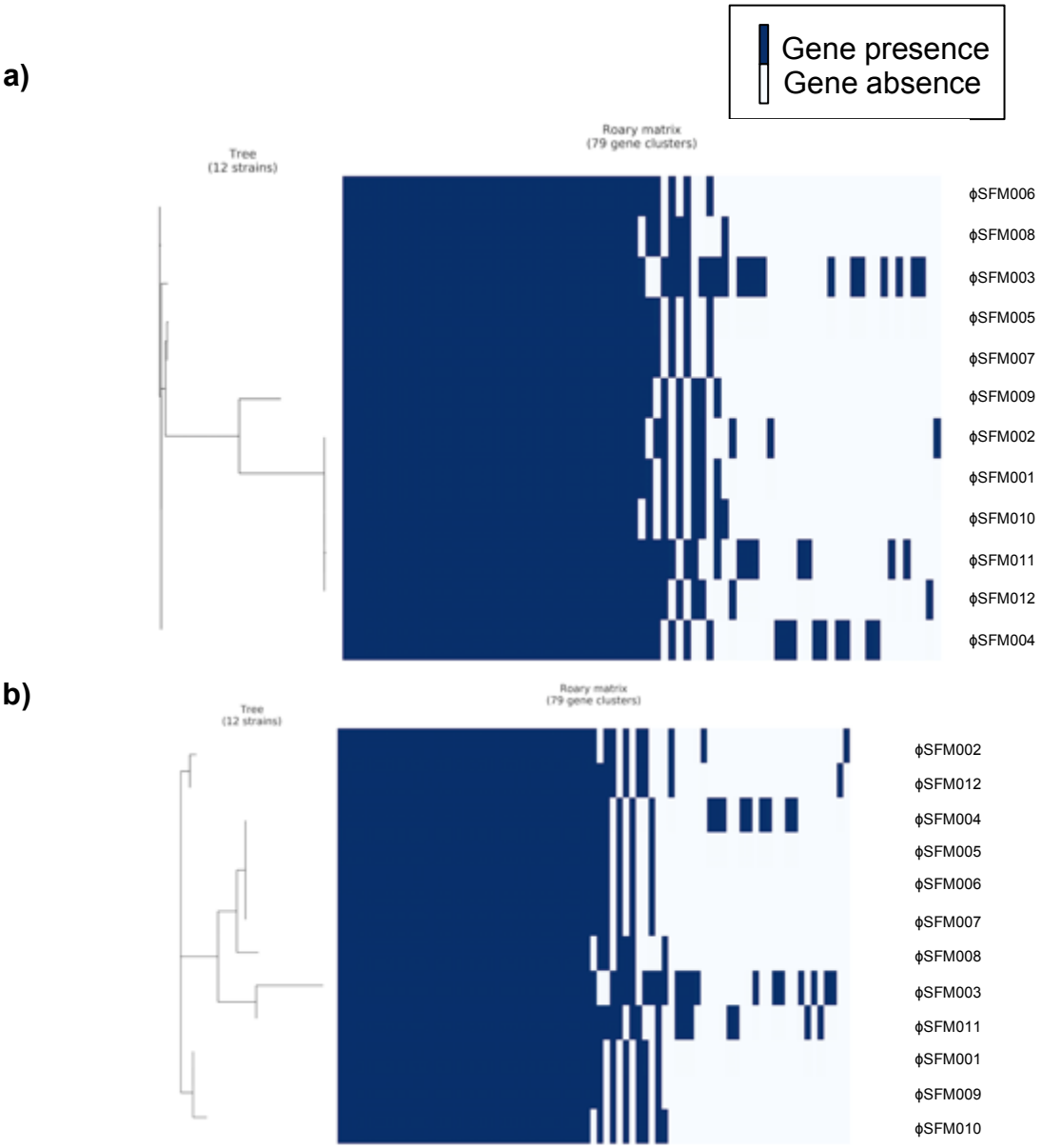

Figure 5-10: Core (a) and accessory genes (b) comparison using Roary. The annotated assemblies in GFF3 format of the samples were analysed using the Roary software that calculates their pan genome. A phylogenetic tree using their core (a) and accessory genes (b) along with the presence and absence of genes figure, were created.

	ϕSFM001	ϕSFM002	ϕSFM003	ϕSFM004	ϕSFM005	ϕSFM006	ϕSFM007	ϕSFM008	ϕSFM009	ϕSFM010	ϕSFM011	ϕSFM012
DNA ligase (2 copies)	1	1	1 and 2	2	2	2	2	2	1	1	1 and 2	1
T7 RNA polymerase (5 copies)	1	1, 3 and 5	1, 2 and 4	2	2	2	2	1	1	1	4	1 and 3
Exonuclease				1 (920 aa)								
DNA polymerase				1 (329 aa)								
Bacterial RNA polymerase inhibitor (2 copies)			1 (197 aa)								2 (197 aa)	
Tail tubular protein gp 12			1 (437 aa)									
Peptidoglycan hydrolases gp 16 (4 copies)		4 (488 aa)	1 (1532 aa) 2 (488 aa) 3 (371 aa)									
Capsid assembly scaffolding protein												1 (416 aa)

Table 5-3: Extra gene copies for each bacteriophage genome. Analysis was performed using Roary.

5.2.3 Analysis of tail fibre protein

In an attempt to decipher the variability of the tail fibre proteins, alignment of all the nucleotide and amino acid sequences were performed. Although there was an area that contained more SNPs than the rest of the sequence, these were only found for ϕSFM009 and it only changed one amino acid in the protein sequence (Figure 5-11). This alignment could explain some affinity for *P. atrosepticum* as there was a group of bacteriophages that contained the same SNPs and these were found to produce plaques in this host (namely ϕSFM001, ϕSFM002, ϕSFM010, ϕSFM011 and ϕSFM012 in Section 3.2.1 and Table 3-2). These differences could not explain the higher affinity that ϕSFM010 has for its host, thus more genes should be involved in host recognition.

a)

Figure 5- 11 (a): Nucleotide alignment of the tail fibre protein in all the isolates. Mismatches are shown on the consensus row as missing, the area shown corresponds to the highest containing SNPs region (between 430 and 570nt).

b)

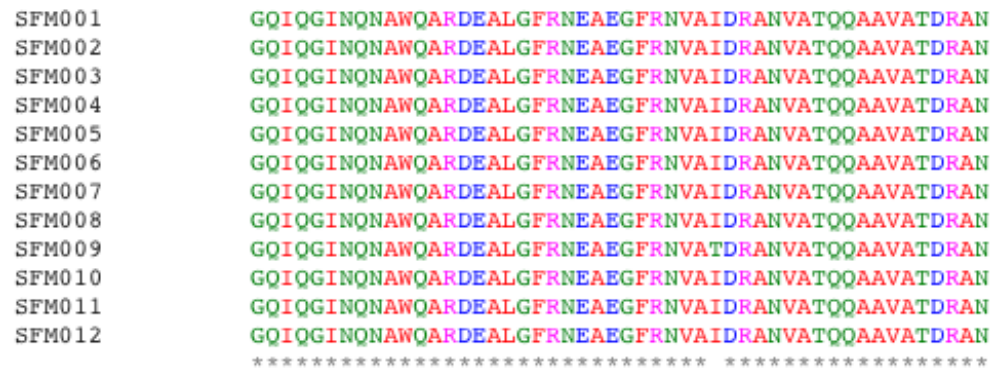

Figure 5-11 (b): Amino acid alignment of the tail fibre protein of all the isolates. Mismatches are shown on the consensus row as missing, the area shown corresponds to the highest containing SNPs region (between 430 and 570nt).

5.2.4 Average Nucleotide Identity (ANI) and phylogenetic analysis of all the bacteriophages isolated

To design an effective phage cocktail, the phages genomes were compared to each other to determine which ones were different from one another. The average nucleotide identity (ANI) of each bacteriophage was calculated and clustered using and all-versus-all approach. All the bacteriophages had 100% similarity between them, making them all variants of the same phage (Figure 5-12), the comparison against their closest homologues showed that they had at least 75% homology with the *Vibrio* phage AP10 and approximately 65-70% with the *Pectobacterium* phage DU_PP_II, being the lowest at 60% with phage T7 (Figure 5-12). These results reflected how similar these sequences are, but also how much they differ from existent sequenced phage genomes.

Even though previous results showed that the isolates belong to the same phage species, we still wanted to infer evolutionary relationships between the phage isolates. Two methods were used in a combined attempt for the phylogenetic analyses of the large subunit of the terminase and the DNA polymerase genes: one using ClustalW and another using MAFFT. From the first analysis of the DNA polymerase alignment, two groups were formed (Figure 5-13 a, i): one included ϕSFM001, ϕSFM002, ϕSFM009, ϕSFM010, ϕSFM011 and ϕSFM012, the other group included the remaining phages. From the large subunit of the terminase gene, there were again two groups

formed (Figure 5-13 a, ii): one contained ϕSFM001, ϕSFM002, ϕSFM010, ϕSFM011 and ϕSFM012 and the other group included the remaining phages. The results for the DNA polymerase and terminase genes using MAFFT were almost the same (Figure 5-13 b, i and ii) as the ones obtained using ClustalW. Independently from the method used, both DNA polymerase and terminase gene analyses agreed on their results.

In order to complete the analysis of the evolutionary relationships, whole genome phylogenetic analysis using MAFFT and VICTOR software were performed (section 2.13.7 in Materials and methods). Whole genome alignment using MAFFT and VICTOR showed the same results as the polymerase gene alignment (Figure 5-14 a and b), and VICTOR results also agreed on the previous findings that grouped all the bacteriophages under the same species. Either by using single gene or whole genome analysis produced the same phylogenetic trees.

To test the similarities our phage isolates have with other already sequenced bacteriophages, a genome-wide proteomic tree was generated using the VIPTree server. The viral proteome tree generated (Figure 5-15) placed our isolates between *Erwinia* spp. and *Yersinia* phages, all well within the *Podoviridae* family of viruses and the Gammaproteobacteria host group. Whole proteome analysis included our isolates within other soil bacteria (Erwinia and *Pectobacterium*) and Enterobacteria.

To classify our isolates within the *Autographivirinidae* subfamily (characterised by having their own RNA polymerase), a phylogenetic tree was produced that included all RNA polymerases from our isolates and other representative viruses from this subfamily (Table 2-12 in section 2.13.7 in Materials and methods). The RNA polymerase analysis confirmed that the isolates formed a different clade linked to other *T7likevirus* (Figure 5-16) such as ϕT7, ϕT3, ϕvB_YenP_AP10 or ϕPP74. All our isolates belong to the T7 viruslike genus.

All the phylogenetic profile methods used included very small branch lengths, as a reflection on how closely related our isolates are. There were two distinct groups, either using single gene or whole genome analysis. Whole proteome analysis placed our phages within the Gammaproteobacteria host group and the *Podoviridae* family. From the RNA polymerase analysis, our isolates belonged to the genus T7virus, closely related to T7 and T3 phages.

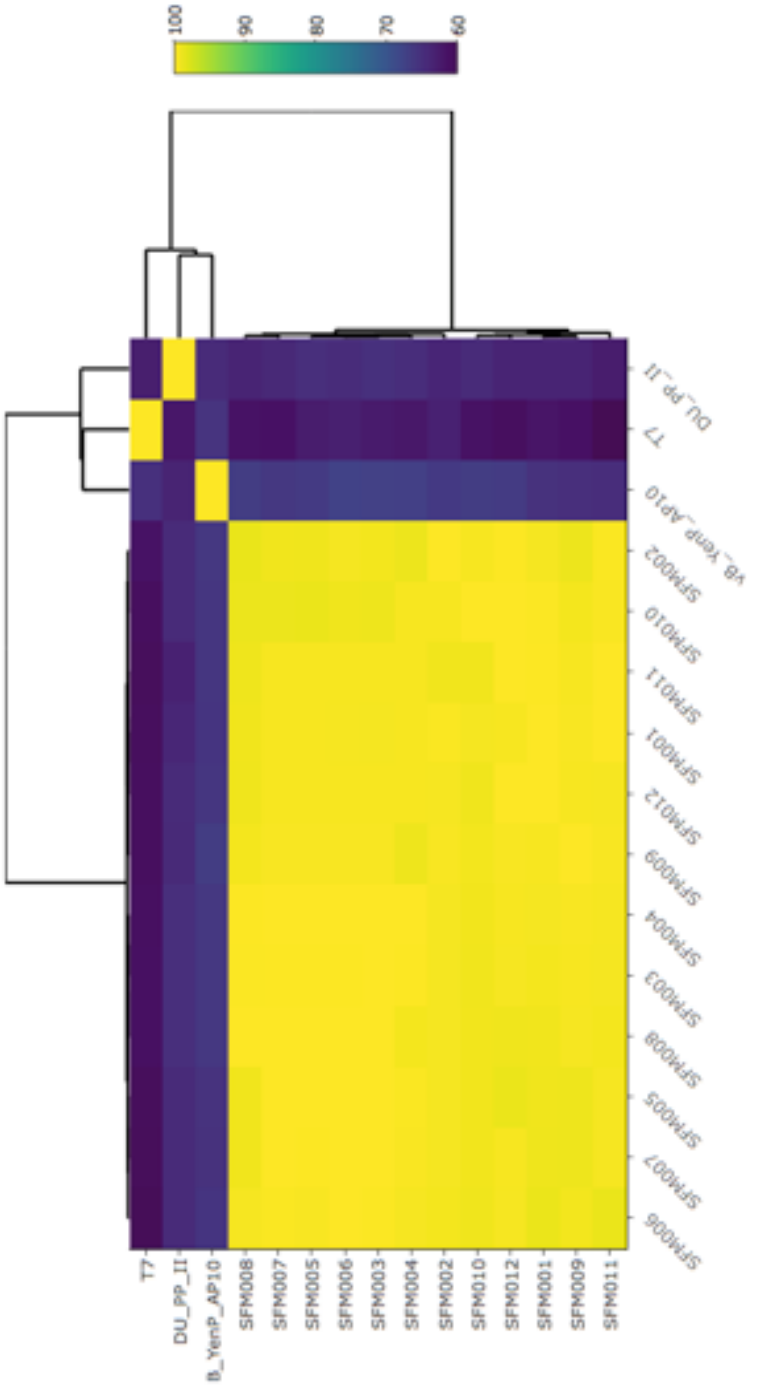

Figure 5-12: Average nucleotide identity comparison of the phage genomes. Clustering of each bacteriophage isolate was based on Average Nucleotide Identity (ANI), using an average linkage for the Euclidean distance in the phylogenetic tree, using autoANI analysis and R packages for the heatmap. Bacteriophages ϕT7, ϕDU_PP_II and ϕvB_YenP_AP10 were added for comparison.

a)

i)

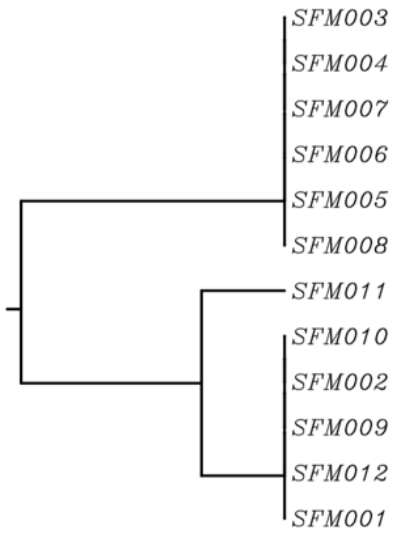

ii)

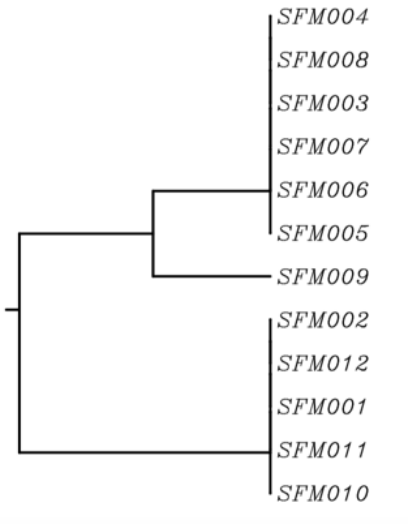

Figure 5-13 (a): Phylogenetic trees originated from the DNA polymerase (i) and the large terminase subunit gene (ii) using ClustalW. The phylogenetic trees originated from *polA* (i) and from *terL* (ii) Both phylogenetic trees (a) were originated using ClustalW using default parameters.

b)

ii)

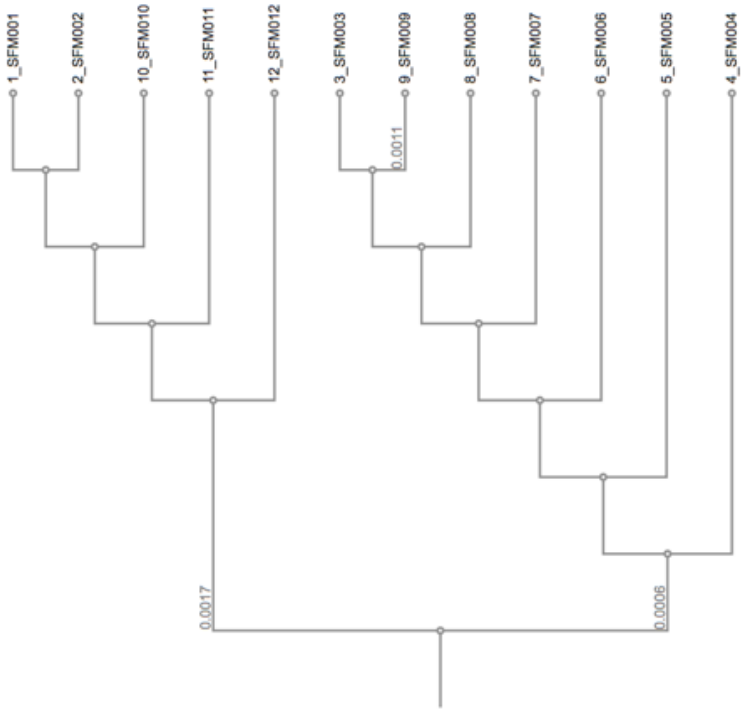

i)

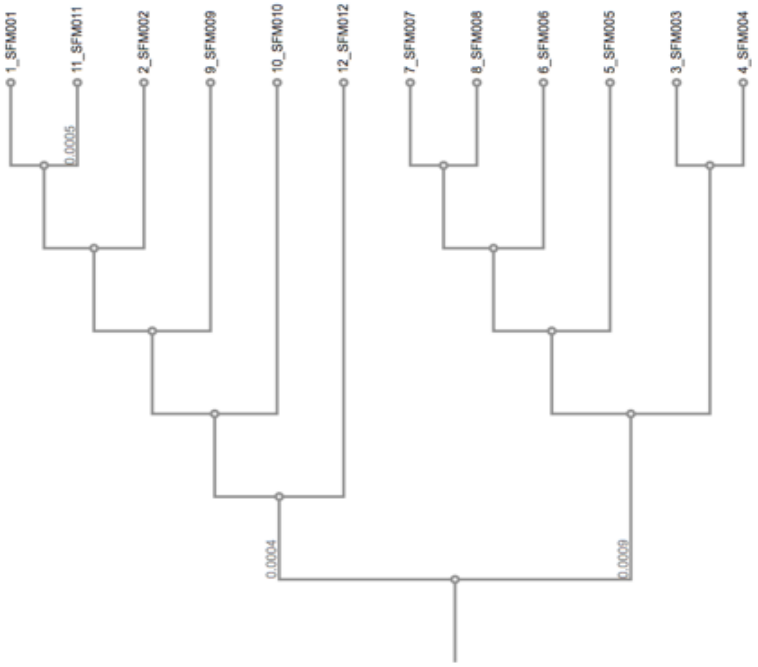

Figure 5-13 (b): Phylogenetic trees originated from the DNA polymerase (i) and the large terminase subunit gene (ii) using MAFFT. The phylogenetic trees originated from *polA* (i) and *terL* (ii). Both phylogenetic trees (b) were originated using MAFFT using default parameters.

a)

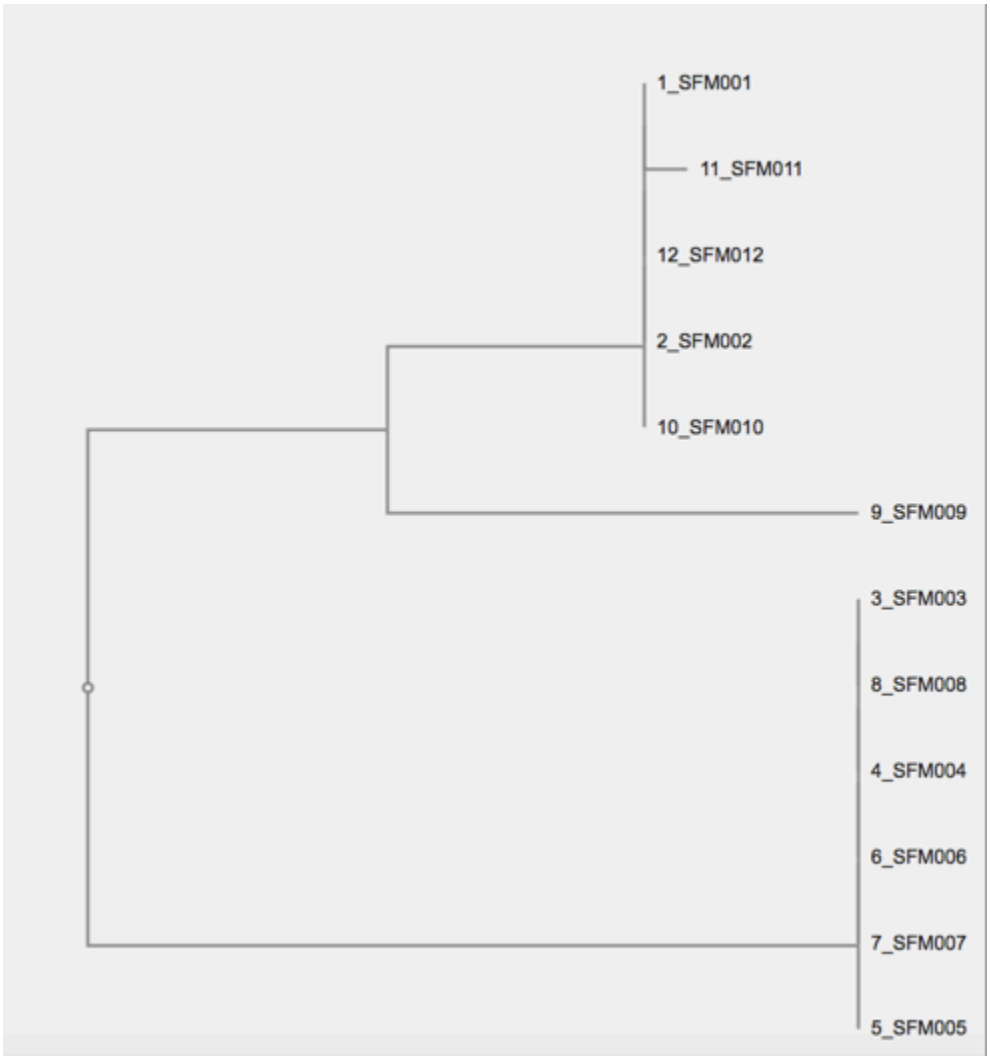

Figure 5-14 (a): Whole genome alignment using MAFFT. This phylogenetic tree was originated using MAFFT with default parameters and visualised with Archaeopterix.

b)

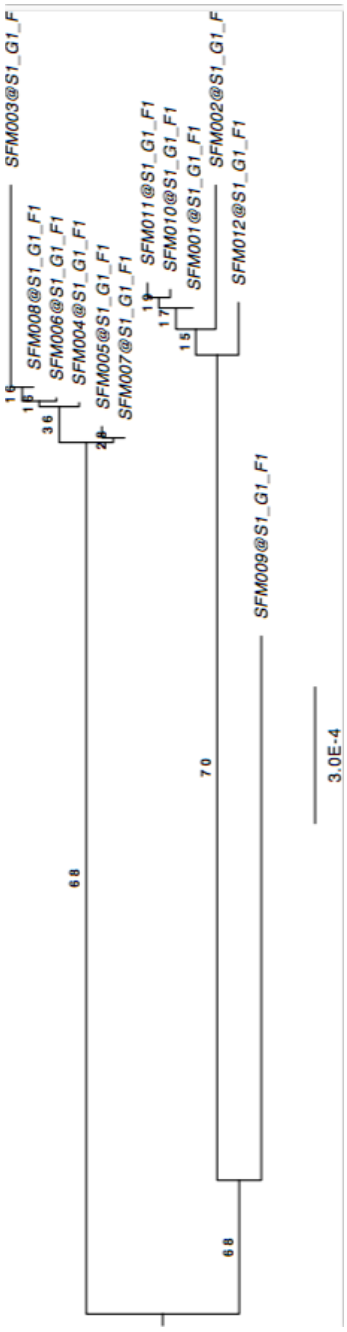

Figure 5-14 (b): Genome nucleotide comparison of the bacteriophage isolates using VICTOR (Virus Classification and Tree building Online Resource). Bacteriophage whole genomes were used for this analysis. Phylogenetic GBDP tree with a yielding average of 31%, the numbers above the branches are GBDP pseudo-bootstrap support values from 100 replications. The branch lengths of the resulting tree are scaled. The OPTSIL clustering yielded one species, one genus and one family clusters.

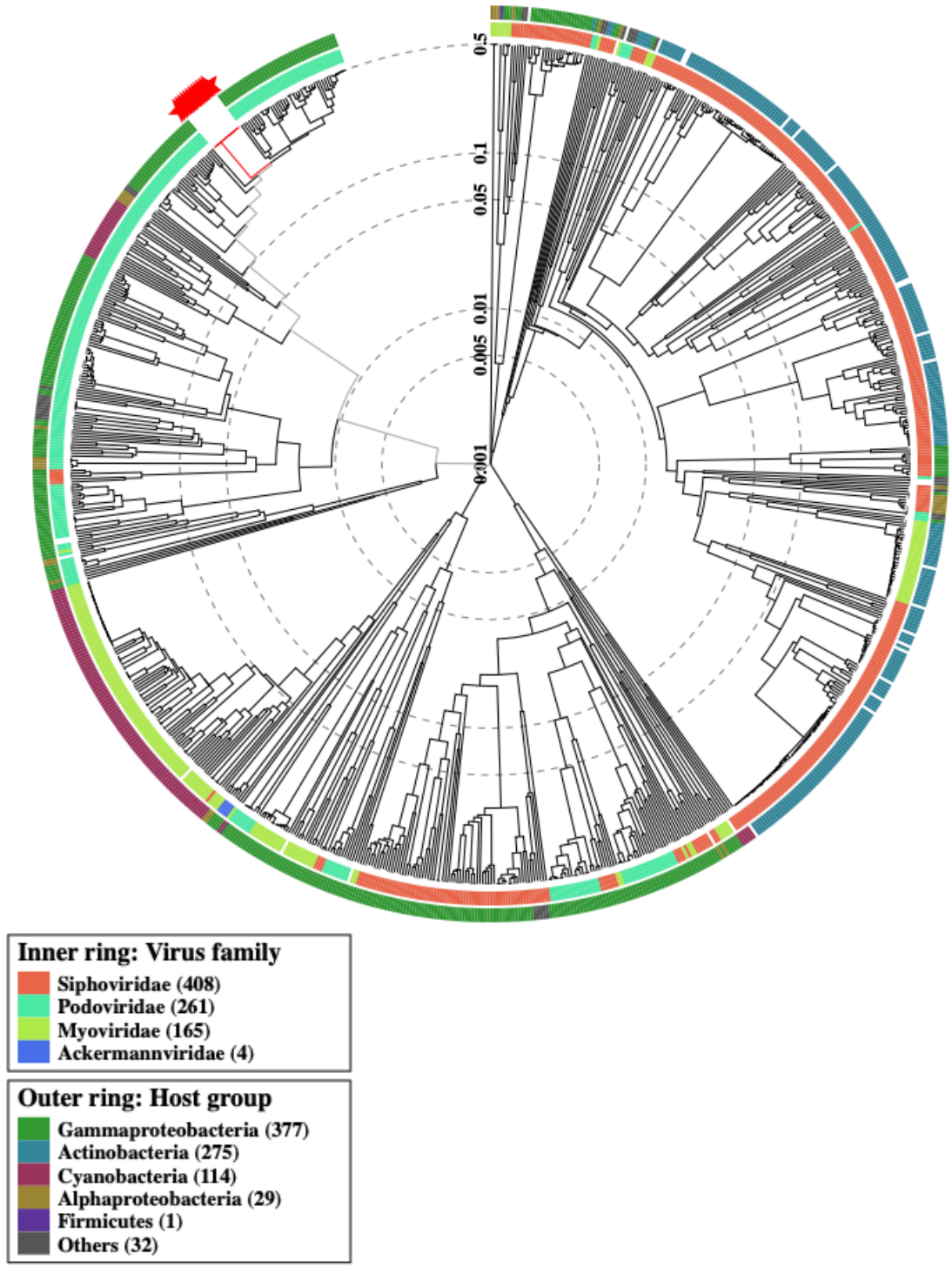

Figure 5-15: Global genomic similarity relationship of the isolated phages using VIPTree. This proteomic tree was generated using the VIPTree server using genome-wide proteomic similarities, our isolates are highlighted in red.

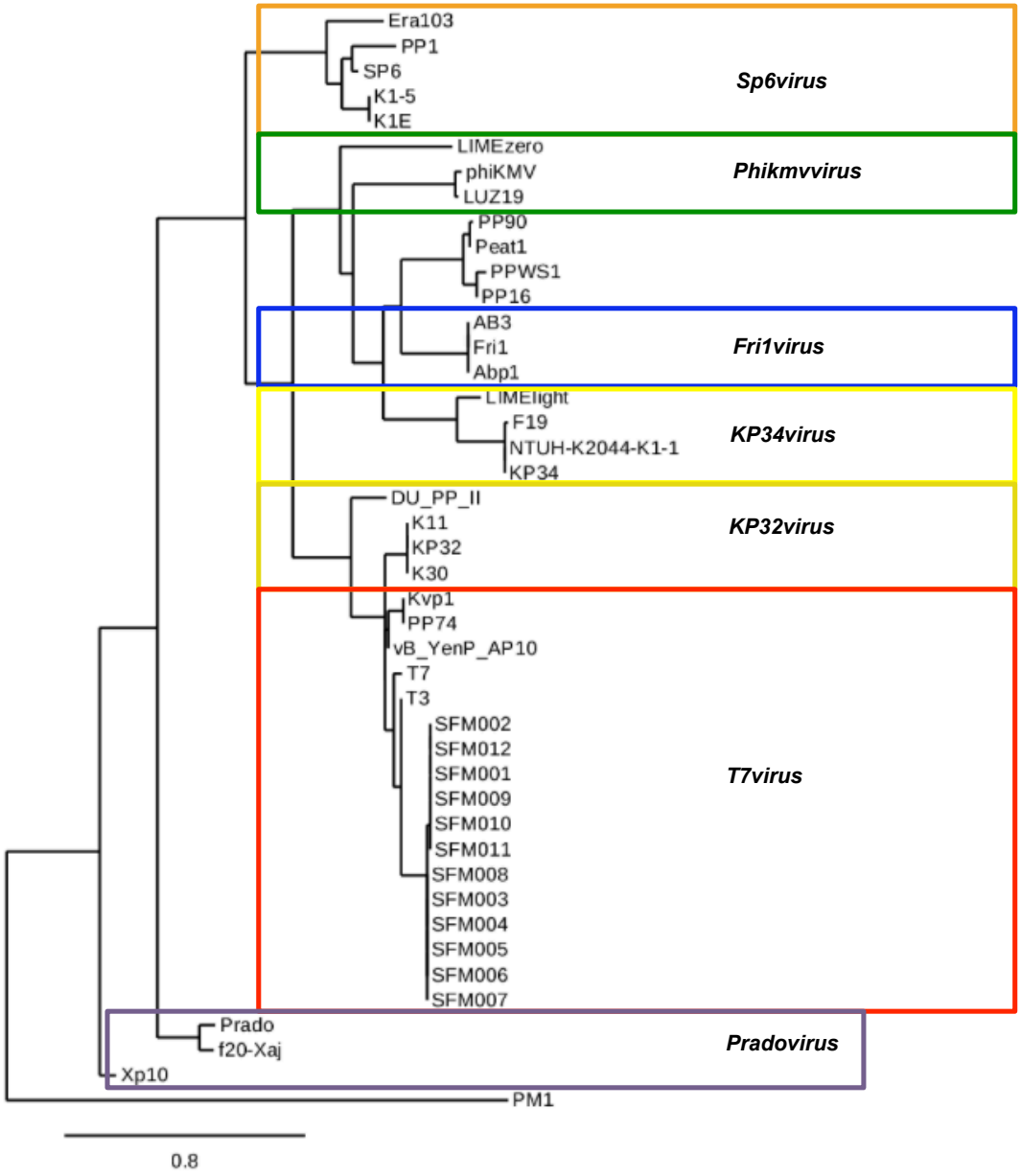

Figure 5-16: Neighbor-joining tree analysis of the RNA Polymerases of phages from the seven genera within the *Podoviridae* subfamily *Autographivirinae.* The phylogenetic tree was constructed using a MUSCLE alignment and the maximum likelihood method in PhyML program. Phage genera as defined by ICTV are delimited by the coloured areas with the type species for each genus.

5.3 Discussion

Obtaining the complete genome sequence of a bacteriophage is an essential step for regulatory approval for phage-based biocontrol and therapy applications in any industry.

Phage genomes have been successfully sequenced even at low coverages (Klumpp *et al.*, 2012; Rihtman *et al.*, 2016), this can present an advantage to other more used methods such as Illumina sequencing that may misinterpret the presence of repetitive sequence stretches (Klumpp *et al.*, 2012), or else it could present a disadvantage as sequencing errors could not be picked up. Nevertheless, recent advances have allowed the sequence of phage genomes from a single plaque (Kot *et al.*, 2014).

From the general features of the genomes analysed, there are a few aspects that require further questioning. The fact that the bacteriophages have circular dsDNA genome clashes with the previous concept that all tailed bacteriophages contain linear dsDNA (Casjens and Gilcrease, 2009), since this point would complicate the packaging and DNA injection processes as they happen through a narrow portal protein that does not accommodate two parallel dsDNA threads (Simpson *et al.*, 2000). Moreover, the circularity of the phages DNA was supported not only from the overlapping sequences of each isolate, but from the restriction enzyme analysis where the number of fragments produced agreed with the existence of a circular DNA molecule (Figure 5-3, a to d), for example, PacI cuts the genome only twice, BssHII cuts it between 2 and 3 times depending on the isolate, BglII cuts the genomes between 3 and 4 times, AvaI cuts between 4 and 5 times and SpeI cuts the genome 4 times. Most of these results reinforce the idea of a circular DNA, which is the form that the genome would take in the cytoplasm to avoid degradation by the host defense mechanisms. Contrarily, analysis of the GC skew in these isolates switches polarity upstream from the terminase gene, with a positive GC skew for half of the genome and close to zero for the other half (Figures 5-7 and 5-8). This change in polarity is indicative of the replication origins in adenoviruses and it changes linearly across the linear genomes (Grigoriev, 1999), supporting the fact that the genome is linear.

A common feature in all the published soft rot *Enterobacteriaceae* phage genomes is their genome organisation (Czajkowski, 2016a). All the analysis performed was indicative that these isolates were closely related, if not the same bacteriophage. From their genome sizes, varying only about 700bp, to their GC content of 50.2% in almost every sample, and restriction maps of the phage genomes were generated in order to verify genome size and/or contig alignment (Klumpp *et al.*, 2012)(Figure 5-3, a to d). The dot plot analysis, CCT view, Easyfig and Roary software only served to support this and previously sequenced genomes were included in the analysis in order to illustrate these similarities. The ANI results showed that all the samples were members of the same bacteriophage species (Figure 5-12), even though they were isolated from different raw materials and at different times (Table

3-1). This same result also happened when isolating phages active against *Pectobacterium parmentieri* in Poland (Smolarska *et al.*, 2018), indicating that there is some sequence conservation across globally distributed soils and that soil viral communities may have some broad biogeographical adaptation (Emerson *et al.*, 2012; Brum *et al.*, 2015; Roux *et al.*, 2016; Emerson *et al.*, 2018); this could be an effect from living in a soil environment where encountering a possible host is scarce. Within habitats, viral communities were characterised as endemic and were structured by soil depth (Emerson *et al.*, 2018). In addition, it has been observed that phages living in liquid medium have three times more SNPs than the same phages grown on plates (Magill *et al.*, 2017), as a direct result from more diffusion of phage and bacteria in liquid conditions.

From the analysis of some genomic features and their position within the genome, we can gather some more information about how the infection develops. The presence of their own RNA polymerase suggests that, like with ϕT7 and ϕT3, they use the host RNA polymerase to transcribe early genes, but then continue to use their own RNA polymerase to activate middle and late promoters (Klimuk *et al.*, 2013; Shadrin *et al.*, 2013). Middle genes, such as the ssDNA-binding proteins all displayed a final phenylalanine residue (data not shown) that increases affinity for the DNA polymerase (Ghosh *et al.*, 2009). The presence of an exonuclease downstream of the structural genes, suggests that nucleotides are required in high numbers for the replisome at this point (Lee and Richardson, 2011). These demands reflect that infection is a carefully regulated and temporally scheduled process (Young, 2014), and supports the idea that genes are only kept if they improve their survival (Sandmeler, 1994; Scholl and Merril, 2005; Thompson *et al.*, 2011).

Whole genome analysis showed high homology with genomes of two other bacteriophages from the *Enterobacteriaceae* family: *Escherichia coli* phage T7 and *Yersinia enterocolitica* phage vB_YenP_AP10. All these phages have non-overlapping host ranges, and a similar case happenned with the *Dickeya solani* phage LIMEstone1 (Adriaenssens *et al.*, 2012)

The genome alone, and subsequently the nucleotide sequence, does not exclusively explain the main differences between these samples, but their proteome could indicate their infection mechanism. For instance, a feature that is typical of T7-like genomes is the position of the endolysin, with predicted *N*-acetyl-*L*-muramoyl amidase activity within the early region and is homologous to ϕT7 gp3.5. This endolysin is present between the ssDNA-binding protein and the DNA primase/helicase genes (Figure 5-9 a) in all the genomes sequenced, and has great similarity with the endolysin from ϕDU_PP_II. It not only breaks the amide bond between the N-acetylmuramic acid and L-alanine in the peptidoglycan layer of bacterial cell walls but also interacts with the viral RNA polymerase inhibiting its transcription (Inouye *et al.*, 1973; Cheng *et al.*, 1994). A second endolysin similar to the *Yersinia* phage vB_YenP_AP10 was present in ϕSFM002 and ϕSFM003. Other

endolysins were found in the structural region of the genome, corresponding to late genes. Including a transglycosilase within the internal virion proteins (although some of these regions were not recognised depending on the annotation software used), with activity against peptidoglycan and an accessory function in DNA translocation in the procapsid (Rydman and Bamford, 2000; Rydman and Bamford, 2002), and a T7likevirus-type spanin or endopeptidase between both subunits of the terminase gene that is involved in the disruption of the outer membrane of the host (Young, 2014). Endolysins are a product of phage evolution and are highly specific through their requirement to continuously adapt to counteract host peptidoglycan dynamics (Glauner *et al.*, 1988), but also as a result from horizontal gene transfer events.

Restriction modification systems are ubiquitous and can be considered as early immune systems from bacteria (Vasu and Nagaraja, 2013). The phage genomes are thought to be unmethylated, like that of phage T3, which is expected as they code for a S-adenosylmethionine hydrolase that removes the methyl group donor (Molineux, 2012) and is part of the phage defense against the host type I restriction systems as this molecule is required as a cofactor for DNA cleavage (Studier and Movva, 1976; Bandyopadhyay *et al.*, 1985; Vasu and Nagaraja, 2013). Type I restriction-modification systems are large pentameric proteins that require ATP, Mg^{+2} and S-adenosylmethionine for both REase and MTase activities (Loenen *et al.*, 2014). Most bacterial genomes have only one Type I system, although three or more are common and once their infecting bacteriophages acquire resistance to the REases, the bacteria are no longer protected (Loenen *et al.*, 2014).

Toxin-antitoxin (TA) systems are also a bacterial defense mechanism. They are formed by a toxic protein and a neutralising antitoxin that have an important role in bacterial physiology, including stress response (Christensen *et al.*, 2001), programmed cell death (Hazan and Engelberg-Kulka, 2004), initiation of persister cells (Schumacher *et al.*, 2009), biofilm formation (Kim *et al.*, 2009) and abortive infection mechanism upon phage infection (Hazan and Engelberg-Kulka, 2004; Fineran *et al.*, 2009; Koga *et al.*, 2011). An inhibitor of a TA system was detected in the phage genome as gp4.5, a protein with 102aa, this protein in ϕT7 codes for a short protein (89aa) that overcomes the abortive infection required by the TA system (Sberro *et al.*, 2013) through interaction with the Lon protease in *E. coli* consequently overcoming the rapid destabilisation of the antitoxin protein. In reality, the bacterial proteases appear to be the weakest link in the TA-mediated defense mechanism, since all rely on the activity of just a single protease for multiple TA systems in the same host (Roberts *et al.*, 1994; Lehnherr and Yarmolinsky, 1995; Aizenman *et al.*, 1996; Van Melderen *et al.*, 1996; Christensen *et al.*, 2001; Cherny and Gazit, 2004).

The determination of phage termini reflects the different DNA replication strategies and DNA packaging by the bacteriophage terminase gene (Casjens and Gilcrease, 2009). In our samples, the termini were similar to

ϕT7 with short direct repeats (Figure 5-4 b) and no *cos* ends (Figure 5-4 a), which are linked to a linear DNA replication strategy and formation of concatemers for DNA packaging. These results were supported by the analysis of the amino acid sequences of the terminase gene in our samples and other characterised phages as previously done by Grose *et al.* (2014) (data not shown). Thus, concatemer formation and a DNA packaging strategy similar to that of phage T7 is likely to happen.

Tail proteins feature binding domains, that mediate host recognition with the cell surface and they are highly strain- or even serovar specific (Klumpp *et al.*, 2013; Lim *et al.*, 2014) and much research has taken advantage that host range is linked to tail fibre composition in some phages (Yoichi *et al.*, 2005; Mahichi *et al.*, 2009; Lin *et al.*, 2012; Le *et al.*, 2013). The tail fiber of bacteriophage T7 is a trimeric coiled-coil protein (Steven *et al.*, 1988) with a C-terminal β-propeller responsible for binding the receptor on the cell surface (Mahichi *et al.*, 2009; Garcia-Doval and van Raaij, 2012; Lee *et al.*, 2012; Minjung Park *et al.*, 2012; Lim *et al.*, 2017). Considering that the most manageable mode of resistance to a phage that a host can develop involves receptor variability and/or changes in accessibility to their receptor, it is obvious that most variations that occur are adsorption-related in the form of SNPs (Magill *et al.*, 2017). In-depth analysis of the tail fibre sequences would bring to light varying levels of co-occurrence between SNPs (Magill *et al.*, 2017), thus explaining where the host range variability resides within our isolates.

Phylogenetic analyses are important for comparison and to locate sequence similarities within a variety of different phages. Phage classification has worked well based on just one criterion, for example using the terminase sequence (Serwer *et al.*, 2004) or the RNA polymerase in the specific case of *Autographivirinae* phages, but it would work better using more phage characteristics (Ackermann, 2011). In this project, single gene analysis matched whole genome/proteome analysis but because phages in general have evolved vertically and by horizontal gene transfer from other phages and hosts. As a result, they should be classified based on whole genomes (Lawrence *et al.*, 2002), but also based on other viral properties such as presence of sugars and/or modified bases in phage DNA and particle weight. From all the genomic data collected, there are many regions that are present in some of the samples but not in others. These rearrangements, duplications and losses are a clear effect of recombination processes, and they mainly occur in close proximity to more conserved regions, such as the structural components in the genome.

Genome sequencing is the ultimate technique to study phage-encoded proteins. However, it only shows translational potential and not the proteins that are actually expressed during the host infection process (Pardini *et al.*, 2017). Thus, other omic approaches including proteomics, transcriptomics and metabolomics could be used in combination in order to completely understand their interaction (Horgan *et al.*, 2010; Leon-Velarde *et al.*, 2014).

Also, homology comparisons to characterised Pfam domains (Finn *et al.*, 2016) and three-dimensional protein structural modeling (Emerson *et al.*, 2018) will decipher the function of the hypothetical proteins in the future, once more phage genomes become available.

5.4 Conclusions and future work

Different variants from the same phage species were identified, their genomes sequenced and characterised both morphologically and through their infective properties. Despite having different host ranges, these isolates share close to 100% homology and future work could locate the areas of genetic heterogeneity that may be responsible for this different phenotype (Magill *et al.*, 2017), this will be important as it potentially could predict the rate at which these phages can evolve and change, either restricting or enlarging their host range.

This newly isolated phage is safe to use as a biocontrol agent, either on its own or as part of a phage cocktail. The immobilisation onto nanoparticles using the corona discharge method should be the next optimisation, as well as *in planta* tests to check its efficiency.

Routinely sequencing of this phage genome should be performed in the future, in particular if used as a phage treatment. As a living system, the host could develop new defence mechanisms that would protect it from viral infection, and special effort should be put into screening for tail fiber proteins, endolysins, R-M and TA systems in both hosts and bacteriophages.

6.0 Results

Characterisation and optimisation of bacteriophage-coated nanoparticles

6.1 Introduction

6.1.1 Immobilisation of bacteriophages using plasma treatment

The main drawback when using bacteriophage treatments in the past has been their vulnerability to environmental factors (Malik *et al.*, 2017). Phages are protein structures that are susceptible to external factors, such as UV light and sunlight (Jones *et al.*, 2007; Czajkowski *et al.*, 2015), temperature (Briers *et al.*, 2008), pH (Briers *et al.*, 2008; Knezevic *et al.*, 2011), presence of organic solvents (Puapermpoonsiri *et al.*, 2009) and/or proteases (Vranova *et al.*, 2013). Different methods have been used to improve storage and increase the shelf life of bacteriophage-based products, these include encapsulation (Stanford *et al.*, 2010) or freeze drying (Davies and Kelly, 1969; Ackermann *et al.*, 2004) to name a few. The immobilisation by corona discharge would give phages structural support, thus making them more resilient.

Plasma treatment or corona discharge has been used to enhance the attachment between polymers (Barton *et al.*, 2003; Canavan *et al.*, 2006) and different biological elements (Conte *et al.*, 2008; Luna *et al.*, 2011; Kerkeni *et al.*, 2013; Recek *et al.*, 2014) to different surfaces. Corona discharge is an electric discharge between two electrodes or one electrode and a surface. The direct application of a corona discharge onto a polymer causes surface modification between oxygen and nitrogen functional groups on its surface. This, in turn, allows the formation of covalent bonds with molecules containing carboxyl groups (Chan *et al.*, 1996), followed by crosslinking of these groups to the amines in proteins such as those found on the surface of phages (Pearson *et al.*, 2013). The increased content of oxygen-containing polar groups on the plasma treated surfaces, such as peroxide groups, carboxyl groups and hydroxyl groups explain their increased wettability or hydrophilicity (Wang *et al.*, 2016), and this improves phage attachment (Wang *et al.*, 2016).

Plasma treatments have proved more effective at immobilisation than other treatments (Wang *et al.*, 2016), though the viral particles must retain their active conformation. One of the main problems for successful immobilisation is the correct orientation of the viruses in order to stop steric hindrance (Richter *et al.*, 2017): virions should be arranged in a tail-up orientation that would expose their receptor-binding proteins (Richter *et al.*, 2017). In a constant electric field, bacteriophages are positioned as a result of the nonzero permanent dipole moment of the virions (Richter *et al.*, 2016), which is around 5600 Debye in phage T7 (Kosturko *et al.*, 1979). The origin of the dipole moment is a result of the electrophoretic movement of counterions within the zeta potential surface, as a function of the applied electric field, the time over which the field is applied and the size of the polymer (Chou *et al.*, 2002). The total force acting on a polyelectrolyte in an external electric field is the sum of the electrophoretic force (F_e) due to the net effective linear charge

density (β) of the polymer and the dielectrophoretic force (F_d) due to the induced dipole moment.

The electrophoretic force on a polyelectrolyte in an electric field is proportional to the local applied electrical field (E) and originates a constant velocity (v_e):

$$v_e = \mu_e E; \quad F_e = \zeta v_e = \zeta \mu_e E$$

where μ_e is the electrophoretic mobility of the polymer, v_e is the electrophoretic velocity, and ζ is the drag coefficient between the electrophoretic velocity and the force (Chou *et al.*, 2002).
The zeta potential of phage T7 is -21.1 ± 1.4mV in deionised water (Han *et al.*, 2014), the negative charge being present in the head as a result of containing the DNA while the positively charged tail fibers are electrostatically attracted to bacterial membranes, that are negatively charged (Baran and Bloomfield, 1978), thus facilitating infection. The tail-up orientation also increases the theoretical maximum density of phage and the denominated jamming or maximum coverage is the steric limit to further adsorption at a particular surface attachment reaction temperature (Naidoo *et al.*, 2012); this is approximately 100 phages per μm^{-2} in optimal conditions (Richter *et al.*, 2017).

The advantages of this phage immobilisation include low preparation costs, uniformity of the surface treated, no requirement of any coupling agents, temperature and pH stability, in some cases endurance to proteases (Schwind *et al.*, 1992) and organic solvents (Olofsson *et al.*, 1998) and the possibility of scaling up for industrial and commercial production (Chan *et al.*, 1996; Hosseinidoust *et al.*, 2014).

6.1.2 Cellulose and nylon particle properties

The two materials used for attachment are cellulose and nylon particles. Cellulose nanocrystals have many interesting properties, including high tensile strength, low density, low coefficients of thermal expansion, high aspect ratio, high surface area as well as optical and electrical functionality (Lagerwall *et al.*, 2014). These properties, together with the comparable ease of surface modification due to the hydroxyl groups makes this material very popular at the nanoscale level (Hosseinidoust *et al.*, 2015). On the other hand, nylon nanoparticles are interesting for their electrostatic electrochemistry, as they can carry out electron transfer reactions between two different polymers (Liu and Bard, 2009). As listed in the Triboelectric Series (Reches *et al.*, 2009) this material tends to give up electrons causing it to become positively charged, with a contact potential of about 4.2V, mainly due to its amide-amide secondary linkages (Arridge, 1967), ultra-pure nylon membranes are extensively used for DNA/RNA extraction.

6.1.3 Uses of immobilised bacteriophages

The many uses of phage immobilisation includes sensory/detection platforms, such as optical detection methods (Smietana *et al.*, 2011), microbead assays (Horikawa *et al.*, 2011), drug delivery systems (Pande *et al.*, 2010), mass-based techniques (Guntupalli *et al.*, 2012), surface plasmon resonance (Ktari *et al.*, 2012), cantilevers (Fu *et al.*, 2011) and electrochemical sensing (Yemini *et al.*, 2007; Kang *et al.*, 2010). Different surfaces that have been used include gold nanoparticles (Singh *et al.*, 2009; Arya *et al.*, 2011), cellulose (Anany *et al.*, 2011) and silica surfaces (Cademartiri *et al.*, 2010). Detection platforms are a fast and sensitive alternative to current methods and it has been applied in food (Loessner *et al.*, 1996) and hospital (Oda *et al.*, 2004; Tanji *et al.*, 2004) environments. Bacterial pathogens were infected by bacteriophages attached to hard surfaces in food processing environments, but only with MOI values of 1000 (Hibma *et al.*, 1997; Abuladze *et al.*, 2008) or more (Sharma *et al.*, 2005). Some platforms have successfully reduced the numbers of *Salmonella* in cheese (Modi *et al.*, 2001), chicken (Goode *et al.*, 2003) and melon slices (B. Leverentz *et al.*, 2001). The importance of these treatments is that they are an alternative to chemical sanitisers on food surfaces.

6.1.4 Aims and objectives

Once the isolates were fully characterised, the attachment to nanoparticles was begun. In order to determine the most effective material, nylon and cellulose nanoparticles were compared to each other and the best for attachment was selected. In addition, other parameters such as size, convenience to use stability and infection potential were also investigated.

After selection of the most appropriate nanoparticle, stability tests were also performed to ensure that phage-coated nanoparticles were more stable at different temperatures over time than free phages.

Bacteriophage ϕSFM002 was used for all the tests as this variant was the most characterised of all of them.

6.2 Immobilisation characterisation

Resistance of bacteriophage to external factors has been a bottleneck for phage treatments (Malik *et al.*, 2017). Attachment to nanoparticles or other surfaces confers structural stability, thus making them more resilient to environmental factors (Fister *et al.*, 2016). In this chapter, the ability of bacteriophage-coated nanoparticles to infect bacteria was performed and compared to that of free bacteriophages and also their stability to temperature over time.

6.2.1 Comparison between the use of cellulose and nylon particles

The comparison of the two different materials, with different sizes, available for attachment: nylon and cellulose, was performed. Before attachment, calculations were made in order to use the same titre of phage per square centimetre, assuming that the nanoparticles were spherical, the grams required per nanomaterial were calculated (see section 2.14 in Materials and methods),.After attachment, the nanoparticles were washed a number of times to discard any free phages, the methods used included centrifugation and membrane filtration and the number of steps required depended on the ability of the supernatants to form plaques (once the supernatants could not form any plaques, the nanoparticle suspension was ready for further testing). This optimisation served to choose cellulose over nylon particles for various reasons, including better infectivity after attachment, the plaques formed were bigger and visible after various dilutions, ease of manipulation as nylon could not be used for dilution, being immiscible in the buffer used (Figure 6-1) and the centrifugation step could not be performed successfully, also the cellulose nanoparticles were active even after the nylon cellulose stopped forming plaques. The cellulose nanoparticles were the most appropriate particles to use for attachment given the results.

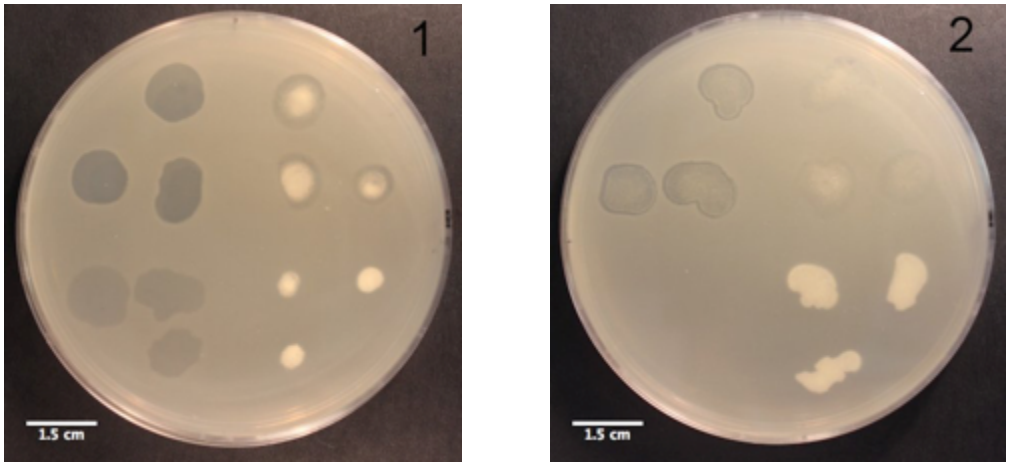

Figure 6-1: Plaques formed by free phages (left half of the plates) and plaques formed by bacteriophage-coated particles (right half of the plates). From the top right quadrant and clockwise, comparison between cellulose, nylon, supernatant from the nanoparticles and free phages (1), the same samples one week later (2). These samples were used for the stability test presented in figure 6-3. Each sample was done in triplicate and 10µl were spot-inoculated per replicate, 1.5 cm scale bars are shown.

6.2.2 Comparison between phage-coated nanoparticles and free bacteriophages

ϕSFM002-coated cellulose nanoparticles were tested for their infection ability against *Pectobacterium atrosepticum* (not its original host) and *Pectobacterium atrosepticum* SCRI 1043. The OxoPlate® method was used and included different MOIs of free bacteriophages for comparison (2.7.2.1 in Materials and methods). There were two different outcomes depending on the bacteria used, ϕSFM002 was not effective against *Pectobacterium atrosepticum* and only free bacteriophages with 0.001 MOI slowed infection down, though briefly (Figure 6-2 a). When using *Pectobacterium atrosepticum* SCRI 1043 all the treatments used slowed down bacterial growth at different levels (Figure 6-2 b), for example free ϕSFM002 with a MOI of 0.000001 only dropped growth briefly whereas MOI of 1 inhibited growth completely (like the negative control containing sterile nanoparticles), all the other treatments tested worked similarly to one another (free ϕSFM002 with MOI of 0.001, diluted and undiluted ϕSFM002-coated cellulose), retarded growth by two hours at the end of the run (the pO_2 levels were between 50-60%, and were achieved six hours after the start of the experiment on the positive control) . Therefore, ϕSFM002-coated cellulose nanoparticles in suspension were as effective as free ϕSFM002 with 0.001 MOI.

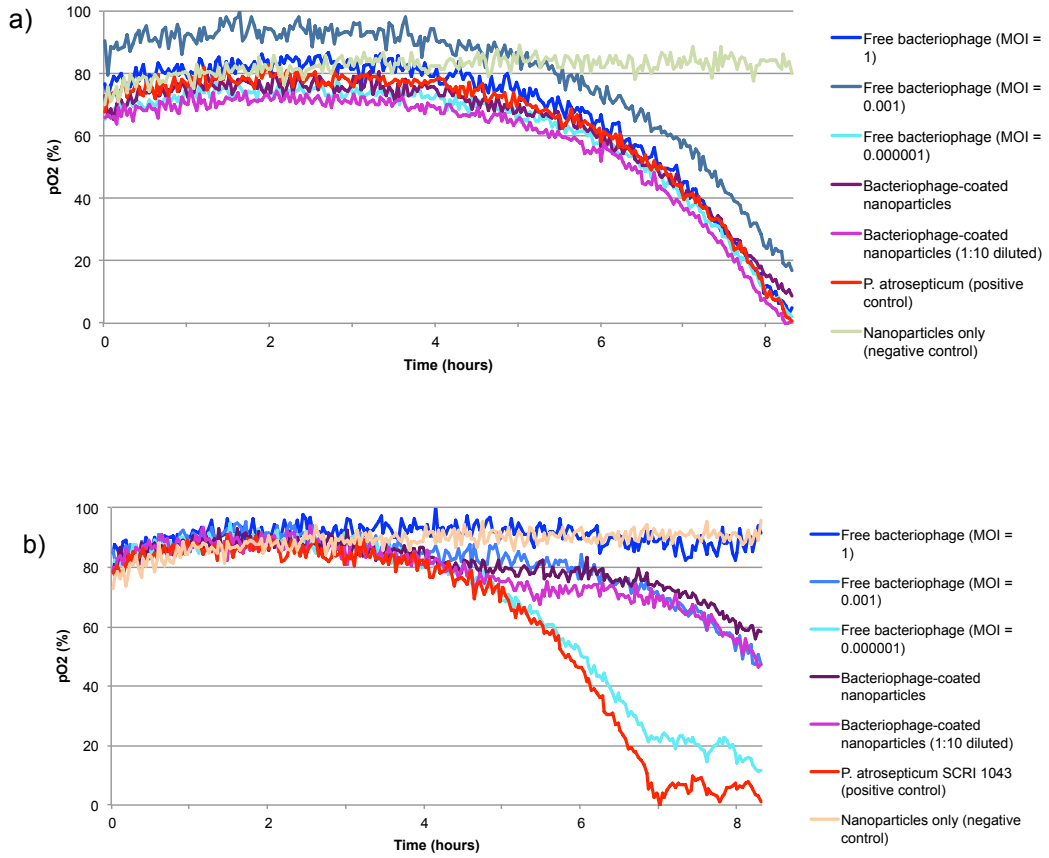

Figure 6-2: Prevention of bacterial growth in liquid media using free bacteriophages and bacteriophage-coated nanoparticles. Oxoplate® results comparing free bacteriophages against bacteriophage-coated nanoparticles against *P. atrosepticum* (a) and *P. atrosepticum* SCRI 1043 (b) using different dilutions of ϕSFM002. Samples were read every five minutes for eight hours at room temperature, a solution containing sterile nanoparticles was used as the negative control, whereas untreated bacteria were used as positive control, three different MOIs were tested with free bacteriophages and two different dilutions were tested for bacteriophage-coated nanoparticles (MOIs could not be calculated). The results shown were the average from six replicates.

6.2.3 Temperature stability of phage-coated particles, compared to free phages

Temperature stability was compared between ϕSFM002-coated cellulose nanoparticles and free ϕSFM002. Their ability to form plaques was measured after incubation at 4°C, room temperature, 30°C and 37°C over a period of time (6 days for free phages and four weeks for the attached ones). The free ϕSFM002 were incubated for a week since decrease in numbers was seen after just one day for all the samples (Figure 6-3 a): the same starting stock of approximately 10^9pfu/ml was used, after one day all the samples lessened approximately 10-fold with the exception of the samples incubated at 37°C where the decrease was higher. By day 2, only the samples kept at 4°C declined another order of magnitude, whereas room temperature was slightly more and both 30°C and 37°C incubations dropped 100-fold compared to day 1. Six days after the start of the experiment the only samples left were the ones incubated at 4°C and at room temperature, that had both the same titre as the 30°C and 37°C two days after the start of the experiment (just below 10^6pfu/ml). The ϕSFM002-coated nanoparticles were incubated for approximately a month (Figure 6-3 b) with differing starting stocks: all the samples had 10^7pfu/ml apart from the 37°C which had 10^6pfu/ml. The 4°C sample remained the same throughout the whole experiment and the 37°C sample did not form any plaques after the starting week. On the other hand, the room temperature sample dropped slightly on week one and maintained this titre for weeks two and three to drop to 10^5pfu/ml on the last week. The samples incubated at 30°C decreased by 10-fold on week one, another 10-fold decline on week two and then remained more or less the same for the rest of the experiment. When comparing both sets, the samples incubated at 37°C did not survive after one week independently of being attached or not, followed by the samples incubated at 30°C which did not last after one week if unattached but they survived well after four weeks if attached to nanoparticles. The samples incubated at room temperature dropped from 10^9pfu/ml to 10^5pfu/ml in less than a week as free ϕSFM002, whereas the attached ϕSFM002 declined from 10^7pfu/ml to 10^5pfu/ml after four weeks, if kept at 4°C free ϕSFM002 decreased from 10^9pfu/ml to 10^6pfu/ml, while they remained at constant levels after four weeks incubation when attached. In conclusion, attachment to nanoparticles did increase their temperature stability, especially at lower temperatures.

a)

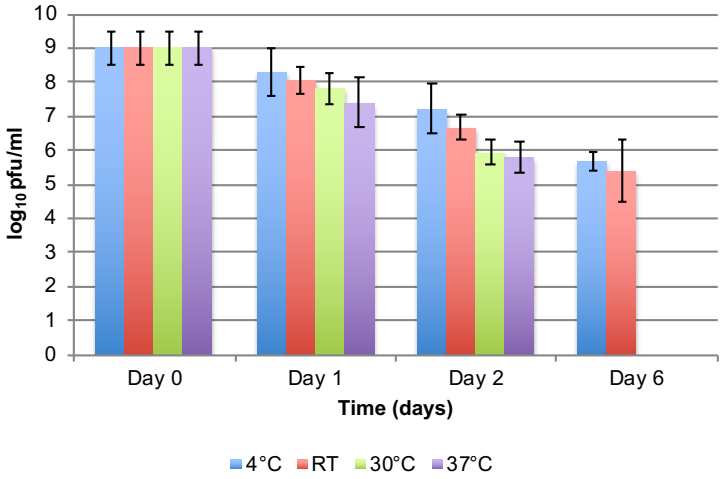

b)

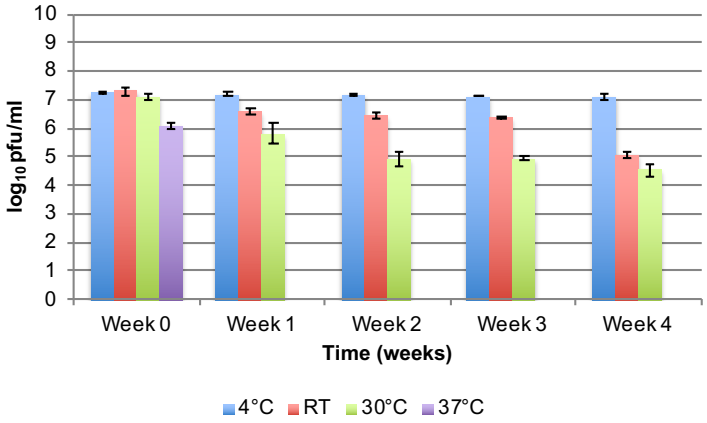

Figure 6-3 (a and b): Stability test results of free bacteriophages (a) and bacteriophage-coated particles (b). Stability test performed on free bacteriophages (a) and on bacteriophage-coated cellulose nanoparticles (b) at different temperatures. This experiment measured the ability to form plaques (pfu/ml) over a period of time, data was taken on triplicate and using only one biological replicate for the nanoparticles, whereas twelve biological replicates were used for the free bacteriophages samples. Note that time scales and initial phage stocks are different (days for free phages and weeks for bacteriophage-coated nanoparticles).

6.3 Discussion

The differences between nylon and cellulose nanoparticles did not just rely on their size but their physical and chemical properties. When using nylon, the phage infectivity was worse that when using cellulose, and this could be caused by steric hindrance of the phage receptor and/or non-covalent bonding of the nanoparticle but attachment through electrostatic interactions. The immiscibility in water of the nylon particles made them very unpractical to use. If we add that nylon plays an important part in the increasing issue regarding plastic pollution from human activities and waste in the oceans and within the gastrointestinal tract of fishes in rivers and at sea (Tanaka and Takada, 2016; McGoran *et al.*, 2017), it seems unethical the use of nylon nanoparticles for this purpose as they will pollute the environment and may be banned for use in the future. This issue does not present with cellulose as it is a ubiquitous material, present in every plant cell wall and its disposal cannot be an issue since cellulases are present in many bacteria and fungi, including *Pectobacterium* spp. (Sethi *et al.*, 2013), being mostly degraded on site. Another good alternative would be quitin as it is widely spread in nature.

Obtaining high concentrations of phage was always a limiting factor, thus the required optimisations and biological replicates of the experiment could not be completed but some considerations previous and after phage attachment were taken into account, including the buffer, the use of any coupling agents and mixing with a protective solution. The buffer used must be of high ionic strength as virions are unstable in low osmotic strength solutions (Leibo and Mazur, 1966), varying the ionic strength can alter electrostatic interactions between phages (Naidoo *et al.*, 2012), PBS ionic strength rises strongly at pHs below 3 and above 6 and it was used previously in other attachment experiments (Zhou *et al.*, 2017). The coupling agents, such as carbodiimide, glutaraldehide, vinylsulfonylethylene ether or triazine could improve attachment or stabilising agents like trehalose that could help maintain phage viability and infectivity (Scott and Mattey, 2009). Immersion in a 5% suspension of skimmed milk buffer immediately after the plasma treatment could block any surface unoccupied by phages with casein and avoid the nonspecific binding of bacterial cells (Richter *et al.*, 2017). All these different solutions could be tested to improve phage orientation and attachment.

Experiments previously used to immobilise phages on cellulose, relied on applying positively charged chemicals to modify their surface and bind phages electrochemically (Anany *et al.*, 2011). More recent methods resulted in an optimal phage orientation and surface coverage used an additional step to achieve the deposition of phages in al alternating electric field (Richter *et al.*, 2017), taking advantage that the phages aligned as a result from electrostatic interactions in close proximity to the surface. Adding the fact that phages, as colloidal unsymmetrical particles, have a permanent dipole moment, this is they have a negatively charged head and positively charged

tail fibers (Baran and Bloomfield, 1978), thus their orientation can be modified using an electric field (Shurdov and Gruzdev, 1984).

The voltage and frequency applied for phage orientation were not optimised, this may improve the orientation of the phages or deactivate them during the corona treatment, although the positive potential applied should have enhanced phage deposition. Phage orientation is related to the Debye length (k^{-1}) on the nanoparticles (Anany *et al.*, 2011), the viral particles align along the lines of the electric field within the small volume when k^{-1} is larger than the size of the phage, if k^{-1} is smaller then the orientation of the phage happens from electrostatic interactions (Zweckstetter *et al.*, 2004; Sadeghi *et al.*, 2011). Asymmetrical phage immobilisation on biosensors without a favored orientation normally show low efficiency detecting bacteria (Hosseinidoust *et al.*, 2011), as a result only 3-10% of receptors are available for infection as seen previously (Richter *et al.*, 2017). To prove this, more characterisations are required, like selectivity analysis using stained cells in confocal microscopy or limit of detection of the nanoparticles (Wang *et al.*, 2016; Richter *et al.*, 2017), this is the lowest concentration of bacteria that can be detected and is statistically different from a blank (Zhou *et al.*, 2017).

The measurement of dissolved oxygen in solution is a reliable method that measures cell viability. In this regard, the OxoPlate® has been used for both bacterial (Hutter and John, 2004) and cancer cells (Cook *et al.*, 2012; Kim *et al.*, 2015) to measure their oxygen consumption over time. The OxoPlate® results showed the infectivity potential of the attached phages, and demonstrated that there are threshold concentrations in phage below which infection can be interrupted (Figure 6-2 a) (Chibani-Chennoufi *et al.*, 2004) and, in general, higher MOIs result in higher bacterial inactivation (Leverentz *et al.*, 2003; Guenther *et al.*, 2009), as seen on free phages during the OxoPlate® experiment (Figure 6-2 b). Other experiments that measure the infectivity potential of attached phage include the disk-diffussion method (Andrews, 2009) or electrochemical impedance spectroscopy (Zhou *et al.*, 2017), this last method would determine the latent period of the phage when attached (Zhou *et al.*, 2017). To test the presence of covalent bonding on the nanoparticles, attenuated total reflectance-Fourier transform infrared spectroscopy (ATR-FTIR) measurements would detect amide bonds, carboxyl and hydroxyl groups on the nanoparticles (Zhou *et al.*, 2017). A negative control sample, with no voltage applied could also be tested.

Over time, the treated surfaces can return to their untreated states. The stability test (Figure 6-3 a and b) showed that after one month, the samples at 4°C remained highly active against their host compared to the others kept at higher temperatures, if phages do detach from the nanoparticles, they would have not maintained their titre as they did (Figure 6-3 a). Two processes can explain the hydrophobic recovery and loss of functional groups on plasma-treated surfaces over time: one is the loss of polar chemical groups from the surface of the material (Schamberger *et al.*, 1994) or by diffusion of these functional groups into the matrix (Paynter, 2000).

Understanding the longevity of the plasma treatment through stability tests helps stablishing a shelf life (Wang *et al.*, 2016). In addition to this, storage conditions of immobilised phages can affect their efficacy to infect, for example drying the samples could alter their orientation or deactivate the receptor binding proteins (Hosseinidoust *et al.*, 2014), in this case lyophilisation was effectively proven to retain activity on ϕT4 (Wang *et al.*, 2016), as an alternative.

With all the experiments performed on attached nanoparticles, more biological samples are required to support these results and to fully characterise the immobilisation method and obtain the highest infectivity and the lowest sensitivity in the attached nanoparticles. On the other hand, other stability tests should be added such as pH stability or UV treatment.

7.0 Results

Efficiency of bacteriophage treatment in preventing pectinolytic bacteria development *in planta*

7.1 Introduction

7.1.1 Importance of soil microbiomes in plant growth

In the last decade, soil microbiome research has highlighted the importance that plant-associated microbial mutualists have for maintaining growth and health of their plant hosts. Roots secrete many organic compounds derived from the photosynthetic activity to the rhizosphere (Dakora and Phillips, 2002), in a process known as rhizodeposition that is believed to attract and sustain the rhizobial microbiota (Jones *et al.,* 2009; Lundberg *et al*., 2012; Lebeis *et al.,* 2015; Berg *et al*., 2017; Edwards *et al*., 2015; İnceoğlu *et al*., 2011; Bai *et al.,* 2015). The bacterial communities from the rhizome in maize were different to those from the surrounding bulk soil (Gomes *et al*., 2001; Sanguin *et al*., 2006; Haichar *et al*., 2008; Bouffaud *et al*., 2012; Peiffer *et al*., 2013) and they provide defense to their host acting as a protective barrier against pathogens (Berendsen *et al*., 2012; Mueller and Sachs, 2015; Wei *et al*., 2015), in a similar way as the gut microbiomes.

Endophytes (Dobereiner, 1992), or symbionts living inside plants, play a role in reducing the effect of environmental stresses in plants such as heat, drought, nutrient limitations, excessive salinity and exposure to pollutants (Ryan *et al*., 2008; Redman *et al*., 2011; Khan *et al*., 2012; Bulgarelli *et al*., 2013; Chang *et al*., 2014; Wani *et al*., 2015; Santoyo *et al*., 2016; Rho *et al*., 2018). They also produce plant growth chemicals such as indole acetic acid (Beyeler *et al*., 1999) or cytokinins (Timmusk *et al*., 1999), enhancing seed germination and increasing their fruit yield. Multiple studies in this field used a mixture of endophytic species, also called consortia, to prove a synergistic effect on the host plant (da Silva *et al*., 2014). These communities are complex yet stable and their composition is influenced by interactions within the community, such as microbes (Mee *et al*., 2014), the plant host (Lebeis *et al*., 2015; Bodenhausen *et al*., 2014; Peiffer *et al*., 2013; Aira *et al*., 2010; Bouffaud *et al*., 2012) and the spatial distribution of the soil (Kim *et al*., 2008; Aira *et al*., 2010; Johnston-Monje *et al*., 2014), although the effect of phages in this environment has also been reported (Ofek *et al*., 2014).

7.1.2 Use of antibiotics in agriculture

The importance of these bacterial communities in the soil has been neglected through the use of antibiotics for crop protection, which has been indispensable in the United States for over 50 years (Stockwell and Duffy, 2012). One of the major problems with antibiotics is their broad spectrum of activity that kills not only the target bacteria but other non-target commensal bacteria (Tamma *et al*., 2012). As a result, antibiotic treament affects the microbiome and can cause plants to develop an antibiotic-associated infection (Davies and Davies, 2010; Tamma *et al*., 2012). Antibiotics are used on plants as a prophylactic, and for treatment of perennial plants such

as pear or apple trees (Stockwell and Duffy, 2012). Spraying antibiotics on the field might increase the frequency of antibiotic resistance genes and, in fact, streptomycin resistance was detected between five to ten years after antibiotic application (Jones and Schnabel, 2000; McManus *et al.*, 2002) and was even detected ten years after the application was stopped (Moller *et al.*, 1981). Other antibiotics include oxytetracycline, gentamicin and oxolinic acid that are used for different bacterial pathogens of plants including *Pectobacterium* spp. (Stockwell and Duffy, 2012). At present, the development of plant disease risk models that are based on environmental parameters and the potential of pathogen populations present in plants is used to calculate the amount of antibiotic required to prevent bacterial infection (Billing, 2000), for example streptomycin treatment (or also known as plantomycin) is used at concentrations between 50 and 150µg/ml and oxytetracycline between 150 and 200µg/ml, with residue tolerance levels on plant of 0.25 and 0.35ppm, respectively (Stockwell and Duffy, 2012).

More recently, the emergence of a carbapenem-resistant *Enterobacteriaceae* containing a highly-transmisable plasmid with the resistance gene for the New Delhi metallo-beta-lactamase (NDM) (Kumarasamy *et al.*, 2010; Yang Wang *et al.*, 2012) has put the use of antibiotics for farming under question. By 2006 the European Union banned all nonmedicinal use of antibiotics in animals and more recently, the United Kingdom government committed to significantly cut antibiotic use in animals reaching the target of 50mg/kg in farm animals by 2016 (two years earlier than proyected) (Veterinary Medicines Directorate, 2016). Other studies proved that antibiotics used in medicine or agriculture are unlikely to alter phage resistance or phage-antibiotic cross-resistance in the environment (Allen *et al.*, 2017), though they do affect the bacterial microbiomes in soil.

The high specificity that is characteristic of phage treatment results in fewer off-target effects on other commensal microflora than antibiotics do (Loc-Carrillo and Abedon, 2011), additionally the self-replicating quality of bacteriophages, their simple, rapid and low production costs make them suitable for use as antimicrobial agents (Loc-Carrillo and Abedon, 2011). Phages are intimately linked to the ecology and evolution of their hosts (Grose and Casjens, 2014), and the pharmacokinetics of phage therapy replicate predator-prey models of population dynamics as opposed to classical peak-distribution-elimination phases typical of antibiotic treatment (Levin and Bull, 2004). The combination of both antibiotic and phages can work in synergy and prevent bacterial resistance (Torres-Barceló and Hochberg, 2016), and in some cases phage resistance can reinstate antibiotic susceptibility (Chan *et al.*, 2016).

7.1.3 Role of bacteriophages in soil communities

Phage ecology can be divided into four categories: phage organismal ecology that includes the adaptations of phage that increase the resilience in

between hosts, phage population ecology or the intrinsic properties of phage growth and phage-phage competition for their host, phage community ecology or the stability of the environment that contains phage populations, and phage ecosystem ecology that studies the impact phages have on energy flow and nutrient cycling within environments (Gill and Abedon, 2003).

Phage densities are very large in the environment: it is estimated that there are as many as 100 million or more per gram of soil or ml of aquatic environment (Wommack and Colwell, 2000; Ashelford *et al.*, 2003), although the actual number of phages capable of infecting a specific bacterial strain are much smaller (Gill and Abedon, 2003). One of the factors that make bacteriophages important is their role in genetic transfer, and their contribution to the evolution of bacterial cells by acquiring and spreading DNA horizontally through transduction (Navarro and Muniesa, 2017) that occurs once every 10^8 phage particles (Bushman, 2002; Chibani-Chennoufi *et al.*, 2004), and actively contributes to the equilibrium of the natural bacterial flora (De Paepe *et al.*, 2014).

Plant-associated symbiotic bacteriophages are classified into helpful (mutual) or harmful (pathogens). Temperate phages are helpful as they protect their bacterial host from infection by homoimmune phages (Gill and Abedon, 2003; Dedrick *et al.*, 2017; Howard-Varona *et al.*, 2017) and they can also modify the host phenotype in a process called phage conversion. As a result, lysogeny plays a role in sustaining the phage population size at the environmental carrying capacity by extending the time for bacterial lysis (Gill and Abedon, 2003). Additionally plants can induce bacterial lysogens in an attempt to eliminate bacterial pathogens (Erskine, 1973; Gvozdyak, 1993). In plants, bacteriophages with lytic life cycle effects are limited to phage-induced bacterial lysis and result in a reduction in plant growth or plant nitrogen content (Ahmad and Morgan, 1994; Johnson, 1994; Hammad, 1998). The development of resistance mechanisms against phages usually comes at a metabolic cost for the bacteria and can potentially change the plant-interaction phenotypes (Lennon *et al.*, 2007; Avrani *et al.*, 2011; Oechslin *et al.*, 2017).

In most crop soil environments, the soil is only partially hydrated which impedes diffusion of free phages, and without mixing of soil, the existing bacterial microcolonies associated with the rhizosphere could exhibit periods of growth or death regarding phage infection (Gill and Abedon, 2003). In addition, phages can become trapped in biofilms (Storey and Ashbolt, 2001) or become reversibly adsorbed to particles commonly found in soil (Burge and Enkiri, 1978; Williams *et al.*, 1987) as a result of their surface chemistry, virion size and pH (Chattopadhyay and Puls, 2000), adsorption to clays could have a protective effect by maintaining phages within a hydrated environment (Williams *et al.*, 1987), and acidic soils can permanently inactivate phages (Sykes *et al.*, 1981; Pantastico-Caldas *et al.*, 1992). In contrast, phages present on the phyllosphere are exposed to UV light,

dessication or also high temperature ranges (Adams, 1959; Ritchie *et al.*, 1977), but their presence is mainly the result of plant germination and growth. In fact, some phages were found in water irrigation systems (Okabe and Goto, 1963) or even arthropods (Erskine, 1973) probably following similar paths to those used by their host bacteria (Gotō, 1992).

7.1.4 Use of bacteriophages as biocontrol agents

There is a strong reciprocal selective pressure for the phage to become more infective and the bacteria to become resistant (Buckling and Rainey, 2002), if phage-resistant bacteria are present, the bacteriophages do not interact with them, are selected and could potentially replace the existing communities (Lenski and Levin, 1985; Dennehy, 2012). Selecting certain bacterial traits, preventing viral reproduction and continuing bacterial progeny (Avrani and Lindell, 2015). Phage-resistance in bacteria is often accompanied by a fitness cost, either by a higher susceptibility to other phages (Avrani *et al.*, 2011; Marston *et al.*, 2012; Castillo *et al.*, 2014; Oechslin *et al.*, 2017) or by slowing their growth rate (Chao *et al.*, 1977; Bohannan and Lenski, 2000; Middelboe, 2000; Lennon *et al.*, 2007), this characteristic was successfully used for vaccine development against *S. enterica* and *S. aureus* (Capparelli *et al.*, 2010).

In contrast to antibiotic resistance, phage-resistance remains under control through coevolution, in different studies the appearance of phage-resistant bacteria did not result in a selection over the susceptible colonies (Connerton *et al.*, 2004). Recently, the entire *sap* operon was proven to play a role in phage susceptibility in T4 and T7 phages (Parra-Lopez *et al.*, 1993) by encoding an ABC transporter that transfers antimicrobial agents to the bacterial cytoplasm. Despite this, the stringent starvation protein A gene (*sspA*) provided phage resistance (Cowley *et al.*, 2018) through transcriptional regulation but the mechanisms are still unknown; althought it is known that SspA works in association to the RNA polymerase and prevents the accumulation of H-NS to upregulate various stress defence systems (Hansen *et al.*, 2005).

The main concern about using bacteriophages to control plant pathogens is their narrow host range (Jones *et al.*, 2007; Jones *et al.*, 2012). Therefore the combination of various phages in a cocktail is common for treatment of a wide range of bacteria that cause the infection (Pires *et al.*, 2016). Selection of appropriate phages for use as biocontrol agents is an essential step (Jones *et al.*, 2012), and they can be applied to the rhizosphere or the phyllosphere of the plant. Factors such as sunlight irradiation (Buckling *et al.*, 2006), temperature, nature of adsorption, pH, clay type, organic matter, nutrient availability for the host (Friman and Buckling, 2013; Friman and Buckling, 2014; Gómez *et al.*, 2015), heavy metal concentrations, acid pollutants, ionic strength (salinity) and moisture are some of the factors that

affect phage viability (Iriarte *et al.*, 2007; Kimura *et al.*, 2008). From all these factors mentioned, only adsorption (Goyal and Gerba, 1979; Farrah and Bitton, 1990), UV irradiation (Iriarte *et al.*, 2007) and temperature (Hurst *et al.*, 1980; Straub *et al.*, 1992; Leonardopoulos *et al.*, 1996) are the main factors for phage survival. Besides, the success of a singular phage treatment is influenced by phage and host densities (Johnson, 1994), but also the timing of phage application (Payne and Jansen, 2000; Payne and Jansen, 2003), phage burst size and bacterial fitness of resistant bacteria. Thus, the specific interaction between phage and host relies on characterisation of each phage treatment under certain conditions before use as biocontrol agents, without the possibility of extrapolating to a different bacterial or phage system (Gill and Abedon, 2003). In addition, phage uptake by the plant depends on the plant species, plant size, age and type of soil or media in which the plant is grown (Iriarte *et al.*, 2012).

The use of phage cocktails has been successfully used in veterinary medicine (Carrillo *et al.*, 2005; Carvalho *et al.*, 2010; Hawkins *et al.*, 2010; Chan *et al.*, 2013), food industry (Britta Leverentz *et al.*, 2003; Bigwood *et al.*, 2008; Garcia *et al.*, 2008; Spricigo *et al.*, 2013) and agriculture (Bae *et al.*, 2012; Adriaenssens *et al.*, 2012). Even some phage-based products have received approval for treatment of food produce, this is the case for ListShield™, EcoShield™ and SalmoFresh™ from Intralitix to control *Listeria monocytogenes, Escherichia coli* O157:H7 and *Salmonella enterica*, respectively, in foods or food-processing environments, Salmonelex™ and Listex™ P100 from Micreos to prevent respectively, *Salmonella* and *Listeria monocytogenes* spread during food processing and AgriPhage™ from OmniLytics to control *Xanthomonas campestris* and *Pseudomonas syringae* on tomato and pepper plants (Pires *et al.*, 2016).

Proof-of-concept experiments to use therapeutic phages were successfully performed against *P. carotovorum* subsp. *carotovorum* on potato plants (Eayre *et al.*, 1995), lettuce (Lim *et al.*, 2013) and on calla lily plants (Ravensdale *et al.*, 2007) and for prevention of potato soft rot development by *P. atrosepticum* (Balogh *et al.*, 2010). The number of characterised phages that infect soft rot *Enterobacteriaceae* grows (Czajkowski, 2016a) and in the near future it is likely that a phage cocktail will target the main soft rot and blackleg producing organisms in just one application (Smolarska *et al.*, 2018).

Disease management on potato relies on host plant resistance, sanitation and cultural practices (Norelli *et al.*, 2003). For example, classification systems of seed potato tubers were introduced to assess quality of the propagation material and rely mainly on visual inspections of both crops and harvested seeds (Shepard and Claflin, 1975) but ignore any latent incubation of the bacteria (Perombelon and Hyman, 1995; Toth *et al.*, 2011). As such, there is no requirement by the European Union to test for these bacterial species in potato. Currently, potato seed treatments contain chemicals such as captan, thiophanate methyl, mancozeb, bleach and fludioxonil (Yangui *et*

al., 2013) and they all are, apart from bleach, fungicides. Both heat and sodium hypochlorite are effective control measures of soft rot (Ranganna *et al.*, 1998; Soriano and Climent, 2006) though not feasible for toxicity and economic reasons. Chlorine bleach is the standard for post-harvest sanitation but it is environmentally harmful and not effective once the seeds have been infected (Bartz, 1999). The importance of alternative treatments to reduce fungicide and insecticide use in crops is the main objective of the project VIROPLANT that aims at developing viral-based treatments to protect crop plants from phytopathogenic bacteria.

The established regulatory frameworks for drugs and procedures do not consider the biological properties of phages, and some experts have tried to set up new guidelines specific for phage therapy in the European Union (Verbeken *et al.*, 2014). The requirement of regulatory approval for phage therapy added to other issues such as the development of bacterial resistance to phages, their narrow host range and the concern about the immunogenicity of phage therapy were not considered (Lu and Koeris, 2011).

7.1.5 Aims and objectives

With the use of cellulose nanoparticles optimised (Chapter 6), our next aim was to test their efficiency for preventing soft rot development in living plants when bound to bacteriophages. In order to prove the hypothesis that different combinations could be used to test the effect of cellulose nanoparticles and bacteria in controlling *Pectobacterium* infections of potatoes and tomato seeds.

Since all the isolates obtained belong to the same species of bacteriophages, the experiments *in vivo* were focused on ϕSFM002 solely as this was the most characterised (Chapter 4).

The first test performed was on tomato seeds (*Solanum lycopersicum* cv Moneymaker), different combinations were used in order to test both the effect of cellulose nanoparticles and bacteria (and them combined) in plant germination.

Translocation:, that is the ability to uptake phage from the roots to the apical parts of the plant, has been reported in maize and beans (Ward and Mahler, 1982), lettuce (Wei *et al.*, 2010) or tomato plants (Iriarte *et al.*, 2012). Phage uptake depend on different factors including phage morphology, plant species and size and type of soil or substrate where the plant grows (Iriarte *et al.*, 2012). In this case, we wanted to test if the tomato seeds could uptake nanoparticles alone during development, and if so what tissues were affected in the growing plant.

The last experiment performed in plants was on potato slices (*Solanum tuberosum*), using different combinations and incubation temperatures in order to determine under what storage conditions each treatment could prevent soft rot development.

7.2 *In planta* tests

The objectives of this section were to investigate that the cellulose nanoparticles bound to bacteriophages did not alter the normal development of the plant or that they could prevent soft rot on grown fruit were.

7.2.1 Effect of different treatments on tomato seeds (*Solanum lycopersicum* cv Moneymaker) growth and development

In order to test any adverse effects by ϕSFM002-coated cellulose nanoparticles on plant growth, tomato seeds were germinated containing bacteriophage-coated particles on their surface and their development was followed and compared to untreated ones (section 2.15.1 in Materials and methods). Tomato seeds were treated and left to germinate, the treatments included sterile nanoparticles, free ϕSFM002 stock, sterile nanoparticles and bacteria, free ϕSFM002 and bacteria, ϕSFM002-coated nanoparticles and bacteria and ϕSFM002-coated nanoparticles (Table 7-1), after seed germination the stem length was measured daily up to fourteen days after inoculation (Figures 7-1 a and b) and the non geminated seeds were also taken into account at the end of the experiment. Seeds took approximately three days before germination started (Figure 7-1 b), and after they were taken into a day/night photoperiod, when they grew at their maximum rate until they plateaued approximately ten to eleven days after the start of the experiment (as seen in the negative control). The samples that grew best were the untreated ones, reaching approximately eight centimeters at the end of the experiment, followed by the samples treated with sterile nanoparticles that grew approximately six centimeters, and then by the sterile nanoparticles and bacteria-treated samples that reached almost six centimeters, the free ϕSFM002 treated seeds alone grew just over four centimeters, the ϕSFM002-coated nanoparticles and the free ϕSFM002 with bacteria only developed about three centimeters, the coated nanoparticles and bacteria grew an average of 0.5 cm per sample and the bacteria-treated samples did not germinate at all (Figure 7-1 a and b). The presence of bacteria in the samples clearly affected the germination of seeds (positive control) as well as negatively affected plant growth if compared to the same samples without the bacteria (Figure 7-1 b).

Testing the effect of the nanoparticles on plant development was also an objective of the previous experiment. Thus, during the previous experiment the development of cotyledons and leaves was recorded as part of normal development compared to the untreated samples (Figure 7-1 c). By the end of the experiment (fourteen days), the untreated samples had all their seeds germinated, they developed their first cotyledons from day eight and their leaves on day twelve (Figure 7-1 c), all the other treatments developed at least one cotyledon from day eight but only the free ϕSFM002 and the sterile nanoparticles developed leaves (Figure 7-1 c) by the end of the experiment. The germination rate varied between 100% on the untreated samples,

followed by the sterile nanoparticles and by the sterile nanoparticles and bacteria samples at 75%, only the free ϕSFM002 samples, the free ϕSFM002 with bacteria samples and the phage-coated nanoparticles samples achieved 50%, whereas the phage-coated nanoparticles with bacteria samples only got 30% of their seeds germinated, none of the bacteria treated samples germinated. In accordance to the previous results, the presence of bacteria on the seeds slowed down their development as seen when grown with free ϕSFM002 and with sterile nanoparticles (Figure 7-1 c) as they did not develop leaves (the samples grown without bacteria did) and their germination rate slowed down for those samples. Presence of bacteria in seeds prevented germination and slowed growth in presence of other treatments (as compared to the treatments alone), likewise presence of any treatment slowed growth or development of tomato plants compared to the negative controls.

Treatment	**Concentration**
Sterile nanoparticles	1 mg/ml
Free ϕSFM002	10^{10} pfu/ml
Sterile nanoparticles and bacteria	1 mg/ml and 10^{8} cfu/ml
Free ϕSFM002 and bacteria	10^{10} pfu/ml and 10^{8} cfu/ml
ϕSFM002-coated nanoparticles and bacteria	N/A and 10^{8} cfu/ml
SFM002-coated nanoparticles	N/A
Bacteria (positive control)	10^{8} cfu/ml
Distilled sterile water (negative control)	N/A

Table 7-1: Treatments used for seed development assay.

a)

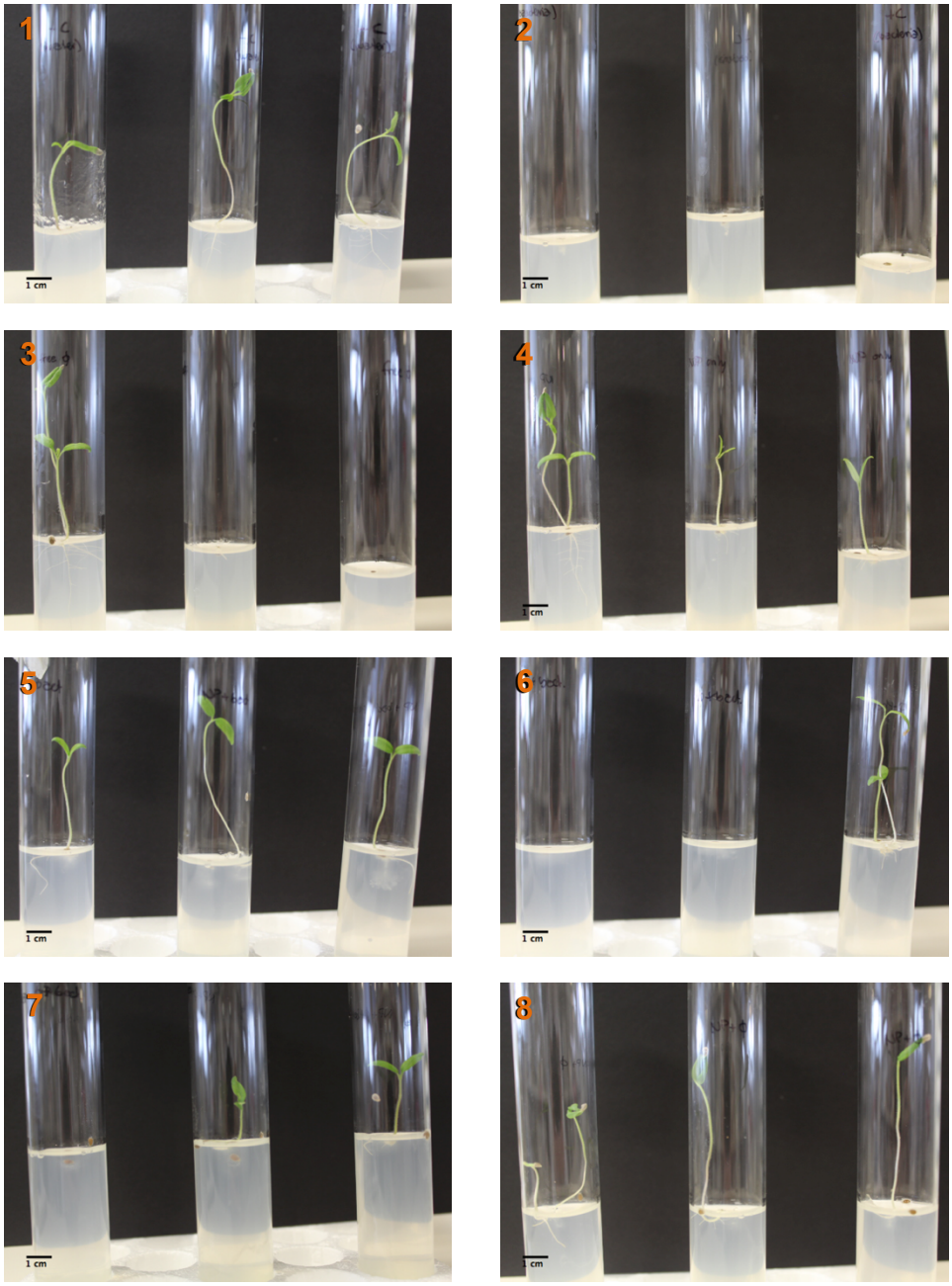

Figure 7-1 (a): Tomato seed germination and growth in the presence of different treatments. Seed germination experiment started by surface-sterilisation of the seeds (*Solanum lycopersicum* cv Moneymaker) and incubation in the dark at 25°C until germination started (6 days), the germinated seeds were then transferred to a long day photoperiod incubator (16L/8D) for the remaining of the experiment. The images correspond (in ascending order): 1 is the negative control (untreated), 2 is the positive control (incubated with bacteria), 3 is free ϕSFM002, 4 is sterile cellulose particles, 5 is cellulose particles and bacteria, 6 is free ϕSFM002 and bacteria, 7 is bacteria and ϕSFM002-coated particles and 8 is ϕSFM002-coated particles. Each treatment was done in triplicates and their growth was measured daily, the bacterial stock used contained 10^8 cfu/ml and the phage stock 10^{10} pfu/ml. All scale bars correspond to 1cm.

b)

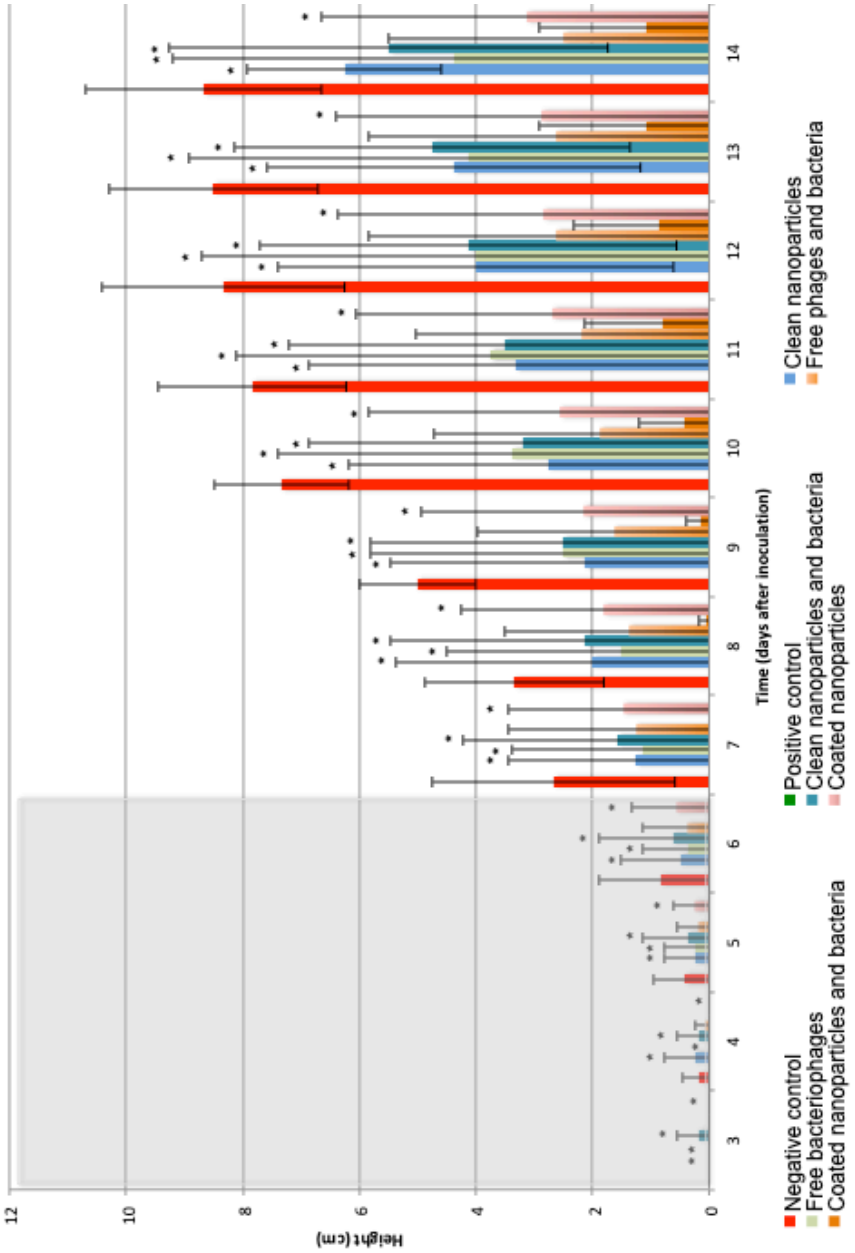

Figure 7-1 (b): Tomato seed germination and growth in the presence of different treatments. Seed treatment experiment started by surface-sterilisation of the seeds (*Solanum lycopersicum* cv Moneymaker) and incubated in the dark at 25°C until germination started (6 days, shown as a shadowed area), the samples were then transferred to a long day photoperiod incubator (16L/8D) for the remaining of the experiment. Each treatment was done in triplicate and their growth was measured daily, the bacterial stock used contained 10^8cfu/ml and the phage stock 10^{10}pfu/ml. Results were plotted (mean ± sd) and Bonferroni's means comparison test (one-way ANOVA with $p \leq 0.05$) was performed.

c)

Samples	Days after inoculation						
	8	9	10	11	12	13	14
Negative control	33	100	100	100	100	100	100
Positive control	0	0	0	0	0	0	0
Free bacteriophages	25	50	50	50	50	50	50
Clean nanoparticles	25	25	50	50	50	75/25*	75/25*
Clean nanoparticles and bacteria	25	50	50	50	75	75	75
Bacteriophage and bacteria	25	25	50	50	50	50	50
Coated nanoparticles and bacteria	0	0	30	30	30	30	30
Coated nanoparticles	25	25	37.5	37.5	37.5	37.5	50

c)

Figure 7-1 (c): Tomato seed germination and growth in the presence of different treatments. Each treatment was done in triplicate and their growth was measured daily as well as cotyledon (red) and leaf (green) development as a percentage, the bacterial stock used contained 10^8 cfu/ml and the phage stock 10^{10} pfu/ml. The (*) represents the only seed out of four that developed real leaves.

7.2.2 Translocation of cellulose particles by the tomato plant

With the objective of testing translocation in the tomato plants, the sterile nanoparticles and the negative control were used to test nanoparticle uptake by the plant using confocal microscopy (Figure 7-2 a to c). The confocal microscopy showed the difference between leaf, stem and root tissues in the plant and allowed recording of the autofluorescence from the cellulose within the plant cell wall and the chloroplasts (Figure 7-2 a), this signal could not be distinguished from that of the nanoparticles, if any (Figure 7-2 b), a faint signal was detected from the nanoparticles alone (Figure 7-2 c), but what was more interesting was the fact the nanoparticles were not spherical as previously thought. No clear signal was detected from the nanoparticles that could be discriminated from the normal cellulose within the plant, on the other hand, this technique has helped establish the irregular shape of the cellulose nanoparticles (Figure 7-2 c).

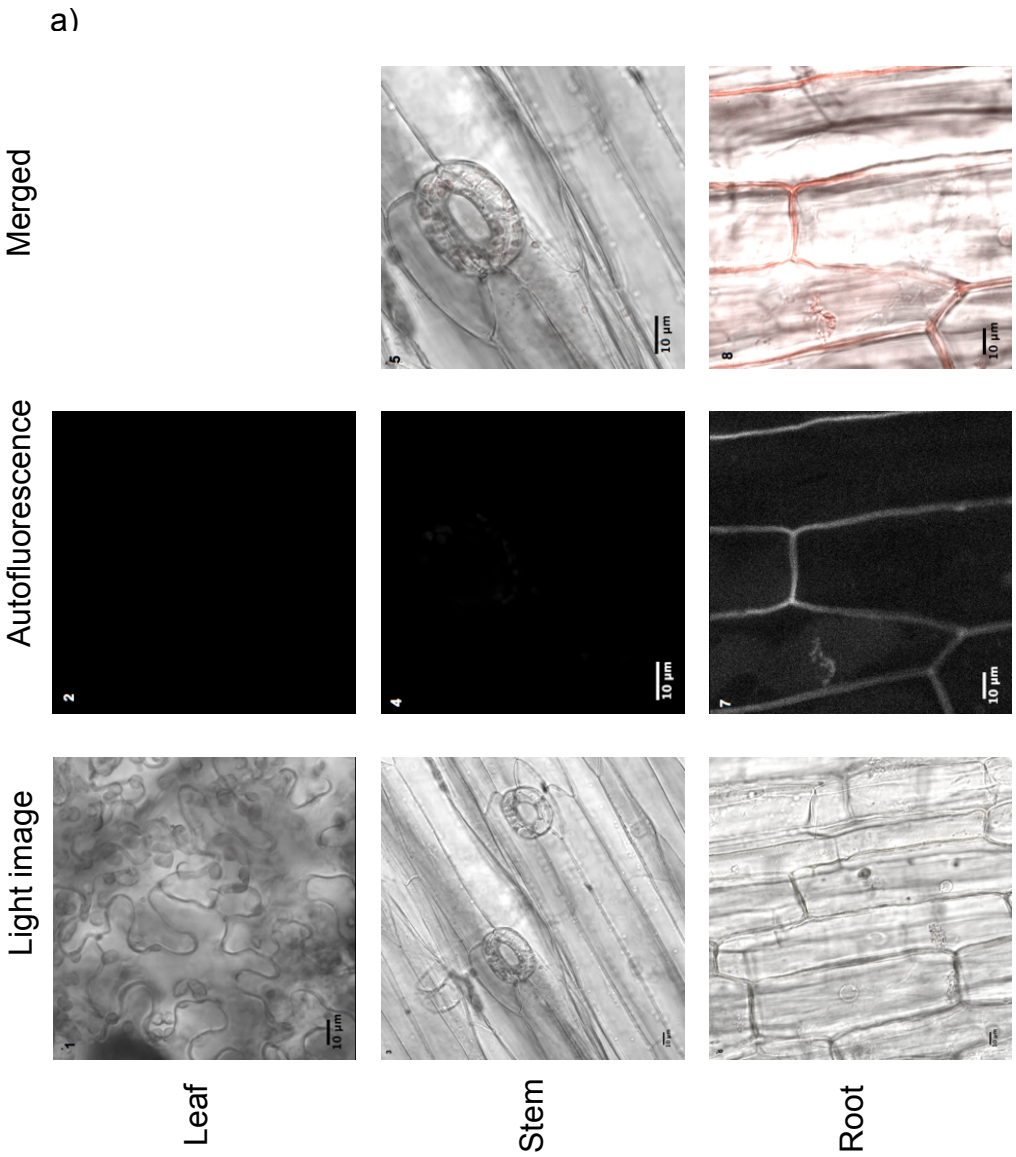

Figure 7-2 (a): Determination of autofluorescence from the tomato plant cellulose. Tomato seeds (*Solanum lycopersicum* cv Moneymaker) were germinated in presence of sterile cellulose nanoparticles and allowed to grow for 28 days, a negative control without nanoparticles was used. Samples were taken from leaves (1 and 2), stems (3 to 5) and roots (6 to 8) using a scalpel and transferred onto glass slides with no fixation. Confocal light images represent the first column, residual autofluorescence are the second column and autofluorescence corresponds to the third column. All scale bars correspond to 10µm.

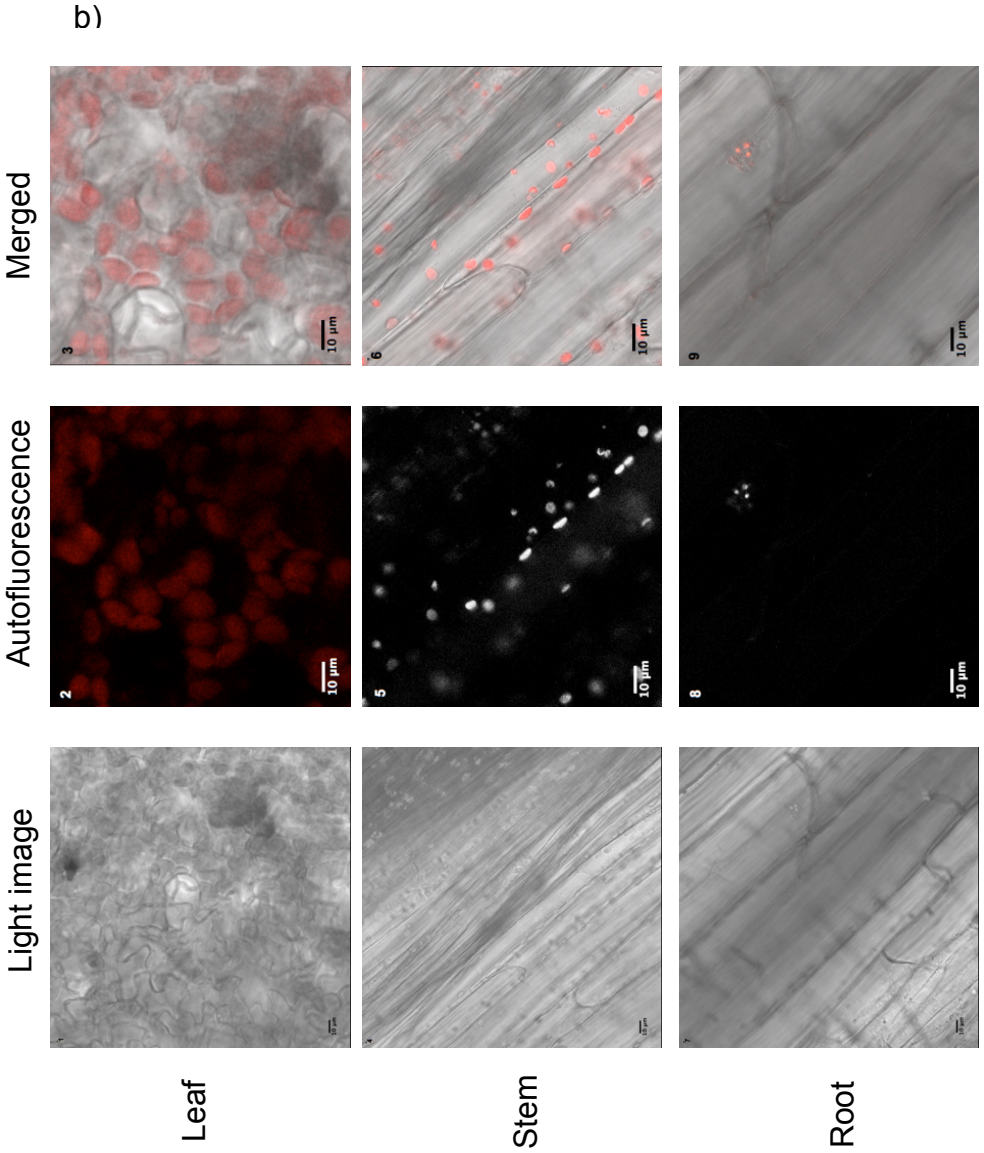

Figure 7-2 (b): Determination of cellulose translocation by the tomato plant. Tomato seeds (*Solanum lycopersicum* cv Moneymaker) were germinated in presence of sterile cellulose nanoparticles and allowed to grow for 28 days, a negative control without nanoparticles was used. Samples were taken from leaves (1 to 3), stems (4 to 6) and roots (7 to 9) using a scalpel and transferred onto glass slides with no fixation. Confocal light images represent the first column, residual autofluorescence are the second column and autofluorescence correspond to the third column. All scale bars correspond to 10µm.

c)

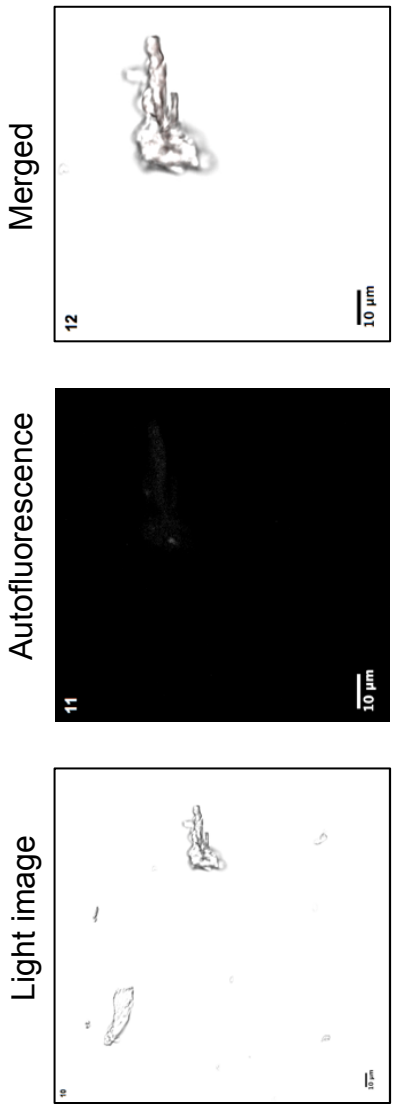

Figure 7-2 (c): Determination of autofluorescence by the cellulose particles. Cellulose samples (10 to 12) were transferred onto glass slides with no fixation and analysed. The first image corresponds to a light image, the second is the autofluorescence of the plant and the third is the merged image. All scale bars correspond to 10µm.

7.2.3 Efficiency of bacteriophage-coated particles to control soft rot development

To measure the efficiency of the phage-coated nanoparticles in preventing soft rot development *in vivo*, potato tubers (*Solanum tuberosum*) were used for inoculation of different treatments and incubated posteriorly at different temperatures (4°C, room temperature and 30°C), soft rot was measured as development of rotten or discoloured tissue on the potato surface every day for three days (Figure 7-3 a) and the infected area was plotted as a percentage of the total tissue area available (Figure 7-3 b), treatments were performed in quadruplets and included free ϕSFM002, ϕSFM002-coated cellulose nanoparticles, two negative controls: one using nothing and the other using PBS and two positive controls: one using *P. atrosepticum* and the other using *P. atrosepticum* SCRI 1043. There was no soft rot in most samples incubated at 4°C after 3 days (Figure 7-3 a), but only small darkened areas were observed even for the negative controls that reached up to 20% by day three (Figure 7-3 b), in all the samples tested at 4°C soft rot developed linearly during the experiment (Figure 7-3 b) and all the samples retained their initial moisture. Furthermore, incubation at room temperature was the worst for soft rot development (Figure 7-3 a), specially for both positive controls and ϕSFM002-coated nanoparticles where soft rot developed linearly and by day three reached 47% for *P. atrosepticum* SCRI 1043, 25% on *P. atrosepticum* and 15% for ϕSFM002-coated nanoparticles (Figure 7-3 b), no soft rot was seen on the negative controls and ϕSFM002 maintained the soft rot levels after the first day, approximately 8% of the total area. Besides, the highest temperature for incubation was the worst for ϕSFM002-coated nanoparticles (Figure 7-3 a) as it reached values of 30% and increased linearly (Figure 7-3 b) whereas free ϕSFM002 remained constant with 5% of total available tissue for the whole experiment, the PBS samples did produce some soft rot for the three days at around 4% of the total area and both positive controls increased their soft rot areas linearly every day, reaching 25% for *P. atrosepticum* SCRI 1043 and 35% for *P. atrosepticum,* the samples incubated at this temperature lost their moisture and their surface appeared dry to the naked eye. In conclusion, phage-coating nanoparticles did not have an effect on preventing or stopping soft rot at 30°C, and its effect was only better than free ϕSFM002 at 4°C. In general, soft rot developed whilst there was moisture on the samples and low temperatures slowed soft rot from developing further.

a)

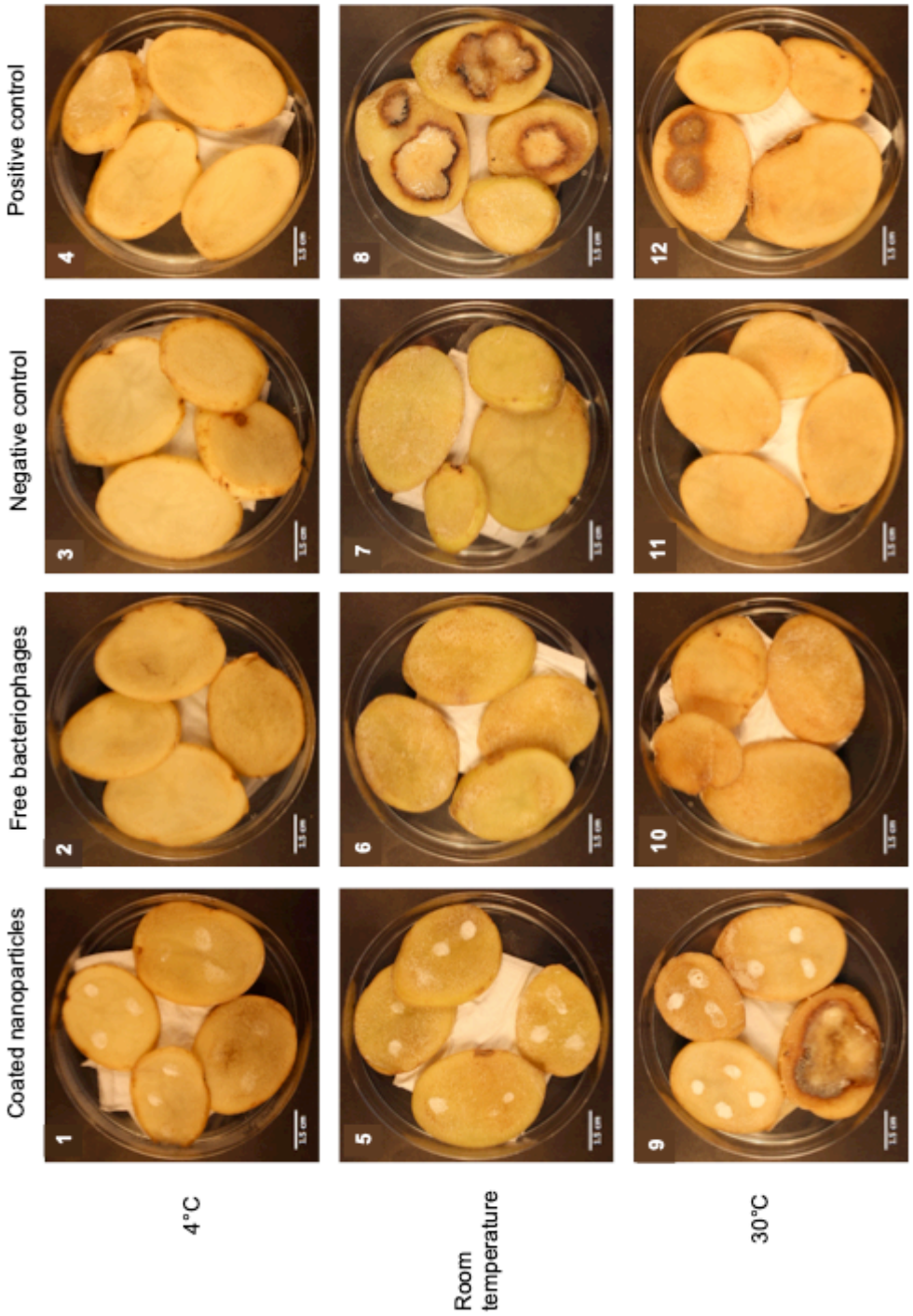

Figure 7-3 (a): Soft rot development on potato slices using different treatments. Potato tuber infection assay measured the area of degradation of potato slices after incubation for 3 days under different incubation temperatures: 4°C (1 to 4), room temperature (5 to 8) and 30°C (9 to 12). The images correspond to the third day for ϕSFM002-coated cellulose (1st column), free ϕSFM002 (2nd column), negative control (3rd column) and the positive control *P. atrosepticum* SCRI 1043 (4th column). The area of degradation was manually selected and compared to the total tissue area available. All scale bars correspond to 1.5 cm.

b)

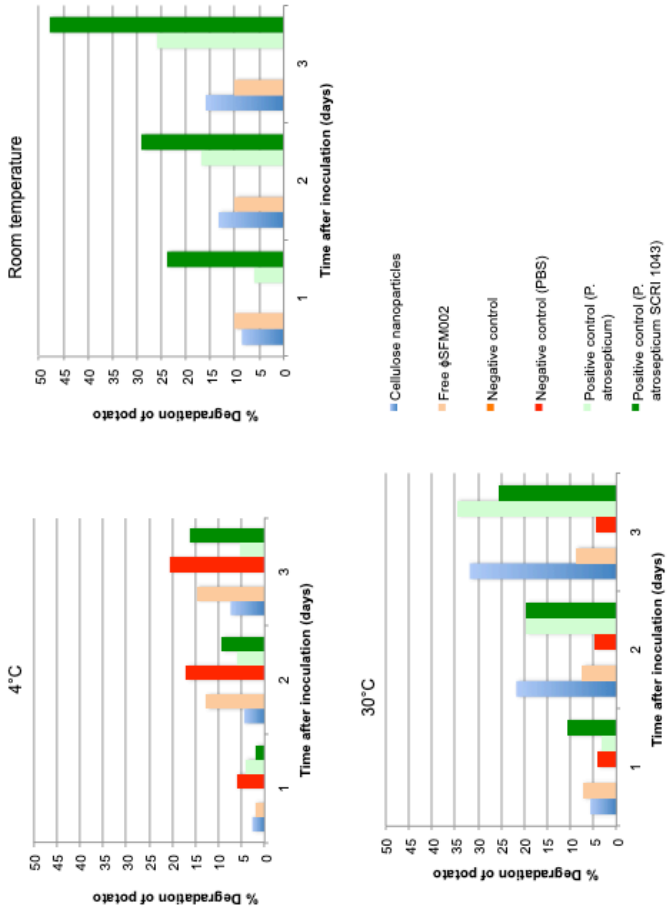

Figure 7-3 (b): Soft rot development of potato slices using different treatments. Potato tuber infection assay was performed by measuring the area of degradation of potato slices after incubation for 3 days under different incubation temperatures: 4°C, room temperature and 30°C. The area of degradation was manually selected and compared to the total tissue area available. Data (means) are representative of one experiment with one biological replicate containing four tuber slices each, the standard deviation should be added when performing repeat experiments as these only measure the percentage of potato tuber infection and are relative to the total area used.

7.3 Discussion

The importance of bacteriophages in the environment must not be overlooked. Viruses infect approximately one-third of the ocean microorganisms every day (Suttle, 2007; Brum and Sullivan, 2015), and their abundance can predict the global carbon flux from the ocean surface to the deep sea (Guidi *et al.*, 2016). They can also shape microbial communities in the human gut either for healthy or pathogenic conditions (Mirzaei and Maurice, 2017). Viral infections contribute to soil ecosystem equilibrium and by knowing soil viral ecology we may understand biogeochemical models and population dynamics (Emerson *et al.*, 2018). Some soil viral metagenomic reports have been generated (Williamson *et al.*, 2017) and demonstrated that soil viromes have the potential to indirectly (through infection of key microbial carbon cyclers) alter the carbon cycling in certain ecosystems (Emerson *et al.*, 2018) or change bacterial metabolism with phage-encoded metabolic genes (Hurwitz and U'Ren, 2016) or bring bacterial blooms to an end through lysogen induction (Brum *et al.*, 2016). For example, virus-encoded glycoside hydrolases contribute to a network of carbon degradation of plant-derived polymers to oligosaccharides or monosaccharides, that are broken down by other soil bacteria to methane and carbon dioxide, in accordance to reports of horizontal gene transfer of lignin-degrading genes (Strachan *et al.*, 2014). At the same time, viral abundances could predict porewater carbon chemistry, for instance $\delta^{13}C$ of porewater methane, an index of the methane production pathway and the methane consumption used in ecosystem and climate models (McCalley *et al.*, 2014) was significantly predicted by methanogen and methanotroph viral concentration (Emerson *et al.*, 2018).

Similarly to the results presented in this chapter, some previous results on phage therapy in plants must be treated with caution as they only used a unique phage isolate and a large-scale field trail should be performed (Czajkowski, 2016b). On a practical level, the selection process of phages with treatment potential should include more bacterial strains to reflect the bacterial soil diversity which, in fact is significantly correlated to viral soil community composition (Fierer and Jackson, 2006). As a matter of fact, the effectiveness of phage therapy relies not only on the susceptibility of the bacterial host but also on the environmental factors that influence phage survival (Iriarte *et al.*, 2007). Temperature can affect phage viability through damaging essential viral components for infection, such as conformational changes of the phage recognition site (Harvey and Ryan, 2004). However, presence of proteases in the soil from bacteria, plant root exudates, animal excrements or decomposition processes can degrade the viral capsid (Vranova *et al.*, 2013). It is also possible that low moisture increase phage stability by enhancing the adsorption process (Mell *et al.*, 2014). Copper-based bactericides reduced phage populations in vitro (Balogh *et al.*, 2005) and UV radiation can damage bacteriophages by different mechanisms (Pfeifer, 1997). Application time of phage treatments should also be considered, if it is best in the evening and stability is enhanced by using

formulated phages (Balogh, 2002). In general, phage treatment is most effective as a preventative measure, since application of viral particles is more effective before bacterial infection develops, this is in accordance to other reports where phage colonisation of the roots avoided phytopathogen invasion (Fujiwara *et al.*, 2011; Bae *et al.*, 2012). Some requirements before commercial use of phage treatments include dynamics of phage populations, timing of application details and phage survival, consistency of control in the field, long-term ecotoxicological risks, if any (Smolarska *et al.*, 2018), biocontainment and safety (Clokie, 2009), such as the potential role in global gene transfer (Verheust *et al.*, 2010), that must be evaluated in a risk assessment.

Another factor to take into account is that selection for phage-resistance is higher in the soil than in vitro (Gomez and Buckling, 2011). Virus-host interactions increase the bacterial mutation rates, thus increasing the bacterial chances to adapt and survive predation and/or changing environmental conditions (Pal *et al.*, 2007). The need for better *in vivo* and *in vitro* models for prediction of phage-bacterial host dynamics, as well as their impact on the energy and nutrient availability in their niche microbiota (Reyes *et al.*, 2012), should be included in the development of experimental and computational methods for efficient analysis of temporal variation in model microbial communities (Reyes *et al.*, 2012). Phages may become redundant after time as a result from co-evolution from being used in phage treatment, this is why phages should be tested individually for their evolutionary dynamic in the ecological context and predict the likelihood of resistance emerging (Gill and Abedon, 2003). Nevertheless, this coevolution does not eradicate bacterial or viral populations as each one needs the other (Oechslin, 2018). The best possible experimental setting would be to apply the Koch postulate inoculating the phages to the environmental bacteria and evaluate their infectivity (Oechslin, 2018).

From the fluorescent microscope results, we learned that the nanoparticles were not spherical as initially suspected, making the calculations for the phage/area ratio inaccurate and these calculations, instead of being as a factor of phage density per surface, they were calculated as phage density per milligram of particles. On the other hand, more effort should be put into the cellulose uptake by the plant: either by staining the cellulose nanoparticles with a dye that does not affect the autofluorescence wavelength of the cellulose so they can be easily discriminated. Once this characterisation is completed more focus, is required for field experiments and/or prevention measures by treating the seed produce.

As previously mentioned, phages should be used before infection starts so we must understand the mechanisms that trigger the infective process. The virulence factors of *P. atrosepticum* are regulated by quorum sensing (QS), this is a bacterial communication system that responds to environmental changes such as nutrient availability, temperature or pH, it is density-dependent (Whitehead *et al.*, 2001) and consists of small diffusible signal

molecules. Plant pathogenic bacteria produce N-acyl homoserine lactones (AHLs), and some research suggest that virulence can be attenuated by controlling the QS system, for example, *P. atrosepticum* secretes virulence factors like pectate lyases, cellulases and proteases that are induced by AHL (Toth *et al.*, 2004; Liu *et al.*, 2008). The use of quorum sensing inhibitors, such as hydroxytyrosol-rich extract (Yangui *et al.*, 2013), piericidin A and glucopiericidin A (Kang *et al.*, 2016), have been suggested as potential control agents of soft rot or by using bacterial strains that express AHL-lactonase, like the *Pseudomonas fluorescens* P3 strain (Molina *et al.*, 2003) or *Bacillus thuringiensis* COT1 (Dong *et al.*, 2004).

There are other different methods that evaluate plant infection development, like measuring the amount of degraded plant matter (Wang *et al.*, 2000; Shabuer *et al.*, 2015b), using potato infusion agar (Shabuer *et al.*, 2015b) or by using the penetration diameter of soft rot in potato tubers (Lapwood *et al.*, 1984), analysis of volatiles, such as acetic acid ethenyl ester (vinyl acetate) for *P. atrosepticum* or cyclohexene, diazene and methoxy-(1,1-dimethyl-2-hydroxyethyl)-amine for *P. carotovorum* subsp. *carotovorum* on potato (Lui *et al.*, 2005), these phenolic acids are good indicators of infection or injury as they are formed as a defense mechanism in potatoes (Ghanekar *et al.*, 1984; Kumar *et al.*, 1991). Presence of saprophytic fungi on decay tissue was not observed during the experiment, though additional tests such as PCR and light microscope identification (Yangui *et al.*, 2013) could be included.

The presence of bacteria avoided completely seed germination and decreased both germination and seed development when used combined with nanoparticles or free bacteriophages. On the other hand, soft rot developed better when moisture was present within the samples and it was temperature–dependent, this was detected on the potato tuber assay. Still these results were inconclusive as there were not enough biological replicates for both the seeds germination and the tuber assay experiments, once replicates are completed, disease reduction can be evaluated based on efficacy and consistency (Byrne *et al.*, 2005), where efficacy is the percentage of mean disease reduction and consistency is the variability between experiments based on standard deviations, the ratio between these two parameters is called Biological Control Index (Byrne *et al.*, 2005). These results do not yet explain the role that *P. atrosepticum* plays within their ecosystem and/or the interactions that explain its presence in soil, therefore more interest on this matter should be taken.

8.0 Discussion and future development

The use of bacteriophages as biocontrol agents involves the characterisation of viral particles as well as understanding of viral/host interactions as these will determine the efficiency of any bacteriophage treatment after multiple applications.

All the bacteriophages isolated for this project are fully characterised using standard methods but also sequencing. This is an uncommon quality as most of the sequences uploaded onto the NCBI database lack any other characteristics apart from their genome sequences, making it more difficult when comparing between phage characteristics. They all produce clear plaques with no halos, characteristic of lytic bacteriophages. Based on their host range, ϕSFM001, ϕSFM002, ϕSFM003, ϕSFM010, ϕSFM011 and ϕSFM012 are the best for phage treatment as they are the most infective. Their morphological properties classify them as part of the *Podoviridae* family: with icosahedral heads and short non-contractile tails, from this analysis ϕSFM002, ϕSFM008 and ϕSFM010 have the longest tails.

The infective process occurs within 20 minutes of encounter and it develops in a guorum-sensing manner: as real-time microscopy indicated that the bacterial bursts happened most at the same time, in a choreographed way.

Genome sequencing should be mandatory for any bacteriophage formulation destined to be used as a treatment and, as a dynamic process, routine sequencing of bacteriophage and their host should be done. An essential part must include the determination of host receptors and the characterisation of those as a result from different environmental conditions as well as determination of prophage and virulence factors from the host genomes as to avoid transferring any contamination in phage stocks. By knowing the defense mechanisms present in their genomes we could understand how phage-host resistance mechanisms develop over time, allowing the implementation of predictive models of virulence. For instance, the absence of CRISPR-Cas in the host genome would allow effective bacteriophage treatments even at low MOIs.

Infection is a carefully regulated process and genes are only maintained if they are required for survival. The bacterial cell wall breaks by the action of an endolysin and also inhibits the host RNA polymerase. The phages avoid the bacterial immune system using a type I restriction-modification system (by the presence of methylases in the phage genome) and toxin-antitoxin inhibitors that are equivalent to gp 4.5 from ϕT7 From the genomic analysis we can place the origin of replication upstream the terminase gene (or the arbitrary starting point for the CCT analysis), this is evident by the switch in polarity of the GC skew. The bacteriophages have similar termini as ϕT7 with short direct repeats and no cos ends, typical of linear DNA replication. Structural regions of the genome tend to be more conserved but locating areas of heterogeneity can help the prediction of mutation rates. Within the structural region is the spanin, responsible for breaking the bacterial cell wall in our bacteriophage isolates.

Phylogenetic analysis divided our isolates in two groups: one containing ϕSFM001, ϕSFM002, ϕSFM010, ϕSFM011 and ϕSFM012, and the other with the remaining seven. Even though different analytical programs placed them in the same viral species (dot plot analysis using GEPARD, nucleotide comparison using CCT view, Roary, average nucleotide identity and whole proteomic tree analysis using VIPTree) they are probably different variant belonging to the same viral species, and variability within them could explain the regions in the genome most likely to change upon infection. Even though these bacteriophages are very similar to each other, they are very different from any others that have been sequenced up to date, sharing 60% homology to their closest bacteriophage genome (results from the average nucleotide identity analysis).

Some of the techniques used should be optimised in order to obtain further results. For example, time-lapse microscopy could include the use of immunofluorescence staining to quantify the bacteria (using labeled antibodies), but also viral particles (either by using SYBR Green or SYTOX Orange). The development of a method to reliably obtain high phage titres and to optimise the orientation/attachment of phage particles onto cellulose (and their quantification) with the aim of further characterise their infective properties. Optimisation of the attachment process should be performed either by using an electric field to orientate the bacteriophages, by modifying the voltage/frequency applied or by using protective emulsions that may aid the stability of the end product. More test would include the measurement of covalent bonds by detecting the presence of amide bonds using attenuated total reflectance-Fourier transform infrared spectroscopy (ATR-FTIR) and by measuring the stability of the phage-coated nanoparticles using different conditions such as pH or UV exposure and for longer periods of time. Other analysis required to complete this project include the in-depth analysis of tail fibre proteins using 3D protein structural modeling that could explain the bacteriophage recognition mechanisms, so far from the SNP analysis of the tail ϕSFM001, ϕSFM002, ϕSFM010, ϕSFM011 and ϕSFM012 showed that they are identical, which does not explain the different host range but agrees with the efficiency of plating and the phylogenetic analysis.

The presence of “hibernating” isolated cells during the time-lapse microscopy experiment could reflect more accurately what happens in the environment upon infection. Determination of growth parameters under different nutrient availability as well as expression profiles of these dormant bacteria (and the possible role toxin-antitoxin systems have in this development) may improve our understanding of persister cell development.

The use of nanoparticles can be useful to increase phage stability or shelf life of phage-based products, and cellulose was the best candidate as it was easier to handle than nylon, although other alternatives like chitin would have been interesting to test.

The soil environment is mainly static, relying on mechanical mixing and/or watering processes in order to change its structure. This could explain why all the isolates from this project were so similar to each other and how they could only infect the bacterial strain that was closest geographically.

From this project this role remains unclear and it would be necessary to analyse the interaction that happen after phage therapy and how the bacterial populations respond both spatial and temporally. Bacteriophages may become redundant over time, produce a dysbiosis or cause horizontal gene transfer events from the bacterial lysis. Alternatively, the combined use of phages and bacteria that express AHL-lactonases (inhibiting QS) could require lower MOIs for treatment. Ultimately, the presence of *Pectobacterium* spp. and their bacteriophages as normal inhabitants of soil may reflect an essential role within this ecosystem. Thus, determination of the role this bacterium and its phage have in the soil ecosystem will prove useful in terms of development of control strategies.

9.0 References

Abatángelo, V., Peressutti Bacci, N., Boncompain, C.A., Amadio, A.A., Carrasco, S., Suárez, C.A., and Morbidoni, H.R. (2017) Broad-range lytic bacteriophages that kill Staphylococcus aureus local field strains. *PLoS One* **12**: e0187387.

Abedon, S.T. (2009) Disambiguating bacteriophage pseudolysogeny: an historical analysis of lysogeny, pseudolysogeny, and the phage carrier state. In *Contemporary Trends in Bacteriophage Research*. Adams, H.T. (ed.). Nova Publishers, New York. pp. 285–307.

Abedon, S.T. (2011) Communication among phages, bacteria, and soil environments. In *Biocommunication in Soil Microorganisms*. Witzany, G. (ed.). Springer Berlin Heidelberg, Berlin, Heidelberg. pp. 37–65.

Abedon, S.T. (2011) Lysis from without. *Bacteriophage* **1**: 46–49.

Abedon, S.T. (2012) Bacterial 'immunity' against bacteriophages. *Bacteriophage* **2**: 50–54.

Abedon, S.T. (2017) Information phage therapy research should report. *Pharmaceuticals* **10**: E43.

Abedon, S.T., Herschler, T.D., and Stopar, D. (2001) Bacteriophage latent-period evolution as a response to resource availability. *Appl Environ Microbiol* **67**: 4233–41.

Abedon, S.T., Hyman, P., and Thomas, C. (2003) Experimental examination of bacteriophage latent-period evolution as a response to bacterial availability. *Appl Environ Microbiol* **69**: 7499–506.

Abedon, S.T., and Lejeune, J.T. (2007) Why bacteriophage encode exotoxins and other virulence factors. *Evol Bioinform Online* **1**: 97–110.

Abedon, S.T., and Yin, J. (2009) Bacteriophage plaques: theory and analysis. *Methods Mol Biol* **501**: 161–174.

Abuladze, T., Li, M., Menetrez, M.Y., Dean, T., Senecal, A., and Sulakvelidze, A. (2008) Bacteriophages reduce experimental contamination of hard surfaces, tomato, spinach, broccoli, and ground beef by Escherichia coli O157:H7. *Appl Environ Microbiol* **74**: 6230–6238.

Ackermann, H.-W., and Eisenstark, A. (1974) The present state of phage taxonomy. *Intervirology* **3**: 201–219.

Ackermann, H.W. (2011) Bacteriophage taxonomy. *Microbiol Aust* 90–94.

Ackermann, H.W., and Kropinski, A.M. (2007) Curated list of prokaryote viruses with fully sequenced genomes. *Res Microbiol* **158**: 555–566.

Ackermann, H.W., and Nguyen, T.M. (1983) Sewage coliphages studied by electron microscopy. *Appl Environ Microbiol* **45**: 1049–1059.

Ackermann, H.W., Tremblay, D., and Moineau, S. (2004) Long term bacteriophage preservation. *WFCC Newsl* **38**: 35–40.

Adams, M.H. (1959) *Bacteriophages*. Interscience Publishers, New York.

Adeolu, M., Alnajar, S., Naushad, S., and Gupta, R.S. (2016) Genome-based phylogeny and taxonomy of the 'Enterobacteriales': proposal for enterobacterales ord. nov. divided into the families Enterobacteriaceae, Erwiniaceae fam. nov., Pectobacteriaceae fam. nov., Yersiniaceae fam. nov., Hafniaceae fam. nov., Morganellaceae fam. nov., and Budviciaceae fam. nov. *Int J Syst Evol Microbiol* **66**: 5575–5599.

Adriaenssens, E.M., and Brister, J.R. (2017) How to name and classify your phage: an informal guide. *Viruses* **9**: 70.

Adriaenssens, E.M., Ceyssens, P.-J., Dunon, V., Ackermann, H.-W., Vaerenbergh, J. Van, Maes, M., Proft, M. De, and Lavigne, R. (2011) Bacteriophages LIMElight and LIMEzero of Pantoea agglomerans, belonging to the "phiKMV-like viruses." *Appl Environ Microbiol* **77**: 3443–3450.

Adriaenssens, E.M., Vaerenbergh, J. Van, Vandenheuvel, D., Dunon, V., Ceyssens, P.-J., Proft, M. De, Kropinski, A.M., Noben, J.-P., Maes, M., and Lavigne, R. (2012) T4-related bacteriophage LIMEstone isolates for the control of soft rot on potato caused by "Dickeya solani." *PLoS One* **7**: e33227.

Afek, U., and Orenstein, J. (2002) Disinfecting potato tubers using steam treatments. *Can J Plant Pathol* **24**: 36–39.

Afgan, E., Baker, D., van den Beek, M., Blankenberg, D., Bouvier, D., Čech, M., Chilton, J., Clements, D., Coraor, N., Eberhard, C., Grüning, B., Guerler, A., Hillman-Jackson, J., Von Kuster, G., Rasche, E., Soranzo, N., Turaga, N., Taylor, J., Nekrutenko, A., and Goecks, J. (2016) The Galaxy platform for accessible, reproducible and collaborative biomedical analyses: 2016 update. *Nucleic Acids Res* **44**: W3–W10.

Agrios, G. (2005) Plant diseases caused by nematodes. In *Plant Pathology*. Elsevier Academic Press, Burlington. pp. 838–842.

Ahern, S.J., Das, M., Bhowmick, T.S., Young, R., and Gonzalez, C.F. (2014) Characterization of novel virulent broad-host-range phages of Xylella fastidiosa and Xanthomonas. *J Bacteriol* **196**: 459–471.

Ahmad, M.H., and Morgan, V. (1994) Characterization of a cowpea (Vigna unguiculata) rhizobiophage and its effect on cowpea nodulation and growth. *Biol Fertil Soils* **18**: 297.

Ahmad, N., Sharma, S., Singh, V.N., Shamsi, S.F., Fatma, A., and Mehta, B.R. (2011) Biosynthesis of silver nanoparticles from desmodium triflorum: a novel approach towards weed utilization. *Biotechnol Res Int* **2011**: 8.

Aira, M., Gómez-Brandón, M., Lazcano, C., Bååth, E., and Domínguez, J. (2010) Plant genotype strongly modifies the structure and growth of maize rhizosphere microbial communities. *Soil Biol Biochem* **42**: 2276–2281.

Aizenman, E., Engelberg-Kulka, H., and Glaser, G. (1996) An Escherichia coli chromosomal "addiction module" regulated by guanosine [corrected] 3',5'-bispyrophosphate: a model for programmed bacterial cell death. *Proc Natl Acad Sci* **93**: 6059–6063.

Akhtar, M.S., Panwar, J., and Yun, Y.S. (2013) Biogenic synthesis of metallic nanoparticles by plant extracts. *ACS Sustain Chem Eng* **1**: 591–602.

Al-Attar, S., Westra, E.R., Oost, J. Van Der, and Brouns, S.J.J. (2011) Clustered regularly interspaced short palindromic repeats (CRISPRs): the hallmark of an ingenious antiviral defense mechanism in prokaryotes. *Biol Chem* **392**: 277–289.

Allen, R.C., Pfrunder-Cardozo, K.R., Meinel, D., Egli, A., and Hall, A.R. (2017) Associations among antibiotic and phage resistance phenotypes in natural and clinical Escherichia coli isolates. *MBio* **8**.

Amitai, G., and Sorek, R. (2016) CRISPR–Cas adaptation: insights into the mechanism of action. *Nat Rev Microbiol* **14**: 67–76.

Anany, H., Chen, W., Pelton, R., and Griffiths, M.W. (2011) Biocontrol of Listeria monocytogenes and Escherichia coli O157:H7 in meat by using phages immobilized on modified cellulose membranes. *Appl Environ Microbiol* **77**: 6379–6387.

Andam, C.P., Doroghazi, J.R., Campbell, A.N., Kelly, P.J., Choudoir, M.J., and Buckley, D.H. (2016) A latitudinal diversity gradient in terrestrial bacteria of the genus Streptomyces. *MBio* **7**: e02200-15.

Anderson, B., Rashid, M.H., Carter, C., Pasternack, G., Rajanna, C., Revazishvili, T., Dean, T., Senecal, A., and Sulakvelidze, A. (2011) Enumeration of bacteriophage particles: comparative analysis of the traditional plaque assay and real-time QPCR- and nanosight-based assays. *Bacteriophage* **1**: 86–93.

Andrews, J.M. (2009) BSAC standardized disc susceptibility testing method (version 8). *J Antimicrob Chemother* **64**: 454–489.

Anisimova, M., and Gascuel, O. (2006) Approximate likelihood-ratio test for branches: a fast, accurate, and powerful alternative. *Syst Biol* **55**: 539–552.

Aprea, G., D'Angelo, A.R., Prencipe, V.A., and Migliorati, G. (2015) Bacteriophage morphological characterization by using transmission electron microscopy. *J Life Sci* **9**: 214–220.

Arridge, R.G.C. (1967) The static electrification of nylon 66. *Br J Appl Phys* **18**: 1311–1316.

Arya, S.K., Singh, A., Naidoo, R., Wu, P., McDermott, M.T., and Evoy, S. (2011) Chemically immobilized T4-bacteriophage for specific Escherichia coli detection using surface plasmon resonance. *Analyst* **136**: 486–492.

Ashelford, K.E., Day, M.J., and Fry, J.C. (2003) Elevated abundance of bacteriophage infecting bacteria in soil. *Appl Environ Microbiol* **69**: 285–289.

Avrani, S., and Lindell, D. (2015) Convergent evolution toward an improved growth rate and a reduced resistance range in Prochlorococcus strains resistant to phage. *Proc Natl Acad Sci U S A* **112**: E2191-200.

Avrani, S., Wurtzel, O., Sharon, I., Sorek, R., and Lindell, D. (2011) Genomic island variability facilitates Prochlorococcus–virus coexistence. *Nature* **474**: 604–8.

Aziz, R.K., Bartels, D., Best, A.A., DeJongh, M., Disz, T., Edwards, R.A., Formsma, K., Gerdes, S., Glass, E.M., Kubal, M., Meyer, F., Olsen, G.J., Olson, R., Osterman, A.L., Overbeek, R.A., McNeil, L.K., Paarmann, D., Paczian, T., Parrello, B., Pusch, G.D., Reich, C., Stevens, R., Vassieva, O., Vonstein, V., Wilke, A., and Zagnitko, O. (2008) The RAST Server: Rapid Annotations using Subsystems Technology. *BMC Genomics* **9**: 75.

Bae, Y.J., Wu, J., Lee, H.J., Jo, E.J., Murugaiyan, S., Chung, E., and Lee, S.W. (2012) Biocontrol potential of a lytic bacteriophage PE204 against bacterial wilt of tomato. *J Microbiol Biotechnol* **22**: 1613–1620.

Baer, A., and Kehn-Hall, K. (2014) Viral concentration determination through plaque assays: using traditional and novel overlay systems. *J Vis Exp* **93**: e52065.

Baker, C.J., Mock, N., Atkinson, M.M., and Hutcheson, S. (1990) Inhibition of the hypersensitive response in tobacco by pectate lyase digests of cell wall and of polygalacturonic acid. *Physiol Mol Plant Pathol* **37**: 155–167.

Balaraju, K., Kim, C.J., Park, D.J., Nam, K.W., Zhang, K., Sang, M.K., and Park, K. (2016) Paromomycin derived from Streptomyces sp AG-P 1441 induces resistance against two major pathogens of chili pepper. *J Microbiol Biotechnol* **26**: 1542–1550.

Balogh, B. (2002) Strategies for improving the efficacy of bacteriophages for controlling bacterial spot on tomato. .

Balogh, B., Canteros, B.I., Stall, R.E., and Jones, J.B. (2008) Control of citrus canker and citrus bacterial spot with bacteriophages. *Plant Dis* **92**: 1048–1052.

Balogh, B., Jones, J.B., Iriarte, F.B., and Momol, M.T. (2010) Phage therapy for plant disease control. *Curr Pharm Biotechnol* **11**: 48–57.

Balogh, B., Jones, J.B., Momol, M.T., and Olson, S.M. (2005) Persistence of bacteriophages as biocontrol agents in the tomato canopy. *Acta Hortic* **695**:

299–302.

Balogh, B., Jones, J.B., Momol, M.T., Olson, S.M., Obradovic, a., King, P., and Jackson, L.E. (2003) Improved efficacy of newly formulated bacteriophages for management of bacterial spot on tomato. *Plant Dis* **87**: 949–954.

Bandyopadhyay, P.K., Studier, F.W., Hamilton, D.L., and Yuan, R. (1985) Inhibition of the type I restriction-modification enzymes EcoB and EcoK by the gene 0.3 protein of bacteriophage T7. *J Mol Biol* **182**: 567–578.

Bankevich, A., Nurk, S., Antipov, D., Gurevich, A.A., Dvorkin, M., Kulikov, A.S., Lesin, V.M., Nikolenko, S.I., Pham, S., Prjibelski, A.D., Pyshkin, A. V, Sirotkin, A. V, Vyahhi, N., Tesler, G., Alekseyev, M.A., and Pevzner, P.A. (2012) SPAdes: a new genome assembly algorithm and its applications to single-cell sequencing. *J Comput Biol* **19**: 455–77.

Baran, G.J., and Bloomfield, V.A. (1978) Tail fiber attachement in bacteriophage T4D studied by quasielastic light scattering band electrophoresis. *Biopolymers* **17**: 2015–2028.

Barlow, S., Chesson, A., Collins, J.D., Flynn, A., Hardy, A., Knaap, A., Kuiper, H., Larsen, J.C., Neindre, P. Le, Schans, J., Silano, V., Skerfving, S., Vannier, P., EFSA Panel on Biological Hazards (BIOHAZ), Andreoletti, O., Budka, H., Buncic, S., Colin, P., Collins, J.D., De, A., Griffin, J., Havelaar, A., Hope, J., Klein, G., Kruse, H., Magnino, S., López, M., Mclauchlin, J., Nguyen-the, C., Noeckler, K., Noerrung, B., Maradona, M.P., Roberts, T., Vågsholm, I., Vanopdenbosch, E., European Food Safety Authority, and European Food Safety Authorty (2009) The use and mode of action of bacteriophages in food production 1 Scientific Opinion of the Panel on Biological Hazards Adopted on 22 April 2009. .

Barnard, A.M.L., Bowden, S.D., Burr, T., Coulthurst, S.J., Monson, R.E., and Salmond, G.P.C. (2007) Quorum sensing, virulence and secondary metabolite production in plant soft-rotting bacteria. *Philos Trans R Soc Lond B Biol Sci* **362**: 1165–83.

Barrangou, R. (2015) The roles of CRISPR-Cas systems in adaptative immunity and beyond. *Curr Opin Immunol* **32**: 36–41.

Barrangou, R., Fremaux, C., Deveau, H., Richards, M., Boyaval, P., Moineau, S., Romero, D.A., and Horvath, P. (2007) CRISPR provides acquired resistance against viruses in prokaryotes. *Science (80-)* **315**: 1709–1712.

Barrangou, R., and Oost, J. Van Der (2015) Bacteriophage exclusion, a new defence system. *EMBO J* **34**: 134–135.

Barras, F., Gijsegem, F. van, and Chatterjee, A.K. (1994) Extracellular enzymes and pathogenesis of soft-rot Erwinia. *Annu Rev Phytopathol* **32**: 201–234.

Barry, G., and Goebel, W. (1951) The effect of chemical and physical agents on the phage receptor of Phase II Shigella sonnei. *J Exp Med* **94**: 387–400.

Barton, D., Short, R.D., Fraser, S., and Bradley, J.W. (2003) The effect of ion energy upon plasma polymerization deposition rate for acrylic acid. *Chem Commun (Camb)* **2003**: 348–349.

Bartz, J. (1999) Supression of bacterial soft rot in potato tubers by application of kasugamycin. *Am J Potato Res* **76**: 127–136.

Bartz, J.A. (1999) Washing fresh fruits and vegetables: lessons from treatment of tomatoes and potatoes with water. *Dairy Food Environ Sanit* **19**: 853–864.

Bartz, J.A., and Kelman, A. (1986) Reducing the potential for bacterial soft rot in potat otubers by chemical treatments and drying. *Am J Potato Res* **63**: 481–493.

Basset, A., Khush, R.S., Braun, A., Gardan, L., Boccard, F., Hoffmann, J.A., and Lemaitre, B. (2000) The phytopathogenic bacteria Erwinia carotovora infects Drosophila and activates an immune response. *Proc Natl Acad Sci U S A* **97**: 3376–3381.

Bassler, B.L., Wright, M., and Silverman, M.R. (1994) Multiple signalling systems controlling expression of luminescence in Vibrio harveyi: sequence and function of genes encoding a second sensory pathway. *Mol Microbiol* **13**: 273–286.

Baz, C., Lahbabi, D., Samri, S., Val, F., Hamelin, G., Madore, I., Bouarab, K., Beaulieu, C., Ennaji, M.M., and Barakate, M. (2012) Control of potato soft rot caused by Pectobacterium carotovorum and Pectobacterium atrosepticum by Moroccan actinobacteria isolates. *World J Microbiol Biotechnol* **28**: 303–311.

Bell, K.S., Sebaihia, M., Pritchard, L., Holden, M.T.G., Hyman, L.J., Holeva, M.C., Thomson, N.R., Bentley, S.D., Churcher, L.J.C., Mungall, K., Atkin, R., Bason, N., Brooks, K., Chillingworth, T., Clark, K., Doggett, J., Fraser, A., Hance, Z., Hauser, H., Jagels, K., Moule, S., Norbertczak, H., Ormond, D., Price, C., Quail, M. a, Sanders, M., Walker, D., Whitehead, S., Salmond, G.P.C., Birch, P.R.J., Parkhill, J., and Toth, I.K. (2004) Genome sequence of the enterobacterial phytopathogen Erwinia carotovora subsp. atroseptica and characterization of virulence factors. *Proc Natl Acad Sci U S A* **101**: 11105–10.

Berendsen, R.L., Pieterse, C.M.J., and Bakker, P.A. (2012) The rhizosphere microbiome and plant health. *Trends Plant Sci* **17**: 478–486.

Bertozzi Silva, J., Storms, Z., Sauvageau, D., Ainsworth, S., Sadovskaya, I., Vinogradov, E., Bae, H., Cho, Y., Baptista, C., Matsumoto, H., *et al.* (2016) Host receptors for bacteriophage adsorption. *FEMS Microbiol Lett* .

Beyeler, M., Keel, C., Michaux, P., and Haas, D. (1999) Enhanced

production of indole-3-acetic acid by a genetically modified strain of Pseudomonas fluorescens CHA0 affects root growth of cucumber, but does not improve protection of the plant against Pythium root rot. *FEMS Microbiol Ecol* **28**: 225–233.

Bickle, T.A., and Kruger, D.H. (1993) Biology of DNA restriction. *Microbiol Rev* **57**: 434–450.

Bigwood, T., Hudson, J.A., Billington, C., Carey-Smith, G. V., and Heinemann, J.A. (2008) Phage inactivation of foodborne pathogens on cooked and raw meat. *Food Microbiol* **25**: 400–6.

Bikard, D., Euler, C.W., Jiang, W., Nussenzweig, P.M., Goldberg, G.W., Duportet, X., Fischetti, V.A., and Marraffini, L.A. (2014) Exploiting CRISPR-Cas nucleases to produce sequence-specific antimicrobials. *Nat Biotechnol* **32**: 1146–1150.

Billing, E. (2000) Fire blight risk assessment systems and models. In *Fire blight: the disease and its causative agent, Erwinia amylovora.* Vanneste, J.L. (ed.). CAB International, Wallingford, UK. pp. 293–318.

Blower, T.R., Chai, R., Przybilski, R., Chindhy, S., Fang, X., Kidman, S.E., Tan, H., Luisi, B.F., Fineran, P.C., and Salmond, G.P.C. (2017) Evolution of Pectobacterium bacteriophage M1 to escape two bifunctional type III toxin-antitoxin and abortive infection systems through mutations in a single viral gene. *Appl Environ Microbiol* **83**: e03229-16.

Blower, T.R., Evans, T.J., Fineran, P.C., Toth, I.K., Foulds, I.J., and Salmond, G.P.C. (2010) Phage-receptor interactions and phage abortive infection: potential biocontrol factors in a bacterial plant pathogen. In *International Society for Molecular Plant-Microbe Interactions*. Minnesota (USA). p. 7.

Blower, T.R., Pei, X.Y., Short, F.L., Fineran, P.C., Humphreys, D.P., Luisi, B.F., and Salmond, G.P.C. (2011) A processed noncoding RNA regulates an altruistic bacterial antiviral system. *Nat Struct Mol Biol* **18**: 185–190.

Blower, T.R., Short, F.L., Fineran, P.C., and Salmond, G.P.C. (2012) Viral molecular mimicry circumvents abortive infection and suppresses bacterial suicide to make hosts permissive for replication. *Bacteriophage* **2**: 234–238.

Blower, T.R., Short, F.L., Rao, F., Mizuguchi, K., Pei, X.Y., Fineran, P.C., Luisi, B.F., and Salmond, G.P.C. (2012) Identification and classification of bacterial Type III toxin-antitoxin systems encoded in chromosomal and plasmid genomes. *Nucleic Acids Res* **40**: 6158–6173.

Bodenhausen, N., Bortfeld-Miller, M., Ackermann, M., and Vorholt, J.A. (2014) A synthetic community approach reveals plant genotypes affecting the phyllosphere microbiota. *PLoS Genet* **10**: e1004283.

Bohannan, B.J.M., and Lenski, R.E. (2000) Linking genetic change to

community evolution: insights from studies of bacteria and bacteriophage. *Ecol Lett* **3**: 362–377.

Bonde, R., and Souza, P. de (1954) Studies on the control of potato bacterial seed-piece decay and blackleg with antibiotics. *Am Potato J* **31**: 311–316.

Borges, A.L., Davidson, A.R., and Bondy-Denomy, J. (2017) The discovery, mechanisms, and evolutionary impact of anti-CRISPRs. *Annu Rev Virol* **4**: 37–59.

Borges, A.L., Zhang, J.Y., Rollins, M.F., Osuna, B.A., Wiedenheft, B., and Bondy-Denomy, J. (2018) Bacteriophage cooperation suppresses CRISPR-Cas3 and Cas9 immunity. *Cell* **174**: 917–925.

Born, Y., Fieseler, L., Marazzi, J., Lurz, R., Duffy, B., and Loessner, M.J. (2011) Novel virulent and broad-host-range Erwinia amylovora bacteriophages reveal a high degree of mosaicism and a relationship to Enterobacteriaceae Phages. *Appl Environ Microbiol* **77**: 5945–5954.

Bouffaud, M.L., Kyselkova, M., Gouesnard, B., Grundmann, G., Muller, D., and Moenne-Loccoz, Y. (2012) Is diversification history of maize influencing selection of soil bacteria by roots? *Mol Ecol* **21**: 195–206.

Brader, G., Sjöblom, S., Hyytiäinen, H., Sims-Huopaniemi, K., and Palva, E.T. (2005) Altering substrate chain length specificity of an acylhomoserine lactone synthase in bacterial communication. *J Biol Chem* **280**: 10403–10409.

Branston (2012) A natural solution to tackle potential soft rot. *http://www.branston.com/news/a-natural-solution-to-takle-potential-soft-rot/* .

Breitbart, M. (2012) Marine viruses: truth or dare. *Ann Rev Mar Sci* **4**: 425–448.

Breitbart, M., Miyake, J.H., and Rohwer, F. (2004) Global distribution of nearly identical phage-encoded DNA sequences. *FEMS Microbiol Lett* **236**: 249–256.

Brettin, T., Davis, J.J., Disz, T., Edwards, R.A., Gerdes, S., Olsen, G.J., Olson, R., Overbeek, R., Parrello, B., Pusch, G.D., Shukla, M., Thomason, J.A., Stevens, R., Vonstein, V., Wattam, A.R., and Xia, F. (2015) RASTtk: a modular and extensible implementation of the RAST algorithm for building custom annotation pipelines and annotating batches of genomes. *Sci Rep* **5**: 8365.

Briers, Y., Miroshnikov, K., Chertkov, O., Nekrasov, A., Mesyanzhinov, V., Volckaert, G., and Lavigne, R. (2008) The structural peptidoglycan hydrolase gp181 of bacteriophage φKZ. *Biochem Biophys Res Commun* **374**: 747–751.

Brouns, S.J.J., Jore, M.M., Lundgren, M., Westra, E.R., Slijkhuis, R.J.H., Snijders, A.P.L., Dickman, M.J., Makarova, K.S., Koonin, E. V., and Oost, J.

van der (2008) Small CRISPR RNAs guide antiviral defense in prokaryotes. *Science (80-)* **321**: 960–964.

Brown, T.L., Petrovski, S., Dyson, Z.A., Seviour, R., and Tucci, J. (2016) The formulation of bacteriophage in a semi solid preparation for control of propionibacterium acnes growth. *PLoS One* **11**: e0151184.

Brum, J.R., Hurwitz, B.L., Schofield, O., Ducklow, H.W., and Sullivan, M.B. (2016) Seasonal time bombs: dominant temperate viruses affect Southern Ocean microbial dynamics. *ISME J* **10**: 437–49.

Brum, J.R., Ignacio-Espinoza, J.C., Roux, S., Doulcier, G., Acinas, S.G., Alberti, A., Chaffron, S., Cruaud, C., Vargas, C. de, Gasol, J.M., Gorsky, G., Gregory, A.C., Guidi, L., Hingamp, P., Iudicone, D., Not, F., Ogata, H., Pesant, S., Poulos, B.T., Schwenck, S.M., Speich, S., Dimier, C., Kandels-Lewis, S., Picheral, M., Searson, S., Tara Oceans Coordinators, T.O., Bork, P., Bowler, C., Sunagawa, S., Wincker, P., Karsenti, E., and Sullivan, M.B. (2015) Ocean plankton. Patterns and ecological drivers of ocean viral communities. *Science (80-)* **348**: 1261498.

Brum, J.R., and Sullivan, M.B. (2015) Rising to the challenge: accelerated pace of discovery transforms marine virology. *Nat Rev Microbiol* **13**: 147–159.

Bryan, D., El-Shibiny, A., Hobbs, Z., Porter, J., and Kutter, E.M. (2016) Bacteriophage T4 infection of stationary phase E. coli: life after log from a phage perspective. *Front Microbiol* **7**: 1391.

Buckling, A., and Brockhurst, M. (2012) Bacteria-virus coevolution. *Adv Exp Med Biol* **751**: 347–370.

Buckling, A., and Rainey, P.B. (2002) Antagonistic coevolution between a bacterium and a bacteriophage. *Proceedings Biol Sci* **269**: 931–6.

Buckling, A., Wei, Y., Massey, R.C., Brockhurst, M.A., and Hochberg, M.E. (2006) Antagonistic coevolution with parasites increases the cost of host deleterious mutations. *Proceedings Biol Sci* **273**: 45–9.

Bulgarelli, D., Rott, M., Schlaeppi, K., Themaat, E.V.L. van, Ahmadinejad, N., Assenza, F., Rauf, P., Huettel, B., Reinhardt, R., Schmelzer, E., Peplies, J., Gloeckner, F.O., Amann, R., Eickhorst, T., and Schulze-Lefert, P. (2012) Revealing structure and assembly cues for Arabidopsis-root inhabiting bacterial microbiota. *Nature* **488**: 91–95.

Bulgarelli, D., Schlaeppi, K., Spaepen, S., Themaat, E.V.L. van, and Schulze-Lefert, P. (2013) Structure and functions of the bacterial microbiota of plants. *Annu Rev Plant Biol* **64**: 807–38.

Burge, W.D., and Enkiri, N.K. (1978) Virus adsorption by five soils. *J Environ Qual* **7**: 73.

Burr, T., Barnard, A.M.L., Corbett, M.J., Pemberton, C.L., Simpson, N.J.L., and Salmond, G.P.C. (2006) Identification of the central quorum sensing regulator of virulence in the enteric phytopathogen, Erwinia carotovora: the VirR repressor. *Mol Microbiol* **59**: 113–125.

Bushman, F. (2002) *Lateral DNA transfer : mechanisms and consequences*. Cold Spring Harbor Laboratory Press, New York.

Buts, L., Lah, J., Dao-Thi, M.H., Wyns, L., and Loris, R. (2005) Toxin-antitoxin modules as bacterial metabolic stress managers. *Trends Biochem Sci* **30**: 672–679.

Buttimer, C., Hendrix, H., Lucid, A., Neve, H., Noben, J.-P., Franz, C., O'Mahony, J., Lavigne, R., and Coffey, A. (2018) Novel N4-like bacteriophages of Pectobacterium atrosepticum. *Pharmaceuticals* **11**: 45.

Buttimer, C., McAuliffe, O., Ross, R.P., Hill, C., O'Mahony, J., and Coffey, A. (2017) Bacteriophages and bacterial plant diseases. *Front Microbiol* **8**: 34.

Byers, J.T., Lucas, C., Salmond, G.P.C., and Welch, M. (2002) Nonenzymatic turnover of an Erwinia carotovora quorum-sensing signaling molecule. *J Bacteriol* **184**: 1163–1171.

Byrne, J.M., Dianese, A.C., Ji, P., Campbell, H.L., Cuppels, D.A., Louws, F.J., Miller, S.A., Jones, J.B., and Wilson, M. (2005) Biological control of bacterial spot of tomato under field conditions at several locations in North America. *Biol Control* **32**: 408–418.

Cademartiri, R., Anany, H., Gross, I., Bhayani, R., Griffiths, M., and Brook, M.A. (2010) Immobilization of bacteriophages on modified silica particles. *Biomaterials* **31**: 1904–1910.

Calendar, R., and Abedon, S.T. (2005) *The bacteriophages*. 1st ed., Springer, Boston, MA.

Canavan, H.E., Cheng, X., Graham, D.J., Ratner, B.D., and Castner, D.G. (2006) A plasma-deposited surface for cell sheet engineering: advantages over mechanical dissociation of cells. *Plasma Process Polym* **3**: 516–523.

Capparelli, R., Nocerino, N., Lanzetta, R., Silipo, A., Amoresano, A., Giangrande, C., Becker, K., Blaiotta, G., Evidente, A., Cimmino, A., Iannaccone, M., Parlato, M., Medaglia, C., Roperto, S., Roperto, F., Ramunno, L., and Iannelli, D. (2010) Bacteriophage-resistant Staphylococcus aureus mutant confers broad immunity against Staphylococcal infection in mice. *PLoS One* **5**: e11720.

Carlson, K., and Miller, E.S. (1994) Enumerating phage. In *Molecular Biology of Bacteriophage T4*. Karam, J.D. (ed.). ASM Press, Washington, DC. pp. 427–429.

Carrillo, C.L., Atterbury, R.J., Dillon, E., Scott, a, Connerton, I.F., and

Connerton, P.L. (2005) Bacteriophage therapy to reduce Campylobacter jejuni colonization of broiler chickens. *Appl Environ Microbiol* **71**: 6554–6563.

Carvalho, C.M., Gannon, B.W., Halfhide, D.E., Santos, S.B., Hayes, C.M., Roe, J.M., and Azeredo, J. (2010) The in vivo efficacy of two administration routes of a phage cocktail to reduce numbers of Campylobacter coli and Campylobacter jejuni in chickens. *BMC Microbiol* **10**: 232.

Casey, E., Sinderen, D. van, and Mahony, J. (2018) In vitro charactersitics of phages to guide “real life” phage therapy suitability. *Viruses* **10**: 163.

Casjens, S.R. (2005) Comparative genomics and evolution of the tailed-bacteriophages. *Curr Opin Microbiol* **8**: 451–458.

Casjens, S.R. (2008) Diversity among the tailed-bacteriophages that infect the Enterobacteriaceae. *Res Microbiol* **159**: 340–348.

Casjens, S.R., and Gilcrease, E.B. (2009) Determining DNA packaging strategy by analysis of the termini of the chromosomes in tailed-bacteriophage virions. *Methods Mol Biol* **502**: 91–111.

Casjens, S.R., Gilcrease, E.B., Winn-Stapley, D.A., Schicklmaier, P., Schmieger, H., Pedulla, M.L., Ford, M.E., Houtz, J.M., Hatfull, G.F., and Hendrix, R.W. (2005) The generalized transducing Salmonella bacteriophage ES18: complete genome sequence and DNA packaging strategy. *J Bacteriol* **187**: 1091–1104.

Casjens, S.R., and Molineux, I.J. (2012) Short noncontractile tail machines: adsorption and DNA delivery by podoviruses. *Adv Exp Med Biol* **728**: 143–179.

Castillo, D., Christiansen, R.H., Espejo, R., and Middelboe, M. (2014) Diversity and geographical distribution of Flavobacterium psychrophilum isolates and their phages: patterns of susceptibility to phage infection and phage host range. *Microb Ecol* **67**: 748–57.

Castresana, J. (2000) Selection of conserved blocks from multiple alignments for their use in phylogenetic analysis. *Mol Biol Evol* **17**: 540–552.

Catalano, C.E. (2005) *Viral genome packaging machines: genetics, structure, and mechanism*. 1st ed., Springer US, .

Catalano, C.E., Cue, D., and Feiss, M. (1995) Virus DNA packaging: the strategy used by phage λ. *Mol Microbiol* 16.

Ceyssens, P.-J., Glonti, T., Kropinski, ndrew M., Lavigne, R., Chanishvili, N., Kulakov, L., Lashkhi, N., Tediashvili, M., and Merabishvili, M. (2011) Phenotypic and genotypic variations within a single bacteriophage species. *Virol J* **8**: 134.

Ceyssens, P.-J., Minakhin, L., Bossche, A. Van den, Yakunina, M., Klimuk, E., Blasdel, B., Smet, J. De, Noben, J.-P., Blasi, U., Severinov, K., and

Lavigne, R. (2014) Development of giant bacteriophage KZ Is independent of the host transcription apparatus. *J Virol* **88**: 10501–10510.

Chan, B.K., Abedon, S.T., and Loc-Carrillo, C. (2013) Phage cocktails and the future of phage therapy. *Future Microbiol* **8**: 769–783.

Chan, B.K., Sistrom, M., Wertz, J.E., Kortright, K.E., Narayan, D., and Turner, P.E. (2016) Phage selection restores antibiotic sensitivity in MDR Pseudomonas aeruginosa. *Sci Rep* **6**: 26717.

Chan, C.M., Ko, T.M., and Hiraoka, H. (1996) Polymer surface modification by plasmas and photons. *Surf Sci Rep* **24**: 1–54.

Chang, C.Y., Kemp, P., and Molineux, I.J. (2010) Gp15 and gp16 cooperate in translocating bacteriophage T7 DNA into the infected cell. *Virology* **398**: 176–186.

Chang, P., Gerhardt, K.E., Huang, X.D., Yu, X.M., Glick, B.R., Gerwing, P.D., and Greenberg, B.M. (2014) Plant growth-promoting bacteria facilitate the growth of barley and oats in salt-impacted soil: implications for phytoremediation of saline soils. *Int J Phytoremediation* **16**: 1133–47.

Chankhamhaengdecha, S., Hongvijit, S., Srichaisupakit, A., Charnchai, P., and Panbangred, W. (2013) Endophytic actinomycetes: a novel source of potential acyl homoserine lactone degrading enzymes. *Biomed Res Int* .

Chao, L., Levin, B.R., and Stewart, F.M. (1977) A complex community in a simple habitat: an experimental study with bacteria and phage. *Ecology* **58**: 369–378.

Charkowski, A.O. (2006) The soft rot Erwinia. In *Plant-Associated Bacteria*. Gnanamanickam S.S. (ed.). Springer, Netherlands, pp. 423–505.

Charkowski, A.O. (2015) Biology and control of Pectobacterium in potato. *Am J Potato Res* **92**: 223–229.

Chatterjee, A., Cui, Y., and Chatterjee, A.K. (2002) RsmA and the quorum-sensing signal, N-[3-oxohexanoyl]-L-homoserine lactone, control the levels of rsmB RNA in Erwinia carotovora subsp. carotovora by affecting its stability. *J Bacteriol* **184**: 4089–4095.

Chatterjee, S., and Rothenberg, E. (2012) Interaction of bacteriophage λ with Its E. coli receptor, LamB. *Viruses* **4**: 3162–3178.

Chattopadhyay, S., and Puls, R.W. (2000) Forces dictating colloidal interactions between viruses and soil. *Chemosphere* **41**: 1279–86.

Chen, J., Quiles-Puchalt, N., Chiang, Y.N., Bacigalupe, R., Fillol-Salom, A., Chee, M.S.J., Fitzgerald, J.R., and Penadés, J.R. (2018) Genome hypermobility by lateral transduction. *Science (80-)* **362**: 207 LP-212.

Chen, L., Xun, W., Sun, L., Zhang, N., Shen, Q., and Zhang, R. (2014) Effect

of different long-term fertilization regimes on the viral community in an agricultural soil of Southern China. *Eur J Soil Biol* **62**: 121–126.

Cheng, X., Zhang, X., Pflugrath, J.W., and Studier, F.W. (1994) The structure of bacteriophage T7 lysozyme, a zinc amidase and an inhibitor of T7 RNA polymerase. *Proc Natl Acad Sci U S A* **91**: 4034–8.

Cherny, I., and Gazit, E. (2004) The YefM antitoxin defines a family of natively unfolded proteins: Implications as a novel antibacterial target. *J Biol Chem* **279**: 8252–8261.

Chevallereau, A., Blasdel, B.G., Smet, D., Monot, J., Zimmermann, M., and Kogadeeva, M. (2016) Next-generation -omics approaches reveal a massive alteration of host RNA metabolism during bacteriophage infection of Pseudomonas aeruginosa. *PLoS Genet* **12**: 1006134.

Chevenet, F., Brun, C., Bañuls, A.L., Jacq, B., and Christen, R. (2006) TreeDyn: towards dynamic graphics and annotations for analyses of trees. *BMC Bioinformatics* **7**: 439.

Chibani-Chennoufi, S., Bruttin, A., Dillmann, M.L., and Brüssow, H. (2004) Phage-host interaction: an ecological perspective. *J Bacteriol* **186**: 3677–3686.

Chibani-Chennoufi, S., Dillmann, M.L., Marvin-Guy, L., Rami-Shojaei, S., and Brüssow, H. (2004) Lactobacillus plantarum bacteriophage LP65: a new member of the SPO1-like genus of the family myoviridae. *J Bacteriol* **186**: 7069–7083.

Chopin, M.C., Chopin, A., and Bidnenko, E. (2005) Phage abortive infection in lactococci: variations on a theme. *Curr Opin Microbiol* **8**: 473–479.

Chou, C.-F., Tegenfeldt, J.O., Bakajin, O., Chan, S.S., Cox, E.C., Darnton, N., Duke, T., and Austin, R.H. (2002) Electrodeless dielectrophoresis of single-and double-stranded DNA. *Biophys* **83**: 2170–2179.

Christensen, S.K., Mikkelsen, M., Pedersen, K., and Gerdes, K. (2001) RelE, a global inhibitor of translation, is activated during nutritional stress. *Proc Natl Acad Sci* **98**: 14328–14333.

Clokie, M.R.J. (2009) *Bacteriophages : methods and protocols volume 1: isolation, characterization, and interactions*. 1st ed., Humana Press, .

Clokie, M.R.J., and Kropinski, A.M. (2009) *Bacteriophages: methods and protocols, volume 2: molecular and applied aspects*. 1st ed., Humana Press, .

Clokie, M.R.J., Millard, A.D., Letarov, A. V., and Heaphy, S. (2011) Phages in nature. *Bacteriophage* **1**: 31–45.

Cohen, S.S. (1949) Growth requirements of bacterial viruses. *Bacteriol Rev* **13**: 1–24.

Colombet, J., Sime-Ngando, T., Cauchie, H.M., Fonty, G., Hoffmann, L., and Demeure, G. (2006) Depth-related gradients of viral activity in Lake Pavin. *Appl Environ Microbiol* **72**: 4440–4445.

Comeau, A.M., and Krisch, H.M. (2008) The capsid of the T4 phage superfamily: the evolution, diversity, and structure of some of the most prevalent proteins in the biosphere. *Mol Biol Evol* **25**: 1321–1332.

Connerton, P.L., Loc Carrillo, C.M., Swift, C., Dillon, E., Scott, A., Rees, C.E.D., Dodd, C.E.R., Frost, J., and Connerton, I.F. (2004) Longitudinal study of Campylobacter jejuni bacteriophages and their hosts from broiler chickens. *Appl Environ Microbiol* **70**: 3877–3883.

Considina, D.M., and Considine, G.D. (1995) *Foods and food production encyclopedia*. NY: Springer, New York.

Conte, A., Buonocore, G.G., Sinigaglia, M., Lopez, L.C., Favia, P., d'agostino, R., and Nobile, M.A. Del (2008) Antimicrobial activity of immobilized lysozyme on plasma-treated polyethylene films. *J Food Prot* **71**: 119–125.

Cook, C.C., Kim, A., Terao, S., Gotoh, A., and Higuchi, M. (2012) Consumption of oxygen: a mitochondrial-generated progression signal of advanced cancer. *Cell Death Dis* **3**: e258–e258.

Corbett, M., Virtue, S., Bell, K., Birch, P., Burr, T., Hyman, L., Lilley, K., Poock, S., Toth, I., and Salmond, G. (2005) Identification of a new quorum-sensing-controlled virulence factor in Erwinia carotovora subsp. atroseptica secreted via the type II targeting pathway. *Mol Plant Microbe Interact* **18**: 334–342.

Cormier, J., and Janes, M. (2014) A double layer plaque assay using spread plate technique for enumeration of bacteriophage MS2. *J Virol Methods* **196**: 86–92.

Cowley, L.A., Low, A.S., Pickard, D., Boinett, C.J., Dallman, T.J., Day, M., Perry, N., Gally, D.L., Parkhill, J., Jenkins, C., and Cain, A.K. (2018) Transposon insertion sequencing elucidates novel gene involvement in susceptibility and resistance to phages T4 and T7 in Escherichia coli O157. *MBio* **9**: 705–723.

Cox, A.R.J., Thomson, N.R., Bycroft, B., Stewart, G.S.A.B., Williams, P., and Salmond, G.P.C. (1998) A pheromone-independent CarR protein controls carbapenem antibiotic synthesis in the opportunistic human pathogen Serratia marcescens. *Microbiology* **144**: 201–209.

Crépin, A., Barbey, C., Beury-Cirou, A., Hélias, V., Taupin, L., Reverchon, S., Nasser, W., Faure, D., Dufour, A., Orange, N., Feuilloley, M., Heurlier, K., Burini, J.-F., and Latour, X. (2012) Quorum sensing signaling molecules produced by reference and emerging soft-rot bacteria (Dickeya and Pectobacterium spp.). *PLoS One* **7**: e35176.

Crepin, A., Barbey, C., Cirou, A., Tannieres, M., Orange, N., Feuilloley, M., Dessaux, Y., Burini, J.-F., Faure, D., and Latour, X. (2012) Biological control of pathogen communication in the rhizosphere: a novel approach applied to potato soft rot due to Pectobacterium atrosepticum. *Plant Soil* **358**: 25–35.

Crick, F.H.C., Leslie Barnett, F.R.S., Brenner, S., and Watts-Tobin, R.J. (1961) General nature of the genetic code for proteins. *Nature* **192**: 1227–1232.

Cronin, D., Moenne-Loccoz, Y., Fenton, A., Dunne, C., Dowling, D.N., and O'Gara, F. (1997) Ecological interaction of a biocontrol Pseudomonas fluorescens strain producing 2,4-diacetylphloroglucinol with the soft rot potato pathogen Erwinia carotovora subsp. atroseptica. *FEMS Microbiol Ecol* **23**: 95–106.

Cuccuru, G., Orsini, M., Pinna, A., Sbardellati, A., Soranzo, N., Travaglione, A., Uva, P., Zanetti, G., and Fotia, G. (2014) Orione, a web-based framework for NGS analysis in microbiology. *Bioinformatics* **30**: 1928–1929.

Cui, Y., Chatterjee, A., Liu, Y., Dumenyo, C.K., and Chatterjee, A.K. (1995) Identification of a global repressor gene, rsmA, of Erwinia carotovora subsp. carotovora that controls extracellular enzymes, N-(3-oxohexanoyl)-L-homoserine lactone, and pathogenicity in soft-rotting Erwinia spp. *J Bacteriol* **177**: 5108–5115.

Cui, Y., Mukherjee, A., Dumenyo, C.K., Liu, Y., and Chatterjee, A.K. (1999) rsmC of the soft-rotting bacterium Erwinia carotovora subsp. carotovora negatively controls extracellular enzyme and harpin(Ecc) production and virulence by modulating levels of regulatory RNA (rsmB) and RNA-binding protein (RsmA). *J Bacteriol* **181**: 6042–6052.

Culley, A.I., Lang, A.S., and Suttle, C.A. (2003) High diversity of unknown picorna-like viruses in the sea. *Nature* **424**: 1054–1057.

Culley, S., Towers, G., Selwood, D., Henriques, R., Grove, J., Culley, S., Towers, G.J., Selwood, D.L., Henriques, R., and Grove, J. (2016) Infection Counter: automated quantification of in vitro virus replication by fluorescence microscopy. *Viruses* **8**: 201.

Czajkowski, R. (2016a) Bacteriophages of soft rot Enterobacteriaceae-a minireview. *FEMS Microbiol Lett* **363**: fnv230.

Czajkowski, R. (2016b) Bacteriophages of soft rot Enterobacteriaceae —a minireview. *FEMS Microbiol Lett* **363**: fnv230.

Czajkowski, R., Ozymko, Z., and Lojkowska, E. (2014) Isolation and characterization of novel soilborne lytic bacteriophages infecting Dickeya spp. biovar 3 ('D. solani'). *Plant Pathol* **63**: 758–772.

Czajkowski, R., Pérombelon, M.C.M., Jafra, S., Lojkowska, E., Potrykus, M., Wolf, J.M. Van Der, and Sledz, W. (2015) Detection, identification and

differentiation of Pectobacterium and Dickeya species causing potato blackleg and tuber soft rot: a review. *Ann Appl Biol* **166**: 18–38.

Czajkowski, R., Pérombelon, M.C.M., Veen, J. a. van, and Wolf, J.M. van der (2011) Control of blackleg and tuber soft rot of potato caused by Pectobacterium and Dickeya species: a review. *Plant Pathol* **60**: 999–1013.

Dakora, F.D., and Phillips, D.A. (2002) Root exudates as mediators of mineral acquisition in low-nutrient environments. *Plant Soil* 245.

Danis-Wlodarczyk, K., Olszak, T., Arabski, M., Wasik, S., Majkowska-Skrobek, G., Augustyniak, D., Gula, G., Briers, Y., Jang, H. Bin, Vandenheuvel, D., Duda, K.A., Lavigne, R., and Drulis-Kawa, Z. (2015) Characterization of the newly isolated lytic bacteriophages KTN6 and KT28 and their efficacy against Pseudomonas aeruginosa biofilm. *PLoS One* **10**: e0137015.

Davey, T., Hodge, C., and Saddler, G.S. (2016) Identification of factors which may be influencing the incidence of blackleg in Scottish seed potatoes. *Proc Crop Prot North Britain 2016, 23-24 Febr 2016, Dundee, UK* 197–202.

Davies, J., and Davies, D. (2010) Origins and evolution of antibiotic resistance. *Microbiol Mol Biol Rev* **74**: 417–433.

Davies, J.D., and Kelly, M.J. (1969) The preservation of bacteriophage H1 of Corynebacterium ulcerans U 103 by freeze-drying. *J Hyg (Lond)* **67**: 573–83.

Davis Ii, E.W., Weisberg, A.J., Tabima, J.F., Grunwald, N.J., and Chang, J.H. (2016) Gall-ID: tools for genotyping gall-causing phytopathogenic bacteria. *PeerJ* **4**: e2222.

Debarbieux, L., Pirnay, J.P., Verbeken, G., Vos, D. De, Merabishvili, M., Huys, I., Patey, O., Schoonjans, D., Vaneechoutte, M., Zizi, M., and Rohde, C. (2016) A bacteriophage journey at the European Medicines Agency. *FEMS Microbiol Lett* **363**: fnv225.

Dedrick, R.M., Jacobs-Sera, D., Guerrero Bustamante, C.A., Garlena, R.A., Mavrich, T.N., Pope, W.H., Cervantes Reyes, J.C., Russell, D.A., Adair, T., Alvey, R., Bonilla, J.A., Bricker, J.S., Brown, B.R., Byrnes, D., Cresawn, S.G., Davis, W.B., Dickson, L.A., Edgington, N.P., Findley, A.M., Golebiewska, U., Grose, J.H., Hayes, C.F., Hughes, L.E., Hutchison, K.W., Isern, S., Johnson, A.A., Kenna, M.A., Klyczek, K.K., Mageeney, C.M., Michael, S.F., Molloy, S.D., Montgomery, M.T., Neitzel, J., Page, S.T., Pizzorno, M.C., Poxleitner, M.K., Rinehart, C.A., Robinson, C.J., Rubin, M.R., Teyim, J.N., Vazquez, E., Ware, V.C., Washington, J., and Hatfull, G.F. (2017) Prophage-mediated defence against viral attack and viral counter-defence. *Nat Microbiol* **9**: 16251.

Dees, M.W., Lebecka, R., Perminow, J.I.S., Czajkowski, R., Grupa, A., Motyka, A., Zoledowska, S., Śliwka, J., Lojkowska, E., and Brurberg, M.B. (2017) Characterization of Dickeya and Pectobacterium strains obtained from

diseased potato plants in different climatic conditions of Norway and Poland. *Eur J Plant Pathol* **148**: 839–851.

Delcher, A.L., Bratke, K.A., Powers, E.C., and Salzberg, S.L. (2007) Identifying bacterial genes and endosymbiont DNA with Glimmer. *Bioinformatics* **23**: 673–679.

Delcher, A.L., Harmon, D., Kasif, S., White, O., and Salzberg, S.L. (1999) Improved microbial gene identification with GLIMMER. *Nucleic Acids Res* **27**: 4636–4641.

Delepelaire, P. (2004) Type I secretion in gram-negative bacteria. *Biochim Biophys Acta - Mol Cell Res* **1694**: 149–161.

Delesalle, V.A., Tanke, N.T., Vill, A.C., and Krukonis, G.P. (2016) Testing hypotheses for the presence of tRNA genes in mycobacteriophage genomes. *Bacteriophage* **6**: e1219441.

Denes, F.S., and Manolache, S. (2004) Macromolecular plasma-chemistry: an emerging field of polymer science. *Prog Polym Sci* **29**: 815–885.

Dennehy, J.J. (2012) What can phages tell us about host-pathogen coevolution? *Int J Evol Biol* **2012**: 12.

Dennis, P.G., Miller, A.J., and Hirsch, P.R. (2010) Are root exudates more important than other sources of rhizodeposits in structuring rhizosphere bacterial communities? *FEMS Microbiol Ecol* **72**: 313–327.

Dereeper, A., Guignon, V., Blanc, G., Audic, S., Buffet, S., Chevenet, F., Dufayard, J.-F., Guindon, S., Lefort, V., Lescot, M., Claverie, J.-M., and Gascuel, O. (2008) Phylogeny.fr: robust phylogenetic analysis for the non-specialist. *Nucleic Acids Res* **36**: W465–W469.

Deveau, H., Barrangou, R., Garneau, J.E., Labonte, J., Fremaux, C., Boyaval, P., Romero, D.A., Horvath, P., and Moineau, S. (2008) Phage response to CRISPR-encoded resistance in Streptococcus thermophilus. *J Bacteriol* **190**: 1390–1400.

Deyn, G.B. De, Cornelissen, J.H.C., and Bardgett, R.D. (2008) Plant functional traits and soil carbon sequestration in contrasting biomes. *Ecol Lett* **11**: 516–531.

Diaz-Munoz, S.L., and Koskella, B. (2014) Bacteria-phage interactions in natural environments. *Adv Appl Microbiol Vol 89* **89**: 135–183.

Doan, T.T., Bouvier, C., Bettarel, Y., Bouvier, T., Henry-des-Tureaux, T., Janeau, J.L., Lamballe, P., Nguyen, B. Van, and Jouquet, P. (2014) Influence of buffalo manure, compost, vermicompost and biochar amendments on bacterial and viral communities in soil and adjacent aquatic systems. *Appl Soil Ecol* **73**: 78–86.

Dobbins, A.T., George, M., Basham, D.A., Ford, M.E., Houtz, J.M., Pedulla,

M.L., Lawrence, J.G., Hatfull, G.F., and Hendrix, R.W. (2004) Complete genomic sequence of the virulent Salmonella bacteriophage SP6. *J Bacteriol* **186**: 1933–44.

Dobereiner, J. (1992) History and new perspectives of diazotrophs in association with nonleguminous plants. *Symbiosis* **13**: 1–13.

Doffkay, Z., Dömötör, D., Kovács, T., and Rákhely, G. (2015) Bacteriophage therapy against plant, animal and human pathogens. *Acta Biol Szeged* **59**: 291–302.

Dong, Y.H., Zhang, X.F., Xu, J.L., and Zhang, L.H. (2004) Insecticidal Bacillus thuringiensis silences Erwinia carotovora virulence by a new form of microbial antagonism, signal interference. *Appl Environ Microbiol* **70**: 954–960.

Doron, S., Melamed, S., Ofir, G., Leavitt, A., Lopatina, A., Keren, M., Amitai, G., and Sorek, R. (2018) Systematic discovery of antiphage defense systems in the microbial pangenome. *Science (80-)* **359**: eaar4120.

Doulatov, S., Hodes, A., Dai, L., Mandhana, N., Liu, M., Deora, R., Simons, R.W., Zimmerly, S., and Miller, J.F. (2004) Tropism switching in Bordetella bacteriophage defines a family of diversity-generating retroelements. *Nature* **431**: 476–481.

Drulis-Kawa, Z., Mackiewicz, P., Kęsik-Szeloch, A., Maciaszczyk-Dziubinska, E., Weber-Dąbrowska, B., Dorotkiewicz-Jach, A., Augustyniak, D., Majkowska-Skrobek, G., Bocer, T., Empel, J., and Kropinski, A.M. (2011) Isolation and characterisation of KP34—a novel φKMV-like bacteriophage for Klebsiella pneumoniae. *Appl Microbiol Biotechnol* **90**: 1333–1345.

Duckworth, D.H. (1987) History and basic properties of bacterial viruses. In *Phage Ecology* . Wiley, New York, USA. p. 321.

Dunn, J.J., Studier, F.W., and Gottesman, M. (1983) Complete nucleotide sequence of bacteriophage T7 DNA and the locations of T7 genetic elements. *J Mol Biol* **166**: 477–535.

Dussoix, D., and Arber, W. (1962) Host specificity of DNA produced by Escherichia coli: II. Control over acceptance of DNA from infecting phage λ. *J Mol Biol* **5**: 37–49.

Dy, R.L., Przybilski, R., Semeijn, K., Salmond, G.P.C., and Fineran, P.C. (2014) A widespread bacteriophage abortive infection system functions through a Type IV toxin-antitoxin mechanism. *Nucleic Acids Res* **42**: 4590–4605.

Eayre, C.G., Bartz, J.A., and Concelmo, D.E. (1995) Bacteriophages of Erwinia carotovora and Erwinia ananas isolated from freshwater lakes. *Plant Dis* **79**: 801–804.

Edgar, R.C. (2004) MUSCLE: multiple sequence alignment with high accuracy and high throughput. *Nucleic Acids Res* **32**: 1792–1797.

Elford, W.J., and Andrews, C.H. (1932) The sizes of different bacteriophages. *Brit J Exp Path* **13**: 446–456S.

Ellis, E.L., and Delbruck, M. (1939) The growth of bacteriophage. *J Gen Physiol* **22**: 365–384.

Elphinstone, J.G., Cahill, G., Davey, T., Harper, G., Humphris, S., Saddler, G.S., Toth, I.K., and Wale, S.J. (2018) Effect of storage conditions on bacterial loading of seed potato tubers. Kenilworth, Warwickshire.

Emerson, J.B., Roux, S., Brum, J.R., Bolduc, B., Woodcroft, B.J., Jang, H. Bin, Singleton, C.M., Solden, L.M., Naas, A.E., Boyd, J.A., Hodgkins, S.B., Wilson, R.M., Trubl, G., Li, C., Frolking, S., Pope, P.B., Wrighton, K.C., Crill, P.M., Chanton, J.P., Saleska, S.R., Tyson, G.W., Rich, V.I., and Sullivan, M.B. (2018) Host-linked soil viral ecology along a permafrost thaw gradient. *Nat Microbiol* **3**: 870–880.

Emerson, J.B., Thomas, B.C., Andrade, K., Allen, E.E., Heidelberg, K.B., and Banfield, J.F. (2012) Dynamic viral populations in hypersaline systems as revealed by metagenomic assembly. *Appl Environ Microbiol* **78**: 6309–20.

Erez, Z., Steinberger-Levy, I., Shamir, M., Doron, S., Stokar-Avihail, A., Peleg, Y., Melamed, S., Leavitt, A., Savidor, A., Albeck, S., Amitai, G., and Sorek, R. (2017) Communication between viruses guides lysis–lysogeny decisions. *Nature* **541**: 488–493.

Eriksson, H., Maciejewska, B., Latka, A., Majkowska-Skrobek, G., Hellstrand, M., Melefors, Ö., Wang, J.T., Kropinski, A.M., Drulis-Kawa, Z., and Nilsson, A.S. (2015) A suggested new bacteriophage genus, “Kp34likevirus”, within the Autographivirinae subfamily of podoviridae. *Viruses* **7**: 1804–1822.

Erskine, J.M. (1973) Characteristics of Erwinia amylovora bacteriophage and its possible role in the epidemiology of fire blight. *Can J Microbiol* **19**: 837–845.

Essarts, Y.R. des, Cigna, J., Quêtu-Laurent, A., Caron, A., Munier, E., Beury-Cirou, A., Hélias, V., and Faure, D. (2016) Biocontrol of the potato blackleg and soft rot diseases caused by Dickeya dianthicola. *Appl Environ Microbiol* **82**: 268–278.

Evans, T.J., Ind, A., Komitopoulou, E., and Salmond, G.P.C. (2010) Phage-selected lipopolysaccharide mutants of Pectobacterium atrosepticum exhibit different impacts on virulence. *J Appl Microbiol* **109**: 505–514.

Fagerlund, R.D., Wilkinson, M.E., Klykov, O., Barendregt, A., Pearce, F.G., Kieper, S.N., Maxwell, H.W.R., Capolupo, A., Heck, A.J.R., Krause, K.L., Bostina, M., Scheltema, R.A., Staals, R.H.J., and Fineran, P.C. (2017) Spacer capture and integration by a type I-F Cas1–Cas2-3 CRISPR

adaptation complex. *Proc Natl Acad Sci* **114**: E5122-5128.

Fajola, A.O. (1979) The post-harvest fruit rots of tomato (Lycopersicum esculentum) in Nigeria. *Nahrung* **23**: 105–109.

Fan, X.Y., Chen, J., and Xie, J.P. (2012) The progress of nanomedicine inspired by bacteriophage. *Yaoxue Xuebao* **47**: 29–33.

FAO (2009) New light on a hidden treasure - an end of year review. Rome.

FAOSTAT (2011) *Food Agric Organ United Nations* .

Farrah, S.R., and Bitton, G. (1990) Viruses in the soil environment. In *Soil biochemistry. vol. 6*. Bollag, J.-M., and Stotzky, G. (eds). M. Dekker, New York, USA. pp. 529–556.

Farris, J.S. (1972) Estimating phylogenetic trees from distance matrices. *Am Nat* **106**: 645–668.

Ferguson, S., Roberts, C., Handy, E., and Sharma, M. (2013) Lytic bacteriophages reduce Escherichia coli O157: H7 on fresh cut lettuce introduced through cross-contamination. *Bacteriophage* **3**: e24323.

Feynman, R.P. (2012) There's plenty of room at the bottom: an invitation to enter a new field of physics. In *Handbook of Nanoscience, Engineering, and Technology*. CRC Press, Boca Raton, FL. pp. 3–12.

Fierer, N., and Jackson, R.B. (2006) The diversity and biogeography of soil bacterial communities. *Proc Natl Acad Sci U S A* **103**: 626–631.

Filée, J., Bapteste, E., Susko, E., and Krisch, H.M. (2006) A selective barrier to horizontal gene transfer in the T4-type bacteriophages that has preserved a core genome with the viral replication and structural genes. *Mol Biol Evol* **23**: 1688–1696.

Fineran, P.C., Blower, T.R., Foulds, I.J., Humphreys, D.P., Lilley, K.S., and Salmond, G.P.C. (2009) The phage abortive infection system, ToxIN, functions as a protein-RNA toxin-antitoxin pair. *Proc Natl Acad Sci U S A* **106**: 894–9.

Finn, R.D., Attwood, T.K., Babbitt, P.C., Bateman, A., Bork, P., Bridge, A.J., Chang, H.-Y., Dosztányi, Z., El-Gebali, S., Fraser, M., Gough, J., Haft, D., Holliday, G.L., Huang, H., Huang, X., Letunic, I., Lopez, R., Lu, S., Marchler-Bauer, A., Mi, H., Mistry, J., Natale, D.A., Necci, M., Nuka, G., Orengo, C.A., Park, Y., Pesseat, S., Piovesan, D., Potter, S.C., Rawlings, N.D., Redaschi, N., Richardson, L., Rivoire, C., Sangrador-Vegas, A., Sigrist, C., Sillitoe, I., Smithers, B., Squizzato, S., Sutton, G., Thanki, N., Thomas, P.D., Tosatto, S.C.E., Wu, C.H., Xenarios, I., Yeh, L.-S., Young, S.-Y., and Mitchell, A.L. (2017) InterPro in 2017-beyond protein family and domain annotations. *Nucleic Acids Res* **45**: D190–D199.

Finn, R.D., Coggill, P., Eberhardt, R.Y., Eddy, S.R., Mistry, J., Mitchell, A.L.,

Potter, S.C., Punta, M., Qureshi, M., Sangrador-Vegas, A., Salazar, G.A., Tate, J., and Bateman, A. (2016) The Pfam protein families database: towards a more sustainable future. *Nucleic Acids Res* **44**: D279–D285.

Firakova, S., Sturdikova, M., and Muckova, M. (2007) Bioactive secondary metabolites produced by microorganisms associated with plants. *Biologia (Bratisl)* **62**: 251–257.

Fischetti, V.A. (2010) Bacteriophage endolysins: a novel anti-infective to control Gram-positive pathogens. *Int J Med Microbiol* **300**: 357–362.

Fister, S., Robben, C., Witte, A.K., Schoder, D., Wagner, M., and Rossmanith, P. (2016) Influence of environmental factors on phage-bacteria interaction and on the efficacy and infectivity of phage P100. *Front Microbiol* **7**: 1152.

Flaks, J.G., and Cohen, S.S. (1957) The enzymic synthesis of 5-hydroxymethyldeoxycytidylic acid. *Biochim Biophys Acta* **25**: 667–668.

Fox, G.E., Stackebrandt, E., Hespell, R.B., Gibson, J., Maniloff, J., Dyer, T.A., Wolfe, R.S., Balch, W.E., Tanner, R.S., Magrum, L.J., Zahlen, L.B., Blakemore, R., Gupta, R., Bonen, L., Lewis, B.J., Stahl, D.A., Luehrsen, K.R., Chen, K.N., and Woese, C.R. (1980) The phylogeny of prokaryotes. *Science (80-)* **209**: 457–463.

Frampton, R. a., Pitman, A.R., and Fineran, P.C. (2012) Advances in bacteriophage-mediated control of plant pathogens. *Int J Microbiol* **2012**: 326452.

Friman, V.-P., and Buckling, A. (2013) Effects of predation on real-time host-parasite coevolutionary dynamics. *Ecol Lett* **16**: 39–46.

Friman, V.-P., and Buckling, A. (2014) Phages can constrain protist predation-driven attenuation of Pseudomonas aeruginosa virulence in multienemy communities. *ISME J* **8**: 1820–1830.

Fu, L., Li, S., Zhang, K., Chen, I.-H., Barbaree, J.M., Zhang, A., and Cheng, Z. (2011) Detection of Bacillus anthracis spores using phage-immobilized magnetostrictive milli/micro cantilevers. *IEEE Sens J* **11**: 1684–1691.

Fuhrman, J.A. (1999) Marine viruses and their biogeochemical and ecological effects. *Nature* **399**: 541–548.

Fujisawa, H., and Morita, M. (2003) Phage DNA packaging. *Genes to Cells* **2**: 537–545.

Fujiwara, A., Fujisawa, M., Hamasaki, R., Kawasaki, T., Fujie, M., and Yamada, T. (2011) Biocontrol of Ralstonia solanacearum by treatment with lytic bacteriophages. *Appl Environ Microbiol* **77**: 4155–62.

Gallet, R., Kannoly, S., and Wang, I.-N. (2011) Effects of bacteriophage traits on plaque formation. *BMC Microbiol* **11**: 181.

Gao, N.L., Zhang, C., Zhang, Z., Hu, S., Lercher, M.J., Zhao, X.-M., Bork, P., Liu, Z., and Chen, W.-H. (2018) MVP: a microbe–phage interaction database. *Nucleic Acids Res* **46**: D700–D707.

Garcia-Doval, C., and Raaij, M.J. van (2012) Structure of the receptor-binding carboxy-terminal domain of bacteriophage T7 tail fibers. *Proc Natl Acad Sci* **109**: 9390–9395.

García-Martínez, J., Maldonado, R.D., Guzmán, N.M., and Mojica, F.J.M. (2018) The CRISPR conundrum: evolve and maybe die, or survive and risk stagnation. *Microb cell* **5**: 262–268.

Garcia, L.R., Garcia, G., and Molineux, I.J. (1995) Rate of translocation of bacteriophage T7 DNA across the membranes of Escherichia coli. *J Bacteriol* **177**: 4066–4076.

Garcia, P., Martinez, B., Obeso, J.M., and Rodriguez, A. (2008) Bacteriophages and their application in food safety. *Lett Appl Microbiol* **47**: 479–85.

Garge, S.S., and Nerurkar, A.S. (2016) Attenuation of quorum sensing regulated virulence of Pectobacterium carotovorum subsp. carotovorum through an AHL lactonase produced by Lysinibacillus sp. Gs50. *PLoS One* **11**: e0167344.

Garneau, J.E., Dupuis, M.-È., Villion, M., Romero, D.A., Barrangou, R., Boyaval, P., Fremaux, C., Horvath, P., Magadán, A.H., and Moineau, S. (2010) The CRISPR/Cas bacterial immune system cleaves bacteriophage and plasmid DNA. *Nature* **468**: 67–71.

Garneau, J.R., Depardieu, F., Fortier, L.-C., Bikard, D., and Monot, M. (2017) PhageTerm: a tool for fast and accurate determination of phage termini and packaging mechanism using next-generation sequencing data. *Sci Rep* **7**: 8292.

Geiduschek, E.P., and Kassavetis, G.A. (2010) Transcription of the T4 late genes. *Virol J* **7**: 288.

Gerdes, K., Christensen, S.K., and Løbner-Olesen, A. (2005) Prokaryotic toxin-antitoxin stress response loci. *Nat Rev Microbiol* **3**: 371–382.

Gerdes, K., and Maisonneuve, E. (2012) Bacterial persistence and toxin-antitoxin loci. *Annu Rev Microbiol* **66**: 103–123.

Gerratana, B., Stapon, A., and Townsend, C.A. (2003) Inhibition and alternate substrate studies on the mechanism of carbapenam synthetase from Erwinia carotovora. *Biochemistry* **42**: 7836–7847.

Ghanekar, A.S., Padwal-Desai, S.R., and Nadkarni, G.B. (1984) The involvement of phenolics and phytoalexins in resistance of potato to soft rot. *Potato Res* **27**: 189–199.

Ghosh, S., Marintcheva, B., Takahashi, M., and Richardson, C.C. (2009) C-terminal phenylalanine of bacteriophage T7 single-stranded DNA-binding protein Is essential for strand displacement synthesis by T7 DNA polymerase at a nick in DNA. *J Biol Chem* **284**: 30339–30349.

Gill, J., and Abedon, S.T. (2003) Bacteriophage ecology and plants. *APSnet Featur* .

Gill, J.J., and Hyman, P. (2010) Phage choice, isolation, and preparation for phage therapy. *Curr Pharm Biotechnol* **11**: 2–14.

Glauner, B., Holtje, J.-V., and Schwarz, U. (1988) The composition of the murein of Escherichia coli*. *J Biol Chem* **263**: 10088–10096.

Glonti, T., Chanishvili, N., and Taylor, P.W. (2010) Bacteriophage-derived enzyme that depolymerizes the alginic acid capsule associated with cystic fibrosis isolates of Pseudomonas aeruginosa. *J Appl Microbiol* **108**: 695–702.

Gnanamanickam, S.S. (2006) *Plant-associated bacteria*. 1st ed., Springer Netherlands, .

Godde, J.S., and Bickerton, A. (2006) The repetitive DNA elements called CRISPRs and their associated genes: evidence of horizontal transfer among prokaryotes. *J Mol Evol* **62**: 718–729.

Goeders, N., and Melderen, L. Van (2014) Toxin-antitoxin systems as multilevel interaction systems. *Toxins (Basel)* **6**: 304–324.

Göker, M., García-Blázquez, G., Voglmayr, H., Tellería, M.T., and Martín, M.P. (2009) Molecular taxonomy of phytopathogenic Fungi: a case study in Peronospora. *PLoS One* **4**: e6319.

Goldfarb, T., Sberro, H., Weinstock, E., Cohen, O., Doron, S., Charpak-Amikam, Y., Afik, S., Ofir, G., and Sorek, R. (2015) BREX is a novel phage resistance system widespread in microbial genomes. *EMBO J* **34**: 169–83.

Goldman, M., Goldman, a, and Sigmond, R.S. (1985) The corona discharge, its properties and specific uses. *Pure Appl Chem* **57**: 1353–1362.

Golec, P., Karczewska-Golec, J., Łoś, M., and Węgrzyn, G. (2014) Bacteriophage T4 can produce progeny virions in extremely slowly growing Escherichia coli host: comparison of a mathematical model with the experimental data. *FEMS Microbiol Lett* **351**: 156–161.

Gomes, N.C.M., Heuer, H., Schönfeld, J., Costa, R., Mendonça-Hagler, L., and Smalla, K. (2001) Bacterial diversity of the rhizosphere of maize (Zea mays) grown in tropical soil studied by temperature gradient gel electrophoresis. *Plant Soil* **232**: 167–180.

Gómez, P., Ashby, B., and Buckling, A. (2015) Population mixing promotes arms race host-parasite coevolution. *Proceedings Biol Sci* **282**: 20142297.

Gomez, P., and Buckling, A. (2011) Bacteria-phage antagonistic coevolution in soil. *Science (80-)* **332**: 106–109.

Goode, D., Allen, V.M., and Barrow, P.A. (2003) Reduction of experimental Salmonella and Campylobacter contamination of chicken skin by application of lytic bacteriophages. *Appl Environ Microbiol* **69**: 5032–5036.

Gotō, M. (1992) *Fundamentals of bacterial plant pathology*. 1st ed., Academic Press, San Diego, USA.

Goto, M., and Matsumoto, K. (1987) Erwinia carotovora subsp. wasabiae subsp. nov. isolated from diseased rhizomes and fibrous roots of Japanese horseradish (Eutrema wasabi Maxim.). *Int J Syst Bacteriol* **37**: 130–135.

Goyal, S.M., and Gerba, C.P. (1979) Comparative adsorption of human enteroviruses, simian rotavirus, and selected bacteriophages to soils. *Appl Environ Microbiol* **38**: 241–247.

Graham, D.C., and Harper, P.C. (1967) Potato blackleg and tuber soft rot. *Scottish J Agric* **48**: 68–74.

Grant, J.R., Arantes, A.S., and Stothard, P. (2012) Comparing thousands of circular genomes using the CGView Comparison Tool. *BMC Genomics* **13**: 202.

Green, J.L., Bohannan, B.J.M., and Whitaker, R.J. (2008) Microbial biogeography: from taxonomy to traits. *Science (80-)* **320**: 1039–1043.

Grigoriev, A. (1999) Strand-specific compositional asymmetries in double-stranded DNA viruses. *Virus Res* **60**: 1–19.

Grose, J.H., and Casjens, S.R. (2014) Understanding the enormous diversity of bacteriophages: the tailed phages that infect the bacterial family Enterobacteriaceae. *Virology* **468**–**470**: 421–443.

Gross, D.C., Powelson, M.L., Regner, K.M., and Radamaker, G.K. (1991) A bacteriophage-typing system for surveying the diversity and distribution of strains of Erwinia carotovora in potato fields. *Phytopathology* **81**: 220–6.

Guenther, S., Herzig, O., Fieseler, L., Klumpp, J., and Loessner, M.J. (2012) Biocontrol of Salmonella Typhimurium in RTE foods with the virulent bacteriophage FO1-E2. *Int J Food Microbiol* **154**: 66–72.

Guenther, S., Huwyler, D., Richard, S., and Loessner, M.J. (2009) Virulent bacteriophage for efficient biocontrol of listeria monocytogenes in ready-to-eat foods. *Appl Environ Microbiol* **75**: 93–100.

Guidi, L., Chaffron, S., Bittner, L., Eveillard, D., Larhlimi, A., Roux, S., Darzi, Y., Audic, S., Berline, L., Brum, J.R., Coelho, L.P., Espinoza, J.C.I., Malviya, S., Sunagawa, S., Dimier, C., Kandels-Lewis, S., Picheral, M., Poulain, J., Searson, S., Stemmann, L., Not, F., Hingamp, P., Speich, S., Follows, M., Karp-Boss, L., Boss, E., Ogata, H., Pesant, S., Weissenbach, J., Wincker, P.,

Acinas, S.G., Bork, P., Vargas, C. De, Iudicone, D., Sullivan, M.B., Raes, J., Karsenti, E., Bowler, C., and Gorsky, G. (2016) Plankton networks driving carbon export in the oligotrophic ocean. *Nature* **532**: 465–470.

Guindon, S., and Gascuel, O. (2003) A simple, fast, and accurate algorithm to estimate large phylogenies by maximum likelihood. *Syst Biol* **52**: 696–704.

Guntupalli, R., Sorokulova, I., Olsen, E., Globa, L., Pustovyy, O., Moore, T., Chin, B., Barbaree, J., and Vodyanoy, V. (2012) Detection and identification of methicillin resistant and sensitive strains of Staphylococcus aureus using tandem measurements. *J Microbiol Methods* **90**: 182–191.

Guttman, B., Raya, R., and Kutter, E. (2005) Basic phage biology. In *Bacteriophages: Biology and Applications*. Kutter, E., and Sulakvelidze, A. (eds). CRC Press, Boca Raton, FL. p. 39.

Gvozdyak, R.I. (1993) Plant, phage, bacterium: a new hypothesis on their interrelation. *Mikrobiol Zh* **55**: 92–94.

Hadas, H., Einav, M., Fishov, I., and Zaritsky, A. (1997) Bacteriophage T4 development depends on the physiology of its host Escherichia coli. *Microbiology* **143**: 179–185.

Haft, D.H., Selengut, J., Mongodin, E.F., and Nelson, K.E. (2005) A guild of 45 CRISPR-associated (Cas) protein families and multiple CRISPR/Cas subtypes exist in prokaryotic genomes. *PLoS Comput Biol* **1**: e60.

Haichar, F. el Z., Marol, C., Berge, O., Rangel-Castro, J.I., Prosser, J.I., Balesdent, J., Heulin, T., and Achouak, W. (2008) Plant host habitat and root exudates shape soil bacterial community structure. *ISME J* **2**: 1221–1230.

Hall, B.G., Acar, H., Nandipati, A., and Barlow, M. (2014) Growth rates made easy. *Mol Biol Evol* **31**: 232–238.

Hall, C.J.J. Van (1902) Bijdragen tot de kennis der bakteriele plantenziekten (in Dutch). .

Hammad, A. m. m. (1998) Evaluation of alginate-encapsulated Azotobacter chroococcum as a phage-resistant and an effective inoculum. *J Basic Microbiol* **38**: 9–16.

Han, J.-H., Wang, M.S., Das, J., Sudheendra, L., Vonasek, E., Nitin, N., and Kennedy, I.M. (2014) Capture and detection of T7 bacteriophages on a nanostructured interface. *ACS Appl Mater Interfaces* **6**: 4758–4765.

Han, M. V, and Zmasek, C.M. (2009) phyloXML: XML for evolutionary biology and comparative genomics. *BMC Bioinformatics* **10**: 356.

Hanemann, T., and Szabó, D.V. (2010) Polymer-nanoparticle composites: from synthesis to modern applications. *Materials (Basel)* **3**: 3468–3517.

Hansen, A.M., Qiu, Y., Yeh, N., Blattner, F.R., Durfee, T., and Jin, D.J.

(2005) SspA is required for acid resistance in stationary phase by downregulation of H-NS in Escherichia coli. *Mol Microbiol* **56**: 719–34.

Hardoim, P.R., Overbeek, L.S. van, and Elsas, J.D. (2008) Properties of bacterial endophytes and their proposed role in plant growth. *Trends Microbiol* **16**: 463–471.

Harris, R.I. (1979) Chemical control of bacterial soft rot of wounded potato tubers. *Potato Res* **22**: 245–249.

Harrison, B.D., Barker, H., Bock, K.R., Guthrie, E.J., Meredith, G., and Atkinson, M. (1977) Plant viruses with circular single-stranded DNA. *Nature* **270**: 760–762.

Harvey, R.W., and Ryan, J.N. (2004) Use of PRD1 bacteriophage in groundwater viral transport, inactivation, and attachment studies. *FEMS Microbiol Ecol* **49**: 3–16.

Hatfull, G.F. (2008) Bacteriophage genomics. *Curr Opin Microbiol* **11**: 447–453.

Hauben, L., Moore, E.R.B., Vauterin, L., Steenackers, M., Mergaert, J., Verdonck, L., and Swings, J. (1998) Phylogenetic position of phytopathogens within the Enterobacteriaceae. *Syst Appl Microbiol* **21**: 384–397.

Hawkins, C., Harper, D., Burch, D., Änggård, E., and Soothill, J. (2010) Topical treatment of Pseudomonas aeruginosa otitis of dogs with a bacteriophage mixture: a before/after clinical trial. *Vet Microbiol* **146**: 309–13.

Hazan, R., and Engelberg-Kulka, H. (2004) Escherichia coli mazEF-mediated cell death as a defense mechanism that inhibits the spread of phage P1. *Mol Genet Genomics* **272**: 227–234.

He, S.Y., Lindeberg, M., Chatterjee, A.K., and Collmer, A. (1991) Cloned Erwinia chrysanthemi out genes enable Escherichia coli to selectively secrete a diverse family of heterologous proteins to its milieu. *Proc Natl Acad Sci U S A* **88**: 1079–1083.

Heden, C.G. (1951) Studies of the infection of E. coli B with the bacteriophage T2. *Acta Pathol Microbiol Scand Suppl* **88**: 1–121.

Hemminga, M.A., Vos, W.L., Nazarov, P. V., Koehorst, R.B.M., Wolfs, C.J.A.M., Spruijt, R.B., and Stopar, D. (2010) Viruses: incredible nanomachines. New advances with filamentous phages. *Eur Biophys J* **39**: 541–550.

Hendrix, R.W. (1999) Evolution: the long evolutionary reach of viruses. *Curr Biol* **9**: R914–R917.

Hendrix, R.W., Hatfull, G.F., and Smith, M.C.M. (2003) Bacteriophages with tails: chasing their origins and evolution. *Res Microbiol* 154.

Hendrix, R.W., Lawrence, J.G., Hatfull, G.F., and Casjens, S. (2000) The origins and ongoing evolution of viruses. *Trends Microbiol* 8.

Hendrix, R.W., Smith, M.C.M., Burns, R.N., Ford, M.E., and Hatfull, G.F. (1999) Evolutionary relationships among diverse bacteriophages and prophages: all the world's a phage. *Proc Natl Acad Sci* **96**: 2192–2197.

Henke, J.M., and Bassler, B.L. (2004a) Three parallel quorum-sensing systems regulate gene expression in Vibrio harveyi. *J Bacteriol* **186**: 6902–6914.

Henke, J.M., and Bassler, B.L. (2004b) Quorum sensing regulates type III secretion in Vibrio harveyi and Vibrio parahaemolyticus. *J Bacteriol* **186**: 3794–3805.

Heyse, S., Hanna, L.F., Woolston, J., Sulakvelidze, A., and Charbonneau, D. (2015) Bacteriophage cocktail for biocontrol of Salmonella in dried pet food. *J Food Prot* **78**: 97–103.

Hibma, A.M., Jassim, S.A.A., and Griffiths, M.W. (1997) Infection and removal of L-forms of Listeria monocytogenes with bred bacteriophage. *Int J Food Microbiol* **34**: 197–207.

Hirata, H., Kashihara, M., Horiike, T., Suzuki, T., Dohra, H., Netsu, O., and Tsuyumu, S. (2016a) Genome sequence of Pectobacterium carotovorum phage PPWS1, isolated from Japanese horseradish (Eutrema japonicum) showing soft-rot symptoms. *Genome Announc* **4**: e01625-15.

Hirata, H., Kashihara, M., Horiike, T., Suzuki, T., Dohra, H., Netsu, O., and Tsuyumu, S. (2016b) Genome sequence of Pectobacterium carotovorum phage PPWS1, isolated from Japanese horseradish [Eutrema japonicum (Miq.) Koidz] showing soft-rot symptoms. *Genome Announc* **4**: e01625-15.

Horgan, M., O'Sullivan, O., Coffey, A., Fitzgerald, G.F., Sinderen, D. van, McAuliffe, O., and Ross, R.P. (2010) Genome analysis of the Clostridium difficile phage ΦCD6356, a temperate phage of the Siphoviridae family. *Gene* **462**: 34–43.

Horikawa, S., Bedi, D., Li, S., Shen, W., Huang, S., Chen, I.H., Chai, Y., Auad, M.L., Bozack, M.J., Barbaree, J.M., Petrenko, V.A., and Chin, B.A. (2011) Effects of surface functionalization on the surface phage coverage and the subsequent performance of phage-immobilized magnetoelastic biosensors. *Biosens Bioelectron* **26**: 2361–2367.

Hosseinidoust, Z., Alam, M.N., Sim, G., Tufenkji, N., and Ven, T.G.M. Van De (2015) Cellulose nanocrystals with tunable surface charge for nanomedicine. *Nanoscale* **7**: 16647–57.

Hosseinidoust, Z., Olsson, A.L.J., and Tufenkji, N. (2014) Going viral: designing bioactive surfaces with bacteriophage. *Colloids Surfaces B Biointerfaces* **124**: 2–16.

Hosseinidoust, Z., Ven, T.G.M. Van De, and Tufenkji, N. (2011) Bacterial capture efficiency and antimicrobial activity of phage-functionalized model surfaces. *Langmuir* **27**: 5472–80.

Howard-Varona, C., Hargreaves, K.R., Abedon, S.T., and Sullivan, M.B. (2017) Lysogeny in nature: mechanisms, impact and ecology of temperate phages. *ISME J* **11**: 1510–1520.

Hu, B., Margolin, W., Molineux, I.J., and Liu, J. (2013) The bacteriophage T7 virion undergoes extensive structural remodeling during infection. *Sci* **339**: 576–579.

Huang, G., Le, S., Peng, Y., Zhao, Y., Yin, S., Zhang, L., Yao, X., Tan, Y., Li, M., and Hu, F. (2013) Characterization and genome sequencing of phage Abp1, a new phiKMV-like virus infecting multidrug-resistant Acinetobacter baumannii. *Curr Microbiol* **66**: 535–543.

Hugenholtz, P., Goebel, B.M., and Pace, N.R. (1998) Impact of culture-independent studies on the emerging phylogenetic view of bacterial diversity (Journal of Bacteriology (1998) 180:18 (4765-4774)). *J Bacteriol* **180**: 4765–4774.

Hurst, C.J., Gerba, C.P., and Cech, I. (1980) Effects of environmental variables and soil characteristics on virus survival in soil. *Appl Environ Microbiol* **40**: 1067–1079.

Hurwitz, B.L., and U'Ren, J.M. (2016) Viral metabolic reprogramming in marine ecosystems. *Curr Opin Microbiol* 31.

Hutter, B., and John, G.T. (2004) Evaluation of OxoPlate for real-time assessment of antibacterial activities. *Curr Microbiol* **48**: 57–61.

Hyman, P. (2012) Bacteriophages and nanostructured materials. *Adv Appl Microbiol* **78**: 55–73.

Hyman, P., and Abedon, S.T. (2009) Practical methods for determining phage growth parameters. *Methods Mol Biol* **501**: 175–202.

Hyman, P., and Abedon, S.T. (2010) Bacteriophage host range and bacterial resistance. *Adv Appl Microbiol* 70.

Icho, T., and Iino, T. (1978) Isolation and characterization of motile Escherichia coli mutants resistant to bacteriophage chi. *J Bacteriol* **134**: 854–860.

Inouye, M., Arnheim, N., and Sternglanz, R. (1973) Bacteriophage T7 lysozyme is an N-acetylmuramyl-L-alanine amidase. *J Biol Chem* **248**: 7247–52.

Iravani, S., Korbekandi, H., Mirmohammadi, S.V., and Zolfaghari, B. (2014) Synthesis of silver nanoparticles : chemical , physical and biological methods. *Res Pharm Sci* **9**: 385–406.

Iriarte, F.B., Balogh, B., Momol, M.T., Smith, L.M., Wilson, M., and Jones, J.B. (2007) Factors affecting survival of bacteriophage on tomato leaf surfaces. *Appl Env Microbiol* **73**: 1704–1711.

Iriarte, F.B., Obradović, A., Wernsing, M.H., Jackson, L.E., Balogh, B., Hong, J.A., Momol, M.T., Jones, J.B., and Vallad, G.E. (2012) Soil-based systemic delivery and phyllosphere in vivo propagation of bacteriophages: two possible strategies for improving bacteriophage persistence for plant disease control. *Bacteriophage* **2**: 215–224.

Jafra, S., Jalink, H., Schoor, R. van der, and Wolf, J.M. van der (2006) Pectobacterium carotovorum subsp. carotovorum strains show diversity in production of and response to N-acyl homoserine lactones. *J Phytopathol* **154**: 729–739.

Jafra, S., Przysowa, J., Czajkowski, R., Michta, A., Garbeva, P., and Wolf, J.M. van der (2006) Detection and characterization of bacteria from the potato rhizosphere degrading N-acyl-homoserine lactone. *Can J Microbiol* **52**: 1006–1015.

Jain, A., and Jain, S.K. (2008) PEGylation: an approach for drug delivery. A review. *Crit Rev Ther Drug Carr Syst* **25**: 403–407.

Janulaitis, A., Petrusyte, M., Maneliene, Z., Klimasauskas, S., and Butkus, V. (1992) Purification and properties of the Eco57I restriction endonuclease and methylase--prototypes of a new class (type IV). *Nucleic Acids Res* **20**: 6043–6049.

Jeltsch, A., and Pingoud, A. (1996) Horizontal gene transfer contributes to the wide distribution and evolution of type II restriction-modification systems. *J Mol Evol* **42**: 91–96.

Johnson, K. (1994) Dose-response relationships and inundative biological control. *Phytopathology* **84**: 780–784.

Johnston-Monje, D., Mousa, W.K., Lazarovits, G., and Raizada, M.N. (2014) Impact of swapping soils on the endophytic bacterial communities of pre-domesticated, ancient and modern maize. *BMC Plant Biol* **14**: 233.

Jones, A.L., and Schnabel, E.L. (2000) The development of streptomycin-resistant strains of Erwinia amylovora. In *Fire blight: the disease and its causative agent, Erwinia amylovora.* Vanneste, J.L. (ed.). CAB International, Wallingford, UK. pp. 235–25.

Jones, D.L., Nguyen, C., and Finlay, R.D. (2009) Carbon flow in the rhizosphere: carbon trading at the soil root interface. *Plant Soil* **321**: 5–33.

Jones, J.B., Jackson, L.E., Balogh, B., Obradović, A., Iriarte, F.B., and Momol, M.T. (2007) Bacteriophages for plant disease control. *Annu Rev Phytopathol* **45**: 245–62.

Jones, J.B., Vallad, G.E., Iriarte, F.B., Obradović, A., Wernsing, M.H., Jackson, L.E., Balogh, B., Hong, J.C., and Momol, M.T. (2012) Considerations for using bacteriophages for plant disease control. *Bacteriophage* **2**: 208–214.

Jones, L.R. (1901) A soft rot of carrot and other vegetables caused by Bacillus carotovora. *Vt Agric Exp Stat Ann Rept* **13**: 299–332.

Jones, P., Binns, D., Chang, H.-Y., Fraser, M., Li, W., McAnulla, C., McWilliam, H., Maslen, J., Mitchell, A., Nuka, G., Pesseat, S., Quinn, A.F., Sangrador-Vegas, A., Scheremetjew, M., Yong, S.-Y., Lopez, R., and Hunter, S. (2014) InterProScan 5: genome-scale protein function classification. *Bioinformatics* **30**: 1236–1240.

Jover, L.F., Cortez, M.H., and Weitz, J.S. (2013) Mechanisms of multi-strain coexistence in host-phage systems with nested infection networks. *J Theor Biol* **332**: 65–77.

Jun, J.W., Giri, S.S., Kim, H.J., Yun, S.K., Chi, C., Chai, J.Y., Lee, B.C., and Park, S.C. (2016) Bacteriophage application to control the contaminated water with Shigella. *Sci Rep* **6**: 22636.

Jutz, G., and Böker, A. (2011) Bionanoparticles as functional macromolecular building blocks – A new class of nanomaterials. *Polymer (Guildf)* **52**: 211–232.

Kalischuk, M., Hachey, J., and Kawchuk, L. (2015) Complete genome sequence of phytopathogenic Pectobacterium atrosepticum bacteriophage Peat1. *Genome Announc* **3**: e00760-15.

Kang, J.E., Han, J.W., Jeon, B.J., and Kim, B.S. (2016) Efficacies of quorum sensing inhibitors, piericidin A and glucopiericidin A, produced by Streptomyces xanthocidicus KPP01532 for the control of potato soft rot caused by Erwinia carotovora subsp. atroseptica. *Microbiol Res* **184**: 32–41.

Kang, Y.R., Hwang, K.H., Kim, J.H., Nam, C.H., and Kim, S.W. (2010) Disposable amperometric biosensor based on nanostructured bacteriophages for glucose detection. *Meas Sci Technol* **21**: 105804.

Kango, S., Kalia, S., Celli, A., Njuguna, J., Habibi, Y., and Kumar, R. (2013) Surface modification of inorganic nanoparticles for development of organic-inorganic nanocomposites-a review. *Elsevier Prog Polym Sci* **38**: 1232–1261.

Karlovsky, P. (2008) *Secondary metabolites in soil ecology*. 1st ed., Springer-Verlag, Berlin Heidelberg, Germany.

Kasman, L.M., Kasman, A., Westwater, C., Dolan, J., Schmidt, M.G., and Norris, J.S. (2002) Overcoming the phage replication threshold: a mathematical model with implications for phage therapy. *J Virol* **76**: 5557–64.

Kastelein, P., Schepel, E., Mulder, A., Turkensteen, L., and Vuurde, J. Van

(1999) Preliminary selection of antagonists of Erwinia carotovora subsp. atroseptica (Van Hall) Dye for application during green crop lifting of seed potato tubers. *Potato Res* **42**: 161–171.

Katoh, K., Rozewicki, J., and Yamada, K.D. (2017) MAFFT online service: multiple sequence alignment, interactive sequence choice and visualization. *Brief Bioinform* .

Katoh, K., and Standley, D.M. (2013) MAFFT multiple sequence alignment software version 7: improvements in performance and usability. *Mol Biol Evol* **30**: 772–780.

Kemp, P., Garcia, L.R., and Molineux, I.J. (2005) Changes in bacteriophage T7 virion structure at the initiation of infection. *Virology* **340**: 307–317.

Kemp, P., Gupta, M., and Molineux, I.J. (2004) Bacteriophage T7 DNA ejection into cells is initiated by an enzyme-like mechanism. *Mol Microbiol* **53**: 1251–1265.

Kerkeni, A., Behary, N., Dhulster, P., Chihib, N.E., and Perwuelz, A. (2013) Study on the effect of plasma treatment of woven polyester fabrics with respect to nisin adsorption and antibacterial activity. *J Appl Polym Sci* **129**: 866–873.

Khan, Z., Guelich, G., Phan, H., Redman, R., and Doty, S. (2012) Bacterial and yeast endophytes from poplar and willow promote growth in crop plants and grasses. *ISRN Agron* **2012**: 11.

Khayi, S., Cigna, J., Chong, T.M., Quêtu-Laurent, A., Chan, K.G., Helias, V., and Faure, D. (2016) Transfer of the potato plant isolates of Pectobacterium wasabiae to pectobacterium parmentieri sp. nov. *Int J Syst Evol Microbiol* **66**: 5379–5383.

Kim, A., Davis, R., and Higuchi, M. (2015) Intracellular oxygen determined by respiration regulates localization of Ras and prenylated proteins. *Cell Death Dis* **6**: e1825–e1825.

Kim, H.J., Boedicker, J.Q., Choi, J.W., and Ismagilov, R.F. (2008) Defined spatial structure stabilizes a synthetic multispecies bacterial community. *Proc Natl Acad Sci U S A* **105**: 18188–93.

Kim, Y., Wang, X., Ma, Q., Zhang, X.S., and Wood, T.K. (2009) Toxin-antitoxin systems in Escherichia coli influence biofilm formation through YjgK (TabA) and fimbriae. *J Bacteriol* **191**: 1258–1267.

Kimura, M., Jia, Z.J., Nakayama, N., and Asakawa, S. (2008) Ecology of viruses in soils: past, present and future perspectives. *Soil Sci Plant Nutr* **54**: 1–32.

Klimuk, E., Akulenko, N., Makarova, K.S., Ceyssens, P.J., Volchenkov, I., Lavigne, R., and Severinov, K. (2013) Host RNA polymerase inhibitors

encoded by φKMV-like phages of pseudomonas. *Virology* **436**: 67–74.

Klumpp, J., Fouts, D.E., and Sozhamannan, S. (2012) Next generation sequencing technologies and the changing landscape of phage genomics. *Bacteriophage* **2**: 190–199.

Klumpp, J., Fouts, D.E., and Sozhamannan, S. (2013) Bacteriophage functional genomics and its role in bacterial pathogen detection. *Brief Funct Genomics* **12**: 354–365.

Knezevic, P., Obreht, D., Curcin, S., Petrusic, M., Aleksic, V., Kostanjsek, R., and Petrovic, O. (2011) Phages of Pseudomonas aeruginosa: response to environmental factors and in vitro ability to inhibit bacterial growth and biofilm formation. *J Appl Microbiol* **111**: 245–54.

Koch, a L. (1964) The growth of viral plaques during the enlargement phase. *J Theor Biol* **6**: 413–431.

Kocharunchitt, C., Ross, T., and McNeil, D.L. (2009) Use of bacteriophages as biocontrol agents to control Salmonella associated with seed sprouts. *Int J Food Microbiol* **128**: 453–459.

Koga, M., Otsuka, Y., Lemire, S., and Yonesaki, T. (2011) Escherichia coli rnlA and rnlB compose a novel toxin-antitoxin system. *Genetics* **187**: 123–130.

Kõiv, V., and Mäe, a (2001) Quorum sensing controls the synthesis of virulence factors by modulating rsmA gene expression in Erwinia carotovora subsp. carotovora. *Mol Genet genomics* **265**: 287–292.

Kokjohn, T.A., and Miller, R.V. (1992) Gene transfer in the environment: transduction. In *Release of Genetically Engineered and Other Micro-Organisms*. Fry, J.C., and Day, M.J. (eds). Cambridge University Press, Cambridge. p. 5481.

Konishi, Y., Ohno, K., Saitoh, N., Nomura, T., Nagamine, S., Hishida, H., Takahashi, Y., and Uruga, T. (2007) Bioreductive deposition of platinum nanoparticles on the bacterium Shewanella algae. *J Biotechnol* **128**: 648–653.

Koskella, B., and Meaden, S. (2013) Understanding bacteriophage specificity in natural microbial communities. *Viruses* **5**: 806–823.

Kosturko, L.D., Hogan, M., and Dattagupta, N. (1979) Structure of DNA within three isometric bacteriophages. *Cell* **16**: 515–22.

Kot, W., Vogensen, F.K., Sørensen, S.J., and Hansen, L.H. (2014) DPS - a rapid method for genome sequencing of DNA-containing bacteriophages directly from a single plaque. *J Virol Methods* **196**: 152–156.

Krisch, H.M., Hamlett, N. V., and Berger, H. (1972) Polynucleotide ligase in bacteriophage T4D recombination. *Genetics* **72**: 187–203.

Kropinski, A.M. (2009) Measurement of the rate of attachment of bacteriophage to cells. *Methods Mol Biol* **501**: 151–155.

Krueger, A.P. (1931) The sorption of bacteriophage by living and dead susceptible bacteria: I. Equilibrium conditions. *J Gen Physiol* **14**: 493–516.

Krumsiek, J., Arnold, R., and Rattei, T. (2007) Gepard: a rapid and sensitive tool for creating dotplots on genome scale. *Bioinformatics* **23**: 1026–1028.

Ktari, T., Baccar, H., Mejri, M.B., and Abdelghani, A. (2012) Calibration of surface plasmon resonance imager for biochemical detection. *Int J Electrochem* **2012**: 1–5.

Kulakauskas, S., Lubys, A., and Ehrlich, S.D. (1995) DNA restriction-modification systems mediate plasmid maintenance. *J Bacteriol* **177**: 3451–3454.

Kumar, A., Pundhir, V.S., and Gupta, K.C. (1991) The role of phenols in potato tuber resistance against soft rot by Erwinia carotovora ssp. carotovora. *Potato Res* **34**: 9–16.

Kumarasamy, K.K., Toleman, M.A., Walsh, T.R., Bagaria, J., Butt, F., Balakrishnan, R., Chaudhary, U., Doumith, M., Giske, C.G., Irfan, S., Krishnan, P., Kumar, A. V, Maharjan, S., Mushtaq, S., Noorie, T., Paterson, D.L., Pearson, A., Perry, C., Pike, R., Rao, B., Ray, U., Sarma, J.B., Sharma, M., Sheridan, E., Thirunarayan, M.A., Turton, J., Upadhyay, S., Warner, M., Welfare, W., Livermore, D.M., and Woodford, N. (2010) Emergence of a new antibiotic resistance mechanism in India, Pakistan, and the UK: a molecular, biological, and epidemiological study. *Lancet Infect Dis* **10**: 597–602.

Kuraku, S., Zmasek, C.M., Nishimura, O., and Katoh, K. (2013) aLeaves facilitates on-demand exploration of metazoan gene family trees on MAFFT sequence alignment server with enhanced interactivity. *Nucleic Acids Res* **41**: W22–W28.

Kutter, E.. M. (1968) The roles of 5-hydroxymethylcytosine in the DNA of bacteriophage T4, as revealed by mutants defective in genes 56, 46, and 47. .

Kutter, E. (2009) Phage host range and efficiency of plating. *Methods Mol Biol* **501**: 141–149.

Kutter, E., Bryan, D., Ray, G., Brewster, E., Blasdel, B., and Guttman, B. (2018) From host to phage metabolism: hot tales of phage T4's takeover of E. coli. *Viruses* **10**: 387.

Kutter, E., and Guttman, B. (2001) T Phages. In *Encyclopedia of Genetics*. Brenner, S., and Miller, J. (eds). Elsevier, pp. 1921–1930.

Kutter, E., Kellenberger, E., Carlson, K., Eddy, S. Neitel, J., Messinger, L., North, J., and Guttman, B. (1994) Effects of bacterial growth conditions and

physiology on T4 infection. In *Molecular Biology of Bacteriophage T4*. Karam, J.D. (ed.). ASM Press , Washington D. C., USA. pp. 406–418.

Kutter E. M., White T., and Kashlev M. (1994) *Effects on host genome structure and expression*. American Society of Microbiology, Washington DC.

Kutter, E., and Sulakvelidze, A. (2004) *Bacteriophages: biology and applications*. 1st ed., CRC Press, Boca Raton, Florida, USA.

Kwan, T., Liu, J., DuBow, M., Gros, P., and Pelletier, J. (2006) Comparative genomic analysis of 18 Pseudomonas aeruginosa bacteriophages. *J Bacteriol* **188**: 1184–1187.

Laasik, E., Andresen, L., and Mäe, A. (2006) Type II quorum sensing regulates virulence in Erwinia carotovora ssp. carotovora. *FEMS Microbiol Lett* **258**: 227–234.

Labrie, S.J., Samson, J.E., and Moineau, S. (2010) Bacteriophage resistance mechanisms. *Nat Rev Microbiol* **8**: 317–327.

Lagerwall, J.P., Schütz, C., Salajkova, M., Noh, J., Park, J.H., Scalia, G., and Bergström, L. (2014) Cellulose nanocrystal-based materials: from liquid crystal self-assembly and glass formation to multifunctional thin films. *NPG Asia Mater* **6**: 80.

Lammens, E., Ceyssens, P.-J., Voet, M., Hertveldt, K., Lavigne, R., and Volckaert, G. (2009) Representational difference analysis (RDA) of bacteriophage genomes. *J Microbiol Methods* **77**: 207–213.

Landsberger, M., Gandon, S., Meaden, S., Buckling, A., Westra, E.R., Van, S., Correspondence, H., Rollie, C., Chevallereau, A., Lè Ne Chabas, H., and Houte, S. Van (2018) Anti-CRISPR phages cooperate to overcome CRISPR-Cas immunity. *Cell* **174**: 908–916.

Lane, D.J., Pace, B., Olsen, G.J., Stahl, D.A., Sogin, M.L., and Pace, N.R. (1985) Rapid determination of 16S ribosomal RNA sequences for phylogenetic analyses. *Proc Natl Acad Sci U S A* **82**: 6955–6959.

Lapwood, D.H., Read, P.J., and Spokes, J. (1984) Methods for assessing the susceptibility of potato tubers of different cultivars to rotting by Erwinia carotovora subspecies atroseptica and carotovora. *Plant Pathol* **33**: 13–20.

Laslett, D., and Canback, B. (2004) ARAGORN, a program to detect tRNA genes and tmRNA genes in nucleotide sequences. *Nucleic Acids Res* **32**: 11–16.

Lavigne, R., Darius, P., Summer, E.J., Seto, D., Mahadevan, P., Nilsson, A.S., Ackermann, H.W., and Kropinski, A.M. (2009) Classification of myoviridae bacteriophages using protein sequence similarity. *BMC Microbiol* **9**: 224.

Lavigne, R., Noben, J.-P., Hertveldt, K., Ceyssens, P.-J., Briers, Y., Dumont,

D., Roucourt, B., Krylov, V.N., Mesyanzhinov, V. V, Robben, J., and Volckaert, G. (2006) The structural proteome of Pseudomonas aeruginosa bacteriophage KMV. *Microbiology* **152**: 529–534.

Lavigne, R., Seto, D., Mahadevan, P., Ackermann, H.W., and Kropinski, A.M. (2008) Unifying classical and molecular taxonomic classification: analysis of the Podoviridae using BLASTP-based tools. *Res Microbiol* **159**: 406–414.

Lawrence, J.G., Hatfull, G.F., and Hendrix, R.W. (2002) Imbroglios of viral taxonomy: genetic exchange and failings of phenetic approaches. *J Bacteriol* **184**: 4891–905.

Le, S., He, X., Tan, Y., Huang, G., Zhang, L., Lux, R., Shi, W., and Hu, F. (2013) Mapping the tail fiber as the receptor binding protein responsible for differential host specificity of Pseudomonas aeruginosa bacteriophages PaP1 and JG004. *PLoS One* **8**: e68562.

Lebeis, S.L., Paredes, S.H., Lundberg, D.S., Breakfield, N., Gehring, J., McDonald, M., Malfatti, S., Rio, T.G. del, Jones, C.D., Tringe, S.G., and Dangl, J.L. (2015) Salicylic acid modulates colonization of the root microbiome by specific bacterial taxa. *Science (80-)* **349**: 860–864.

Lee, J.-H., Shin, H., Ji, S., Malhotra, S., Kumar, M., Ryu, S., and Heu, S. (2012) Complete genome sequence of phytopathogenic Pectobacterium carotovorum subsp. carotovorum bacteriophage PP1. *J Virol* **86**: 8899–8900.

Lee, J., Chastain, P.D., Kusakabe, T., Griffith, J.D., and Richardson, C.C. (1998) Coordinated leading and lagging strand DNA synthesis on a minicircular template. *Mol Cell* **1**: 1001–10.

Lee, S.-J., and Richardson, C.C. (2011) Choreography of bacteriophage T7 DNA replication. *Curr Opin Chem Biol* **15**: 580–586.

Lefort, V., Desper, R., and Gascuel, O. (2015) FastME 2.0: a comprehensive, accurate, and fast distance-based phylogeny inference program. *Mol Biol Evol* **32**: 2798–800.

Lehman, S.M. (2007) Development of a bacteriophage-based biopesticide for fire blight. .

Lehnherr, H., and Yarmolinsky, M.B. (1995) Addiction protein Phd of plasmid prophage P1 is a substrate of the ClpXP serine protease of Escherichia coli. *Proc Natl Acad Sci U S A* **92**: 3274–3277.

Leibo, S.P., and Mazur, P. (1966) Effect of osmotic shock and low salt concentration on survival and density of bacteriophages T4B and T4Bo1. *Biophys J* **6**: 747–772.

Leiman, P.G., Chipman, P.R., Kostyuchenko, V.A., Mesyanzhinov, V. V., and Rossmann, M.G. (2004) Three-dimensional rearrangement of proteins in the tail of bacteriophage T4 on infection of its host. *Cell* **118**: 419–429.

Lelie, D. van der, Taghavi, S., Monchy, S., Schwender, J., Miller, L., Ferrieri, R., Rogers, A., Wu, X., Zhu, W., Weyens, N., Vangronsveld, J., and Newman, L. (2009) Poplar and its bacterial endophytes: coexistence and harmony. *Crit Rev Plant Sci* **28**: 346–358.

Lennon, J.T., Khatana, S.A.M., Marston, M.F., and Martiny, J.B.H. (2007) Is there a cost of virus resistance in marine cyanobacteria? *ISME J* **1**: 300–312.

Lenski, R.E., and Levin, B.R. (1985) Constraints on the coevolution of bacteria and virulent phage: a model, some experiments, and predictions for natural communities. *Am Nat* **125**: 585–602.

Leon-Velarde, C.G., Kropinski, A.M., Chen, S., Abbasifar, A., Griffiths, M.W., and Odumeru, J.A. (2014) Complete genome sequence of bacteriophage vB_YenP_AP5 which infects Yersinia enterocolitica of serotype O:3. *Virol J* **11**: 188.

Leonardopoulos, J., Papaconstantinou, A., and Georgakopoulou-Papandreou, E. (1996) The meaning of soil characteristics and temperature for the survival of bacteriophages in naturally contaminated soil samples. *Acta Microbiol Hell* **41**: 309–316.

Lepikhov, K., Tchernov, A., Zheleznaja, L., Matvienko, N., Walter, J., and Trautner, T.A. (2001) Characterization of the type IV restriction modification system BspLU11III from Bacillus sp . LU11. *Nucleic Acids Res* **29**: 4691–4698.

Letellier, L., Boulanger, P., Plancon, L., Jacquot, P., and Santamaria, M. (2004) Main features on tailed phage, host recognition and DNA uptake. *Front Biosci* **9**: 1228–1339.

Leverentz, B., Conway, W.S., Alavidze, Z., Janisiewicz, W.J., Fuchs, Y., Camp, M.J., Chighladze, E., and Sulakvelidze, A. (2001) Examination of bacteriophage as a biocontrol method for Salmonella on fresh-cut fruit: a model study. *J Food Prot* **64**: 1116–1121.

Leverentz, B., Conway, W.S., Alavidze, Z., Janisiewicz, W.J., Fuchs, Y., Camp, M.J., Chihiladze, E., and Sulakvelidze, A. (2001) Examination of bacteriophage as a biocontrol method for Salmonella on fresh-cut fruit: a model study. *J Food Prot* **64**: 1116–21.

Leverentz, B., Conway, W.S., Camp, M.J., Janisiewicz, W.J., Abuladze, T., Yang, M., Saftner, R., and Sulakvelidze, A. (2003) Biocontrol of Listeria monocytogenes on fresh-cut produce by treatment with lytic bacteriophages and a bacteriocin. *Appl Environ Microbiol* **69**: 4519–4526.

Leverentz, B., Janisiewica, W., and Conway, W.S. (2003) Biological control of minimally processed fruit and vegetables. In *Microbial safety of minimally processed foods*. Juneja, V.K., Sapers, G.M., and Novak, J.S. (eds). CRC Press, Boca Raton, Fla. pp. 319–332.

Levin, B.R., and Bull, J.J. (2004) Population and evolutionary dynamics of phage therapy. *Nat Rev Microbiol* **2**: 166–173.

Li, R., Stapon, A., and Townsend, C.A. (2000) Three unusual reactions mediate carbapenem and carbapenam biosynthesis. *J Am Chem Soc* **122**: 9296–9297.

Li, S., Fan, H., An, X., Fan, H., Jiang, H., Chen, Y., and Tong, Y. (2014) Scrutinizing virus genome termini by high-throughput sequencing. *PLoS One* **9**: e85806.

Lim, E.S., Zhou, Y., Zhao, G., Bauer, I.K., Droit, L., Ndao, I.M., Warner, B.B., Tarr, P.I., Wang, D., and Holtz, L.R. (2015) Early life dynamics of the human gut virome and bacterial microbiome in infants. *Nat Med* **21**: 1228–1234.

Lim, J.A., Heu, S., Park, J., and Roh, E. (2017) Genomic characterization of bacteriophage vB_PcaP_PP2 infecting Pectobacterium carotovorum subsp. carotovorum, a new member of a proposed genus in the subfamily Autographivirinae. *Arch Virol* **162**: 2441–2444.

Lim, J.A., Jee, S., Lee, D.H., Roh, E., Jung, K., Oh, C., and Heu, S. (2013) Biocontrol of Pectobacterium carotovorum subsp. carotovorum using bacteriophage PP1. *J Microbiol Biotechnol* **23**: 1147–1153.

Lim, J.A., Shin, H., Lee, D.H., Han, S.W., Lee, J.H., Ryu, S., and Heu, S. (2014) Complete genome sequence of the Pectobacterium carotovorum subsp. carotovorum virulent bacteriophage PM1. *Arch Virol* **159**: 2185–2187.

Lin, T.-L., Hsieh, P.-F., Huang, Y.-T., Lee, W.-C., Tsai, Y.-T., Su, P.-A., Pan, Y.-J., Hsu, C.-R., Wu, M.-C., and Wang, J.-T. (2014) Isolation of a bacteriophage and its depolymerase specific for K1 capsule of Klebsiella pneumoniae: implication in typing and treatment. *J Infect Dis* **210**: 1734–1744.

Lin, T.-Y., Lo, Y.-H., Tseng, P.-W., Chang, S.-F., Lin, Y.-T., and Chen, T.-S. (2012) A T3 and T7 recombinant phage acquires efficient adsorption and a broader host range. *PLoS One* **7**: e30954.

Lindberg, A.A. (1973) Bacteriophage receptors. *Annu Rev Microbiol* **27**: 205–241.

Lindell, D., Jaffe, J.D., Coleman, M.L., Futschik, M.E., Axmann, I.M., Rector, T., Kettler, G., Sullivan, M.B., Steen, R., Hess, W.R., Church, G.M., and Chisholm, S.W. (2007) Genome-wide expression dynamics of a marine virus and host reveal features of co-evolution. *Nature* **449**: 83–86.

Lingohr, E.J., Villegas, A., She, Y.-M., Ceyssens, P.-J., and Kropinski, A.M. (2008) The genome and proteome of the Kluyvera bacteriophage Kvp1 – another member of the T7-like Autographivirinae. *Virol J* **5**: 122.

Linkov, I., Steevens, J., Adlakha-Hutcheon, G., Bennett, E., Chappell, M.,

Colvin, V., Davis, J.M., Davis, T., Elder, A., Foss Hansen, S., Hakkinen, P.B., Hussain, S.M., Karkan, D., Korenstein, R., Lynch, I., Metcalfe, C., Ramadan, A.B., and Satterstrom, F.K. (2009) Emerging methods and tools for environmental risk assessment, decision-making, and policy for nanomaterials: summary of NATO Advanced Research Workshop. *J Nanoparticle Res* **11**: 513–527.

Liu, C.-Y., and Bard, A.J. (2009) Electrostatic electrochemistry: nylon and polyethylene systems. *Chem Phys Lett* **485**: 231–234.

Liu, H., Coulthurst, S.J., Pritchard, L., Hedley, P.E., Ravensdale, M., Humphris, S., Burr, T., Takle, G., Brurberg, M.B., Birch, P.R.J., Salmond, G.P.C., and Toth, I.K. (2008) Quorum sensing coordinates brute force and stealth modes of infection in the plant pathogen Pectobacterium atrosepticum. *PLoS Pathog* **4**: e1000093.

Liu, Y., Cui, Y., Mukherjee, A., and Chatterjee, A.K. (1998) Characterization of a novel RNA regulator of Erwinia carotovora ssp. carotovora that controls production of extracellular enzymes and secondary metabolites. *Mol Microbiol* **29**: 219–234.

Liu, Y., Jiang, G., Cui, Y., Mukherjee, A., Ma, W.L., and Chatterjee, A.K. (1999) kdgR(Ecc) negatively regulates genes for pectinases, cellulase, protease, Harpin(Ecc), and a global RNA regulator in Erwinia carotovora subsp. carotovora. *J Bacteriol* **181**: 2411–2421.

Liu, Y., Murata, H., Chatterjee, A., and Chatterjee, A.K. (1993) Characterization of a novel regulatory gene aepA that controls extracellular enzyme production in the phytopathogenic bacterium Erwinia carotovora subsp. carotovora. *Mol Plant Microbe Interact* **6**: 299–308.

Loc-Carrillo, C., and Abedon, S.T. (2011) Pros and cons of phage therapy. *Bacteriophage* **1**: 111–114.

Loenen, W.A.M., Dryden, D.T.F., Raleigh, E.A., and Wilson, G.G. (2014) Type I restriction enzymes and their relatives. *Nucleic Acids Res* **42**: 20–44.

Loessner, M.J. (2005) Bacteriophage endolysins — current state of research and applications. *Curr Opin Microbiol* **8**: 480–487.

Loessner, M.J., Rees, C.E., Stewart, G.S., and Scherer, S. (1996) Construction of luciferase reporter bacteriophage A511::luxAB for rapid and sensitive detection of viable Listeria cells. *Appl Environ Microbiol* **62**: 1133–40.

Lowe, T.M., and Chan, P.P. (2016) tRNAscan-SE On-line: integrating search and context for analysis of transfer RNA genes. *Nucleic Acids Res* **44**: W54–W57.

Lu, T.K., and Koeris, M.S. (2011) The next generation of bacteriophage therapy. *Curr Opin Microbiol* **14**: 524–31.

Lui, L.H., Vikram, A., Abu-Nada, Y., Kushalappa, A.C., Raghavan, G.S.V., and Al-Mughrabi, K. (2005) Volatile metabolic profiling for discrimination of potato tubers inoculated with dry and soft rot pathogens. *Am J Potato Res* **82**: 1–8.

Luna, S.M., Silva, S.S., Gomes, M.E., Mano, J.F., and Reis, R.L. (2011) Cell adhesion and proliferation onto chitosan-based membranes treated by plasma surface modification. *J Biomater Appl* **26**: 101–116.

Luo, M.L., Mullis, A.S., Leenay, R.T., and Beisel, C.L. (2015) Repurposing endogenous type I CRISPR-Cas systems for programmable gene repression. *Nucleic Acids Res* **43**: 674–81.

Luria, S.E., and Delbrück, M. (1943) Mutations of bacteria from virus sensitivity to virus resistance. *Genetics* **28**: 491–511.

Ma, B., Hibbing, M.E., Kim, H., Reedy, R.M., Yedidia, I., Breuer, J., Breuer, J., Glasner, J.D., Perna, N.T., Kelman, A., and Charkowski, A.O. (2007) Host range and molecular phylogenies of the soft rot enterobacterial genera Pectobacterium and Dickeya. *Phytopathology* **97**: 1150–1163.

Mackay, J.M., and Shipton, P.J. (1983) Heat treatment of seed tubers for control of potato blackleg (Erwinia carotovora subsp. atroseptica) and other diseases. *Plant Pathol* **32**: 385–393.

Madigan, M.T., Bender, K.S., Buckley, D.H., Martinko, J.M.., and Stahl, D.A. (2014) *Brock Biology of Microorganisms*. Fourteen edition., Pearson Education, Boston, USA.

Magill, D.J., Kucher, P.A., Krylov, V.N., Pleteneva, E.A., Quinn, J.P., and Kulakov, L.A. (2017) Localised genetic heterogeneity provides a novel mode of evolution in dsDNA phages. *Sci Rep* **7**: 13731.

Mahichi, F., Synnott, A.J., Yamamichi, K., Osada, T., and Tanji, Y. (2009) Site-specific recombination of T2 phage using IP008 long tail fiber genes provides a targeted method for expanding host range while retaining lytic activity. *FEMS Microbiol Lett* **295**: 211–217.

Mahmoudi, E., Hasanzadeh, N., Tabatabaei, B.E.S., and Venturi, V. (2011) Isolation and identification of N-acylhomoserin lactone degrading bacteria from potato rhizosphere. *African J Microbiol Res* **5**: 1635–1642.

Mahony, J., and Sinderen, D. van (2012) Structural aspects of the interaction of dairy phages with their host bacteria. *Viruses* **4**: 1410–1424.

Makarova, K.S., Wolf, Y.I., Alkhnbashi, O.S., Costa, F., Shah, S.A., Saunders, S.J., Barrangou, R., Brouns, S.J.J., Charpentier, E., Haft, D.H., Horvath, P., Moineau, S., Mojica, F.J.M., Terns, R.M., Terns, M.P., White, M.F., Yakunin, A.F., Garrett, R.A., Oost, J. van der, Backofen, R., and Koonin, E. V. (2015) An updated evolutionary classification of CRISPR–Cas systems. *Nat Rev Microbiol* **13**: 722–736.

Malik, D.J., Sokolov, I.J., Vinner, G.K., Mancuso, F., Cinquerrui, S., Vladisavljevic, G.T., Clokie, M.R.J., Garton, N.J., Stapley, A.G.F., and Kirpichnikova, A. (2017) Formulation, stabilisation and encapsulation of bacteriophage for phage therapy. *Adv Colloid Interface Sci* **249**: 100–133.

Mansfield, J., Genin, S., Magori, S., Citovsky, V., Sriariyanum, M., Ronald, P., Dow, M.A.X., Verdier, V., Beer, S. V, Machado, M.A., Toth, I.A.N., Salmond, G., Foster, G.D., Lipm, I.P., and Tolosan, F.-C. (2012) Top 10 plant pathogenic bacteria in molecular plant pathology. *Mol Plant Pathol* **13**: 614–629.

Marrone, P.G. (2014) The market and potential for biopesticides. In *ACS Symposium Series*. Gross, A.D., Coats, J.R., Duke, S.O., and Seiber, J.N. (eds). American Chemical Society, pp. 245–258.

Marschner, H., Romheld, V., Horst, W.J., and Martin, P. (1986) Root-induced changes in the rhizosphere: importance for the mineral nutrition of plants. *Z Pflanz Boden* **149**: 441–456.

Marsh, P., and Wellington, E.M.H. (1994) Phage-host interactions in soil. *FEMS Microbiol Ecol* **15**: 99–107.

Marston, M.F., Pierciey, F.J., Shepard, A., Gearin, G., Qi, J., Yandava, C., Schuster, S.C., Henn, M.R., and Martiny, J.B.H. (2012) Rapid diversification of coevolving marine Synechococcus and a virus. *Proc Natl Acad Sci* **109**: 4544–4549.

Marti, R., Zurfluh, K., Hagens, S., Pianezzi, J., Klumpp, J., and Loessner, M.J. (2013) Long tail fibres of the novel broad-host-range T-even bacteriophage S16 specifically recognize Salmonella OmpC. *Mol Microbiol* **87**: 818–834.

Matthews, C.K., and Allen, J.R. (1983) DNA precursor biosynthesis. In *Bacteriophage T4*. Mathews, C.K., Kutter, E.M., Mosig, G., and Berget, P.B. (eds). American Society for Microbiology, Washington, D.C, USA. pp. 59–70.

Maurice, C.F., Bouvier, C., Wit, R. De, and Bouvier, T. (2013) Linking the lytic and lysogenic bacteriophage cycles to environmental conditions, host physiology and their variability in coastal lagoons. *Environ Microbiol* **15**: 2463–2475.

McAllister, W.T., and Wu, H.L. (1978) Regulation of transcription of the late genes of bacteriophage T7. *Proc Natl Acad Sci U S A* **75**: 804–808.

McCalley, C.K., Woodcroft, B.J., Hodgkins, S.B., Wehr, R.A., Kim, E.H., Mondav, R., Crill, P.M., Chanton, J.P., Rich, V.I., Tyson, G.W., and Saleska, S.R. (2014) Methane dynamics regulated by microbial community response to permafrost thaw. *Nature* **514**: 478–481.

McGoran, A.R., Clark, P.F., and Morritt, D. (2017) Presence of microplastic in the digestive tracts of European flounder, Platichthys flesus, and European

smelt, Osmerus eperlanus, from the River Thames. *Environ Pollut* **22**: 744–751.

McGowan, S.J., Barnard, A.M.L., Bosgelmez, G., Sebaihia, M., Simpson, N.J.L., Thomson, N.R., Todd, D.E., Welch, M., Whitehead, N.A., and Salmond, G.P.C. (2005) Carbapenem antibiotic biosynthesis in Erwinia carotovora is regulated by physiological and genetic factors modulating the quorum sensing-dependent control pathway. *Mol Microbiol* **55**: 526–545.

McGowan, S.J., Sebaihia, M., O'Leary, S., Hardie, K.R., Williams, P., Stewart, G.S., Bycroft, B.W., and Salmond, G.P. (1997) Analysis of the carbapenem gene cluster of Erwinia carotovora: definition of the antibiotic biosynthetic genes and evidence for a novel beta-lactam resistance mechanism. *Mol Microbiol* **26**: 545–556.

McGowan, S.J., Sebaihia, M., Porter, L.E., Stewart, G.S., Williams, P., Bycroft, B.W., and Salmond, G.P. (1996) Analysis of bacterial carbapenem antibiotic production genes reveals a novel beta-lactam biosynthesis pathway. *Mol Microbiol* **22**: 415–426.

McManus, P.S., Stockwell, V.O., Sundin, G.W., and Jones, A.L. (2002) Antibiotic use in plant agriculture. *Annu Rev Phytopathol* **40**: 443–65.

McNair, K., Bailey, B.A., and Edwards, R.A. (2012) PHACTS, a computational approach to classifying the lifestyle of phages. *Bioinformatics* **28**: 614–618.

Mee, M.T., Collins, J.J., Church, G.M., and Wang, H.H. (2014) Syntrophic exchange in synthetic microbial communities. *Proc Natl Acad Sci U S A* **111**: E2149-56.

Mei, C., and Flinn, B.S. (2010) The use of beneficial microbial endophytes for plant biomass and stress tolerance improvement. *Recent Pat Biotechnol* **4**: 81–95.

Meier-Kolthoff, J.P., Auch, A.F., Klenk, H.-P., and Göker, M. (2013) Genome sequence-based species delimitation with confidence intervals and improved distance functions. *BMC Bioinformatics* **14**: 60.

Meier-Kolthoff, J.P., and Göker, M. (2017) VICTOR: genome-based phylogeny and classification of prokaryotic viruses. *Bioinformatics* **33**: 3396–3404.

Meier-Kolthoff, J.P., Hahnke, R.L., Petersen, J., Scheuner, C., Michael, V., Fiebig, A., Rohde, C., Rohde, M., Fartmann, B., Goodwin, L.A., Chertkov, O., Reddy, T.B.K., Pati, A., Ivanova, N.N., Markowitz, V., Kyrpides, N.C., Woyke, T., Gï¿½ker, M., and Klenk, H.P. (2014) Complete genome sequence of DSM 30083T, the type strain (U5/41T) of Escherichia coli, and a proposal for delineating subspecies in microbial taxonomy. *Stand Genomic Sci* **9**: 2.

Melderen, L. Van, Thi, M.H.D., Lecchi, P., Gottesman, S., Couturier, M., and

Maurizi, M.R. (1996) ATP-dependent degradation of CcdA by Lon protease. Effects of secondary structure and heterologous subunit interactions. *J Biol Chem* **271**: 27730–27738.

Mell, L.F.S., Raúl, A., Isidro, M.-Z., José, H., Josefina, L., Benigno, V.J., Cosme, B.-R., Saúl, E.R., Fabiola Sary Mell, L.-S., Raúl, A., Isidro, M.-Z., José Basilio, H., Josefina, L., José Benigno, V.-T., Cosme, B.-R., and Raymundo Saúl, G.-E. (2014) Agricultural soil supports the survival of Ralstonia solanacearum bacteriophage ΦRsS6 with biocontrol potential. *J Exp Biol Agric Sci* **2**: 90–97.

Mendes, R., Kruijt, M., Bruijn, I. de, Dekkers, E., Voort, M. van der, Scheinder, J.H., Piceno, Y.M., DeSantis, T.Z., Andersen, G.L., Bakker, P.A., and Raaijmakers, J.M. (2011) Deciphering the rhizosphere microbiome for disease-supressive bacteria. *Science (80-)* **332**: 1097–1100.

Messer, W., and Noyer-Weidner, M. (1988) Timing and targeting: the biological functions of Dam methylation in E. coli. *Cell* 54.

Middelboe, M. (2000) Bacterial growth rate and marine virus–host dynamics. *Microb Ecol* **40**: 114–124.

Miedzybrodzki, R., Fortuna, W., Weber-Dabrowska, B., and Górski, A. (2007) Phage therapy of staphylococcal infections (including MRSA) may be less expensive than antibiotic treatment. *Postepy Hig Med Dosw (Online)* **61**: 461–465.

Miller, M.T., Bachmann, B.O., Townsend, C. a, and Rosenzweig, A.C. (2002) The catalytic cycle of beta -lactam synthetase observed by x-ray crystallographic snapshots. *Proc Natl Acad Sci U S A* **99**: 14752–14757.

Miller, M.T., Gerratana, B., Stapon, A., Townsend, C.A., and Rosenzweig, A.C. (2003) Crystal structure of carbapenam synthetase (CarA). *J Biol Chem* **278**: 40996–41002.

Miller, R. V. (2001) Environmental bacteriophage-host interactions: Factors contribution to natural transduction. *Antonie van Leeuwenhoek, Int J Gen Mol Microbiol* **79**: 141–7.

Miller, S.T., Xavier, K.B., Campagna, S.R., Taga, M.E., Semmelhack, M.F., Bassler, B.L., and Hughson, F.M. (2004) Salmonella typhimurium recognizes a chemically distinct form of the bacterial quorum-sensing signal AI-2. *Mol Cell* **15**: 677–687.

Mills, A.A.S., Platt, H.W.B., and Hurta, R.A.R. (2006) Sensitivity of Erwinia spp. to salt compounds in vitro and their effect on the development of soft rot in potato tubers in storage. *Postharvest Biol Technol* **41**: 208–214.

Mirzaei, M.K., and Maurice, C.F. (2017) Ménage à trois in the human gut: interactions between host, bacteria and phages. *Nat Rev Microbiol* **15**: 397–408.

Modi, R., Hirvi, Y., Hill, A., and Griffiths, M.W. (2001) Effect of phage on survival of Salmonella enteritidis during manufacture and storage of cheddar cheese made from raw and pasteurized milk. *J Food Prot* **64**: 927–933.

Mohapatra, S.S., Fioravanti, A., and Biondi, E.G. (2014) DNA methylation on Caulobacter and other Alphaproteobacteria during cell cycle progression. *Trends Microbiol* **22**: 528–535.

Moldovan, R., Chapman-McQuiston, E., and Wu, X.L. (2007) On kinetics of phage adsorption. *Biophys J* **93**: 303–315.

Molina, L., Constantinescu, F., Michel, L., Reimmann, C., Duffy, B., and DÃ©fago, G. (2003) Degradation of pathogen quorum-sensing molecules by soil bacteria: a preventive and curative biological control mechanism. *FEMS Microbiol Ecol* **45**: 71–81.

Molineux, I.J. (2001) No syringes please, ejection of phage T7 DNA from the virion is enzyme driven. *Mol Microbiol* **40**: 1–8.

Molineux, I.J. (2012) The T7 group. In *The Bacteriophages.* Calendar, R. (ed.). Oxford University Press, New York. pp. 277–301.

Moller, W.J., Schroth, M.., and Thomson, S.V. (1981) The scenario of fire blight and streptomycin resistance. *Plant Dis* **65**: 563–568.

Monie, C., Reay, G., and Wardlaw, J. (2017) Arable crops and potato stores. Pesticide usage in Scotland. Edinburgh.

Moré, M.I., Finger, L.D., Stryker, J.L., Fuqua, C., Eberhard, A., and Winans, S.C. (1996) Enzymatic synthesis of a quorum-sensing autoinducer through use of defined substrates. *Science (80-)* **272**: 1655–1658.

Morschhäuser, J., Kohler, G., Ziebuhr, W., Blum-Oehler, G., Dobrindt, U., and Hacker, J. (2000) Evolution of microbial pathogens. *Philos.trans.r.soc.l B BiolSci* **355**: 695–704.

Mueller, U.G., and Sachs, J.L. (2015) Engineering microbiomes to improve plant and animal health. *Trends Microbiol* **23**: 606–617.

Muniz, C.A., Jaillard, D., Lemaitre, B., and Boccard, F. (2007) Erwinia carotovora Evf antagonizes the elimination of bacteria in the gut of Drosophila larvae. *Cell Microbiol* **9**: 106–119.

Murray, N.E. (2000) Type I restriction systems: sophisticated molecular machines (a legacy of Bertani and Weigle). *Microbiol Mol Biol Rev* **64**: 412–434.

Nabergoj, D., Modic, P., and Podgornik, A. (2018) Effect of bacterial growth rate on bacteriophage population growth rate. *Microbiologyopen* **7**: e00558.

Nachin, L., and Barras, F. (2000) External pH: an environmental signal that helps to rationalize pel gene duplication in Erwinia chrysanthemi. *Mol Plant*

Microbe Interact **13**: 882–886.

Nadarasah, G., and Stavrinides, J. (2011) Insects as alternative hosts for phytopathogenic bacteria. *FEMS Microbiol Rev* **35**: 555–575.

Naidoo, R., Singh, A., Arya, S.K., Beadle, B., Glass, N., Tanha, J., Szymanski, C.M., and Evoy, S. (2012) Surface-immobilization of chromatographically purified bacteriophages for the optimized capture of bacteria. *Bacteriophage* **2**: 15–24.

Narr, A., Nawaz, A., Wick, L.Y., Harms, H., and Chatzinotas, A. (2017) Soil viral communities vary temporally and along a land use transect as revealed by virus-like particle counting and a modified community fingerprinting approach (fRAPD). *Front Microbiol* **8**: 1975.

Navarro, F., and Muniesa, M. (2017) Phages in the Human Body. *Front Microbiol* **8**: 566.

Nishimura, Y., Yoshida, T., Kuronishi, M., Uehara, H., Ogata, H., and Goto, S. (2017) ViPTree: the viral proteomic tree server. *Bioinformatics* **33**: 2379–2380.

Norelli, J.., Jones, A.., and Aldwinckle, H.S. (2003) Fire blight management in the twenty-first century using new technologies that enhance host resistance in apple. .

O'Farrell, P.H. (1975) High resolution two-dimensional electrophoresis of proteins. *J Biol Chem* **250**: 4007–21.

Oda, M., Morita, M., Unno, H., and Tanji, Y. (2004) Rapid detection of Escherichia coli O157 : H7 by using green fluorescent protein-labeled PP01 bacteriophage. *Appl Environ Microbiol* **70**: 527–534.

Oechslin, F. (2018) Resistance development to bacteriophages occurring during bacteriophage therapy. *Viruses* **10**: 351.

Oechslin, F., Piccardi, P., Mancini, S., Gabard, J., Moreillon, P., Entenza, J.M., Resch, G., and Que, Y.-A. (2017) Synergistic interaction between phage therapy and antibiotics clears Pseudomonas aeruginosa infection in endocarditis and reduces virulence. *J Infect Dis* **215**: jiw632.

Oerke, E.-C. (2006) Crop losses to pests. *J Agric Sci* **144**: 31–43.

Ofek, M., Voronov-Goldman, M., Hadar, Y., and Minz, D. (2014) Host signature effect on plant root-associated microbiomes revealed through analyses of resident vs. active communities. *Environ Microbiol* **16**: 2157–67.

Ofir, G., Melamed, S., Sberro, H., Mukamel, Z., Silverman, S., Yaakov, G., Doron, S., and Sorek, R. (2018) DISARM is a widespread bacterial defence system with broad anti-phage activities. *Nat Microbiol* **3**: 90–98.

Ofir, G., and Sorek, R. (2018) Contemporary phage biology: from classic

models to new insights. *Cell* **172**: 1260–1270.

Ohmori, H., Haynes, L.L., and Rothman-Denes, L.B. (1988) Structure of the ends of the coliphage N4 genome. *J Mol Biol* **202**: 1–10.

Okabe, N., and Goto, M. (1963) Bacteriophages of plant pathogens. *Annu Rev Phytopathol* **1**: 397–418.

Oliveira, H., Melo, L.D.R., Santos, S.B., Nóbrega, F.L., Ferreira, E.C., Cerca, N., Azeredo, J., and Kluskens, L.D. (2013) Molecular aspects and comparative genomics of bacteriophage endolysins. *J Virol* **87**: 4558–70.

Olofsson, L., Ankarloo, J., and Nicholls, I.A. (1998) Phage viability in organic media: insights into phage stability. *J Mol Recognit* **11**: 91–93.

Oost, J. van der, Jore, M.M., Westra, E.R., Lundgren, M., and Brouns, S.J.J. (2009) CRISPR-based adaptive and heritable immunity in prokaryotes. *Trends Biochem Sci* **34**: 401–407.

Overbeek, R., Olson, R., Pusch, G.D., Olsen, G.J., Davis, J.J., Disz, T., Edwards, R.A., Gerdes, S., Parrello, B., Shukla, M., Vonstein, V., Wattam, A.R., Xia, F., and Stevens, R. (2014) The SEED and the Rapid Annotation of microbial genomes using Subsystems Technology (RAST). *Nucleic Acids Res* **42**: D206-14.

Paepe, M. De, Leclerc, M., Tinsley, C.R., and Petit, M.-A. (2014) Bacteriophages: an underestimated role in human and animal health? *Front Cell Infect Microbiol* **4**: 39.

Page, A.J., Cummins, C.A., Hunt, M., Wong, V.K., Reuter, S., Holden, M.T.G., Fookes, M., Falush, D., Keane, J.A., and Parkhill, J. (2015) Roary: rapid large-scale prokaryote pan genome analysis. *Bioinformatics* **31**: 3691–3693.

Pajunen, M.I., Elizondo, M.R., Skurnik, M., Kieleczawa, J., and Molineux, I.J. (2002) Complete nucleotide sequence and likely recombinatorial origin of bacteriophage T3. *J Mol Biol* **319**: 1115–1132.

Pal, C., Maciá, M.D., Oliver, A., Schachar, I., and Buckling, A. (2007) Coevolution with viruses drives the evolution of bacterial mutation rates. *Nature* **450**: 1079–1081.

Panda, P., Vanga, B.R., Lu, A., Fiers, M., Fineran, P.C., Butler, R., Armstrong, K., Ronson, C.W., and Pitman, A.R. (2016) Pectobacterium atrosepticum and Pectobacterium carotovorum harbor distinct, independently acquired integrative and conjugative elements encoding coronafacic acid that enhance virulence on potato stems. *Front Microbiol* **7**: 397.

Pande, J., Szewczyk, M.M., and Grover, A.K. (2010) Phage display: concept, innovations, applications and future. *Biotechnol Adv* 28.

Pantastico-Caldas, M., Duncan, K.E., Istock, C.A., and Bell, J.A. (1992)

Population dynamics of bacteriophage and Bacillus subtilis in soil. *Ecology* **73**: 1888–1902.

Paolozzi, L., and Ghelardini, P. (2006) The bacteriophage Mu. In *The Bacteriophages*. Richard Calendar (ed.). Oxford University Press, Oxford. pp. 469–498.

Pardini, M.T., Silva B, L., Aguiar, L.A., and Soto, M.E. (2017) Bacteriophage genome sequencing: a new alternative to understand biochemical interactions between prokaryotic cells and phages. *J Microb Biochem Technol* **9**: 169–173.

Parikka, K.J., Romancer, M. Le, Wauters, N., and Jacquet, S. (2017) Deciphering the virus-to-prokaryote ratio (VPR): insights into virus-host relationships in a variety of ecosystems. *Biol Rev* **92**: 1081–1100.

Park, J.W., Lee, S.W., Balaraju, K., Kim, C.J., and Park, K. (2012) Chili - Pepper protection from Phytophthora capsici and Pectobacterium carotovorum SCC1 by encapsulated paromycin derived from Streptomyces sp. AMG-P1. *J Pure Appl Microbiol* **6**: 1517–1522.

Park, M., Lee, J.H., Shin, H., Kim, M., Choi, J., Kang, D.H., Heu, S., and Ryu, S. (2012) Characterization and comparative genomic analysis of a novel bacteriophage, SFP10, simultaneously inhibiting both Salmonella enterica and Escherichia coli O157:H7. *Appl Environ Microbiol* **78**: 58–69.

Parra-Lopez, C., Baer, M.T., and Groisman, E.A. (1993) Molecular genetic analysis of a locus required for resistance to antimicrobial peptides in Salmonella typhimurium. *EMBO J* **12**: 4053–4062.

Parsek, M.R., Val, D.L., Hanzelka, B.L., Cronan, J.E., and Greenberg, E.P. (1999) Acyl homoserine-lactone quorum-sensing signal generation. *Proc Natl Acad Sci U S A* **96**: 4360–4365.

Paul, J.H. (2008) Prophages in marine bacteria: dangerous molecular time bombs or the key to survival in the seas? *ISME J* **2**: 579–589.

Payne, R.J.H., and Jansen, V.A.A. (2000) Phage therapy: the peculiar kinetics of self-replicating pharmaceuticals. *Clin Pharmacol Ther* **68**: 225–30.

Payne, R.J.H., and Jansen, V.A.A. (2003) Pharmacokinetic principles of bacteriophage therapy. *Clin Pharmacokinet* **42**: 315–25.

Paynter, R.W. (2000) XPS studies of the ageing of plasma-treated polymer surfaces. *Surf Interface Anal* **29**: 56–64.

Pearson, H.A., Sahukhal, G.S., Elasri, M.O., and Urban, M.W. (2013) Phage-bacterium war on polymeric surfaces: can surface-anchored bacteriophages eliminate microbial infections? *Biomacromolecules* **14**: 1257–1261.

Pedulla, M.L., Ford, M.E., Houtz, J.M., Karthikeyan, T., Wadsworth, C., Lewis, J.A., Jacobs-Sera, D., Falbo, J., Gross, J., Pannunzio, N.R., Brucker,

W., Kumar, V., Kandasamy, J., Keenan, L., Bardarov, S., Kriakov, J., Lawrence, J.G., Jacobs, W.R., Hendrix, R.W., and Hatfull, G.F. (2003) Origins of highly mosaic mycobacteriophage genomes. *Cell* **113**: 171–182.

Peiffer, J.A., Spor, A., Koren, O., Jin, Z., Tringe, S.G., Dangl, J.L., Buckler, E.S., and Ley, R.E. (2013) Diversity and heritability of the maize rhizosphere microbiome under field conditions. *Proc Natl Acad Sci U S A* **110**: 6548–53.

Penadés, J.R., Chen, J., Quiles-Puchalt, N., Carpena, N., and Novick, R.P. (2015) Bacteriophage-mediated spread of bacterial virulence genes. *Curr Opin Microbiol* **23**: 171–178.

Pérombelon, M.C.M. (2002) Potato diseases caused by soft rot erwinias: an overview of pathogenesis. *Plant Pathol* **51**: 1–12.

Perombelon, M.C.M., Burnett, E.M., Melvin, J.S., and Black, S. (1989) Preliminary studies on the control of potato blackleg by a hot water treatment of seed tubers. In *Vascular wilt diseases of Plants: Basic studies and control*. Tjamos, E.C., and Beckman, C.H. (eds). Springer-Verlag: NATO Advanced Science Institutes Series, New York, USA. pp. 557–566.

Perombelon, M.C.M., and Hyman, L.J. (1995) Serological methods to quantify potato seed contamination by Erwinia carotovora subsp. atroseptica. *EPPO Bull* **25**: 195–202.

Pérombelon, M.C.M., and Kelman, A. (1980) Ecology of soft rot erwinias. *Annu Rev Phytopatology* **18**: 361–387.

Perombelon, M.C.M., and Salmond, G.P.C. (1995) Bacterial soft rots. In *Pathogenesis and host specificity in plant disease*. Singh, U.S., Singh, R.P., and Kohmoto, K. (eds). Permagon Press Ltd., Oxford, UK. pp. 1–20.

Pfeifer, G.P. (1997) Formation and processing of UV photoproducts: effects of DNA sequence and chromatin environment. *Photochem Photobiol* 65.

Phillips, J.A., and Kelman, A. (1982) Direct fluorescent antibody stain procedure applied to insect transmission of Erwinia carotovora. *Phytopathology* **72**: 898–901.

Pires, D., Sillankorva, S., Faustino, A., and Azeredo, J. (2011) Use of newly isolated phages for control of Pseudomonas aeruginosa PAO1 and ATCC 10145 biofilms. *Res Microbiol* **162**: 798–806.

Pires, D.P., Cleto, S., Sillankorva, S., Azeredo, J., and Lu, T.K. (2016) Genetically engineered phages: a review of advances over the last decade. *Microbiol Mol Biol Rev* **80**: 523–43.

Põllumaa, L., Alamäe, T., and Mäe, A. (2012) Quorum sensing and expression of virulence in pectobacteria. *Sensors* **12**: 3327–49.

Pradeep Ram, A.S., and Sime-Ngando, T. (2010) Resources drive trade-off between viral lifestyles in the plankton: evidence from freshwater microbial

microcosms. *Environ Microbiol* **12**: 467–479.

Price, M.N., Dehal, P.S., and Arkin, A.P. (2010) FastTree 2 – Approximately maximum-likelihood trees for large alignments. *PLoS One* **5**: e9490.

Przybilski, R., Richter, C., Gristwood, T., Clulow, J.S., Vercoe, R.B., and Fineran, P.C. (2011) Csy4 is responsible for CRISPR RNA processing in Pectobacterium atrosepticum. *RNA Biol* **8**: 517–528.

Puapermpoonsiri, U., Spencer, J., and Walle, C.F. van der (2009) A freeze-dried formulation of bacteriophage encapsulated in biodegradable microspheres. *Eur J Pharm Biopharm* **72**: 26–33.

Py, B., Barras, F., Harris, S., Robson, N., and Salmond, G.P.C. (1998) Extracellular enzymes and their role in Erwinia virulence. *Methods Microbiol* **27**.

Rajaure, M., Berry, J., Kongari, R., Cahill, J., and Young, R. (2015) Membrane fusion during phage lysis. *Proc Natl Acad Sci* **112**: 5497–5502.

Rakhuba, D. V, Kolomiets, E.I., Dey, E.S., and Novik, G.I. (2010) Bacteriophage receptors, mechanisms of phage adsorption and penetration into host cell. *Polish J Microbiol* **59**: 145–55.

Rakonjac, J., Bennett, N.J., Spagnuolo, J., Gagic, D., and Russel, M. (2011) Filamentous bacteriophage: biology, phage display and nanotechnology applications. *Curr Issues Mol Biol* **13**: 51–76.

Ranganna, B., Raghavan, G.S.V., and Kushalappa, A.C. (1998) Hot water dipping to enhance storability of potatoes. *Postharvest Biol Technol* **13**: 215–223.

Rao, V.B., and Feiss, M. (2008) The bacteriophage DNA packaging motor. *Annu Rev Genet* **42**: 647–681.

Rath, D., Amlinger, L., Hoekzema, M., Devulapally, P.R., and Lundgren, M. (2015) Efficient programmable gene silencing by Cascade. *Nucleic Acids Res* **43**: 237–246.

Ravensdale, M., Blom, T.J., Gracia-Garza, J.A., Svircev, A.M., and Smith, R.J. (2007) Bacteriophages and the control of Erwinia carotovora subsp. carotovora. *Can J Plant Pathol / Rev Can Phytopathol* **29**: 121–130.

Ray, D.K., Mueller, N.D., West, P.C., and Foley, J.A. (2013) Yield trends are insufficient to double global crop production by 2050. *PLoS One* **8**: e66428.

Recek, N., Mozetic, M., Jaganjac, M., Milkovic, L., Zarkovic, N., and Vesel, A. (2014) Adsorption of proteins and cell adhesion to plasma treated polymer substrates. *Int J Polym Mater Polym Biomater* **63**: 685–691.

Reches, M., Snyder, P.W., and Whitesides, G.M. (2009) Folding of electrostatically charged beads-on-a-string as an experimental realization of

a theoretical model in polymer science. *Proc Natl Acad Sci* **106**: 17644–17649.

Redford, A.J., Bowers, R.M., Knight, R., Linhart, Y., and Fierer, N. (2010) The ecology of the phyllosphere: geographic and phylogenetic variability in the distribution of bacteria on tree leaves. *Environ Microbiol* **12**: 2885–2893.

Redman, R.S., Kim, Y.O., Woodward, C.J.D.A., Greer, C., Espino, L., Doty, S.L., and Rodriguez, R.J. (2011) Increased fitness of rice plants to abiotic stress via habitat adapted symbiosis: a strategy for mitigating impacts of climate change. *PLoS One* **6**: e14823.

Reeves, P.J., Whitcombe, D., Wharam, S., Gibson, M., Allison, G., Bunce, N., Barallon, R., Douglas, P., Mulholland, V., Stevens, S., Walker, D., and Salmond, G.P.C. (1993) Molecular cloning and characterization of 13 out genes from Erwinia carotovora subspecies carotovora: genes encoding members of a general secretion pathway (GSP) widespread in Gram-negative bacteria. *Mol Microbiol* **8**: 443–456.

Research and markets (2015) Global nanotechnology market outlook 2022. Uttar Pradesh, India.

Retamales, J., Vasquez, I., Santos, L., Segovia, C., Ayala, M., Alvarado, R., Nuñez, P., and Santander, J. (2016) Complete genome sequences of lytic bacteriophages of Xanthomonas arboricola pv. juglandis. *Genome Announc* **4**: e00336-16.

Reyes, A., Semenkovich, N.P., Whiteson, K., Rohwer, F., and Gordon, J.I. (2012) Going viral: next-generation sequencing applied to phage populations in the human gut. *Nat Rev Microbiol* **10**: 607–617.

Rezzonico, F., Smits, T., and Duffy, B. (2011) Diversity, evolution and functionality of CRISPR regions in the fire blight pathogen Erwinia amylovora. *Appl Environ Microbiol* **77**: 3819–3829.

Rho, H., Hsieh, M., Kandel, S.L., Cantillo, J., Doty, S.L., and Kim, S.H. (2018) Do endophytes promote growth of host plants under stress? A meta-analysis on plant stress mitigation by endophytes. *Microb Ecol* **75**: 407–418.

Richter, Å., Matuła, K., Leśniewski, A., Kwašnicka, K., Łoś, J., Łoś, M., Paczesny, J., and Hołyst, R. (2016) Ordering of bacteriophages in the electric field: application for bacteria detection. *Sensors Actuators, B Chem* **224**: 233–240.

Richter, C., Chang, J.T., and Fineran, P.C. (2012) Function and regulation of clustered regularly interspaced short palindromic repeats (CRISPR) / CRISPR associated (Cas) systems. *Viruses* **4**: 2291–2311.

Richter, Ł., Bielec, K., Leśniewski, A., Łoś, M., Paczesny, J., and Hołyst, R. (2017) Dense layer of bacteriophages ordered in alternating electric field and immobilized by surface chemical modification as sensing element for bacteria

detection. *ACS Appl Mater Interfaces* **9**: 19622–19629.

Rihtman, B., Meaden, S., Clokie, M.R.J., Koskella, B., and Millard, A.D. (2016) Assessing Illumina technology for the high-throughput sequencing of bacteriophage genomes. *PeerJ* **4**: e2055.

Ritchie, D.F.F., Kloos, E.J., and Klos, E.J. (1977) Isolation of Erwinia amylovora bacteriophage from aerial parts of apple trees. *Phytopathology* **67**: 101–104.

Roberts, R.C., Ström, A.R., and Helinski, D.R. (1994) The parDE operon of the broad-host-range plasmid RK2 specifies growth inhibition associated with plasmid loss. *J Mol Biol* **237**: 35–51.

Roberts, R.J., Vincze, T., Posfai, J., and Macelis, D. (2015) REBASE-a database for DNA restriction and modification: enzymes, genes and genomes. *Nucleic Acids Res* **43**: D298-299.

Robinson, K., and Foster, G.D. (1987) Control of potato blackleg by tuber pasteurization: the determination of time-temperature combinations for the inactivation of pectolytic erwinia. *Potato Res* **30**: 121–125.

Rocha, A.B.O., Honorio, S.L., Messias, L.C., Oton, M., and Gomez, P. (2015) Effect of UV-C radiation and fluorescent light to control postharvest soft rot in potato seed tubers. *Sci Hortic (Amsterdam)* **181**: 174–181.

Rodriguez-Brito, B., Li, L., Wegley, L., Furlan, M., Angly, F., Breitbart, M., Buchanan, J., Desnues, C., Dinsdale, E., Edwards, R., Felts, B., Haynes, M., Liu, H., Lipson, D., Mahaffy, J., Martin-Cuadrado, A.B., Mira, A., Nulton, J., Pašić, L., Rayhawk, S., Rodriguez-Mueller, J., Rodriguez-Valera, F., Salamon, P., Srinagesh, S., Thingstad, T.F., Tran, T., Thurber, R.V., Willner, D., Youle, M., and Rohwer, F. (2010) Viral and microbial community dynamics in four aquatic environments. *ISME J* **4**: 739–751.

Rodriguez-Valera, F., Martin-Cuadrado, A.-B., Rodriguez-Brito, B., Pašić, L., Thingstad, T.F., Rohwer, F., and Mira, A. (2009) Explaining microbial population genomics through phage predation. *Nat Rev Microbiol* **7**: 828–836.

Rodriguez, R.J., Henson, J., Volkenburgh, E. Van, Hoy, M., Wright, L., Beckwith, F., Kim, Y.O., and Redman, R.S. (2008) Stress tolerance in plants via habitat-adapted symbiosis. *ISME J* **2**: 404–416.

Rohwer, F., and Edwards, R. (2002) The phage proteomic tree: a genome-based taxonomy for phage. *J Bacteriol* **184**: 4529–4535.

Rohwer, F., and Thurber, R.V. (2009) Viruses manipulate the marine environment. *Nature* 459.

Ross, A., Ward, S., and Hyman, P. (2016) More is better: selecting for broad host range bacteriophages. *Front Microbiol* **7**: 1352.

Ross, H. (1986) *Potato breeding - problems and perspectives*. Paul Parey Scientific Pub., Berlin, Germany.

Roux, S., Brum, J.R., Dutilh, B.E., Sunagawa, S., Duhaime, M.B., Loy, A., Poulos, B.T., Solonenko, N., Lara, E., Poulain, J., Pesant, S., Kandels-Lewis, S., Dimier, C., Picheral, M., Searson, S., Cruaud, C., Alberti, A., Duarte, C.M., Gasol, J.M., Vaqué, D., Bork, P., Acinas, S.G., Wincker, P., Sullivan, M.B., and Sullivan, M.B. (2016) Ecogenomics and potential biogeochemical impacts of globally abundant ocean viruses. *Nature* **537**: 689–693.

Ryan, R.P., Germaine, K., Franks, A., Ryan, D.J., and Dowling, D.N. (2008) Bacterial endophytes: recent developments and applications. *FEMS Microbiol Lett* 278.

Rydman, P.S., and Bamford, D.H. (2000) Bacteriophage PRD1 DNA entry uses a viral membrane-associated transglycosylase activity. *Mol Microbiol* **37**: 356–63.

Rydman, P.S., and Bamford, D.H. (2002) The lytic enzyme of bacteriophage PRD1 is associated with the viral membrane. *J Bacteriol* **184**: 104–10.

Sadeghi, G., Schijven, J.F., Behrends, T., Hassanizadeh, S.M., Gerritse, J., and Kleingeld, P.J. (2011) Systematic study of effects of pH and ionic strength on attachment of phage PRD1. *Ground Water* **49**: 12–9.

Sadowski, P.D., and Kerr, C. (1970) Degradation of Escherichia coli B deoxyribonucleic acid after infection with deoxyribonucleic acid- defective amber mutants of bacteriophage T71. *J Virol* **6**: 149–155.

Saha, S., and Raghava, G.P.S. (2007) BTXpred: prediction of bacterial toxins. *In Silico Biol* **7**: 405–412.

Salathé, M., and Soyer, O.S. (2008) Parasites lead to evolution of robustness against gene loss in host signaling networks. *Mol Syst Biol* **4**: 202.

Salzberg, S.L., Delcher, A.L., Kasif, S., and White, O. (1998) Microbial gene identification using interpolated Markov models. *Nucleic Acids Res* **26**.

Samson, J.E., Magadán, A.H., Sabri, M., and Moineau, S. (2013) Revenge of the phages: defeating bacterial defences. *Nat Rev Microbiol* **11**: 675–687.

San Chan, Y.S., and Mat Don, M. (2013) Biosynthesis and structural characterization of Ag nanoparticles from white rot fungi. *Mater Sci Eng C Mater Biol Appl* **33**: 282–288.

Sandaa, R.-A. (2009) Viruses, Environmental. In *Encyclopedia of Microbiology*. Moselio Schaechter (ed.). Academic Press, San Diego, USA. pp. 553–567.

Sanders, M.E., and Klaenhammer, T.R. (1984) Phage resistance in a phage-insensitive strain of Streptococcus lactis: temperature-dependent phage development and host-controlled phage replication. *Appl Environ Microbiol*

47: 979–85.

Sandmeler, H. (1994) Acquisition and rearrangement of sequence motifs in the evolution of bacteriophage tail fibres. *Mol Microbiol* 12.

Sanger, F., Air, G.M., Barrell, B.G., Brown, N.L., Coulson, A.R., Fiddes, J.C., Hutchison, C.A., Slocombe, P.M., and Smith, M. (1977) Nucleotide sequence of bacteriophage φX174 DNA. *Nature* **265**: 687–695.

Sanguin, H., Remenant, B., Dechesne, A., Thioulouse, J., Vogel, T.M., Nesme, X., Moënne-Loccoz, Y., and Grundmann, G.L. (2006) Potential of a 16S rRNA-based taxonomic microarray for analyzing the rhizosphere effects of maize on Agrobacterium spp. and bacterial communities. *Appl Environ Microbiol* **72**: 4302–12.

Santoyo, G., Moreno-Hagelsieb, G., Carmen Orozco-Mosqueda, M. del, and Glick, B.R. (2016) Plant growth-promoting bacterial endophytes. *Microbiol Res* 183.

Savalia, D., Robins, W., Nechaev, S., Molineux, I., and Severinov, K. (2010) The role of the T7 Gp2 inhibitor of host RNA polymerase in phage development. *J Mol Biol* **402**: 118–126.

Savitskaya, E.E., Musharova, O.S., and Severinov, K. V. (2016) Diversity of CRISPR-Cas-mediated mechanisms of adaptive immunity in prokaryotes and their application in biotechnology. *Biochemistry* **81**: 653–661.

Sberro, H., Leavitt, A., Kiro, R., Koh, E., Peleg, Y., Qimron, U., and Sorek, R. (2013) Discovery of functional toxin/antitoxin systems in bacteria by shotgun cloning. *Mol Cell* **50**: 136–48.

Schamberger, P.C., Abes, J.I., and Gardella, J.A. (1994) Surface chemical studies of aging and solvent extraction effects on plasma-treated polystyrene. *Colloids Surfaces B Biointerfaces* **3**: 203–215.

Schauder, S., Shokat, K., Surette, M.G., and Bassler, B.L. (2001) The LuxS family of bacterial autoinducers: biosynthesis of a novel quorum-sensing signal molecule. *Mol Microbiol* **41**: 462–476.

Schlesinger, M. (1932) Adsorption of bacteriophages to homologous bacteria. II. Quantitative investigation of adsorption velocity and saturation. Estimation of the particle size of the bacteriophage. *Immunitaetsforschung* 149–160.

Schmelcher, M., Donovan, D.M., and Loessner, M.J. (2012) Bacteriophage endolysins as novel antimicrobials. *Future Microbiol* 7.

Schmelcher, M., Shen, Y., Nelson, D.C., Eugster, M.R., Eichenseher, F., Hanke, D.C., Loessner, M.J., Dong, S., Pritchard, D.G., Lee, J.C., Becker, S.C., Foster-Frey, J., and Donovan, D.M. (2014) Evolutionarily distinct bacteriophage endolysins featuring conserved peptidoglycan cleavage sites

protect mice from MRSA infection. *J Antimicrob Chemother* **70**: 1453–1465.

Scholl, D., Kieleczawa, J., Kemp, P., Rush, J., Richardson, C.C., Merril, C., Adhya, S., and Molineux, I.J. (2004) Genomic analysis of bacteriophages SP6 and K1-5, an estranged subgroup of the T7 supergroup. *J Mol Biol* **335**: 1151–71.

Scholl, D., and Merril, C. (2005) The genome of bacteriophage K1F, a T7-like phage that has acquired the ability to replicate on K1 strains of Escherichia coli. *J Bacteriol* **187**: 8499–8503.

Schumacher, M.A., Piro, K.M., Xu, W., Hansen, S., Lewis, K., and Brennan, R.G. (2009) Molecular mechanisms of HipA-mediated multidrug tolerance and its neutralization by HipB. *Science (80-)* **323**: 396–401.

Schwarz, D., Thompson, A.J., and Klaring, H.-P. (2014) Guidelines to use tomato in experiments with a controlled environment. *Front Plant Sci* **18**: 625.

Schwind, P., Kramer, H., Kremser, A., Ramsberger, U., and Rasched, I. (1992) Subtilisin removes the surface layer of the phage fd coat. *Eur J Biochem* **210**: 431–436.

Sciara, G., Blangy, S., Siponen, M., Mc Grath, S., Sinderen, D. Van, Tegoni, M., Cambillau, C., and Campanacci, V. (2008) A topological model of the baseplate of lactococcal phage Tuc2009. *J Biol Chem* **283**: 2716–2723.

Scott, H., and Mattey, M. (2009) Immobilisation ans stabilisation of virus. 5.

Seemann, T. (2014) Prokka: rapid prokaryotic genome annotation. *Bioinformatics* **30**: 2068–2069.

Semenova, E., Nagornykh, M., Pyatnitskiy, M., Artamonova, I.I., and Severinov, K. (2009) Analysis of CRISPR system function in plant pathogen Xanthomonas oryzae. *FEMS Microbiol Lett* **296**: 110–116.

Serwer, P., Hayes, S.J., Zaman, S., Lieman, K., Rolando, M., and Hardies, S.C. (2004) Improved isolation of undersampled bacteriophages: finding of distant terminase genes. *Virology* **329**: 412–424.

Serwer, P., Wright, E.T., Hakala, K.W., and Weintraub, S.T. (2008) Evidence for bacteriophage T7 tail extension during DNA injection. *BMC Res Notes* **1**: 36.

Sethi, S., Datta, A., Gupta, B.L., and Gupta, S. (2013) Optimization of cellulase production from bacteria isolated from soil. *ISRN Biotechnol* **2013**: 1–7.

Shabuer, G., Ishida, K., Pidot, S.J., Roth, M., Dahse, H.-M., and Hertweck, C. (2015a) Plant pathogenic anaerobic bacteria use aromatic polyketides to access aerobic territory. *Science (80-)* **350**: 670 LP-674.

Shabuer, G., Ishida, K., Pidot, S.J., Roth, M., Dahse, H.-M., and Hertweck,

C. (2015b) Plant pathogenic anaerobic bacteria use aromatic polyketides to access aerobic territory. *Science* **350**: 670–4.

Shadrin, A., Sheppard, C., Savalia, D., Severinov, K., and Wigneshweraraj, S. (2013) Overexpression of Escherichia coli udk mimics the absence of T7 Gp2 function and thereby abrogates successful infection by T7 phage. *Microbiol (United Kingdom)* **159**: 269–274.

Sharma, M., Ryu, J.H., and Beuchat, L.R. (2005) Inactivation of Escherichia coli O157:H7 in biofilm on stainless steel by treatment with an alkaline cleaner and a bacteriophage. *J Appl Microbiol* **99**: 449–459.

Shepard, J.F., and Claflin, L.E. (1975) Critical analyses of the principles of seed potato certification. *Annu Rev os Phytopathol* **13**: 271–293.

Shivaji, S., Madhu, S., and Singh, S. (2011) Extracellular synthesis of antibacterial silver nanoparticles using psychrophilic bacteria. *Process Biochem* **46**: 1800–1807.

Short, F.L., Akusobi, C., Broadhurst, W.R., and Salmond, G.P.C. (2018) The bacterial Type III toxin-antitoxin system, ToxIN, is a dynamic protein-RNA complex with stability-dependent antiviral abortive infection activity. *Sci Rep* **8**: 1013.

Short, F.L., Pel, X.Y., Blower, T.R., Ong, S.L., Fineran, P.C., Luisi, B.F., and Salmond, G.P.C. (2013) Selectivity and self-assembly in the control of a bacterial toxin by an automatic noncoding RNA pseudoknot. *Proc Natl Acad Sci U S A* **110**: E241-249.

Shurdov, M.A., and Gruzdev, A.D. (1984) Fluorescence polarization study of tertiary structure of DNA within bacteriophage lambda. *FEBS Lett* **165**: 238–242.

Sievers, F., Wilm, A., Dineen, D., Gibson, T.J., Karplus, K., Li, W., Lopez, R., McWilliam, H., Remmert, M., Söding, J., Thompson, J.D., and Higgins, D.G. (2011) Fast, scalable generation of high-quality protein multiple sequence alignments using Clustal Omega. *Mol Syst Biol* **7**: 539.

Silva, D.P. da, Castañeda-Ojeda, M.P., Moretti, C., Buonaurio, R., Ramos, C., and Venturi, V. (2014) Bacterial multispecies studies and microbiome analysis of a plant disease. *Microbiol (United Kingdom)* **160**: 556–66.

Simmonds, P., and Aiewsakun, P. (2018) Virus classification – where do you draw the line? *Arch Virol* **163**: 2037–2046.

Simpson, a a, Tao, Y., Leiman, P.G., Badasso, M.O., He, Y., Jardine, P.J., Olson, N.H., Morais, M.C., Grimes, S., Anderson, D.L., Baker, T.S., and Rossmann, M.G. (2000) Structure of the bacteriophage phi29 DNA packaging motor. *Nature* **408**: 745–750.

Singer, B.S., Gold, L., Gauss, P., and Doherty, D.H. (1982) Determination of

the amount of homology required for recombination in bacteriophage T4. *Cell* **31**: 25–33.

Singh, A., Glass, N., Tolba, M., Brovko, L., Griffiths, M., and Evoy, S. (2009) Immobilization of bacteriophages on gold surfaces for the specific capture of pathogens. *Biosens Bioelectron* **24**: 3645–3651.

Sistla, S., and Rao, D.N. (2004) S-Adenosyl-L-methionine-dependent restriction enzymes. *Crit Rev Biochem Mol Biol* 39.

Skelsey, P., Elphinstone, J.G., Saddler, G.S., Wale, S.J., and Toth, I.K. (2016) Spatial analysis of blackleg-affected seed potato crops in Scotland. *Plant Pathol* **65**: 570–576.

Sleeman, M.C., Smith, P., Kellam, B., Chhabra, S.R., Bycroft, B.W., and Schofield, C.J. (2004) Biosynthesis of carbapenem antibiotics: new carbapenam substrates for carbapenem synthase (carC). *ChemBioChem* **5**: 879–882.

Smet, J. De, Zimmermann, M., Kogadeeva, M., Ceyssens, P.-J., Vermaelen, W., Blasdel, B., Jang, H. Bin, Sauer, U., and Lavigne, R. (2016) High coverage metabolomics analysis reveals phage-specific alterations to Pseudomonas aeruginosa physiology during infection. *ISME J* **10**: 1823–1835.

Smietana, M., Bock, W.J., Mikulic, P., Ng, A., Chinnappan, R., and Zourob, M. (2011) Detection of bacteria using bacteriophages as recognition elements immobilized on long-period fiber gratings. *Opt Express* **19**: 7971–7978.

Smolarska, A., Rabalski, L., Narajczyk M., and Czajkowski R. (2018) Isolation and phenotypic and morphological characterization of the first Podoviridae lytic bacteriophages φA38 and φA41 infecting Pectobacterium parmentieri (former Pectobacterium wasabiae). *Eur J Plant Pathol* **150**: 413–425.

Sorek, R., Lawrence, C.M., and Wiedenheft, B. (2013) CRISPR-mediated adaptive immune systems in bacteria and Archaea. *Annu Rev Biochem* **82**: 237–266.

Soriano, P., and Climent, F. (2006) Region vs. industry effects and volatility transmission. *Financ Anal J* **62**: 52–64.

Sperandio, V., Mellies, J.L., Nguyen, W., Shin, S., and Kaper, J.B. (1999) Quorum sensing controls expression of the type III secretion gene transcription and protein secretion in enterohemorrhagic and enteropathogenic Escherichia coli. *Proc Natl Acad Sci U S A* **96**: 15196–15201.

Sperandio, V., Torres, A.G., Giron, J.A., and Kaper, J.B. (2001) Quorum sensing is a global regulatory mechanism in enterohemorrhagic Escherichia

coli O157:H7. *J Bacteriol* **183**: 5187–5197.

Spricigo, D.A., Bardina, C., Cortés, P., and Llagostera, M. (2013) Use of a bacteriophage cocktail to control Salmonella in food and the food industry. *Int J Food Microbiol* **165**: 169–74.

Srinivasiah, S., Lovett, J., Ghosh, D., Roy, K., Fuhrmann, J.J., Radosevivh, M., and Wommack, K.E. (2015) Dynamics of autochthonous soil viral communities parallels dynamics of host communities under nutrient stimulation. *FEMS Microbiol Ecol* **91**: fiv063.

Stanford, K., McAllister, T.A., Niu, Y.D., Stephens, T.P., Mazzocco, A., Waddell, T.E., and Johnson, R.P. (2010) Oral delivery systems for encapsulated bacteriophages targeted Escherichia coli O157: H7 in feedlot cattle. *J Food Prot* **73**: 1304–12.

Stern, A., and Sorek, R. (2012) The phage-host arms-race : shaping the evolution of microbes. *Bioessays* **33**: 43–51.

Steven, A.C., and Trus, B.L. (1986) Electron microscopy of proteins. In *The structure of bacteriophage T7*. J. R. Harris and R. W. Horne (ed.). Academic Press, London. pp. 1–35.

Steven, A.C., Trus, B.L., Maizel, J. V., Unser, M., Parry, D.A.D., Wall, J.S., Hainfeld, J.F., and Studier, F.W. (1988) Molecular substructure of a viral receptor-recognition protein. The gp17 tail-fiber of bacteriophage T7. *J Mol Biol* **200**: 351–365.

Stockwell, V.O., and Duffy, B. (2012) Use of antibiotics in plant agriculture. *Rev Sci Tech l'OIE* **31**: 199–210.

Storey, M. V., and Ashbolt, N.J. (2001) Persistence of two model enteric viruses (B40-8 and MS-2 bacteriophages) in water distribution pipe biofilms. *Water Sci Technol* **43**: 133–138.

Strachan, C.R., Singh, R., VanInsberghe, D., Ievdokymenko, K., Budwill, K., Mohn, W.W., Eltis, L.D., and Hallam, S.J. (2014) Metagenomic scaffolds enable combinatorial lignin transformation. *Proc Natl Acad Sci* **111**: 10143–8.

Strange, R.R.N., and Scott, P.P.R.P. (2005) Plant disease: a threat to global food security. *Phytopathology* **43**: 83–116.

Straub, T.M., Pepper, I.L., and Gerba, C.P. (1992) Persistence of viruses in desert soils amended with anaerobically digested sewage sludge. *Appl Environ Microbiol* **58**: 636–41.

Studier, F.W., and Movva, N.R. (1976) SAMase gene of bacteriophage T3 is responsible for overcoming host restriction. *J Virol* **19**: 136–145.

Stummeyer, K., Schwarzer, D., Claus, H., Vogel, U., Gerardy-Schahn, R., and Muhlenhoff, M. (2006) Evolution of bacteriophages infecting encapsulated bacteria: lessons from Escherichia coli K1-specific phages. *Mol*

Microbiol **60**: 1123–1135.

Su, P., Im, H., Hsieh, H., Kang'a, S., and Dunn, N.W. (1999) LlaFI, a type III restriction and modification system in Lactococcus lactis. *Appl Environ Microbiol* **65**: 686–693.

Sullivan, M.J., Petty, N.K., and Beatson, S.A. (2011) Easyfig: a genome comparison visualizer. *Bioinformatics* **27**: 1009–1010.

Sun, S., Gao, S., Kondabagil, K., Xiang, Y., Rossmann, M.G., and Rao, V.B. (2012) Structure and function of the small terminase component of the DNA packaging machine in T4-like bacteriophages. *Proc Natl Acad Sci* **109**: 817–822.

Suttle, C. a (2007) Marine viruses--major players in the global ecosystem. *Nat Rev Microbiol* **5**: 801–812.

Suttle, C.A. (2005) Viruses in the sea. *Nature* **437**: 356–361.

Svircev, A.M., Castle, A.J., and Lehman, S.M. (2010) Bacteriophages for control of phytopathogens in food production systems. In *Bacteriophages in the Control of Food- and Waterborne Pathogens*. Sabour, P.M., and Griffiths, M.W. (eds). ASM Press, Washington DC, USA. pp. 79–102.

Swanson, M.M., Fraser, G., Daniel, T.J., Torrance, L., Gregory, P.J., and Taliansky, M. (2009) Viruses in soils: morphological diversity and abundance in the rhizosphere. *Ann Appl Biol* **155**: 51–60.

Swarts, D.C., Makarova, K., Wang, Y., Nakanishi, K., Ketting, R.F., Koonin, E. V, Patel, D.J., and Oost, J. van der (2014) The evolutionary journey of Argonaute proteins. *Nat Struct Mol Biol* **21**: 743–753.

Swiss Institute of Bioinformatics (2013) Viral genome circularization. https://viralzone.expasy.org/3968?outline=all_by_protein.

Sykes, I.K., Lanning, S., and Williams, S.T. (1981) the effect of pH on soil actinophage. *J Gen Microbiol* **122**: 271–280.

Tamma, P.D., Cosgrove, S.E., and Maragakis, L.L. (2012) Combination therapy for treatment of infections with gram-negative bacteria. *Clin Microbiol Rev* **25**: 450–70.

Tanaka, K., and Takada, H. (2016) Microplastic fragments and microbeads in digestive tracts of planktivorous fish from urban coastal waters. *Sci Rep* **6**: 34351.

Tanji, Y., Furukawa, C., Na, S.H., Hijikata, T., Miyanaga, K., and Unno, H. (2004) Escherichia coli detection by GFP-labeled lysozyme-inactivated T4 bacteriophage. *J Biotechnol* **114**: 11–20.

Tétart, F., Desplats, C., and Krisch, H.M. (1998) Genome plasticity in the distal tail fiber locus of the T-even bacteriophage: recombination between

conserved motifs swaps adhesin specificity. *J Mol Biol* **282**: 543–556.

Thompson, J.D., Higgins, D.G., and Gibson, T.J. (1994) CLUSTAL W: improving the sensitivity of progressive multiple sequence alignment through sequence weighting, position-specific gap penalties and weight matrix choice. *Nucleic Acids Res* **22**: 4673–80.

Thompson, J.N. (2005) Coevolution: the geographic mosaic of coevolutionary arms races. *Curr Biol* **15**: R992–R994.

Thompson, L.R., Zeng, Q., Kelly, L., Huang, K.H., Singer, A.U., Stubbe, J., and Chisholm, S.W. (2011) Phage auxiliary metabolic genes and the redirection of cyanobacterial host carbon metabolism. *Proc Natl Acad Sci* **108**: E757–E764.

Thomson, N.R., Cox, a, Bycroft, B.W., Stewart, G.S., Williams, P., and Salmond, G.P. (1997) The rap and hor proteins of Erwinia, Serratia and Yersinia: a novel subgroup in a growing superfamily of proteins regulating diverse physiological processes in bacterial pathogens. *Mol Microbiol* **26**: 531–544.

Thomson, N.R., Nasser, W., McGowan, S., Sebaihia, M., and Salmond, G.P.C. (1999) Erwinia carotovora has two KdgR-like proteins belonging to the IcIR family of transcriptional regulators: Identification and characterization of the RexZ activator and the KdgR repressor of pathogenesis. *Microbiology* **145**: 1531–1545.

Timmusk, S., Nicander, B., Granhall, U., and Tillberg, E. (1999) Cytokinin production by Paenibacillus polymyxa. *Soil Biol Biochem* **31**: 1847–1852.

Tock, M.R., and Dryden, D.T.F. (2005) The biology of restriction and anti-restriction. *Curr Opin Microbiol* **8**: 466–472.

Torres-Barceló, C., and Hochberg, M.E. (2016) Evolutionary rationale for phages as complements of antibiotics. *Trends Microbiol* **24**: 249–256.

Toth, I.K., Bell, K.S., Holeva, M.C., and Birch, P.R.J. (2003) Soft rot erwiniae: from genes to genomes. *Mol Plant Pathol* **4**: 17–30.

Toth, I.K., and Birch, P.R.J. (2005) Rotting softly and stealthily. *Curr Opin Plant Biol* **8**: 424–429.

Toth, I.K., Newton, J.A., Hyman, L.J., Lees, A.K., Daykin, M., Ortori, C., Williams, P., and Fray, R.G. (2004) Potato plants genetically modified to produce N-acylhomoserine lactones increase susceptibility to soft rot erwiniae. *Mol plantmicrobe Interact MPMI* **17**: 880–7.

Toth, I.K., Wolf, J.M. van der, Saddler, G., Lojkowska, E., Hélias, V., Pirhonen, M., Tsror Lahkim, L., and Elphinstone, J.G. (2011) Dickeya species: an emerging problem for potato production in Europe. *Plant Pathol* **60**: 385–399.

Trias, R., Baneras, L., Montesinos, E., and Badosa, E. (2008) Lactic acid bacteria from fresh fruit and vegetables as biocontrol agents of phytopathogenic bacteria and fungi. *Int Microbiol* **11**: 231–236.

Trun, N., and Trempy, J. (2003) Bacteriophages. In *Fundamental Bacterial Genetics*. Blackwell Publishers, Maiden, USA. pp. 105–125.

Tzipilevich, E., Habusha, M., and Ben-Yehuda, S. (2017) Acquisition of phage sensitivity by bacteria through exchange of phage receptors. *Cell* **168**: 186–199.

United Nations, Department of Economic and Social Affairs, P.D. (2015) World population prospects: the 2015 revision. *World Popul Prospect 2015 Revis Key Find Adv Tables* Working paper No. ESA/P/WP.241.

Uroz, S., D'Angelo-Picard, C., Carlier, A., Elasri, M., Sicot, C., Petit, A., Oger, P., Faure, D., and Dessaux, Y. (2003) Novel bacteria degrading N-acylhomoserine lactones and their use as quenchers of quorum-sensing-regulated functions of plant-pathogenic bacteria. *Soc Gen Microbiol J* **149**: 1981–1989.

Vandenbergh, P.A., and Cole, R.L. (1986) Cloning and expression in Escherichia coli of the polysaccharide depolymerase associated with bacteriophage-infected Erwinia amylovora. *Appl Environ Microbiol* **51**: 862–4.

Vasu, K., and Nagaraja, V. (2013) Diverse functions of restriction-modification systems in addition to cellular defense. *Microbiol Mol Biol Rev* **77**: 53–72.

Vendeville, A., Winzer, K., Heurlier, K., Tang, C.M., and Hardie, K.R. (2005) Making "sense" of metabolism: autoinducer-2, LuxS and pathogenic bacteria. *Nat Rev Microbiol* **3**: 383–396.

Verbeken, G., Pirnay, J.-P., Lavigne, R., Jennes, S., Vos, D. De, Casteels, M., and Huys, I. (2014) Call for a dedicated European legal framework for bacteriophage therapy. *Arch Immunol Ther Exp (Warsz)* **62**: 117–129.

Verheust, C., Pauwels, K., Mahillon, J., Helinski, D.R., and Herman, P. (2010) Contained use of bacteriophages : risk assessment and biosafety recommendations. *Appl Biosaf* **15**: 32–44.

Veterinary Medicines Directorate, U. (2016) Highlights Report 2016 UK-VARSS. .

Viazis, S., Akhtar, M., Feirtag, J., Brabban, A.D., and Diez-Gonzalez, F. (2011) Isolation and characterization of lytic bacteriophages against enterohaemorrhagic Escherichia coli. *J Appl Microbiol* **110**: 1323–1331.

Vigneshwaran, N., Ashtaputre, N.M., Varadarajan, P.V., Nachane, R.P., Paralikar, K.M., and Balasubramanya, R.H. (2007) Biological synthesis of silver nanoparticles using the fungus Aspergillus flavus. *Mater Lett* **61**: 1413–

1418.

Vranova, V., Rejsek, K., and Formanek, P. (2013) Proteolytic activity in soil: a review. *Appl Soil Ecol* **70**: 23–32.

Wang, C., Knill, E., Glick, B.R., and Défago, G. (2000) Effect of transferring 1-aminocyclopropane-1-carboxylic acid (ACC) deaminase genes into Pseudomonas fluorescens strain CHA0 and its gacA derivative CHA96 on their growth-promoting and disease-suppressive capacities. *Can J Microbiol* **46**: 898–907.

Wang, C., Sauvageau, D., and Elias, A. (2016) Immobilization of active bacteriophages on polyhydroxyalkanoate surfaces. *ACS Appl Mater Interfaces* **8**: 1128–1138.

Wang, I.-N. (2006a) Lysis timing and bacteriophage fitness. *Genetics* **172**: 17–26.

Wang, I.-N. (2006b) Lysis timing and bacteriophage fitness. *Genetics* **172**: 17–26.

Wang, I.-N., Smith, D.L., and Young, R. (2000) Holins: the protein clocks of bacteriophage infections. *Annu Rev Microbiol* **54**: 799–825.

Wang, Q., and Sabour, P.M. (2010) Encapsulation and controlled release of bacteriophages for food animal production. In Bacteriophages in the Control of Food- and Waterborne Pathogens. In *Bacteriophages in the Control of Food- and Waterborne Pathogens*. Sabour, P.M., and Griffiths, M.W. (eds). ASM Press, Washington. pp. 237–255.

Wang, X., Lord, D.M., Cheng, H.-Y., Osbourne, D.O., Hong, S.H., Sanchez-Torres, V., Quiroga, C., Zheng, K., Herrmann, T., Peti, W., Benedik, M.J., Page, R., and Wood, T.K. (2012) A new type V toxin-antitoxin system where mRNA for toxin GhoT is cleaved by antitoxin GhoS. *Nat Chem Biol* **8**: 855–861.

Wang, X., and Wood, T.K. (2011) Toxin-antitoxin systems influence biofilm and persister cell formation and the general stress response. *Appl Environ Microbiol* **77**: 5577–83.

Wang, Y., Wu, C., Zhang, Q., Qi, J., Liu, H., Wang, Y., He, T., Ma, L., Lai, J., Shen, Z., Liu, Y., and Shen, J. (2012) Identification of New Delhi metallo-β-lactamase 1 in Acinetobacter lwoffii of food animal origin. *PLoS One* **7**: e37152.

Wani, Z.A., Ashraf, N., Mohiuddin, T., and Riyaz-Ul-Hassan, S. (2015) Plant-endophyte symbiosis, an ecological perspective. *Appl Microbiol Biotechnol* 99.

Ward, R.L., and Mahler, R.J. (1982) Uptake of bacteriophage f2 through plant roots. *Appl Environ Microbiol* **43**: 1098–103.

Weber-Dabrowska, B., Jończyk-Matysiak, E., Zaczek, M., Łobocka, M., Łusiak-Szelachowska, M., and Górski, A. (2016) Bacteriophage procurement for therapeutic purposes. *Front Microbiol* **7**: 1177.

Wei, B.L., Brun-Zinkernagel, A.M., Simecka, J.W., Prüß, B.M., Babitzke, P., and Romeo, T. (2001) Positive regulation of motility and flhDC expression by the RNA-binding protein CsrA of Escherichia coli. *Mol Microbiol* **40**: 245–256.

Wei, C., Liu, J., Maina, A.N., Mwaura, F.B., Yu, J., Yan, C., Zhang, R., and Wei, H. (2017) Developing a bacteriophage cocktail for biocontrol of potato bacterial wilt. *Virol Sin* **32**: 476–484.

Wei, J., Jin, Y., Sims, T., and Kniel, K.E. (2010) Manure- and biosolids-resident murine norovirus 1 attachment to and internalization by romaine lettuce. *Appl Environ Microbiol* **76**: 578–583.

Wei, Z., Yang, T., Friman, V.-P., Xu, Y., Shen, Q., and Jousset, A. (2015) Trophic network architecture of root-associated bacterial communities determines pathogen invasion and plant health. *Nat Commun* **6**: 8413.

Weinbauer, M.G., Brettar, I., and Höfle, M.G. (2003) Lysogeny and virus-induced mortality of bacterioplankton in surface, deep, and anoxic marine waters. *Limnol Oceanogr* **48**: 1457–1465.

Weitz, J.S., Mileyko, Y., Joh, R.I., and Voit, E.O. (2008) Collective decision making in bacterial viruses. *Biophys J* **95**: 2673–2680.

Welch, M., Todd, D.E., Whitehead, N. a, McGowan, S.J., Bycroft, B.W., and Salmond, G.P. (2000) N-acyl homoserine lactone binding to the CarR receptor determines quorum-sensing specificity in Erwinia. *EMBO J* **19**: 631–641.

Weyens, N., Lelie, D. van der, Taghavi, S., and Vangronsveld, J. (2009) Phytoremediation: plant-endophyte partnerships take the challenge. *Curr Opin Biotechnol* **20**: 248–254.

Whichard, J.M., Sriranganathan, N., and Pierson, F.W. (2003) Suppression of Salmonella growth by wild-type and large-plaque variants of bacteriophage Felix O1 in liquid culture and on chicken frankfurters. *J Food Prot* **66**: 220–225.

Whitehead, H., East, A., and McIntosh, L. (1953) The so-called 'nascent' bacteriophage phenomenon. *J Dairy Res* **20**: 60–64.

Whitehead, N.A., Barnard, A.M.L., Slater, H., Simpson, N.J.L., and Salmond, G.P.C. (2001) Quorum-sensing in Gram-negative bacteria. *FEMS Microbiol Rev* 25.

Whitehead, N.A., Byers, J.T., Commander, P., Corbelt, M.J., Coulthurst, S.J., Everson, L., Harris, A.K.P., Pemberton, C.L., Simpson, N.J.L., Slater, H., Smith, D.S., Welch, M., Williamson, N., and Salmond, G.P.C. (2002) The

regulation of virulence in phytopathogenic Erwinia species: quorum sensing, antibiotics and ecological considerations. *Antonie Van Leeuwenhoek* **81**: 223–231.

Williams, K.P.., Kassavetis, George, A., Herendeen, Daniel, R., and Geiduschek, E.P. (1994) Regulation of late-gene expression. In *Molecular biology of bacteriophage T4*. Karam, J.D., and Drake, J.W. (eds). American Society of Microbiology, Washington, DC, USA. pp. 161–175.

Williams, S.T., Mortimer, A.M., and Manchester, L. (1987) Ecology of soil bacteriophages. In *Phage ecology.* Gerba, C.P., and Bitton, G. (eds). John Wiley & Sons, New York. pp. 157–179.

Williamson, K.E., Fuhrmann, J.J., Wommack, K.E., and Radosevich, M. (2017) Viruses in soil ecosystems: an unknown quantity within an unexplored territory. *Annu Rev Virol* **4**: 201–219.

Williamson, K.E., Radosevich, M., and Wommack, K.E. (2005) Abundance and diversity of viruses in six Delaware soils. *Appl Environ Microbiol* **71**: 3119–3125.

Williamson, K.E., Wommack, K.E., and Radosevich, M. (2003) Sampling natural viral communities from soil for culture-independent analyses. *Appl Env Microbiol* **69**: 6628–6633.

Willner, I., Baron, R., and Willner, B. (2006) Growing metal nanoparticles by enzymes. *Adv Mater* **18**: 1109–1120.

Wilson, G.G., and Murray, N.E. (1991) Restriction and modification systems. *Annu Rev Genet* **25**: 585–627.

Wolf, J.M. van der, Haan, E. De, Kastelein, P., Krijger, M., Haas, B.H. de, Velvis, H., Mendes, O., Kooman-Gersmann, M., and Zouwen, P. van der (2017) Virulence of Pectobacterium carotovorum subsp. brasiliense on potato compared with that of other Pectobacterium and Dickeya species under climatic conditions prevailing in the Netherlands. *Plant Pathol* **66**: 571–583.

Wommack, K.E., and Colwell, R.R. (2000) Virioplankton : viruses in aquatic ecosystems. *Society* 64.

Wommack, K.E., Williamson, K.E., Helton, R.R., Bench, S.R., and Winget, D.M. (2009) Methods for the isolation of viruses from environmental samples. *Methods Mol Biol* **501**: 3–14.

Wright, R.C.T., Friman, V.-P., Smith, M.C.M., and Brockhurst, M.A. (2018) Cross-resistance is modular in bacteria-phage interactions. *PLoS Biol* **16**: e2006057.

Wyatt, G., and Lund, B. (1981) The effect of antibacterial products on bacterial soft rot of potatoes. *Potato Res* **24**: 315–329.

Xavier, K.B., and Bassler, B.L. (2005) Regulation of uptake and processing of the quorum-sensing autoinducer AI-2 in Escherichia coli. *J Bacteriol* **187**: 238–248.

Yangui, T., Sayadi, S., and Dhouib, A. (2013) Sensitivity of Pectobacterium carotovorum to hydroxytyrosol-rich extracts and their effect on the development of soft rot in potato tubers during storage. *Crop Prot* **53**: 52–57.

Yates, E.A., Philipp, B., Buckley, C., Atkinson, S., Chhabra, S.R., Sockett, R.E., Goldner, M., Dessaux, Y., Cámara, M., Smith, H., and Williams, P. (2002) N-acylhomoserine lactones undergo lactonolysis in a pH-, temperature-, and acyl chain length-dependent manner during growth of Yersinia pseudotuberculosis and Pseudomonas aeruginosa. *Infect Immun* **70**: 5635–5646.

Ye, J., Kostrzynska, M., Dunfield, K., and Warriner, K. (2009) Evaluation of a biocontrol preparation consisting of Enterobacter asburiae JX1 and a lytic bacteriophage cocktail to suppress the growth of Salmonella Javiana associated with tomatoes. *J Food Prot* **72**: 2284–2292.

Yemini, M., Levi, Y., Yagil, E., and Rishpon, J. (2007) Specific electrochemical phage sensing for Bacillus cereus and Mycobacterium smegmatis. *Bioelectrochemistry* **70**: 180–184.

Yin, J. (1993) Evolution of bacteriophage T7 in a growing plaque. *J Bacteriol* **175**: 1272–1277.

Yoichi, M., Abe, M., Miyanaga, K., Unno, H., and Tanji, Y. (2005) Alteration of tail fiber protein gp38 enables T2 phage to infect Escherichia coli O157:H7. *J Biotechnol* **115**: 101–107.

You, L., Suthers, P.F., and Yin, J. (2002) Effects of Escherichia coli physiology on growth of phage T7 in vivo and in silico. *J Bacteriol* **184**: 1888–1894.

You, L., and Yin, J. (1999) Amplification and spread of viruses in a growing plaque. *J Theor Biol* **200**: 365–373.

Young, I., Wang, I., and Roof, W.D. (2000) Phages will out: strategies of host cell lysis. *Trends Microbiol* **8**: 120–128.

Young, R. (1992a) Bacteriophage lysis: mechanism and regulation. *Microbiol Rev* **56**: 430–81.

Young, R. (1992b) Bacteriophage lysis: mechanism and regulation. *Microbiol Rev* **56**: 430–81.

Young, R. (2002) Bacteriophage holins: deadly diversity. *J Mol Microbiol Biotechnol* **4**: 21–36.

Young, R. (2014) Phage lysis: three steps, three choices, one outcome. *J Microbiol* **52**: 243–258.

Young, R., and Gill, J.J. (2015) Phage therapy redux--What is to be done? *Science (80-)* **350**: 1163–1164.

Yu, F., and Mizushima, S. (1982) Roles of lipopolysaccharide and outer membrane protein ompc of Escherichia coli K-12 in the receptor function for bacteriophage T4. *J Bacteriol* **151**: 718–722.

Yuzenkova, J., Nechaev, S., Berlin, J., Rogulja, D., Kuznedelov, K., Inman, R., Mushegian, A., and Severinov, K. (2003) Genome of Xanthomonas oryzae bacteriophage Xp10: an odd T-odd phage. *J Mol Biol* **330**: 735–48.

Zavriev, S.K., and Shemyakin, M.F. (1982) RNA polymerase-dependent mechanism for the stepwise T7 phage DNA transport from the virion into E. coli. *Nucleic Acids Res* **10**: 1635–52.

Zhang, H.-B., Wang, L.-H., and Zhang, L.-H. (2002) Genetic control of quorum-sensing signal turnover in Agrobacterium tumefaciens. *Proc Natl Acad Sci U S A* **99**: 4638–4643.

Zhang, J., Liu, X., and Li, X.-J. (2015) Bioinformatic analysis of phage AB3, a phiKMV-like virus infecting Acinetobacter baumannii. *Genet Mol Res* **14**: 190–198.

Zhang, X., and Studier, F.W. (1995) Isolation of transcriptionally active mutants of T7 RNA polymerase that do not support phage growth. *J Mol Biol* **250**: 156–68.

Zhang, Y., Fan, Q., and Loria, R. (2016) A re-evaluation of the taxonomy of phytopathogenic genera Dickeya and Pectobacterium using whole-genome sequencing data. *Syst Appl Microbiol* **39**: 252–259.

Zhao, M., Sun, B., Wu, L., Gao, Q., Wang, F., Wen, C., Wang, M., Liang, Y., Hale, L., Zhou, J., and Yang, Y. (2016) Zonal soil type determines soil microbial responses to maize cropping and fertilization. *mSystems* **1**: e00075-16.

Zhou, Y., Marar, A., Kner, P., and Ramasamy, R.P. (2017) Charge-directed immobilization of bacteriophage on nanostructured electrode for whole-cell electrochemical biosensors. *Anal Chem* **89**: 5734–5741.

Zhu, J., and Winans, S.C. (2001) The quorum-sensing transcriptional regulator TraR requires its cognate signaling ligand for protein folding, protease resistance and dimerization. *Proc Natl Acad Sci U S A* **98**: 1507–1512.

Zimkus, A.Z., Zavriev, S.K., and Grinius, L.L. (1986) [The role of ATP and membrane potential in the penetration of phage T17 DNA into the cell during infection]. *Mol Biol (Mosk)* **20**: 185–91.

Zmasek, C.M., and Eddy, S.R. (2001) ATV: display and manipulation of annotated phylogenetic trees. *Bioinformatics* **17**: 383–4.

Zweckstetter, M., Hummer, G., and Bax, A. (2004) Prediction of charge-induced molecular alignment of biomolecules dissolved in dilute liquid-crystalline phases. *Biophys J* **86**: 3444–60.

10.0 Appendix

a)

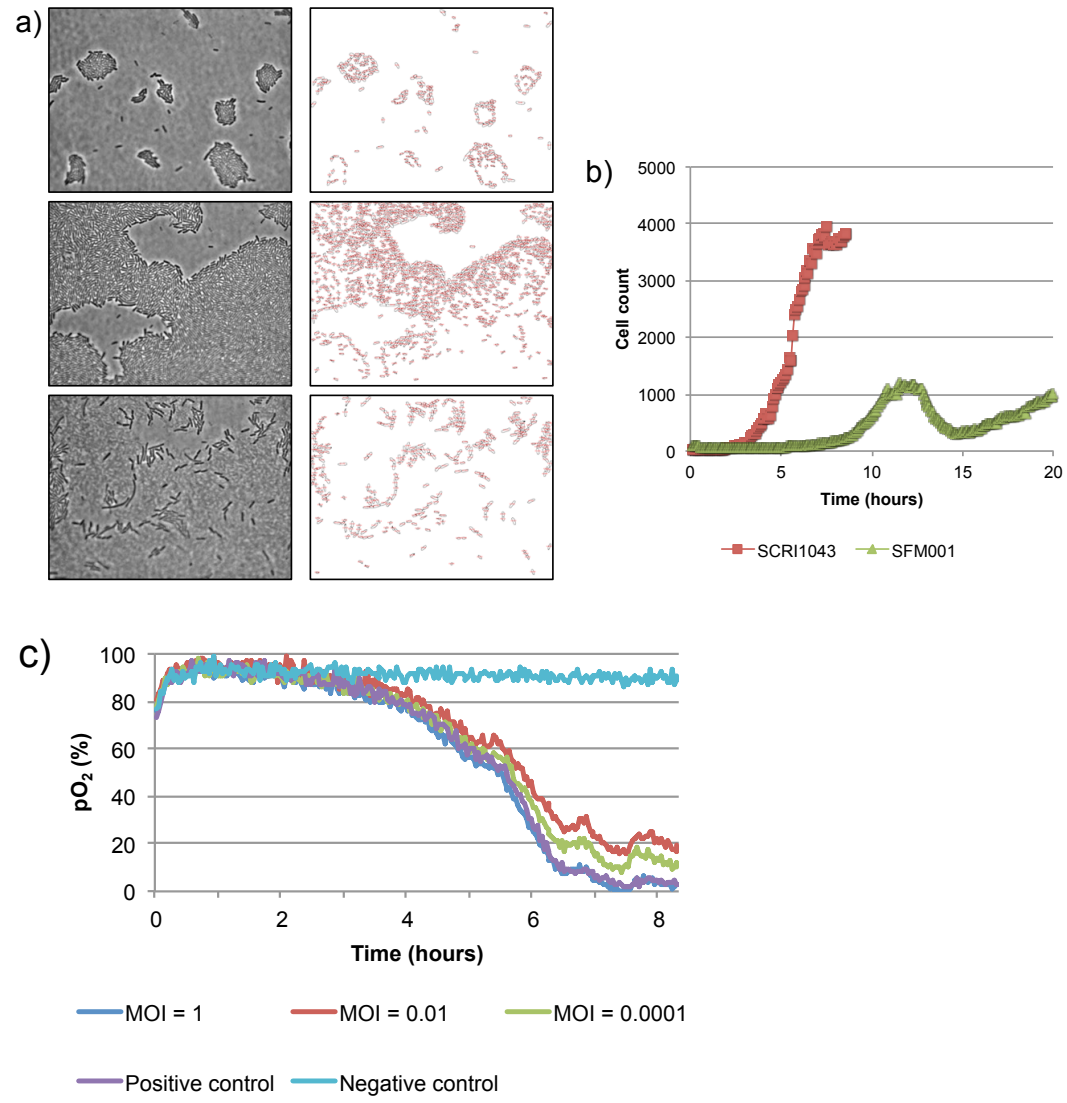

Appendix (a): Infection kinetics on solid and liquid media experiments using ϕSFM001. (a) Images were taken every 5 minutes for up to 20 hours at 1000X magnification using a Nikon TE 2000S inverted microscope and a Hamamatsu Orca-285 Firewire Digital CCD Camera (left column images in a). These images were then processed and quantified using ImageJ 1.50i software (right column images in a) and the results were plotted and compared to a positive control using the growth of their host bacteria alone (red line, b). The OxoPlate® method (c) measured fluorescence intensity every 2 minutes for eight hours, the results were normalised and plotted as pO_2 (in percentage) per time point using *Pectobacterium atrosepticum* SCRI 1043 under the same conditions, being each value the result from six different readings.

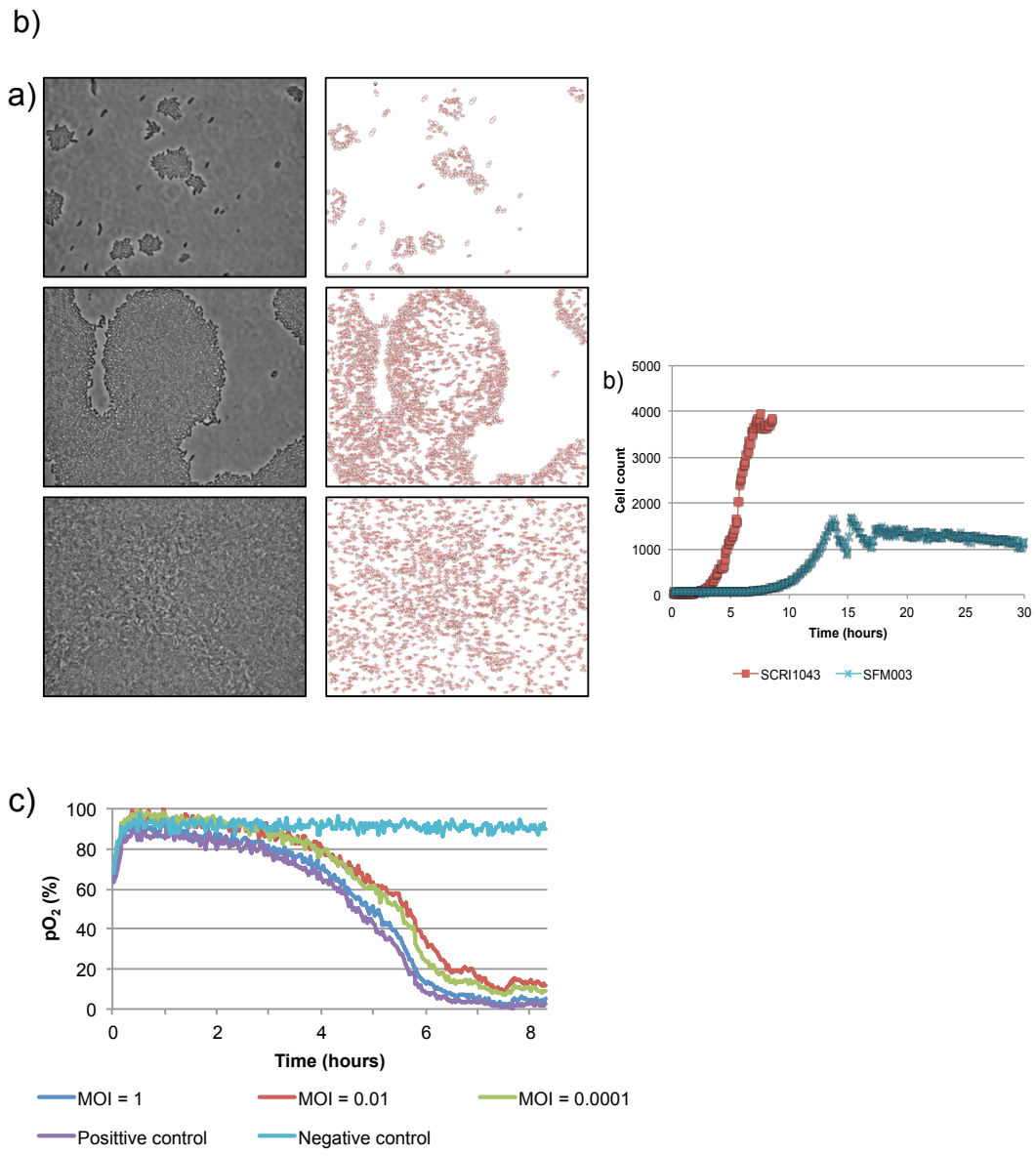

Appendix (b): Infection kinetics on solid and liquid media experiments using ϕSFM003. (a) Images were taken every 5 minutes for up to 30 hours at 1000X magnification using a Nikon TE 2000S inverted microscope and a Hamamatsu Orca-285 Firewire Digital CCD Camera (left column images in a). These images were then processed and quantified using ImageJ 1.50i software (right column images in a) and the results were plotted and compared to a positive control using the growth of their host bacteria alone (red line, b). The OxoPlate® method (c) measured fluorescence intensity every 2 minutes for eight hours, the results were normalised and plotted as pO_2 (in percentage) per time point using *Pectobacterium atrosepticum* SCRI 1043 under the same conditions, being each value the result from six different readings.

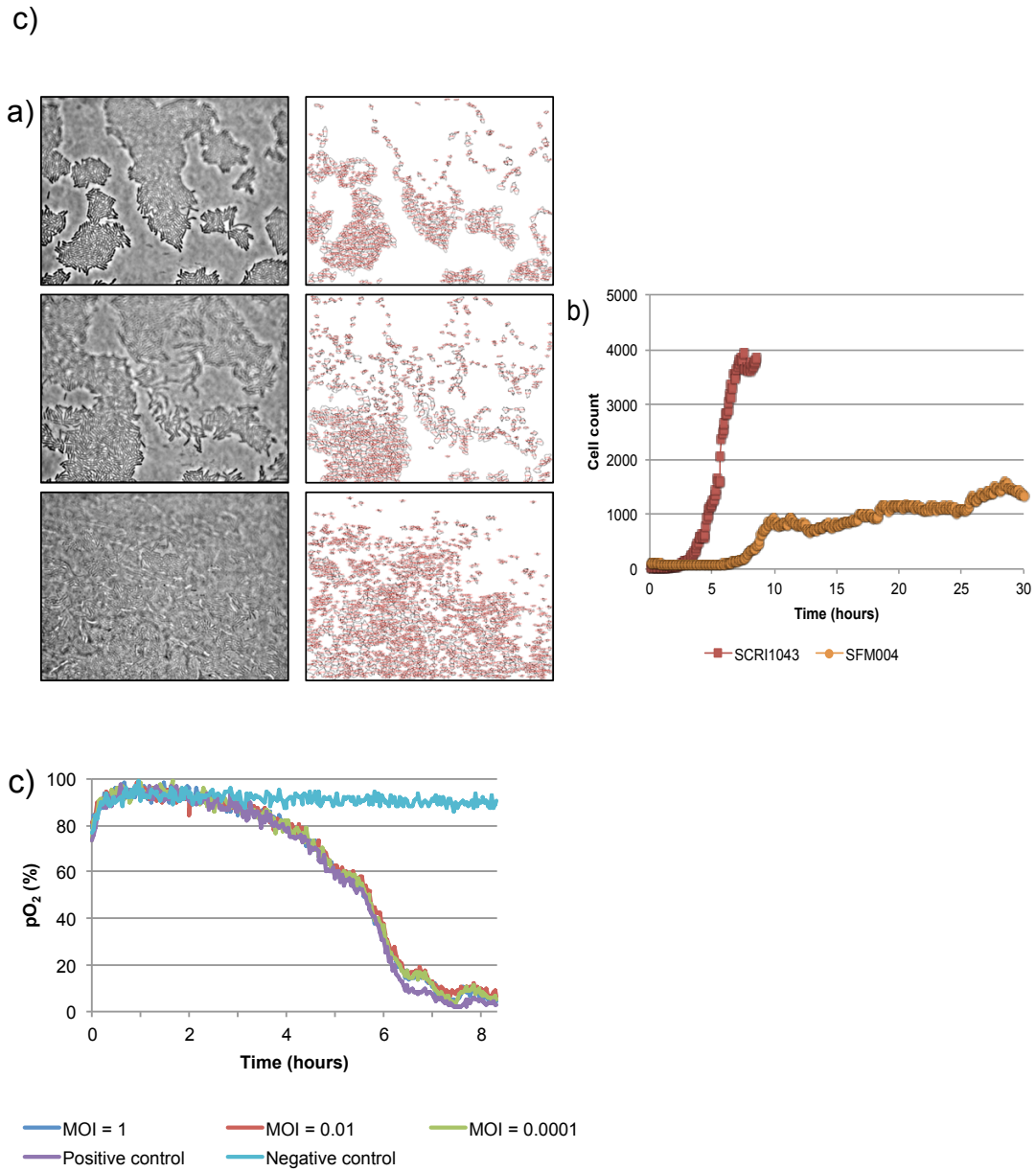

Appendix (c): Infection kinetics on solid and liquid media experiments using ϕSFM004. (a) Images were taken every 5 minutes for up to 30 hours at 1000X magnification using a Nikon TE 2000S inverted microscope and a Hamamatsu Orca-285 Firewire Digital CCD Camera (left column images in a). These images were then processed and quantified using ImageJ 1.50i software (right column images in a) and the results were plotted and compared to a positive control using the growth of their host bacteria alone (red line, b). The OxoPlate® method (c) measured fluorescence intensity every 2 minutes for eight hours, the results were normalised and plotted as pO_2 (in percentage) per time point using *Pectobacterium atrosepticum* SCRI 1043 under the same conditions, being each value the result from six different readings.

d)

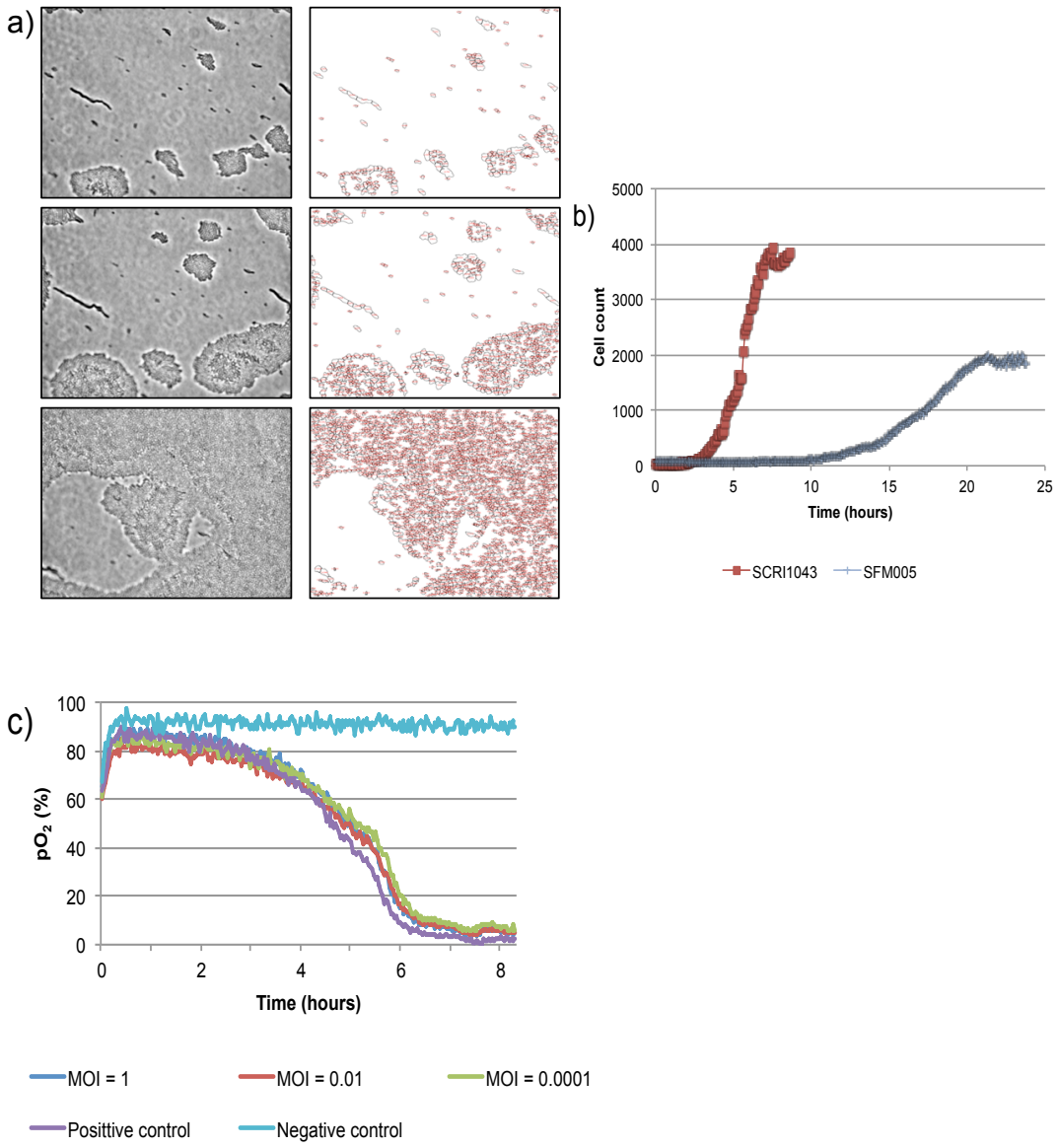

Appendix (d): Infection kinetics on solid and liquid media experiments using ϕSFM005. (a) Images were taken every 5 minutes for up to 25 hours at 1000X magnification using a Nikon TE 2000S inverted microscope and a Hamamatsu Orca-285 Firewire Digital CCD Camera (left column images in a). These images were then processed and quantified using ImageJ 1.50i software (right column images in a) and the results were plotted and compared to a positive control using the growth of their host bacteria alone (red line, b). The OxoPlate® method (c) measured fluorescence intensity every 2 minutes for eight hours, the results were normalised and plotted as pO_2 (in percentage) per time point using *Pectobacterium atrosepticum* SCRI 1043 under the same conditions, being each value the result from six different readings.

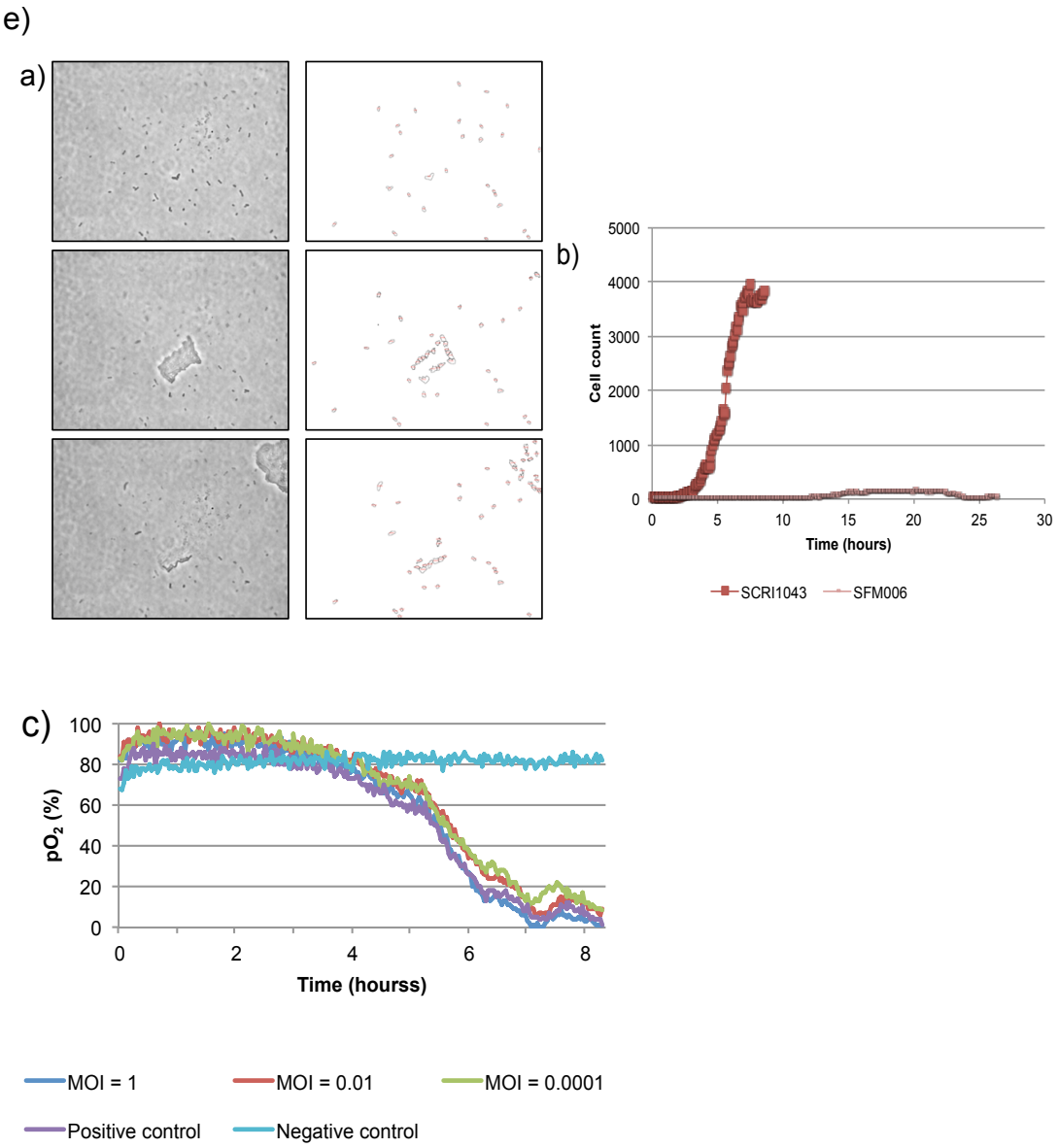

Appendix (e): Infection kinetics on solid and liquid media experiments using ϕSFM006. (a) Images were taken every 5 minutes for up to 25 hours at 1000X magnification using a Nikon TE 2000S inverted microscope and a Hamamatsu Orca-285 Firewire Digital CCD Camera (left column images in a). These images were then processed and quantified using ImageJ 1.50i software (right column images in a) and the results were plotted and compared to a positive control using the growth of their host bacteria alone (red line, b). The OxoPlate® method (c) measured fluorescence intensity every 2 minutes for eight hours, the results were normalised and plotted as pO_2 (in percentage) per time point using *Pectobacterium atrosepticum* SCRI 1043 under the same conditions, being each value the result from six different readings.

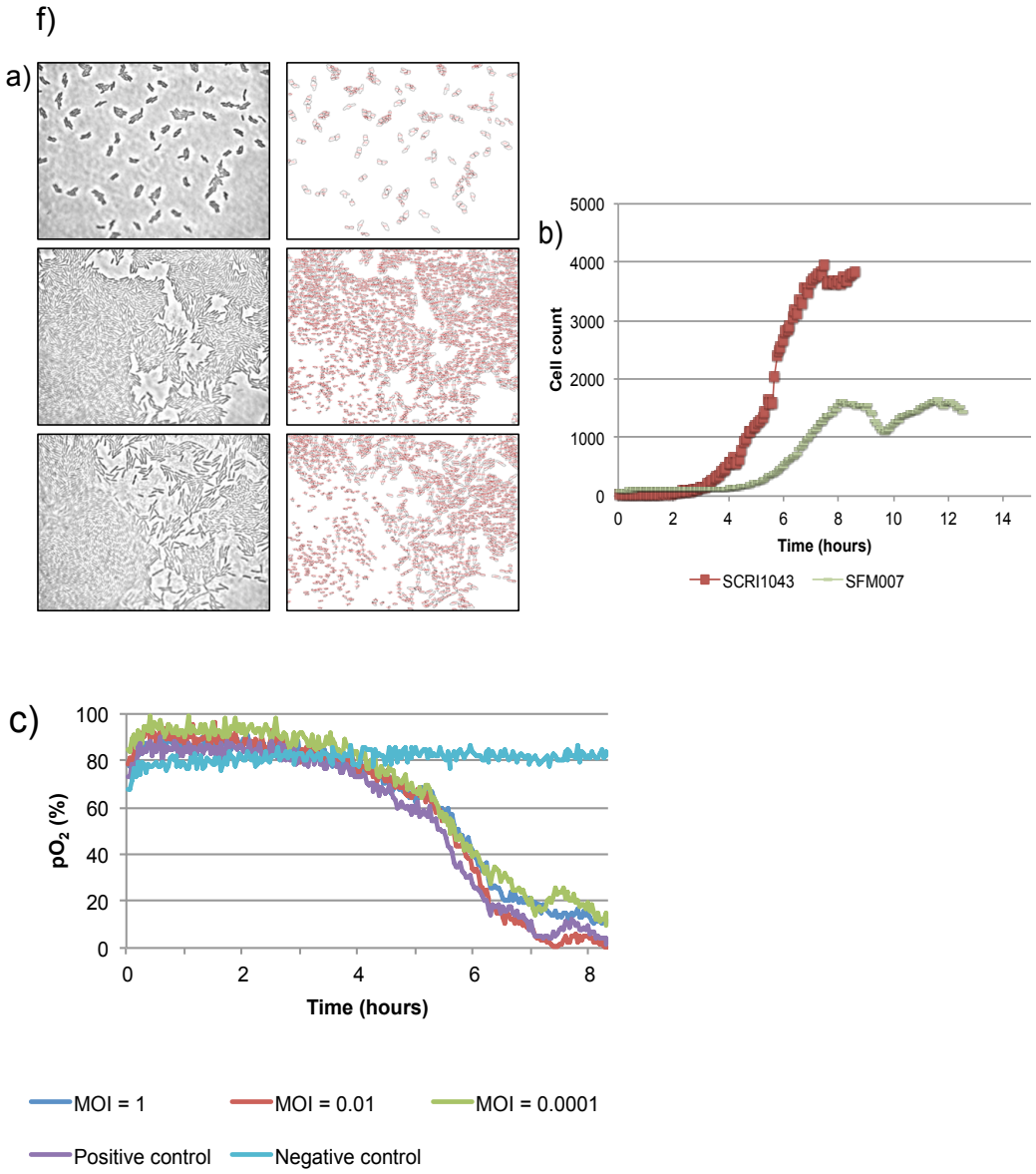

Appendix (f): Infection kinetics on solid and liquid media experiments using ϕSFM007. (a) Images were taken every 5 minutes for up to 15 hours at 1000X magnification using a Nikon TE 2000S inverted microscope and a Hamamatsu Orca-285 Firewire Digital CCD Camera (left column images in a). These images were then processed and quantified using ImageJ 1.50i software (right column images in a) and the results were plotted and compared to a positive control using the growth of their host bacteria alone (red line, b). The OxoPlate® method (c) measured fluorescence intensity every 2 minutes for eight hours, the results were normalised and plotted as pO_2 (in percentage) per time point using *Pectobacterium atrosepticum* SCRI 1043 under the same conditions, being each value the result from six different readings.

g)

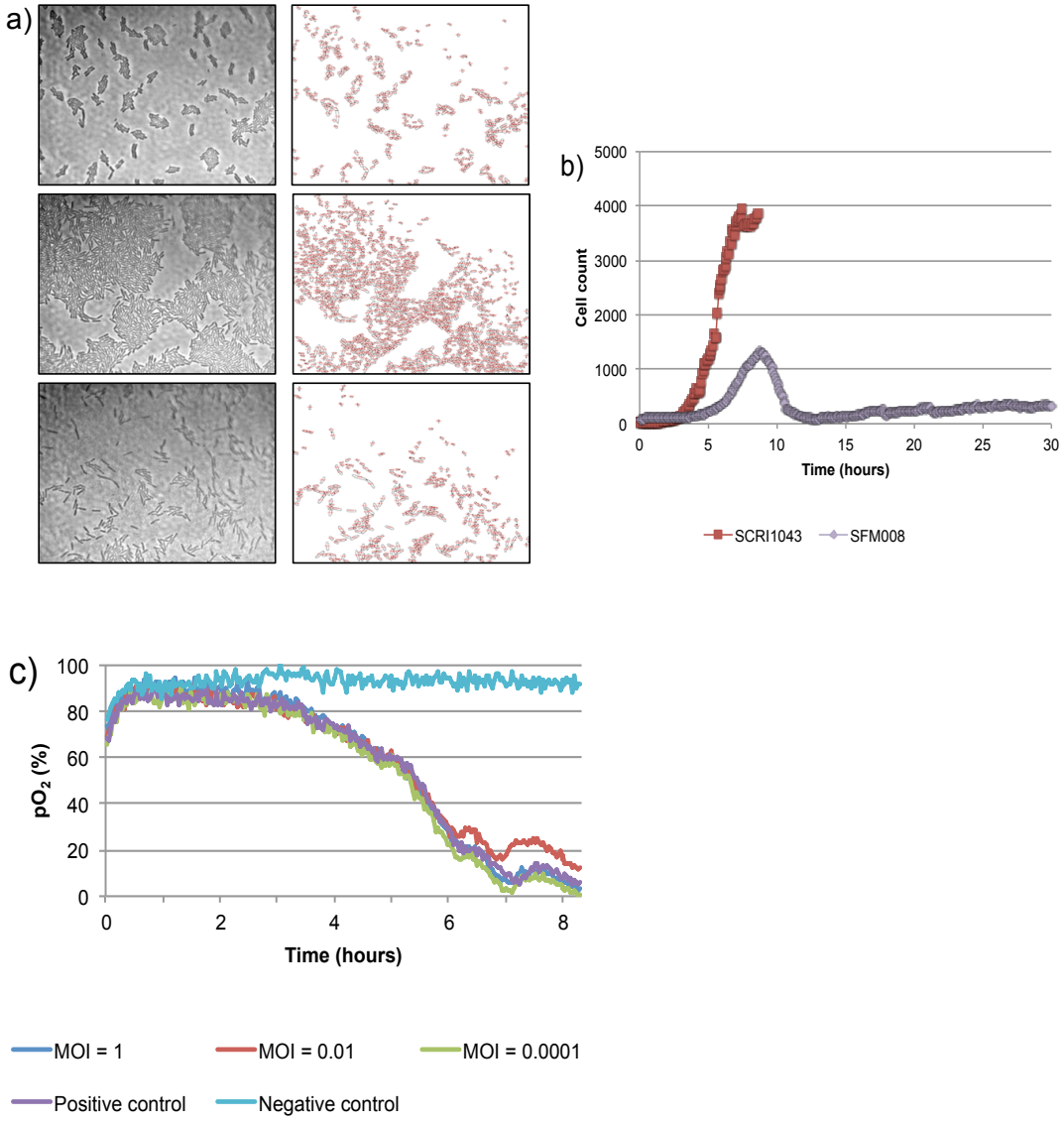

Appendix (g): Infection kinetics on solid and liquid media experiments using ϕSFM008. (a) Images were taken every 5 minutes for up to 30 hours at 1000X magnification using a Nikon TE 2000S inverted microscope and a Hamamatsu Orca-285 Firewire Digital CCD Camera (left column images in a). These images were then processed and quantified using ImageJ 1.50i software (right column images in a) and the results were plotted and compared to a positive control using the growth of their host bacteria alone (red line, b). The OxoPlate® method (c) measured fluorescence intensity every 2 minutes for eight hours, the results were normalised and plotted as pO_2 (in percentage) per time point using *Pectobacterium atrosepticum* SCRI 1043 under the same conditions, being each value the result from six different readings.

h)

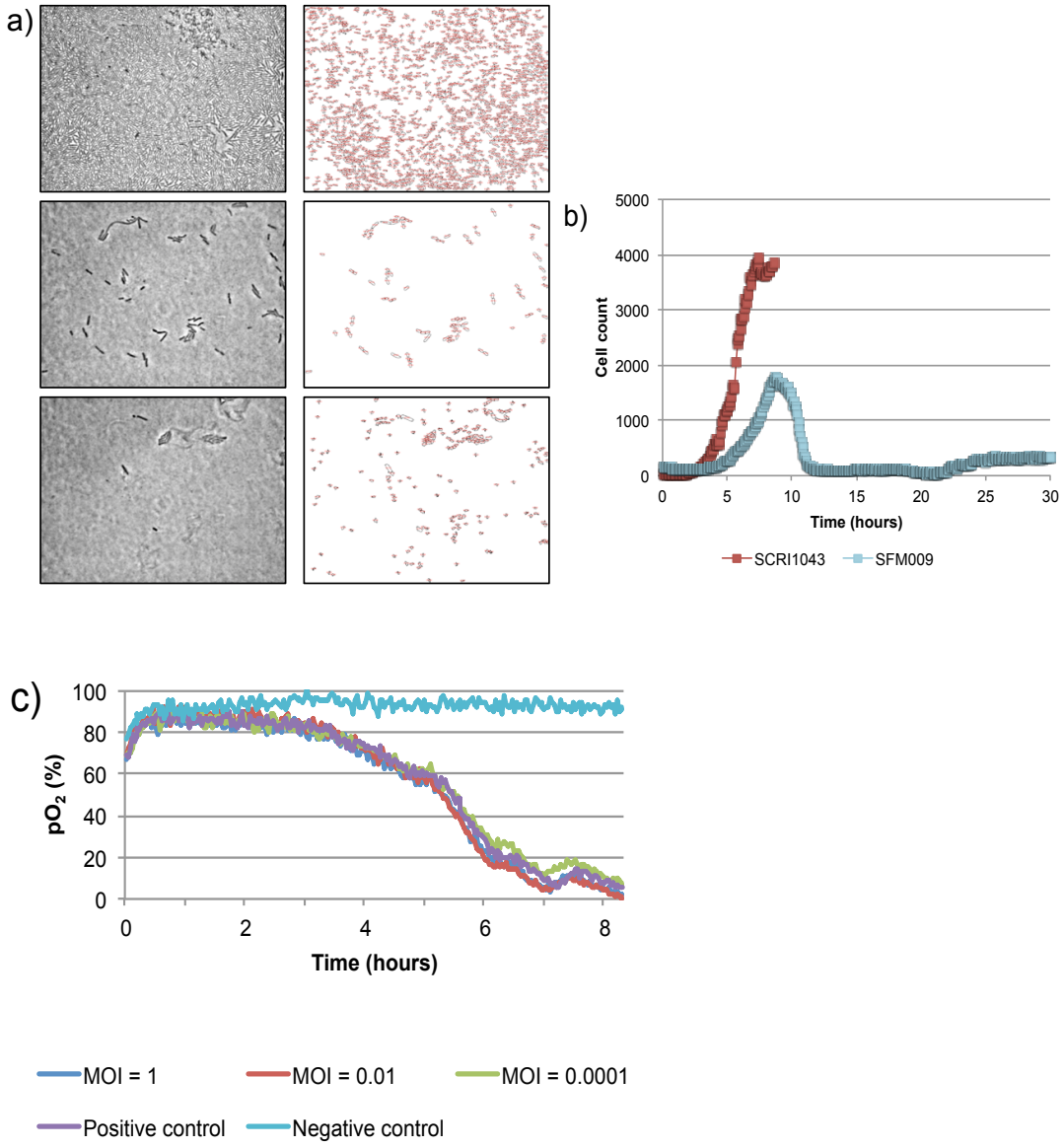

Appendix (h): Infection kinetics on solid and liquid media experiments using ϕSFM009. (a) Images were taken every 5 minutes for up to 30 hours at 1000X magnification using a Nikon TE 2000S inverted microscope and a Hamamatsu Orca-285 Firewire Digital CCD Camera (left column images in a). These images were then processed and quantified using ImageJ 1.50i software (right column images in a) and the results were plotted and compared to a positive control using the growth of their host bacteria alone (red line, b). The OxoPlate® method (c) measured fluorescence intensity every 2 minutes for eight hours, the results were normalised and plotted as pO_2 (in percentage) per time point using *Pectobacterium atrosepticum* SCRI 1043 under the same conditions, being each value the result from six different readings.

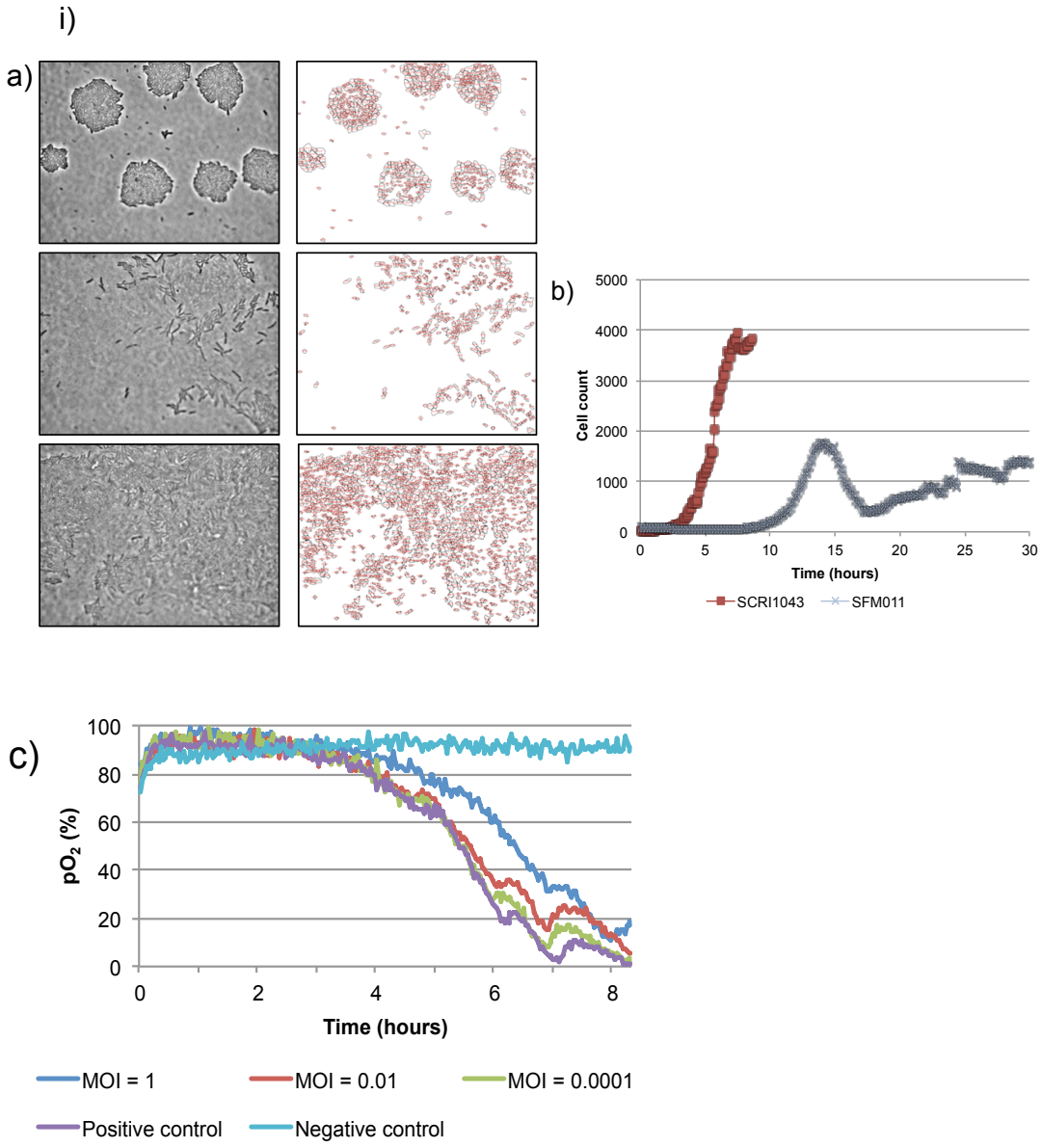

Appendix (i): Infection kinetics on solid and liquid media experiments using ϕSFM011. (a) Images were taken every 5 minutes for up to 30 hours at 1000X magnification using a Nikon TE 2000S inverted microscope and a Hamamatsu Orca-285 Firewire Digital CCD Camera (left column images in a). These images were then processed and quantified using ImageJ 1.50i software (right column images in a) and the results were plotted and compared to a positive control using the growth of their host bacteria alone (red line, b). The OxoPlate® method (c) measured fluorescence intensity every 2 minutes for eight hours, the results were normalised and plotted as pO_2 (in percentage) per time point using *Pectobacterium atrosepticum* SCRI 1043 under the same conditions, being each value the result from six different readings.

j)

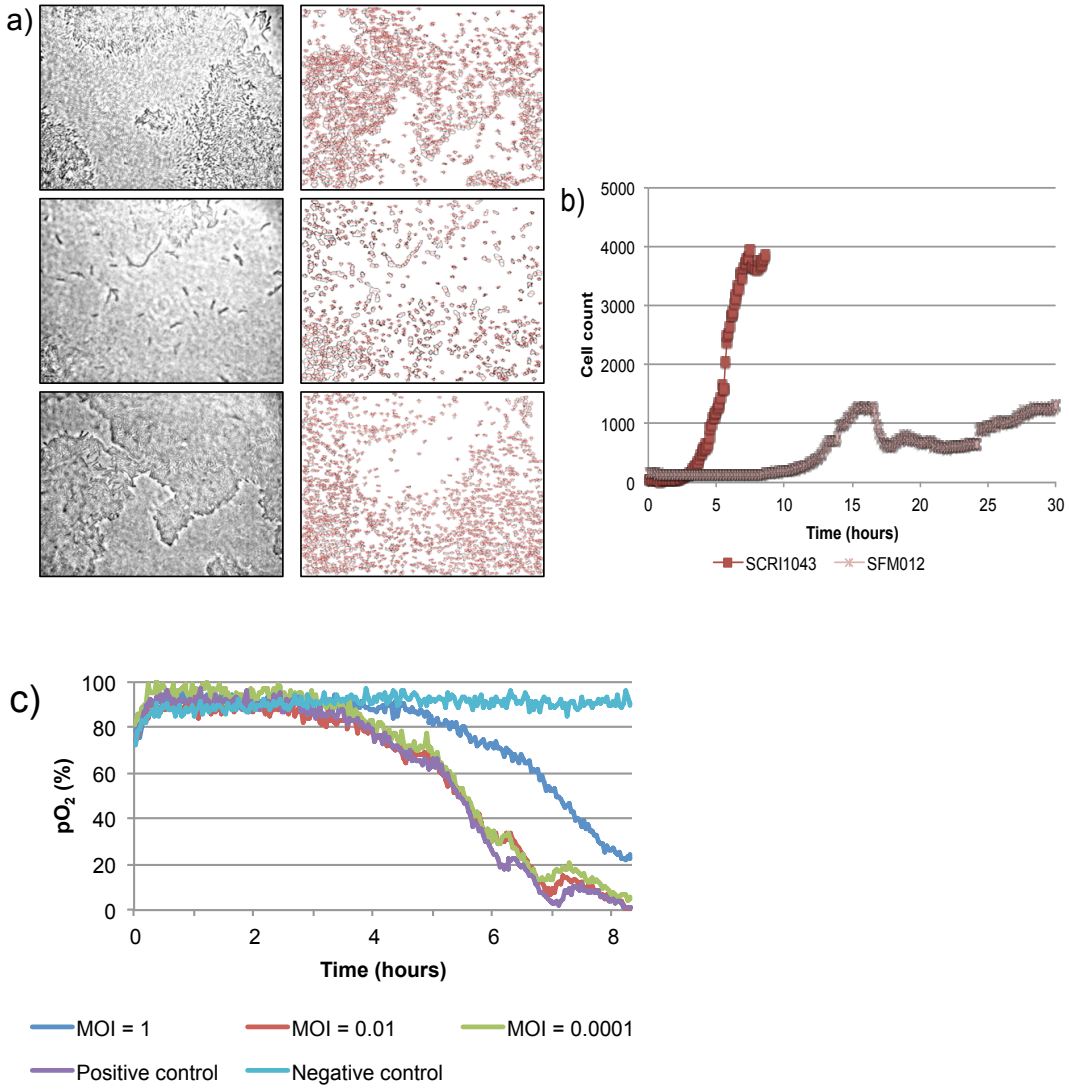

Appendix (j): Infection kinetics on solid and liquid media experiments using ϕSFM012. (a) Images were taken every 5 minutes for up to 30 hours at 1000X magnification using a Nikon TE 2000S inverted microscope and a Hamamatsu Orca-285 Firewire Digital CCD Camera (left column images in a). These images were then processed and quantified using ImageJ 1.50i software (right column images in a) and the results were plotted and compared to a positive control using the growth of their host bacteria alone (red line, b). The OxoPlate® method (c) measured fluorescence intensity every 2 minutes for eight hours, the results were normalised and plotted as pO_2 (in percentage) per time point using *Pectobacterium atrosepticum* SCRI 1043 under the same conditions, being each value the result from six different readings.

k)

Gene number	Position	Pfam	InterProScan	BLASTP
1	0-1760	-	-	DNA packaging protein B (*Yersinia* phage vB_Yen_AP10, *Escherichia* phage ECA2) 0
2	2066-2224	-	-	-
3	3179-3673	-	-	Hypothetical protein (S. pyogenes) 1e-47
4	3670-3867	-	-	Hypothetical protein (Klebsiella phage) 4e-24
5	3851-4249	-	-	Hypothetical protein PP74_02 (Pectobacterium phage PP74) 1e-04
6	4280-5221	-	-	Protein kinase (Stenotrophomonas phage IME15) 1e-59
7	5251-6078	BRO N-terminal domain (275 aa.)	BRO family, N-terminal domain 2.9e-11	Hypothetical protein (P. atrosepticum) 3e-122
8	6149-7054	DNA-directed RNA polymerase, N-terminal 301 aa.	DNA-directed RNA polymerase N-terminal 2e-09	RNA polymerase (Yersinia phage vB_Yen_AP10) 7e-116
9	7153-8079	DNA-directed RNA polymerase, phage-type 308 aa.	DNA-dependent RNA polymerase 1.4e-46	DNA-dependent RNA polymerase (Enterobacteriaceae) 5e-173
10	8118-8867	DNA-directed RNA polymerase, phage-type 249 aa.	DNA-dependent RNA polymerase 1.3e-45	RNA polymerase (Enterobacteria phage T7) 2e-136
11	9025-9582	-	-	Hypothetical protein (Escherichia phage ECA2) 1e-14
12	9639-9821	-	-	Putative lipid II flippase FtsIU (Mycobacterium) 3.3
13	9899-10087	-	-	BTB/Poz and MATH domain-containing protein 2 (Serratia italica) 5.1
14	10121-11230	DNA ligase, ATP-dependent (phage T3-type) 369 aa.	ATP-dependent DNA ligase domain 3.7e-35	DNA ligase (Escherichia phage HZ2R8) 1e-166
15	11232-11339	-	-	Hypothetical protein (Herbaspirillum sp. WT00C) 6.0
16	11429-11689	-	-	Hypothetical protein P2B40kb_p008 (Pectobacterium phage DU_PP_II) 2e-40

17	11686-12480	-	-	Hypothetical protein (Serratia phage SM9-3Y) 2e-46
18	12477-12638	-	-	Hypothetical protein sh2_0013 (Citrobacter phage SH2) 3e-05
19	12635-12832	RNA polymerase inhibitor 65 aa.	RNA polymerase inhibitor 3.6e-22	RNA polymerase inhibitor (Escherichia phage HZ2R8 and phage EG1, and Enterobacteria phage T7) 1e-20
20	13320-13634	-	-	ssDNA-binding protein (Serratia phage SM9-3Y and Citrobacter phage SH1) 1e-24
21	14093-14389	Peptidoglycan recognition protein family domain 98aa.	-	Endolysin (Yersinia phage vB_Yen_AP10) 2e-27
22	14386-14541	N-acetylmuramoyl-L-alanine domain superfamily 51 aa.	-	Endolysin (Pectobacterium phage DU_PP_II) 7e-22
23	14626-16386	Phage T7 (gp 4), DNA primase/helicase, N-terminal 586 aa.	DNA B-like helicase C-terminal domain 1.4e-15	DNA primase/helicase (Yersinia phage phiYe-F10, Serratia phage 2050H2 or Citrobacter phage phiCFP-1) 0
24	16401-16670	-	-	Hypothetical protein RU59_00016 (Enterobacter phage phiEap-1) 4e-08
25	16672-16980	Inhibitor of toxin/antitoxin system 102 aa.	Inhibitor of toxin/antitoxin system (gp 4.5) 1.5e-51	Hypothetical protein (Klebsiella phage vB__kp1) 1e-29
26	17052-17399	-	-	-
27	17411-19588	DNA polymerase A 725 aa.	DNA polymerase family A 2.5e-51	DNA-directed DNA polymerase (Klebsiella phage K5) 0
28	19588-19767	-	-	Portal protein (Pectobacterium phage DU_PP_II) 2e-07
29	19771-20064	Phage T7, gp 5.5 97 aa.	-	Hypothetical protein (Yersinia phage vB_YenP_AP10) 0.037
30	20015-20218	-	-	HNS-binding protein (Pectobacterium phage DU_PP_II) 2e-07
31	20262-20681	-	-	Hypothetical protein (Escherichia phage ZG49) 2e-12
32	20674-21594	-	-	Exonuclease (Pectobacterium phage DU_PP_II) 3e-174
33	21570-21695	-	-	-
34	21884-22129	Phage T7-like, gp 6.5 81 aa.	Hypothetical protein (DUF2717) 7.7e-30	Hypothetical protein (Yersinia phage vB_YenP_AP10) 3e-35

36	22420-22710	Phage T7-like virion assembly protein 96 aa.	Phage T7 virion assembly protein 2.2e-16	Tail assembly protein (Pectobacterium phage DU_PP_II) 8e-27
37	22727-24349	Head-to-tail connector protein, podovirus-type 540 aa.	Phage head-to-tail connecting protein 1.6e-100	Head to tail joining protein (Yersinia phage vB_YenP_AP10) 0
38	24414-25340	Phage T7 capsid assembly 308 aa.	Phage T7 capsid assembly protein 1e-49	Capsid assembly protein (Yersinia phage vB_YenP_AP5) 8e-133
39	25437-26468	-	-	Capsid and scaffold protein (Pectobacterium phage DU_PP_II) 0
40	27102-27692	Tail tubular protein, gp 11	Tail tubular protein 1.6e-56	Tail tubular protein A (Pectobacterium phage DU_PP_II) 3e-118
41	27986-30094	-	-	Tail tubular protein B (Pectobacterium phage DU_PP_II) 0
42	30175-30582	Phage T7, probable scaffold protein gp 13 135 aa.	Hypothetical protein (DUF2833) 1.4e-39	Internal virion protein A (Pectobacterium phage PP74) 6e-51
43	30612-30971	-	-	Internal virion protein B (Yersinia phage vB_YenP_AP10) 8e-45
44	30974-33238	-	-	Internal virion protein C (Yersinia phage vB_YenP_AP10 and Klebsiella phage KP32) 0
45	33258-33746	Lysozyme-like domain superfamily 162 aa.	Transglycosylase SLT domain 9.5e-24	Internal virion protein D (Yersinia phage vB_YenP_AP10) 3e-76
46	33922-37239	-	-	Internal virion protein D (Yersinia phage vB_YenP_AP10) 0
47	37307-38830	Phage T7 tail fibre protein 507 aa.	Phage T7 tail fibre protein 1.2e-52	Tail fibre protein (Pectobacteirum phage DU_PP_II) 0
48	38929-39042	-	-	-
49	39263-39526	DNA maturase, phage T7-like 87 aa.	DNA packaging protein 1.1e-34	DNA packaging protein A (Yersinia phage vB_YenP_AP10) 5e-40
50	39632-40075	Spanin, inner membrane subunit, T7likevirus-type 147 aa.	Phage Rz lysis protein 2.1e-06	Hypothetical protein P2B40kb_p040 (Pectobacterium phage DU_PP_II) 8e-48

Appendix (k): Detailed CDS prediction of ϕSFM002 performed by PROKKA and the individual analysis using InterProScan, Pfam and BLASTP.

I)

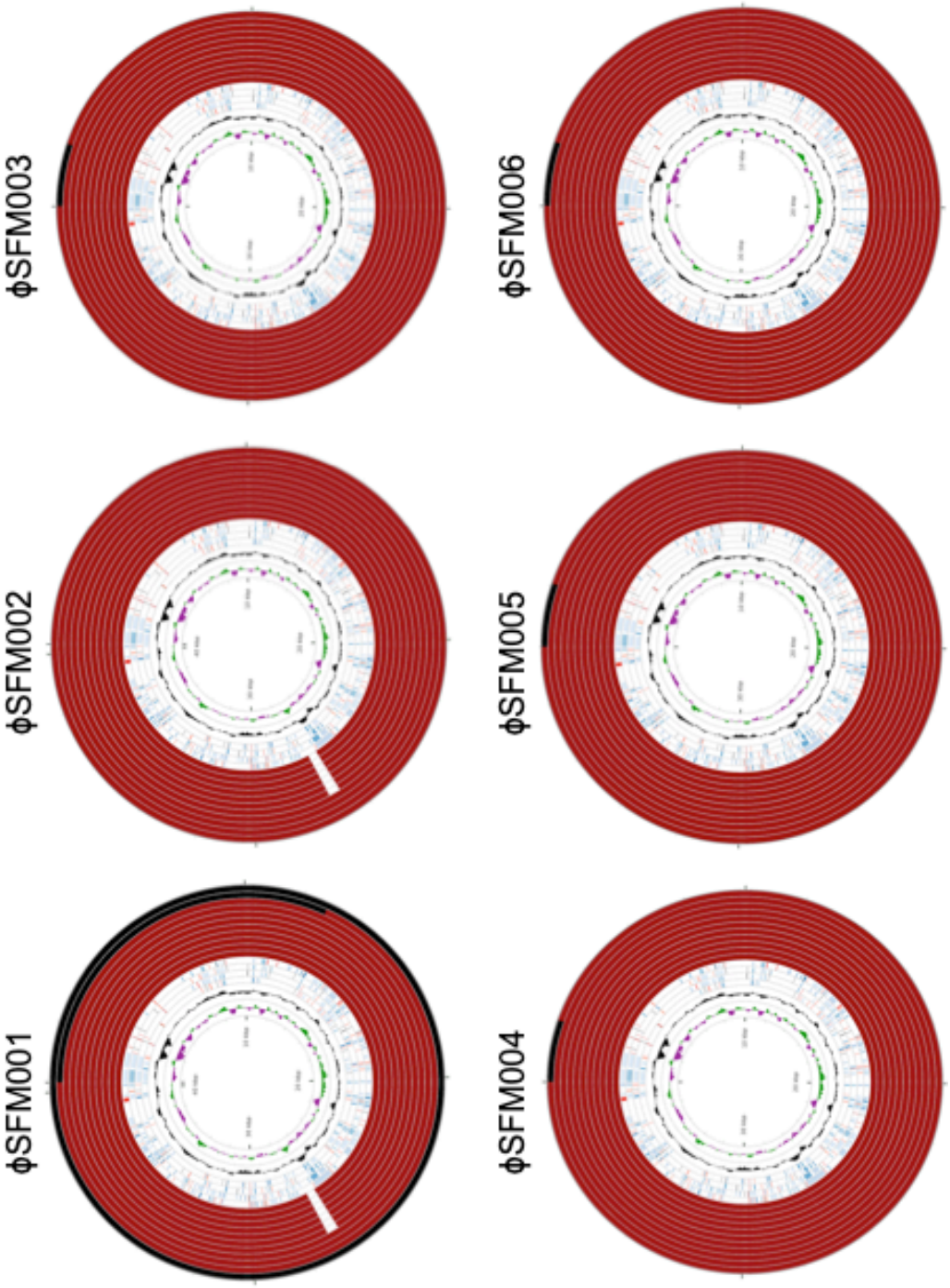

Appendix (I): Nucleotide sequence comparison using CCT view. All phage genomes were manually colinearised placing the starting arbitrary point at the start of the open reading frame of the large terminase subunit gene (1), then each phage was compared individually to each other and the four closest phages from BLASTP results were added (ϕDU_PP_II, ϕPP74, ϕT7 and ϕvB_YenP_AP10 in the internal ring), dark red shows 90% similarity whereas black shows 100%. GC content and GC skews (+ and -) were shown as the innermost rings.

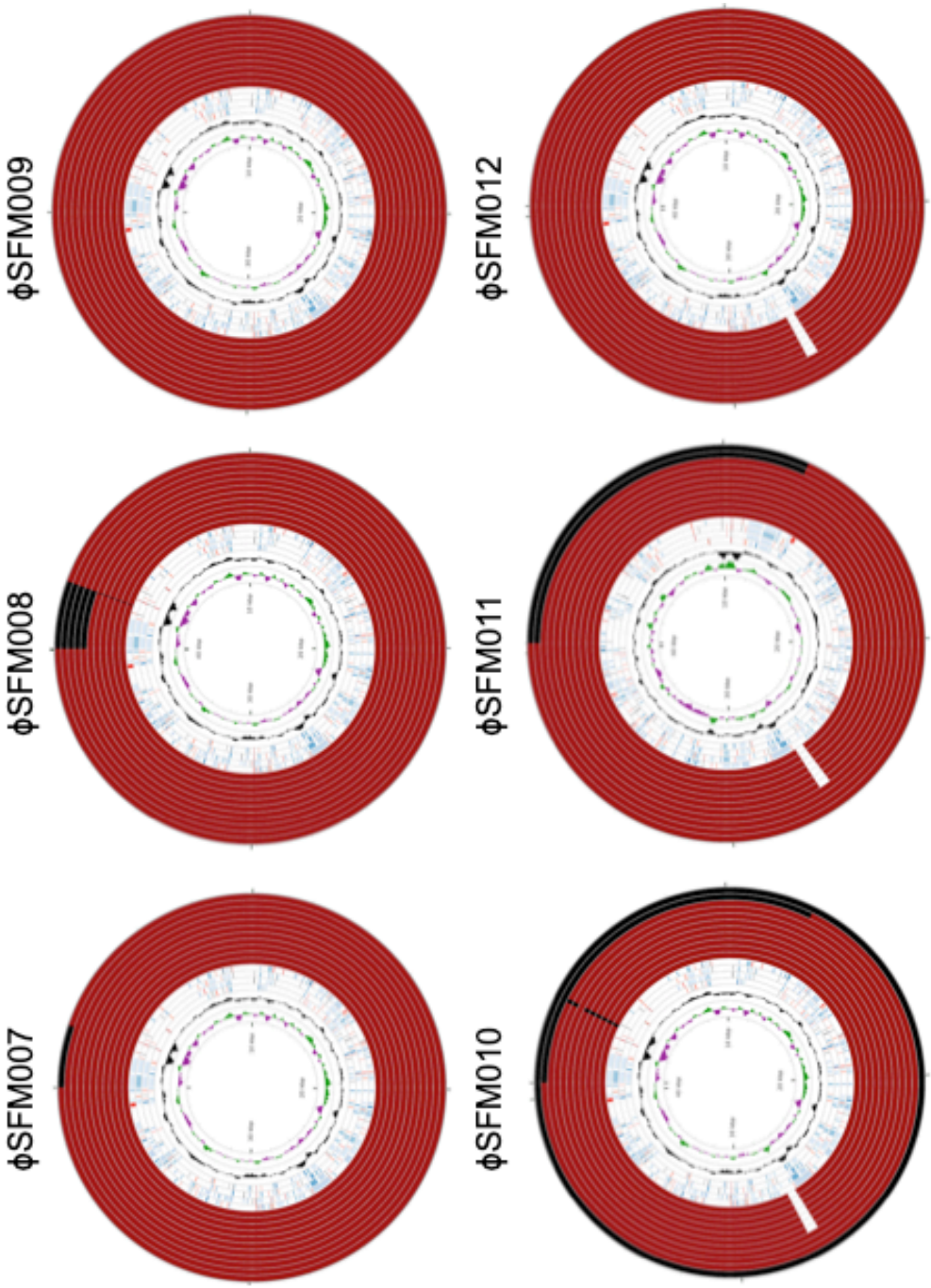

Appendix (I, cont.): Nucleotide sequence comparison using CCT view. All phage genomes were manually colinearised placing the starting arbitrary point at the start of the open reading frame of the large terminase subunit gene (1), then each phage was compared individually to each other and the four closest phages from BLASTP results were added (ϕDU_PP_II, ϕPP74, ϕT7 and ϕvB_YenP_AP10 in the internal ring), dark red shows 90% similarity whereas black shows 100%. GC content and GC skews (+ and -) were shown as the innermost rings.

m)

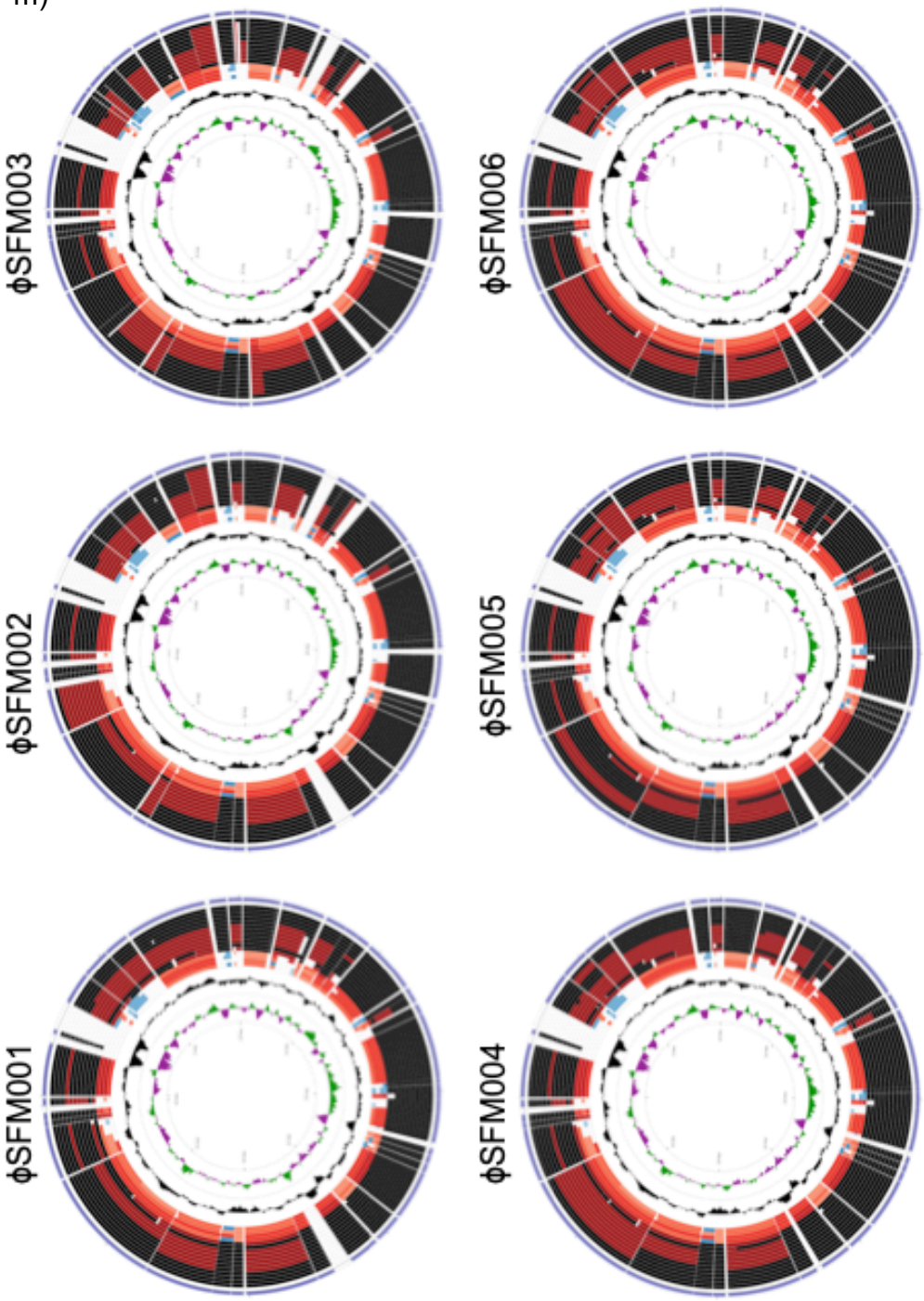

Appendix (m): Phage genome organisation comparison using CCT view. All phage genomes were manually colinearised placing the starting arbitrary point at the start of the open reading frame of the large terminase subunit gene (1), then each phage was compared individually to each other and the four closest phages from BLASTP results were added (ϕDU_PP_II, ϕPP74, ϕT7 and ϕvB_YenP_AP10 in the internal ring), dark red shows 90% similarity whereas black shows 100%. GC content and GC skews (+ and -) were shown as the innermost rings.

m)

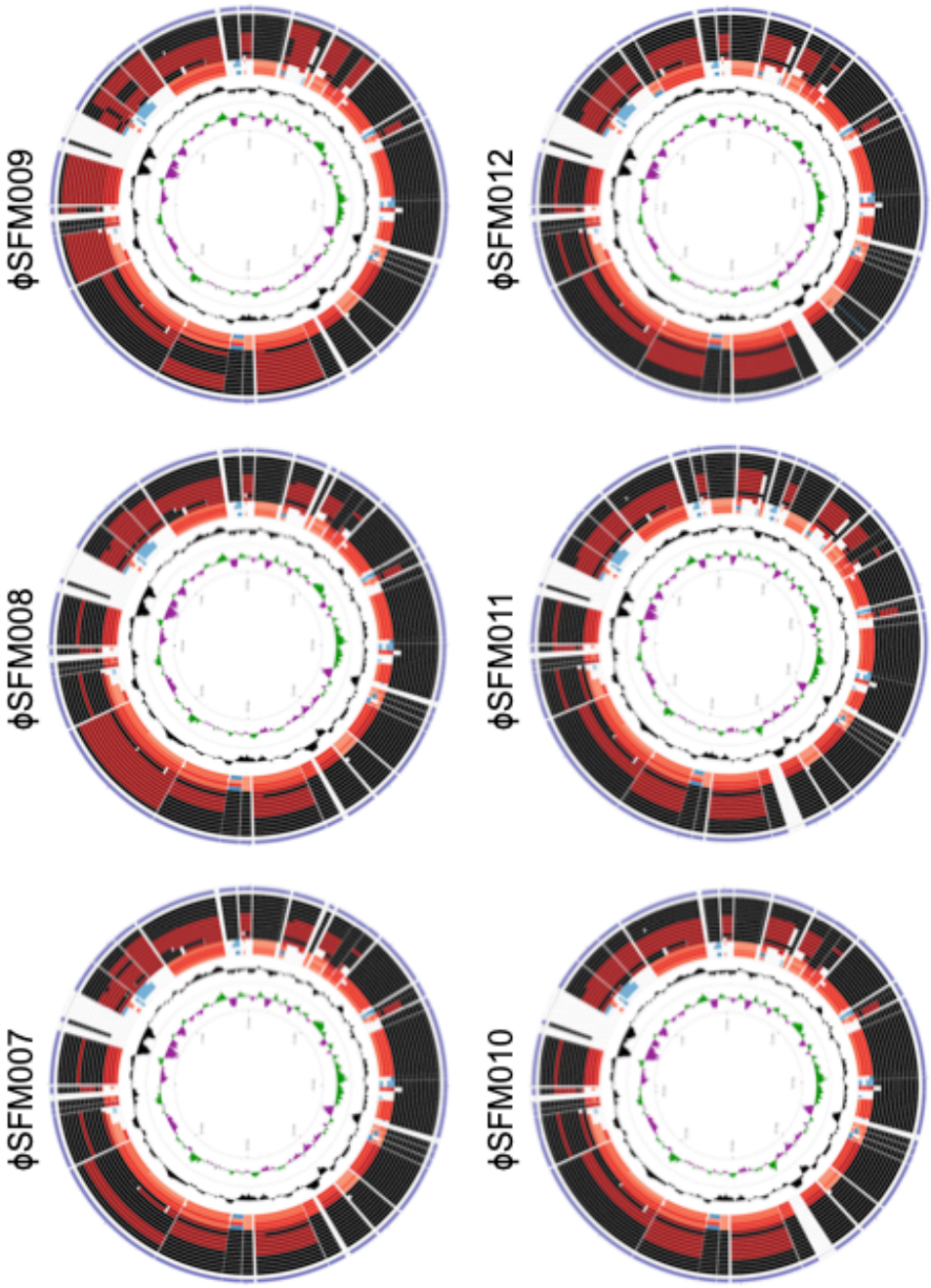

Appendix (m, cont.): Phage genome organisation comparison using CCT view. All phage genomes were manually colinearised placing the starting arbitrary point at the start of the open reading frame of the large terminase subunit gene (1), then each phage was compared individually to each other and the four closest phages from BLASTP results were added (ϕDU_PP_II, ϕPP74, ϕT7 and ϕvB_YenP_AP10 in the internal ring), dark red shows 90% similarity whereas black shows 100%. GC content and GC skews (+ and -) were shown as the innermost rings.

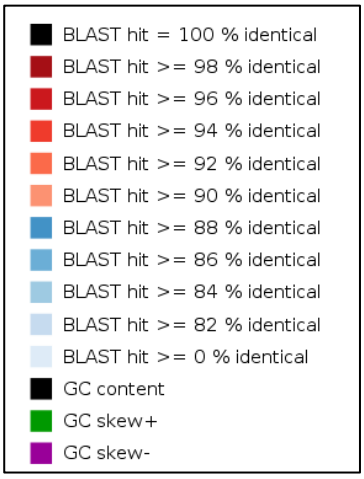
BLAST hit = 100 % identical
BLAST hit >= 98 % identical
BLAST hit >= 96 % identical
BLAST hit >= 94 % identical
BLAST hit >= 92 % identical
BLAST hit >= 90 % identical
BLAST hit >= 88 % identical
BLAST hit >= 86 % identical
BLAST hit >= 84 % identical
BLAST hit >= 82 % identical
BLAST hit >= 0 % identical
GC content
GC skew+
GC skew-